Universität Bremen

GLOMAR

The physiology of coral reef calcifiers under local and global stressors

Dissertation submitted by

Friedrich W. Meyer

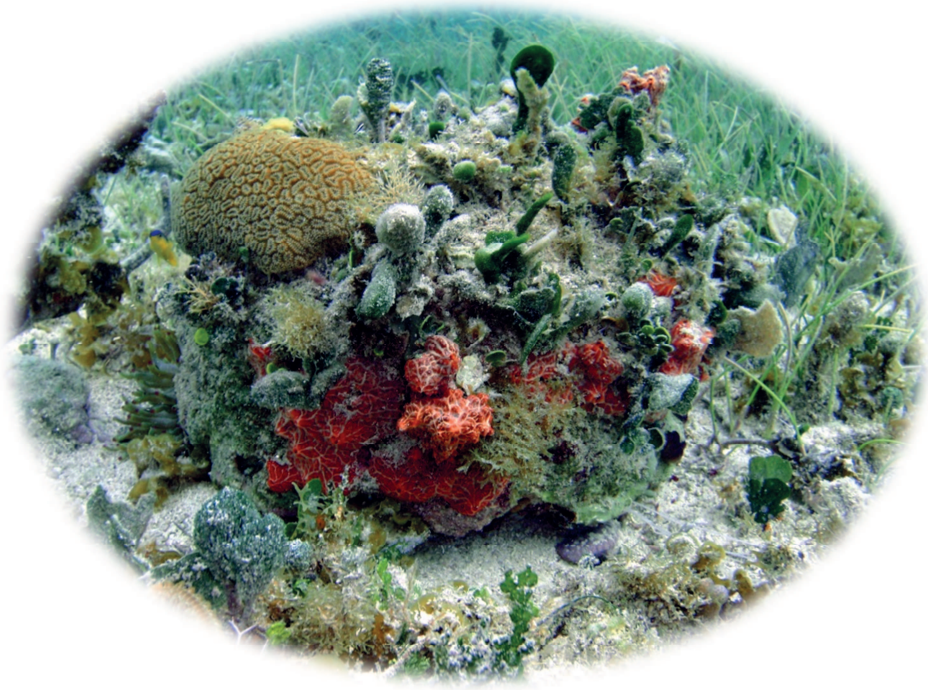

Bremen, 30.07.2015

zmt bremen

Leibniz Association

1st Reviewer: Prof. Dr. Christian Wild, University of Bremen

2nd Reviewer: Dr. Andreas Kunzmann, ZMT Bremen

Date of Colloquium: 04.11.2015

In partial fulfillment of the requirements for the degree of Doctor of Natural Sciences

(Dr. rer. nat.)

First Examiner:

Prof. Christian Wild

Leibniz Center for Tropical Marine Ecology,

Bremen, Germany

Second Examiner:

Dr. Andreas Kunzmann

Leibniz Center for Tropical Marine Ecology,

Bremen, Germany

Additional Examiner :1

Prof. Dr. Kai Bischof

University Bremen,

Bremen, Germany

Additional Examiner 2

Dr. Mirta Teichberg,

Leibniz Center for Tropical Marine Ecology,

Bremen, Germany

Dedicated to my parents and Marianna

Acknowledgements

My sincere thanks to Christian for giving me the opportunity to develop and complete this thesis. Thank you for the tremendous support and supervision, for the countless and helpful comments and ideas. Thank you for your patience and support during the writing process and helping me focus, thus ensuring the successful completion of this thesis. It was great to work with you and be a guest in your working group. A special thanks to my PhD panel: Mirta, Karen and Andreas, my working group leader. Thanks for the support, the formation of ideas, the field trip planning and of course the development of the final papers. It was great being supervised by such diverse a panel. Thank you to Soehnke, who was willing to be part of my panel as an external member. Furthermore I would like to thank Susana Enríquez, Roberto Iglesias Prieto and Nadine Schubert for a great course on "Light and photosynthesis in coral reefs" and for taking me in for a unique research stay in Puerto Morelos. Thanks Nadine for your help and support during the experimental phase, it was great learning from you. Thanks a lot to the research group of Roberto and Susana; I had a great time and learned so much. For the great hospitality and support during my stay at AIMS in Australia, I would like to thank Sven Uthicke and Nikolas Vogel. Thanks a lot to Niko for a comfortable stay at the AIMS and for the highly efficient experimental phase and calmness during "incubation madness". A huge thanks to the CORE and Ecophys working group which I enjoyed being a part of. I am very grateful for the ideas and comments during the presentation and project development.

I am thankful to GLOMAR for the financial and intellectual support during my thesis. To all the great people at GLOMAR, especially to Tina and Karin for being great research theme leaders, the administration as well as leadership of GLOMAR and of course to all the fellow students for the interesting seminars and fun times during conferences and retreats. Thanks to all my co-authors for the development of the manuscripts: to Andre for teaming up with me to investigate the mysteries of calcification and ocean acidification and for the very interesting and constructive discussions. It was fun developing and finalizing ideas with you. Thanks to Ulisse for the contribution in our book chapter and Nils co-supervision. It was fun learning more about nitrogen fixation and carbid. In addition I would like to thank Nils, for being a great student, lab partner, hiwi, co-author and friend. Also thanks to Astrid, Anny and Hauke for the pleasant and insightful cooperation into the world of microbes. Thanks a lot to my hiwis: Flo, Sabrina, Nur and Helen. Thanks Alex for being the best part time office mate! Without you I would have missed out on many squirrels and rabbits. You often made my day and always knew how to keep stress levels manageable. Thanks also to my office neighbors across the hall: Vanessa and CJ, thanks for the great times! Thanks a lot to the technicians at ZMT, specially Matthias, Christian, Steffi, Conny, Doro and Dieter who did priceless work and were eager to answer the many questions and requests I had. Furthermore thanks to Frank and Andreas P for the provision of material and help in any other situation. Thanks also to the IT support, mainly Uli and Chirstoph for

helping to solve digital and analog confusions! A special thanks to Epi, who always had a listening ear and for helping me develop great devices for my laboratory studies. I learned a lot from you. Thanks to the ZMT for the opportunity to develop my PhD thesis and to the administration for their support.

Finally, thanks a lot to my friends and family and of course to Marianna for your endless support, calmness and being always there for me, unconditionally.

Table of Contents

Thesis Abstract

Anthropogenic activities have caused coral reefs worldwide to face extreme changes in their environment at both global and local scales. Rising carbon dioxide (CO_2) concentrations in the atmosphere have led to global warming and seawater temperature rise and an increase in the CO_2 content in the ocean. This phenomenon has led to a decrease in pH and so called ocean acidification (OA) and is greatly affecting aquatic organisms worldwide.

On a local scale, population increase and coastal development has led to an increase in inorganic nutrient inputs to the coast, resulting in eutrophication, which has increased the amount of dissolved organic carbon (DOC) in the ocean. This has had detrimental effects on coral health. However, there is a lack of knowledge of how OA and high availability of DOC affect the physiology of corals and calcifying reef algae individually and in combination, and how this high nutrient content may disturb the future functioning of coral reefs.

This thesis investigated the individual and combined effects of OA as increased dissolved inorganic carbon (DIC) and high availability of DOC on the physiology of reef building corals from the Great Barrier Reef and calcifying green algae from the Indo-Pacific and the Caribbean. More specifically, we investigated various calcification processes, photosynthesis and the nitrogen fixation of the coral holobiont with its associated bacteria and calcifying green algae. An introductory chapter reviews the theory behind OA, the impact it has had on marine life in the tropics and a list suggesting indicator processes for OA (chapter 1). The following three chapters elucidate the physiological response of reef building corals from the Great Barrier Reef and calcifying green algae from the Indo-Pacific and the Caribbean under high DIC and DOC concentrations and the interaction of these two environmental parameters (chapter 2 to 4). As our current understanding of the calcification process in calcifying green algae of the genus *Halimeda* is in its infancy, this process is crucial to understand physiological impacts of both high DIC and DOC availability. Therefore, this thesis is supplemented with two chapters describing the geobiological calcification processes of *Halimeda opuntia* using scanning electron microscopy and known physiological processes (chapter 5). These findings are summarised in a new model for calcification for the green algae of the genus *Halimeda.* Findings were then compared to altered calcification under high DIC conditions to extend this model to the processes of calcification under high DIC conditions (chapter 7). As light drives the most important physiological processes such as photosynthesis and calcification in both algae and corals, the individual and combined effects of reduced light availability and high DIC availability on the physiology of *H. opuntia* and *Acropora millepora* were investigated (chapter 6). To provide a more holistic understanding of the impacts high DIC concentrations have on the coral holobiont, nitrogen fixation, a crucial part of nutrient cycling of coral reefs, was investigated in *Seriatopora hystrix* under high DIC conditions (chapter 8).

The key questions in this thesis are: 1) How do both, OA as elevated DIC and DOC availability affect the physiology of key coral reef calcifiers and how do both stressors interact? 2) What are the main properties of the calcification processes in *H. opuntia*? 3) How is the calcification process of *H. opuntia* influenced by high DIC? 4) How do light and high DIC affect the physiology of key coral reef calcifiers? and 5) How is nitrogen fixation of *S. hystrix* influenced under high DIC?

To answer these questions, comparative physiological measurements under controlled environmental conditions were carried out, and different treatments of altered environmental conditions were compared. Physiological measurements in combination with analysis of the calcification structure using scanning electron microscopy were used to suggest a model for the calcification of *Halimeda* and to investigate the impact of high DIC concentrations on these processes.

Major findings revealed that:

- elevated DIC concentrations reduced the growth and dark calcification of *A. millepora,* it also reduced the daily calcification rates of *H. opuntia*, and reduced the daily calcification rates and primary production of *H. incrassata* and *U. flabellum*. In addition, the nitrogen fixation rates of *S. hystrix* were reduced compared to control conditions and showed a significant correlation to calcification rates.

- under elevated DOC concentrations, the primary production of *H. macroloba, H. opuntia, A. millepora* and *H. incrassata* were reduced. The calcification rates of *H. incrassata* and *U. flabellum* were reduced.

- the combination of elevated DIC and DOC concentrations led to additive effects of both stressors, but also interactive effects were observed as *U. flabellum* showed a further reduction in calcification rates under the combination of both treatments in comparison to the individual treatments.

- the calcification structures of *H. opuntia* showed three distinct features and their formation were separated into two main components: night and day processes in which both, abiotic as well as biotic processes played an important role. Under the influence of high DIC concentrations, the cementation of the segments was mainly impacted, and under high DIC concentrations, the cementation of *H. opuntia* was significantly reduced.

In summary, we disclose that elevated DIC concentrations have multiple impacts on the physiology of both reef algae and corals, leading to reduced primary production rates and lower calcification rates, combined with poor cementation of algal segments. These findings indicate that overall productivity of corals and calcifying algae-dominated communities may decline under future ocean acidification scenarios. Not only does the calcification rate decline, but as shown for *Halimeda,* the calcified structure becomes weaker, leading to reduced competitiveness against biotic and abiotic factors and

ultimately leading to potentially faster erosion rates and lower structural complexity of these important biogenic hard substrates.

This thesis revealed that the physiology of reef corals and algae are affected under high DOC concentrations and that elevated DOC concentrations have strong negative impacts on the physiology (growth, photosynthesis) of the key organisms investigated in this thesis. This could likely reduce the future production of biogenic derived carbon of both coral and algal origin leading to a loss in structural complexity in reefs of the Indo-Pacific and the Caribbean. For *Halimeda* bioherms, reduced competiveness of the living alga due to decreased physical durability of weaker calcified skeletons and reduced growth rates might lead to the reduction of important habitats and a loss in the buffering capacity under future conditions of acidification.

The new model for the calcification process of *Halimeda* will be beneficial for future studies that investigate the effect of environmental changes on the calcification process and easing the interpretation of calcification structures of living and dead material. These findings will be crucial to be able to investigate future reef changes under high DIC and increased DOC concentrations. Our findings on calcification rates and calcification structures can be used as indicators of environmental change and as future predictors.

Zusammenfassung

Weltweit sind Korallenriffe extremen Veränderungen ihrer Umwelt durch anthropogene Einflüsse auf lokaler und globaler Ebene ausgesetzt. Steigende Temperaturen als Resultat des globalen Klimawandels und steigender Kohlendioxid Gehalt (CO_2) in der Atmosphäre haben den CO_2 Gehalt im Wasser ansteigen lassen und damit den pH Wert sinken lassen, was zum Anstieg von gelöstem inorganischem Kohlenstoff (DIC) und der sogenannten „Ozeanversauerung“ (OA) führt und aquatische Organismen weltweit beeinflusst. Auf lokaler Ebene haben Bevölkerungswachstum und Küstenentwicklung zu einer Zunahme von inorganischen Nährstoffen im Wasser und zu einer Überdüngung geführt. Diese hat zu einer Zunahme von gelösten organischen Kohlenstoffen (DOC) im Wasser geführt, von denen bekannt ist, dass sie negative Einflüsse auf den Gesundheitszustand von Korallen haben. Erstaunlicher Weise ist wenig darüber bekannt wie hohe DIC und DOC Verfügbarkeit die Physiologie von Korallen und kalzifizierenden Algen beeinflussen und ob diese sich gegenseitig verstärken und eventuell die Funktionen der Riffe der Zukunft verändern.

Diese Arbeit untersuchte daher die individuellen und kombinierten Effekte von DIC und DOC Verfügbarkeit auf die Physiologie von riffbildenden Korallen aus dem Großen Barriere Riff sowie von kalzifizierenden Algen aus dem Indo-Pazifik und der Karibik. Um einen übergreifenden Einblick in die Prozesse zu gewinnen, die möglicherweise beeinflusst werden, wurden Kalzifizierung, Photosynthese und Stickstofffixierung des Korallen Holobiont inklusive der assoziierten Bakterien und der kalzifizierenden Grünalgen untersucht. In einem einführenden Kapitel wird die Theorie hinter Ozeanversauerung sowie der Einfluss auf marine Lebensformen in den Tropen behandelt und eine Liste mit Indikator Prozessen vorgeschlagen (Kapitel 1). Die nächsten drei Kapitel behandeln die physiologischen Einflüsse von erhöhter DIC und DOC Verfügbarkeit und deren Interaktion auf Riffkorallen von dem Großen Barriere Riff sowie kalzifizierenden Grünalgen aus dem Indo-Pazifik und der Karibik (Kapitel 2 bis 4). Da das derzeitige Wissen über den Kalzifizierungsmechanismus der kalzifizierenden Grünalge *Halimeda* beschränkt ist, aber nötig ist um die physiologischen Einflüsse von OA und DOC zu verstehen, ist diese Arbeit um 2 Kapitel erweitert, die den geobiologischen Kalzifizierungsprozess von *Halimeda opuntia* behandeln und diesen Anhand von Raster Elektronenmikroskopie und bekannten physiologischen Prozessen aufklären (Kapitel 5). Erkenntnisse aus dieser Studie wurden dann auf die Kalzifizierung unter OA Bedingungen erweitert (Kapitel 7). Da Licht ein wichtiger Faktor ist, der Prozesse wie Photosynthese und Kalzifizierung in Algen und Korallen antreibt, wurde der individuelle und kombinierte Effekt von Licht und OA auf die Alge *H. opuntia* und Koralle *Acropora millepora* in einem zusätzlichen Kapitel untersucht (Kapitel 6). Um das Gesamtverständnis der physiologischen Veränderung von Korallen unter OA zu verbessern wurde zudem ein sehr wichtiger Teil des Nährstoffkreislaufes, der Stickstofffixierung der Koralle *Seriatopora hystrix* und erhöhten DIC Bedingungen untersucht (Kapitel 8).

Die Schlüsselfragen dieser Studie waren: 1) Wie beeinflussen erhöhte DIC und DOC Verfügbarkeit die Physiologie von wichtigen Kalzifizierern des Korallenriffes und interagieren diese beiden Stressoren? 2) Was sind die Haupt Charakteristiken der Kalzifizierung von *H. opuntia*? 3) Wie wird dieser Prozess von erhöhter DIC Verfügbarkeit beeinflusst? 4) Wie beeinflussen Licht und DIC die Kalzifizierung von wichtigen Riff Kalzifizierern? 5) Wie wird die Stickstofffixierung von *Seriatopora hystrix* durch erhöhte DIC Konzentrationen beeinflusst?

Um diese Fragen zu beantworten wurden vergleichende Messungen der Physiologie dieser Organismen unter kontrollierten Umweltbedingungen durchgeführt und verschiedene Umweltbedingungen miteinander verglichen. Hierbei wurden physiologische Messungen zusammen mit der Analyse der Kalzifizierungsstruktur benutzt und ein neues Modell der Kalzifizierung von *Halimeda* zu erstellen und dieses um den Einfluss von hohen DIC zu erweitern.

Haupterkenntnisse dieser Arbeit waren:

- Erhöhte DIC Konzentrationen reduzieren das Wachstum und die Kalzifizierung unter Abwesenheit von Licht von *A. millepora,* reduzieren die Tageskalzifizierungsraten von *H. opuntia*, und reduzieren Tageskalzifizierungsraten sowie die Primärproduktion von *Halimeda incrassata* und *Udothea flabellum*. Zusätzlich wurden die Stickstofffixierungsraten von *S. hystrix* im Vergleich zu den Kotrollbedingungen reduziert, und zeigten signifikante Korrelationen mit den Kalzifizierungsraten.

- Unter erhöhten DOC Konzentrationen wurden die Primärproduktion von *H. macroloba, H. opuntia, A. millepora* und *H. incrassata* reduziert. Das Wachstum und die Kalzifizierung von *A. millepora* und die Kalzifizierungsraten von *H. incrassata* und *U. flabellum* wurden ebenso reduziert.

- Erhöhte DIC und DOC Verfügbarkeit führte zu additive Effekten auf die Physiologie von Korallen und Algen, zeigten aber auch interaktive Reaktionen unter dem Einfluss beider Stressoren die in Kombination einen höheren Einfluss auf die Organismen zeigten als im einzelnen indem z.B: die Kalzifizierungsraten von *U. flabellum* noch deutlicher reduziert wurden also von hohen DIC Konzentrationen alleine.

- Die Kalzifizierungsstrukturen von *H. opuntia* ließen sich in drei Typen unterteilen und deren Formierung wurde auf zwei Hauptkomponenten aufgeteilt: Tages- und Nachtprozesse bei denen beide, abiotische sowie biotische Prozesse eine wichtige Rolle spielten. Unter dem Einfluss von hohen DIC Konzentrationen wurde vor allem die Zementierung der einzelnen Segmente von *H. opuntia* beeinflusst und unter diesen Bedingungen wurde diese Zementierung deutlich reduziert.

Zusammenfassend konnten wir zeigen das erhöhte DIC Verfügbarkeit multiple Einflüsse auf die Physiologie von Riffalgen sowie Korallen hat welche zu reduzierten Primärproduktionsraten sowie niedrigen Kalzifizierungsraten kombiniert mit schwacher Zementierung führen. Diese Erkenntnisse

zeigen auf das die Produktivität der von kalzifizierenden Korallen und Algen dominierten Gemeinschaften unter zukünftigen OA Bedingungen drastisch sinken könnte. Nicht nur könnte die Netto Kalzifizierung dieser Gemeinschaften abnehmen, sondern, wie am Beispiel von *Halimeda* gezeigt, wird das gebildete Skelett schwächer und führt letztendlich zur einer reduzierten Widerstandsfähigkeit gegenüber biotischen und abiotischen Faktoren und schlussendlich zu erhöhten Erosionsraten und reduzierter Strukturkomplexität dieser wichtigen Bildner biogener Hartsubstrate.

In dieser Arbeit konnten wir zeigen, dass die Physiologie von Riffkorallen und Algen durch hohe DIC und DOC Verfügbarkeit beeinflusst wird und das hohe DOC Konzentrationen negative Einflüsse auf die Physiologie (Wachstum, Photosyntheseleistung) dieser Schlüsselorganismen hat. Dies wird wahrscheinlich die Produktion von biogenen Karbonaten durch Algen und Korallen verringern was zu einem Verlust von struktureller Komplexität in den Riffen des Indo-Pazifik und der Karibik führen kann. Für die durch *Halimeda* Sande geprägten Ökosysteme bedeutet dies ein Verlust von wertvollem Habitat durch die verringerte Konkurrenzfähigkeit von *Halimeda* aufrgund reduzierten Wachstumes und geringerer physischer Stabilität durch schwächer kalzifizierte Skelette. Dies hat zudem negative Auswirkungen auf die Pufferkapazität dieser Ökosysteme gegenüber weiterer Versauerung, da die *Halimeda* Sande einen natürlichen Carbonat Puffer darstellen.

Das von uns vorgestellte neue Modell zur Kalzifizierung von *Halimeda* wird wertvoll für zukünftige Studien sein, die den Einfaluss von Umweltfaktoren auf den Kalzifizierungsprozess dieser Alge untersuchen werden. Es kann zudem die Interpretation der kalzifizierten Struktur in lebendem um totem Material vereinfachen und Aussagen über die Diagenese zulassen. Diese Erkenntnisse können dazu beitragen Veränderungen in den Riffen der Zukunft und hohen DIC und DOC Gehalten zu untersuchen und vorherzusagen. Zudem können diese Erkenntnisse zu Kalzifizierungsraten sowie deren Kalzifizierungsstruktur also Indikatoren für wechselnde Umwelteinflüsse dienen und Vorhersagen über Karbonatproduktion ermöglichen.

Introduction

Global climate change in combination with local disturbances, such as eutrophication and resource overuse, poses threats to coral reefs worldwide and has led to a decline in live coral cover by up to 80 % in some regions [1,2]. The increase in fossil fuel emissions, deforestation, and other sources of carbon dioxide (CO_2) emissions result in the rising of CO_2 partial pressure in the atmosphere. As over 30 % of the atmospheric CO_2 is taken up by the ocean, this alters the oceans carbonate chemistry, ultimately leading to a drop in pH and causing ocean acidification (OA). Along with a reduction in pH, the saturation state of carbonate ions is reduced [3], making it more difficult for organisms to calcify [4]. This could have a detrimental effect on reef organisms like corals and calcifying algae. In addition, OA has also shown to affect processes like primary production and nutrient acquisition [5–8] (for detailed information on OA chemistry and effects on organisms see chapter 1).

On a local scale, increased sewage and agricultural effluxes lead to an increase in the nutrient concentration of the water column, causing eutrophication of coastal waters and their ecosystems [9–13]. The content of dissolved organic carbon (DOC) has also increased [14,15] along with the introduction of inorganic nutrients, including phosphate, ammonia and nitrate (14,15). In contrast to DOC in the open ocean which is typically of low bioavailability, highly labile DOC from waste waters or algal blooms fuels bacterial growth [16,17] that may cause coral bleaching, trigger diseases and eventual coral mortality [18–20]. In a reef system the nutrient concentrations (inorganic and organic) are generally low [21–23]. These oligotrophic conditions result from the close coupling between metabolic processes and nutrient cycling, featuring the typically high productivity of a reef in a nutrient-depleted environment [24,25]. However, increased urbanisation and fertilizer use can significantly increase the local nutrient concentrations in coral reefs through river discharge [26–28], particularly inorganic nutrients and sewage which alter the content of dissolved organic carbon (DOC) in the water column [14,19]. An increase in DOC also results from the increase in inorganic nutrient availability, which can trigger a macroalgae bloom and change planktonic productivity [29]. In a coral reef, algae and corals are the main producers of DOC although with significant differences in production rates and composition [16,30–34]. Therefore, a shift from a coral to an algae dominated system greatly alters the content and composition of DOC [26,31,32,35,36]. Carbohydrates represent the largest fraction of DOC in algae and corals, followed by lipids and amino acids [31–33]. In laboratory experiments, the carbohydrates lactose and glucose have been used as treatments because they are one of the most abundant sugars released in algae and coral DOC [18,20,31]. These studies have shown the effects of bleaching, tissue loss and eventual death of the coral after being exposed to only a few weeks of elevated DOC concentrations. Apart from these findings, very little is known about the effects of elevated DOC concentrations on the physiology of corals, and no study has investigated the effects on calcifying reef algae. Due to the combined effects that ocean acidification

and increased organic carbon might pose on calcifying organisms in the near future, it is crucial to investigate the effects and identify the changes in the physiology of such organisms when exposed to different levels of these environmental parameters. A loss in productivity and calcification due to OA and increased DOC of coral species that provide reef habitat structure may lead to an imbalance in reef accretion and erosion and consequently to the potential loss of reef structure.

Calcifying algae are another important group of carbonate producers in coral reef and lagoon environments. Species of the genus *Halimeda,* a calcifying green alga, produce large amounts of carbonate sands [37] through their high growth and turnover rates [38,39], significantly contributing to habitat formation of carbonate platform build-ups [40,41] as well as the global carbon budget [42]. Under future acidification scenarios, *Halimeda* species may suffer from reduced productivity due to decreased carbonate production, leading to a loss in the provision of important habitat and a potential impairment in the future buffering capacity of the ocean coastal systems due to a loss in *Halimeda* derived carbonate sands. Studies on the effect of OA on *Halimeda* are partially contrasting [5,43–45], and the mechanisms of calcification are not well understood. The microstructure of the aragonite skeleton in *Halimeda* and parts of the abiotic setting surrounding the individual segments have been described in less recent publications, [46–50] and it is clear that the nucleation and crystallisation processes, as well as the origin of different skeletal features [46] remain unknown. Understanding these processes is essential to be able to interpret experimental results when investigating the calcification response of *Halimeda* towards altered environmental parameters.

Light also plays and important role in the calcification process of algae [51] as it drives photosynthesis. Light seems to be partially involved in the calcification process of corals and algae and it is the main energy supply of these organisms. In combination with riverine runoff, eutrophication and algae blooms, light availability can be strongly reduced [27,36,52] and can greatly affect the health of marine organisms [53,54]. The interaction of light and global stressors like OA during the process of calcification and primary production is under investigated, yet fundamental, to understand the potential cumulative effects. This information would ultimately help identify disturbances in carbon budgets and biogenic carbon evolution during events of increased flood plumes or reduced light availability due to algae blooms.

For corals, it is crucial to maintain the coral/symbiont (dinoflagellate) symbiosis in order to ensure efficient growth and productivity in a low nutrient environment. Although nitrogen recycling is efficient, new nitrogen needs to be supplied via prey capture by assimilating inorganic or organic nitrogen from the water column or by dinitrogen fixation. Many corals have exhibited dinitrogen fixation by harbouring cyanobacteria [55,56] and this process has been evaluated as an important nitrogen source for many coral species [55,56]. It is therefore surprising that no studies have yet investigated the effect of OA on the dinitrogen fixation of corals. A reduction of dinitrogen fixation

through OA could greatly affect the symbiont/host symbiosis, leading to a potential reduction in primary production.

Objectives

The aspiration of this thesis is to identify the individual and combined effects of OA and increased DOC concentrations on the physiology of two key functional groups in coral reefs ecosystems, calcifying green algae and corals, by using multiple physiological measurements under controlled laboratory conditions and a synoptic approach on diverse response parameters of the coral holobiont and the algae. This thesis aims to contribute to the understanding of the calcification process of calcifying green algae of the genus *Halimeda* and to assess how OA alters these processes. To enhance the synoptic view of the organism response towards OA, the effect of light in combination with OA and the effect of OA on the nitrogen fixation of corals is also investigated.

The key questions of this thesis were:

1) How does elevated DIC and DOC availability affect the physiology (primary production, nutrient uptake, growth) of a coral reef species and how do both stressors interact?

2) How does elevated DIC and DOC availability affect the physiology (primary production, nutrient uptake, growth) of a calcifying green algae species from different geographical locations and how do both stressors interact?

3) What are the main microstructural properties in the calcification mechanism of *Halimeda opuntia* and how are these properties related to the presently known physiological processes?

4) How does OA influence the calcification mechanism of *H. opuntia*?

5) How does light and OA affect the physiology of key coral reef calcifiers?

6) How does OA influence the dinitrogen fixation of the hermatypic coral *Seriatopora hystrix*?

References

1. Burke L, Reytar K, Spalding M, Perry A (2011) Reefs at risk revisited. 6-15 p. Available: http://www.pubmedcentral.nih.gov/articlerender.fcgi?artid=3150666&tool=pmcentrez&rendertype=abstract. Accessed 17 July 2013.

2. Wilkinson C (2000) Status of coral reefs of the world: 2004. Chapter. Available: http://www.crisponline.info/Portals/1/Skins/inside_fr/documents/0_statusofcoralreefs.pdf. Accessed 17 July 2013.

3. Zeebe RE, Wolf-Gladrow DA (2001) CO_2 in seawater: equilibrium, kinetics, isotopes. Elsevier Science. Available: http://books.google.com/books?hl=en&lr=&id=VrumU3XvQ-gC&oi=fnd&pg=PP2&dq=Seawater:+Equilibrium,+Kinetics,+Isotopes,+&ots=0lJD0a2k3_&sig=6G0E8lNEEUyMZQByGa-_CV_RNao. Accessed 5 August 2011.

4. Doney SC, Fabry VJ, Feely RA, Kleypas J a. (2009) Ocean Acidification: The Other CO_2 Problem. Ann Rev Mar Sci 1: 169–192. Available: http://www.annualreviews.org/eprint/QwPqRGcRzQM5ffhPjAdT/full/10.1146/annurev.marine.010908.163834. Accessed 28 April 2014.

5. Sinutok S, Hill R, Doblin MA, Wuhrer R, Ralph PJ (2011) Warmer more acidic conditions cause decreased productivity and calcification in subtropical coral reef sediment-dwelling calcifiers. Limnol Oceanogr 56: 1200–1212. Available: http://cat.inist.fr/?aModele=afficheN&cpsidt=24362064. Accessed 21 February 2014.

6. Beman JM, Chow C-E, King AL, Feng Y, Fuhrman JA, et al. (2011) Global declines in oceanic nitrification rates as a consequence of ocean acidification. Proc Natl Acad Sci U S A 108: 208–213. Available: http://www.pnas.org/cgi/content/abstract/108/1/208. Accessed 19 January 2011.

7. Leclercq N, Gattuso J-P, Jaubert J (2002) Primary production, respiration, and calcification of a coral reef mesocosm under increased CO_2 partial pressure. Limnol Oceanogr 47: 558–564. Available: http://www.aslo.org/lo/toc/vol_47/issue_2/0558.html.

8. Anthony KRN, Kline DI, Diaz-Pulido G, Dove SG, Hoegh-Guldberg O (2008) Ocean acidification causes bleaching and productivity loss in coral reef builders. Proc Natl Acad Sci U S A 105: 17442–17446. Available: http://www.ncbi.nlm.nih.gov/pubmed/18988740.

9. Bell P (1992) Eutrophication and coral reefs—some examples in the Great Barrier Reef lagoon. Water Res 26: 553–568. Available: http://www.sciencedirect.com/science/article/pii/004313549290228V. Accessed 24 August 2014.

10. Bell PRF (1991) Status of eutrophication in the Great Barrier Reef lagoon. Mar Pollut Bull 23: 89–93. Available: http://linkinghub.elsevier.com/retrieve/pii/0025326X9190655C.

11. Dubinsky Z, Stambler N, Fabricius KE (n.d.) Factors Determining the Resilience of Coral Reefs to Eutrophication: A Review and Conceptual Model. Coral Reefs: An Ecosystem in Transition. Springer Netherlands. pp. 493–505. Available: http://dx.doi.org/10.1007/978-94-007-0114-4_28.

12. Jessen C, Bednarz VN, Rix L, Teichberg M, Wild C (2015) Marine Eutrophication. In: Armon RH, Ha¨nninen O, editors. Environmental Indicators. doi:10.1007/978-94-017-9499-2_11.

13. Fabricius KE, McCorry D (2006) Changes in octocoral communities and benthic cover along a water quality gradient in the reefs of Hong Kong. Mar Pollut Bull 52: 22–33. Available: http://www.sciencedirect.com/science/article/pii/S0025326X05003590.

14. Ford P, Tillman P, Robson B, Webster IT (2005) Organic carbon deliveries and their flow related dynamics in the Fitzroy estuary. Mar Pollut Bull 51: 119–127. Available: http://www.ncbi.nlm.nih.gov/pubmed/15757714. Accessed 22 August 2014.

15. Alongi DM, McKinnon a D (2005) The cycling and fate of terrestrially-derived sediments and nutrients in the coastal zone of the Great Barrier Reef shelf. Mar Pollut Bull 51: 239–252. Available: http://www.ncbi.nlm.nih.gov/pubmed/15757725. Accessed 24 May 2013.

16. Gregg A, Hatay M, Haas AF, Robinett N, Barott KL, et al. (2013) Biological oxygen demand optode analysis of coral reef-associated microbial communities exposed to algal exudates. PeerJ 1: e107. Available: http://www.pubmedcentral.nih.gov/articlerender.fcgi?artid=3719127&tool=pmcentrez&rendertype=abstract. Accessed 25 April 2014.

17. Haas AF, Nelson CE, Rohwer F, Wegley-Kelly L, Quistad SD, et al. (2013) Influence of coral and algal exudates on microbially mediated reef metabolism. PeerJ 1: e108. Available: http://www.pubmedcentral.nih.gov/articlerender.fcgi?artid=3719129&tool=pmcentrez&rendertype=abstract. Accessed 24 March 2014.

18. Kuntz NM, Kline DI, Sandin SA, Rohwer F (2005) Pathologies and mortality rates caused by organic carbon and nutrient stressors in three Caribbean coral species. Mar Ecol Prog Ser 294: 173–180. Available: http://www.int-res.com/abstracts/meps/v294/p173-180/.

19. Kline DI, Kuntz NM, Breitbart M, Knowlton N, Rohwer F (2006) Role of elevated organic carbon levels and microbial activity in coral mortality. Mar Ecol Prog Ser 314: 119–125. Available: http://www.int-res.com/abstracts/meps/v314/p119-125/.

20. Haas AF, Al-Zibdah M, Wild C (2009) Effect of inorganic and organic nutrient addition on coral–algae assemblages from the Northern Red Sea. J Exp Mar Bio Ecol 380: 99–105. Available: http://linkinghub.elsevier.com/retrieve/pii/S0022098109003712. Accessed 22 June 2011.

21. Rengar DA, Riegel BM (2005) Effect of nutrient enrichment and elevated CO_2 partial pressure on growth rate of atlantic scleractinian coral *Acropora cervicornis*. Mar Ecol Prog Ser 293: 69–76. Available: http://cat.inist.fr/?aModele=afficheN&cpsidt=16887426. Accessed 15 July 2011.

22. Humphrey C, Weber M, Lott C, Cooper TF, Fabricius KE (2008) Effects of suspended sediments, dissolved inorganic nutrients and salinity on fertilisation and embryo development in the coral *Acropora millepora* (Ehrenberg, 1834). Coral Reefs 27: 837–850. Available: http://dx.doi.org/10.1007/s00338-008-0408-1. Accessed 30 June 2011.

23. Nelson CE, Alldredge AL, McCliment E, Amaral-Zettler L, Carlson C (2011) Depleted dissolved organic carbon and distinct bacterial communities in the water column of a rapid-flushing coral reef ecosystem. ISME J 5: 1374–1387. Available: http://www.ncbi.nlm.nih.gov/pubmed/21390080. Accessed 19 July 2011.

24. Schlager W (1981) The paradox of drowned reefs and carbonate platforms. Geol Soc Am Bull 92: 197–211. Available: http://gsabulletin.gsapubs.org/cgi/content/abstract/92/4/197.

25. Hallock P, Schlager W (1986) Nutrient excess and the demise of coral reefs and carbonate platforms. Palaios 1: 389. Available: http://www.jstor.org/stable/3514476?origin=crossref. Accessed 17 October 2011.

26. Fabricius KE, De'ath G, McCook LJ, Turak E, Williams DM (2005) Changes in algal, coral and fish assemblages along water quality gradients on the inshore Great Barrier Reef. Mar Pollut Bull 51: 384–398. Available: http://www.sciencedirect.com/science/article/pii/S0025326X04003923.

27. Fabricius KE (2005) Effects of terrestrial runoff on the ecology of corals and coral reefs: review and synthesis. Mar Pollut Bull 50: 125–146. Available: http://www.sciencedirect.com/science/article/pii/S0025326X04004497.

28. Fabricius KE, De'ath G, De'Ath G (2004) Identifying ecological change and its causes: A case study on coral reefs. Ecol Appl 14: 1448–1465. Available: http://www.esajournals.org/doi/abs/10.1890/03-5320. Accessed 27 July 2011.

29. Hauri C, Fabricius KE, Schaffelke B, Humphrey C (2010) Chemical and physical environmental conditions underneath mat- and canopy-forming macroalgae, and their tffects on understorey corals. PLoS One 5: e12685. Available: http://dx.doi.org/10.1371/journal.pone.0012685.

30. Haas AF, Jantzen C, Naumann MS, Iglesias-Prieto R, Wild C (2010) Organic matter release by the dominant primary producers in a Caribbean reef lagoon: implication for in situ O_2 availability. Mar Ecol Prog Ser 409: 27–39. doi:10.3354/meps08631.

31. Wild C, Naumann MS, Niggl W, Haas AF (2010) Carbohydrate composition of mucus released by scleractinian warm- and cold-water reef corals. Aquat Biol 10: 41–45. doi:10.3354/ab00269.

32. Haas AF, Wild C (2010) Composition analysis of organic matter released by cosmopolitan coral reef-associated green algae. Aquat Biol 10. Available: http://www.int-res.com/abstracts/ab/v10/n2/p131-138/. Accessed 17 January 2014.

33. Nelson CE, Goldberg SJ, Wegley Kelly L, Haas AF, Smith JE, et al. (2013) Coral and macroalgal exudates vary in neutral sugar composition and differentially enrich reef bacterioplankton lineages. ISME J 7: 962–979. Available: http://www.ncbi.nlm.nih.gov/pubmed/23303369. Accessed 19 November 2013.

34. Haas AF, Nelson C, Kelly L, Carlson C (2011) Effects of coral reef benthic primary producers on dissolved organic carbon and microbial activity. PLoS One 6. Available: http://dx.plos.org/10.1371/journal.pone.0027973. Accessed 17 January 2014.

35. Naumann MS, Haas AF, Struck U, Mayr C, El-Zibdah M, et al. (2010) Organic matter release by dominant hermatypic corals of the Northern Red Sea. Coral Reefs 29: 649–659. Available: http://www.springerlink.com/index/10.1007/s00338-010-0612-7. Accessed 14 July 2011.

36. Cooper TF, Uthicke S, Humphrey C, Fabricius KE (2007) Gradients in water column nutrients, sediment parameters, irradiance and coral reef development in the Whitsunday Region, central Great Barrier Reef. Estuar Coast Shelf Sci 74: 458–470. Available: http://www.sciencedirect.com/science/article/pii/S0272771407001412.

37. Wefer G (1980) Carbonate production by algae *Halimeda*, *Penicillus* and *Padina*. Nature 285: 323–324. Available: http://www.nature.com/nature/journal/v285/n5763/abs/285323a0.html. Accessed 11 November 2011.

38. Hillis-Colinvaux L (1980) Ecology and taxonomy of *Halimeda*: primary producer of coral reefs. Adv Mar Biol 17: 1–327. Available: http://www.sciencedirect.com/science/article/pii/S006528810860303X. Accessed 26 July 2011.

39. Drew E (1983) *Halimeda* biomass, growth rates and sediment generation on reefs in the central Great Barrier Reef province. Coral Reefs: 101–110. Available: http://www.pubmedcentral.nih.gov/articlerender.fcgi?artid=3184997&tool=pmcentrez&rendertype=abstract. Accessed 8 April 2014.

40. Multer HG (1988) Growth rate, ultrastructure and sediment contribution of *Halimeda incrassata* and *Halimeda monile*, Nonsuch and Falmouth Bays, Antigua, W.I. Coral Reefs 6: 179–186. Available: http://www.springerlink.com/index/10.1007/BF00302014.

41. Freile D, Milliman JD, Hillis L (1995) Leeward bank margin *Halimeda* meadows and draperies and their sedimentary importance on the western Great Bahama Bank slope. Coral Reefs 14: 27–33. Available: http://link.springer.com/10.1007/BF00304068. Accessed 21 February 2014.

42. Rees S a., Opdyke BN, Wilson P a., Henstock TJ (2006) Significance of *Halimeda* bioherms to the global carbonate budget based on a geological sediment budget for the Northern Great Barrier Reef, Australia. Coral Reefs 26: 177–188. Available: http://link.springer.com/10.1007/s00338-006-0166-x. Accessed 21 February 2014.

43. Hofmann LC, Heiden J, Bischof K, Teichberg M (2014) Nutrient availability affects the response of the calcifying chlorophyte *Halimeda opuntia* (L.) J.V. Lamouroux to low pH. Planta 239: 231–242. Available: http://www.ncbi.nlm.nih.gov/pubmed/24158465. Accessed 23 January 2014.

44. Robbins LL, Knorr PO, Hallock P (2009) Response of *Halimeda* to ocean acidification: field and laboratory evidence. Biogeosciences Discuss 6: 4895–4918. Available: http://www.biogeosciences-discuss.net/6/4895/2009/.

45. Price N, Hamilton S, Tootell J, Smith J (2011) Species-specific consequences of ocean acidification for the calcareous tropical green algae *Halimeda*. Mar Ecol Prog Ser 440: 67–78. Available: http://www.int-res.com/abstracts/meps/v440/p67-78/. Accessed 31 October 2011.

46. Reid RP, Macintyre IANG (1998) Carbonate Recrystallization in Shallow Marine Environments: A Widespread Diagenetic Process Forming Micritized Grains. SEPM J Sediment Res Vol. 68 (1: 1–3. Available: http://search.datapages.com/data/doi/10.1306/D42688B5-2B26-11D7-8648000102C1865D.

47. Larkum AWD (1976) Calcification in the green alga *Halimeda* II. The exchange of Ca^{2+} and the occurrence of age gradients in calcification and photosynthesis. J Exp … 27: 864–878. Available: http://jxb.oxfordjournals.org/content/27/5/864.short. Accessed 25 September 2012.

48. Beer D De, Larkum A (2002) Photosynthesis and calcification in the calcifying algae *Halimeda* discoidea studied with microsensors. Plant Cell Environ: 1209–1217. Available: http://onlinelibrary.wiley.com/doi/10.1046/j.1365-3040.2001.00772.x/full. Accessed 25 September 2012.

49. Wilbur KM, Colinvaux LH, Watabe N (1969) Electron microscope study of calcification in the alga *Halimeda* (order Siphonales) 1. Phycologia 8: 27–35. Available: http://phycologia.org/doi/abs/10.2216/i0031-8884-8-1-27.1?journalCode=phya. Accessed 27 July 2015.

50. Milliman J, Müller G, Förstner F (2012) Recent sedimentary carbonates: Part 1 marine carbonates. Available: https://books.google.com/books?hl=de&lr=&id=SKnxCAAAQBAJ&pgis=1. Accessed 27 July 2015.

51. Borowitzka MA, Larkum AWD (1976) Calcification in the green-alga *Halimeda* 3. Sources of inorganic carbon for photosynthesis and calcification and a model of mechnism of calcification. J Exp Bot 27: 879–893. Available: http://jxb.oxfordjournals.org/content/27/5/879.short. Accessed 21 November 2013.

52. De'ath G, Fabricius KE (2010) Water quality as a regional driver of coral biodiversity and macroalgae on the Great Barrier Reef. Ecol Appl 20: 840–850. Available: http://dx.doi.org/10.1890/08-2023.1.

53. Kendall JJ, Powell EN, Connor SJ, Bright TJ, Zastrow CE (1985) Effects of turbidity on calcification rate, protein concentration and the free amino acid pool of the coral *Acropora cervicornis.* Mar Biol 87: 33–46. Available: http://link.springer.com/10.1007/BF00397003. Accessed 27 July 2015.

54. Kendall J. JJ, Powell EN, Connor SJ, Bright TJ (n.d.) The effects of drilling fluids (Muds) and turbidity on the growth and metabolic state of the coral *Acropora Cervicornis*, with comments on methods of normalization for coral data. Available: http://www.ingentaconnect.com/content/umrsmas/bullmar/1983/00000033/00000002/art00011. Accessed 27 July 2015.

55. Fiore CL, Jarett JK, Olson ND, Lesser MP (2010) Nitrogen fixation and nitrogen transformations in marine symbioses. Trends Microbiol 18: 455–463. Available: http://www.ncbi.nlm.nih.gov/pubmed/20674366. Accessed 25 May 2013.

56. Cardini U, Bednarz VN, Foster RA, Wild C (2014) Benthic N_2 fixation in coral reefs and the potential effects of human-induced environmental change. Ecol Evol 4: 1706–1727. Available: http://www.pubmedcentral.nih.gov/articlerender.fcgi?artid=4063469&tool=pmcentrez&rendertype=abstract. Accessed 27 July 2015.

Publication Outline

This thesis comprises eight chapters, and each chapter is represented by one article. It contains a book chapter that has been published and seven papers out of which four are published, one accepted, one under review and one in preparation for submission. Chapter one describes the theory behind ocean acidification, its spatial and temporal resolution and the impact on marine organisms. In the second chapter, a laboratory experiment highlights the effects of ocean acidification and increased organic carbon content on the physiology (i.e. photosynthesis, calcification) of a prominent reef coral. This chapter is complemented by the third chapter which elucidates the impact of equal environmental settings on the physiology of two calcifying reef algae species. In the fourth chapter effects on the physiology of the previously mentioned environmental settings are then described for two calcifying reef algae from a different geographical setting. The fifth chapter suggests a new model for the important calcification process in the calcifying algae named in chapter 3 and 4. In addition to ocean acidification, also the factor light and its impact on the physiology of calcifying green algae and corals is investigated in chapter 6. To understand the effects of ocean acidification on the calcification process in calcifying green algae, chapter 7 describes the impact of ocean acidification on the calcification mechanism suggested in chapter 5. In order to understand more of the corals holobiont reaction towards altered environmental conditions, in chapter 8, the effect of ocean acidification on coral di-nitrogen fixation is investigated.

Article 1)

Friedrich W. Meyer, Ulisse Cardini, and Christian Wild

Ocean acidification and related indicators

The book chapter has been initiated by C. Wild. The structure of the chapter was designed by Friedrich W. Meyer and C. Wild. Writing of the manuscript was conducted by Friedrich W. Meyer, Ulisse Cardini, and Christian Wild. The book has been published at Springer, DOI: 10.1007/978-94-017-9499-2_41

Article 2)

Friedrich W Meyer, Nikolas Vogel, Karen Diele, Andreas Kunzmann, Sven Uthicke, Christian Wild
Effects of high dissolved inorganic and organic carbon availability on the physiology of the hard coral *Acropora millepora* from the Great Barrier Reef

The design of this study was developed by F. W. Meyer and N. Vogel with the support of C. Wild. F. W. Meyer and N. Vogel carried out the laboratory experiment and analysed the samples and data. The manuscript was written by Friedrich W Meyer, Nikolas Vogel, Karen Diele, Andreas Kunzmann, Sven Uthicke and Christian Wild. The manuscript has been submitted to PLOS ONE.

Article 3)

Friedrich Wilhelm Meyer, Nikolas Vogel, Mirta Teichberg, Sven Uthicke, Christian Wild

The Physiological Response of Two Green Calcifying Algae From the Great Barrier Reef Towards High Dissolved Inorganic and Organic Carbon (DIC and DOC) Availability

The design of this study was developed by F. W. Meyer and N. Vogel with the support of C. Wild. F. W. Meyer and N. Vogel carried out the laboratory experiment and analysed the samples and data.

The manuscript was written by Friedrich Wilhelm Meyer, Nikolas Vogel, Mirta Teichberg, Sven Uthicke and Christian Wild. The manuscript has been accepted in PLOS ONE.

Article 4)

Friedrich W Meyer, Nadine Schubert, Karen Diele, Mirta Teichberg, Christian Wild and Susana Enríquez

Effects of high dissolved organic carbon (DOC) and high dissolved inorganic carbon (DIC) on photosynthesis and calcification in two calcifying green algae from a Caribbean reef lagoon

The collaboration between ZMT and the partners at the Instituto de Ciencias del Mar y Limnología, Mexico was initiated by C. Wild. The design of the study was development by Friedrich W Meyer, Nadine Schubert, Karen Diele, Mirta Teichberg, Christian Wild and Susana Enríquez. The experiment was performed and analysed by Friedrich W Meyer and Nadine Schubert. The manuscript was written by Friedrich W Meyer, Nadine Schubert, Karen Diele, Mirta Teichberg, Christian Wild and Susana Enríquez. The manuscript is in preparation for submission to PLOS ONE.

Article 5)

Andre Wizemann, **Friedrich W. Meyer,** Hildegard Westphal

A new model for the calcification of the green macro-alga *Halimeda opuntia* (Lamouroux)

The idea of this study was developed by Andre Wizemann and Friedrich W. Meyer. Andre Wizemann and Friedrich W. Meyer carried out the laboratory experiment and A Wizemann analysed the data. The manuscript was written by Andre Wizemann, Friedrich W. Meyer, Hildegard Westphal. The manuscript has been published in Coral Reefs, DOI: 10.1007/s00338-014-1183-9

Article 6)

N. Vogel1, **F. W. Meyer,** C. Wild, S. Uthicke

Decreased light availability can amplify negative impacts of ocean acidification on calcifying coral reef organisms

The design of this study was developed by F. W. Meyer and N. Vogel with the support of C. Wild. F. W. Meyer and N. Vogel carried out the laboratory experiment and analysed the samples and data.

The manuscript was written by Nikolas Vogel, Friedrich W Meyer, Sven Uthicke and Christian Wild. The manuscript has been published in Marine Ecology Progress Series, DOI: 10.3354/meps11088

Article 7)

Andre Wizemann, Friedrich W. Meyer, Laurie C. Hofmann, Christian Wild, Hildegard Westphal

Ocean acidification alters the calcareous microstructure of the green macro-alga *Halimeda opuntia*

The publication was initiated by Andre Wizemann and Friedrich W. Meyer. Andre Wizemann and Friedrich W. Meyer carried out the laboratory experiment and A Wizemann analysed the data. Additional data and ideas were provided Laurie C. Hofmann. The manuscript was written by Andre Wizemann, Friedrich W. Meyer, Laurie C. Hofmann, Christian Wild and Hildegard Westphal. The manuscript has been published in Coral Reefs, DOI: 10.1007/s00338-015-1288-9

Article 8)

Nils Rädecker, **Friedrich W. Meyer**, Vanessa N. Bednarz, Ulisse Cardini, Christian Wild

Ocean acidification rapidly reduces dinitrogen fixation associated with the hermatypic coral Seriatopora hystrix

The idea of this study was developed by Nils Rädecker and Christian Wild. Nils Rädecker and Friedrich W. Meyer carried out the laboratory experiment with help from Vanessa N. Bednarz, Ulisse Cardini. Nils Rädecker analysed the samples and data with the help of Friedrich W. Meyer, Vanessa N. Bednarz and Ulisse Cardini. The manuscript was written by Nils Rädecker, Friedrich W. Meyer, Vanessa N. Bednarz, Ulisse Cardini and Christian Wild. The manuscript has been published in Marine Ecology Progress Series, DOI: 10.3354/meps10912

1 - Ocean acidification and related indicators

Friedrich W. Meyer*, Ulisse Cardini, and Christian Wild

Coral Reef Ecology Group (CORE), Leibniz Center for Tropical Marine Ecology (ZMT), Fahrenheitstr. 6, D-28359 Bremen, Germany

*corresponding author

The book chapter has been published at Springer, DOI: 10.1007/978-94-017-9499-2_41

Abstract

Ocean acidification is one of the main consequences of global climate change. It is caused by the increasing input of atmospheric CO_2 in the world ocean, which in turn is affecting the marine carbonate system and resulting by now in a measurable decline in seawater pH. Thus, several key water quality parameters (alkalinity, partial pressure of CO_2, concentration of dissolved inorganic carbon - DIC, and the seawater pH) serve as environmental indicators for ocean acidification. In addition, many pelagic and benthic marine organisms, particularly those that are calcifying, negatively or positively respond to acidification so that their physiological parameters (calcification, photosynthesis, growth) may also act as indicators of this phenomenon. On the ecosystem level, potential environmental indicators for acidification can be found in the sedimentary record (mineralogy, crystallography), in the benthic community (relative abundance of calcifying versus non-calcifying organisms, rugosity), or in the overall production, cementation, and erosion of inorganic carbon.

Keywords: carbonate chemistry, eutrophication, photosynthesis, calcification, Palaeocene-Eocene Thermal Maximum, saturation horizons, cementation, coral

41.1 Introduction

As fossil fuel emissions grow at an alarming rate, earth's climate is changing and temperatures are rising due to the increased concentration of greenhouse gasses. Carbon Dioxide (CO_2), one of the most significant greenhouse gases, also leads to another problem: the so-called ocean acidification (OA). In this chapter, we refer to three sections where we select the main environmental parameters that serve as short and long term identifiers of ocean acidification from the early signs, and the organism level to the ecosystem level.

In the first section, we define the term OA and describe its causes and its detection in seawater. We also compare present and past acidification events in the Earth's history. We move along with a summary on the worldwide distribution of OA with an emphasis on most affected regions, while suggesting indicators that can be used to detect short- and long-term changes in seawater carbonate chemistry.

In the second section of this chapter, we outline the most important physiological processes affected by OA and identify which parameters can potentially serve as indicators. Coral reef ecosystems are found in areas of naturally lower intensity of ocean acidification (see section 41.2.3). While providing ecosystem services for billions of people, at the same time they are being affected by the strongest human pressure through overpopulation, exploitation, and habitat destruction. Therefore, we decided to focus on the effects of OA in these systems, as their study and conservation should be of the highest priority for the above mentioned reasons (see also section 41.4.3). During the description of physiological processes, we focus mainly on coral reef benthic communities and refer to related work in temperate and Polar Regions, for which knowledge on coral reef species is scarce. We then distinguish between short- and long-term effects on organisms' physiology and identify the processes that lead to changes in community composition. By comparing present and predicted alterations in community composition with geological and sedimentary records, we identify indicators on the community composition level. Changes in productivity and shifts in carbon cycling are then discussed as potential indicators of acidification. Ultimately, the effects of OA on the ecosystem level and possible related indicators are discussed.

In the third section, we summarize the outcomes of previously employed OA indicators and provide an outlook on the future expected performance of organisms, communities and ecosystems. We finally conclude the chapter by suggesting priority fields for future research to elucidate management strategies for ocean acidification.

41.2 Definition, causes and distribution of ocean acidification

41.2.1 The 'Other CO_2 Problem' and its effects on the ocean carbonate system

Ocean acidification is a term commonly used to describe the changes in the seawater carbonate chemistry deriving from the ocean uptake of anthropogenic CO_2 from the atmosphere. Since global warming and ocean acidification are both caused by increasing atmospheric CO_2, acidification is commonly referred to as the 'other CO_2 problem' (Doney et al. 2009).

CO_2 in the atmosphere equilibrates with surface water through air-sea gas exchange within a timescale of approximately one year (Doney et al. 2009). Once dissolved, CO_2 gas reacts with water to form carbonic acid (H_2CO_3), which dissociates by losing hydrogen ions (H^+) to form bicarbonate (HCO_3^-) and carbonate (CO_3^{2-}) ions:

$$CO_{2(atm)} \leftrightarrow CO_{2(aq)} + H_2O \leftrightarrow H_2CO_3 \leftrightarrow H^+ + HCO_3^- \leftrightarrow 2H^+ + CO_3^{2-} \quad (1.1)$$

These reactions are reversible and near equilibrium (Millero et al. 2002). Accumulating CO_2 in the oceans alters the seawater carbonate chemistry, increasing aqueous CO_2, bicarbonate, and hydrogen ion concentrations, with the latter lowering pH. On the other hand, carbonate ion concentration declines. This, in turn, cause a decrease in the saturation state (Ω) of calcium carbonate ($CaCO_3$), which is directly dependent on the concentration of dissolved carbonate ions:

$$\Omega = [Ca^{2+}]\,[CO_3^{2-}]/K'_{sp} \quad (1.2)$$

Calcium carbonate occurs in two common polymorphs, calcite and aragonite, the latter being approximately 50% more soluble than calcite (Mucci 1983). In seawater, a natural horizontal boundary is formed as a result of temperature, pressure, and depth, known as the (aragonite or calcite, respectively) saturation horizon (Raven et al. 2005), which represents the transition depth between the supersaturated upper ocean ($\Omega > 1.0$) and the undersaturated deep ocean ($\Omega < 1.0$).

Increasing CO_2 levels (and the resulting lowering in pH and carbonate ion concentration) decreases the saturation state of $CaCO_3$ and raises the saturation horizons of both its mineral forms closer to the surface. This is an important threshold for marine calcifying organisms since $CaCO_3$ deposition generally occurs at $\Omega > 1.0$, while its dissolution occurs at $\Omega < 1.0$ (Fig. 41.1). However, reduced calcification rates following acidification occur for a variety of calcareous organisms even at $\Omega < 1.0$

(Ries et al. 2009). Aside from the slowing and/or reversing of calcification, organisms may suffer several other adverse effects, either indirectly through negative impacts on food resources or directly as reproductive or physiological effects (see Sect. 1.2).

Moreover, a decrease in seawater buffer capacity will arise as a result of the dissolution of anthropogenic CO_2 and the following increase in Dissolved Inorganic Carbon (sum of the dissolved carbonate species, denoted as DIC), causing much greater sensitivity to local variations in DIC and Total Alkalinity (TA) (Egleston et al. 2010). This is posing another threat to marine life, especially in shallow coastal environments in which high biological productivity drives the large natural variability in carbonate chemistry that will be amplified as the buffer capacity of the ocean will decrease (Shaw et al. 2013; see Section 41.3).

The solution chemistry of carbon dioxide in the seawater can be easily calculated and monitored by measuring any two of its four main parameters (TA, DIC, pH , and CO_2 partial pressure (pCO_2)) for a given boron concentration, temperature, salinity, and pressure. This can therefore be used as an effective environmental indicator of ocean acidification, allowing us to detect and investigate regional and local trends. Several Standard Operating Procedures regarding the measurement of each parameter are listed in Dickson et al. (2007), while Riebesell et al. (2010) provide a useful baseline for ocean acidification research and data reporting.

41.2.2 Past acidification events in Earth history compared to present phenomenon

The earth already experienced episodes that involved geologically 'rapid' (<10,000 yrs) changes of ocean carbonate chemistry, such as the Palaeocene-Eocene Thermal Maximum (PETM, ~55 Myr), during which global surface temperatures increased by 5 to 9˚C within a few thousand years (Sluijs et al. 2006; Zachos et al. 2003) and a substantial carbon release occurred, leading to ocean acidification and dissolution of deep-sea carbonates (Ridgwell and Schmidt 2010; Zachos et al. 2005; Zeebe et al. 2009). However, the present rate of carbon input is greater than during any of the geological ocean acidification events identified so far, including the PETM (Riebesell et al. 2010). A recent investigation provided further evidence that the current rate of ocean acidification is faster than at any time in the past 300 million years, and it is occurring at almost 10 times the rate of acidification experienced by the oceans during the PETM (Hönisch et al. 2012). Historically, sustained periods of acidification and CO_2 increase - which were similar, but not as extreme as in the last 1,000 years - have led to the collapse of coral reefs and, in one instance, to the extinction of 96% of marine life (Hönisch et al. 2012).

There is little doubt concerning the link between anthropogenic emissions and ocean acidification, since the current anthropogenic trend already exceeds the level of natural variability by up to 30 times

on regional scales (Friedrich et al. 2012). These results are further verified by hydrographical surveys and time series data (Doney et al. 2009; Dore et al. 2009; Feely et al. 2008; Wootton et al. 2008) that show a direct correlation between rates of increase in surface water pCO_2 and atmospheric CO_2 (Dore et al. 2009), thereby indicating uptake of anthropogenic CO_2 as the major cause for the observed long-term increase in Dissolved Inorganic Carbon (DIC) and decrease in $CaCO_3$ saturation state.

Over the past 250 years, atmospheric CO_2 levels increased by more than 40% from pre-industrial levels of approximately 280 parts per million by volume (ppmv) to 393 ppmv in 2012 (Tans and Keeling 2013). The rate of increase, driven by human fossil fuel combustion and deforestation, was about 1.0% yr^{-1} in the 1990s and reached 3.4% yr^{-1} between 2000 and 2008 (Le Quéré et al. 2009). About one third of the carbon dioxide released by humans into the atmosphere dissolves into the oceans (Sabine et al. 2004).

Since the beginning of the industrial revolution, surface ocean waters have already experienced a 0.1 pH drop or more (representing an approximately 29% increase in H^+), and a further 0.3 – 0.4 pH drop is projected for the end of the 21st century as the oceans absorb more anthropogenic CO_2 (equivalent to approximately a 150% increase in H^+ and 50% decrease in CO_3^{2-} concentrations) (Solomon et al. 2007).

Recently, several trace-element and isotopic tools have become available which have been applied as environmental indicators to study and compare past and present acidification events. It is possible to trace changes in seawater pH through the boron isotopic composition ($\delta^{11}B$) of marine carbonates, to estimate surface ocean aqueous [CO_2] using the stable carbon isotopic composition ($\delta^{13}C$) of organic molecules, and to reveal ambient [CO_3^{2-}] by means of the trace element (such as B, U, and Zn)–to-calcium ratio of benthic and planktonic foraminifer shells (Hönisch et al. 2012).

The assessment of past acidification events through geological records is essential to understand and predict the unknown territory of marine ecosystem change that we are facing. Hence, future studies will have to apply the available tools in order to expand geochemical estimates and reduce uncertainties of past ocean carbonate chemistry and ecological changes.

41.2.3 Regional variability of acidification in the world ocean

Saturation states are highest in shallow, warm tropical waters and lowest in cold high-latitude regions and increasing water depths, reflecting the increase in $CaCO_3$ solubility with decreasing temperature and increasing pressure (Feely et al. 2004). Since high-latitude regions have naturally low carbonate ion concentrations and higher CO_2 solubility, these will be the first regions affected by ocean

acidification and by undersaturated surface waters (Fig. 41.1) (Fabry 2009). Recent investigations showed that areas of aragonite undersaturation already exist in some Northern Polar Seas (Bates and Mathis 2009; Yamamoto-Kawai et al. 2009). Surface waters of the Southern Ocean, Arctic Ocean, and parts of the subarctic Pacific will become undersaturated with respect to aragonite by the end of this century if the current CO_2 emission rates are not mitigated (Orr et al. 2005; Steinacher et al. 2009).

Moreover, anthropogenic CO_2 penetration into the ocean has been concentrated in the upper thermocline (Sabine et al. 2004), which determined the shoaling of saturation horizons by 30–200 m from the pre-industrial period to the present. As a consequence, deep-sea regions will also be soon affected by ocean acidification and undersaturated waters, as the saturation horizons become shallower.

Although major changes are expected to occur only in the future, a recent report already found large quantities of upwelling water undersaturated in aragonite close to the Pacific continental shelf area of North America, a condition that was not predicted to occur in open ocean surface waters until 2050 (Feely et al. 2008). Much of the corrosive character of these waters is due to respiration processes occurring below the euphotic zone. However, in the absence of the anthropogenic signal, the aragonite saturation horizon would have been deeper, and no undersaturated waters would have reached the surface (Feely et al. 2008). Thus, these events are likely to occur more frequently and in the near future, because of the additional inputs of anthropogenic CO_2, exposing continental shelves and their benthic communities to acidified conditions.

Other peculiar point-source environments of low-pH waters are also used as natural laboratories to help unravel the ecosystem-level effects of ocean acidification. These are natural pH gradients, caused by the volcanic vents of CO_2-rich gases or by low-pH, low carbonate saturation groundwater springs, which have been exploited to investigate how species, communities, and ecosystems react to acidified conditions in a natural environment. Most studied are the ones in Italy (Hall-Spencer et al. 2008), Greece (Vizzini et al. 2010), Papua New Guinea (Fabricius et al. 2011; Uthicke et al. 2013), and Mexico (Crook et al. 2013; Crook et al. 2011).

Natural pH gradients, as well as high-latitudes or deep and upwelling areas of the oceans, are presently undergoing large and rapid changes in seawater carbonate chemistry. Therefore, their investigation may help in understanding ocean acidification effects on physiological processes, potential acclimation, and adaptation strategies and future impacts at the population, community, and regional scales. This in turn may provide essential environmental indicators in the form of biological processes, species, or communities that, because of their moderate tolerance to pH and pCO_2 variability, can be effectively used to assess the quality of the environment and how ocean acidification changes over space and time (see Section 41.3).

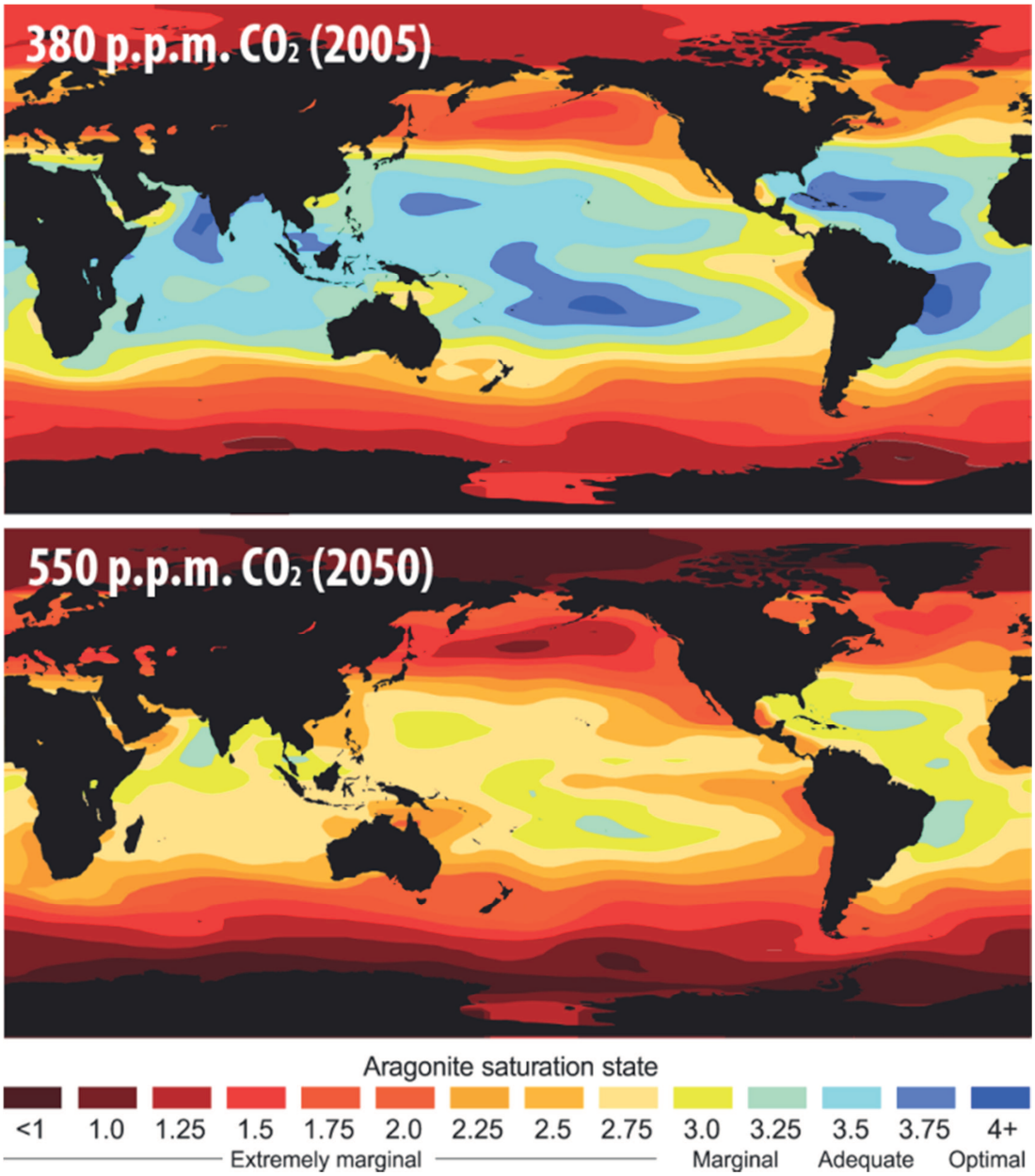

Fig. 41.1 Model showing expected changes in the surface oceans' aragonite saturation state by 2050 due to anthropogenic CO_2 emissions. Modified from Schiermeier (2011).

41.3 Impact on the physiological parameters of organisms and ecosystems

The impacts of OA on the organisms' level have been studied intensively and a vast amount of literature is available for polar, temperate (see reviews by Riebesell et al. 2010; Gattuso and Hansson 2011), and tropical regions. In this section, we concentrate on the effects of OA in tropical regions and in particular on coral reefs and their related benthos, as these represent some of the most productive areas of the world's oceans, which provide a multifarious range of ecosystem services. As coral reefs are located in areas of naturally low acidification (please refer to section 41.2.3), they should be the focus of management and conservation strategies. Furthermore, these areas are amongst the most populated worldwide, and the immense population pressure brings a potential cumulative effect, such as eutrophication, with it (please refer to section 41.4.1). Therefore, the identification of indicators for upcoming acidification in coral reefs is especially needed.

41.3.1 Calcification

Due to the shift in the carbonate system and the lowering of the carbonate saturation state, one of the most apparent indicators of OA on the organism level is the change in calcification. As the forms of carbonate, as well as the calcifying mechanisms, differ across taxa, the response toward OA can vary. However, the most dominant observation is a loss in calcification rate or alteration of calcification structure with increasing OA conditions. This can be observed for temperate and polar species living in the areas most susceptible to OA (Cerrano et al. 2013; Comeau et al. 2012; Fabry et al. 2008; Feely et al. 2004; Hoppe et al. 2011). Many studies on tropical calcifiers, such as corals, calcifying algae, molluscs, echinoderms, and crustaceans, indicate similar effects of OA.

41.3.2 Corals

Corals form the basis and structure of coral reefs. They provide habitat and primary productivity for one of the world's most diverse ecosystems. First results revealed that a reduced pH due to the increase of atmospheric pCO_2 impairs the ability of corals to calcify (Anthony et al. 2008; Krief et al. 2010). The overall trend of reduced calcification has also been identified in many other experiments (Jokiel et al. 2008; Marubini et al. 2008; Marubini et al. 2003), which was also confirmed in field studies (Fabricius et al. 2011; Manzello and Kleypas 2008). Moreover, corals seem to be able to influence the carbonate chemistry on a small scale within their tissues and on a larger scale in the whole reef community. It has been shown that corals are able to elevate the pH of water close to and within their tissue by 0.2 to 0.5 (Venn et al. 2011), and due to calcification activity they modify seawater pCO_2 and alkalinity even downstream of their habitat (Kleypas et al. 2011). Asymbiotic cold

water corals show more pronounced responses toward OA, and a decrease of calcification and reduced distribution can be found along natural pH gradients (Jantzen et al. 2013; Maier et al. 2012).

41.3.3 Algae

Calcifying algae, mainly crustose coralline algae (CCA), play an important role in a reef ecosystem as they strengthen the coral reef framework. Recent studies found that CCAs seem to be the most susceptible to dissolution and productivity loss under OA conditions (Anthony et al. 2008; Kuffner et al. 2007; Martin and Gattuso 2009). Similar results were observed in experiments with *Halimeda* (Price et al. 2011; Robbins et al. 2009), an algae providing important microhabitats and contributing to substrate/sediment production (Drew 1983; Jinendradasa and Ekaratne 2002; Mussaka et al. 2001). Specimens of Halimeda incubated for 3 weeks under pH of 7.5 showed reduced inorganic carbon contents and increased organic carbon contents, suggesting reduced calcification, while high productivity was maintained. The same holds true for other calcifying micro and macro algae (Langer et al. 2006; Martin and Gattuso 2009; Ries et al. 2009) and the results are also supported by recent field data from natural vent sites (Fabricius et al. 2011; Johnson et al. 2012; Porzio et al. 2011).

41.3.4 Other benthic invertebrates

Little is known about the impact of OA on gastropods in tropical reefs. Overall, calcification rates of adult *Littorina* and the whelk *Urosalpinx cinerea* decrease with increasing OA conditions (Ries et al. 2009). Crabs can play an important ecological role by reducing epiphyte growth on corals and calcifying algae (Coen 1988; Stachowicz and Hay 1999; Stachowicz and Hay 1996), as well as by influencing nutrient cycling and ecosystem health with their grazing, omnivorous, detritivorous or scavenging behaviour. Nevertheless, studies on brachyuran crabs and the impacts of OA are rare. A few studies on adult crabs suggest a lowered thermal tolerance of the spider crab *Hyas araneus* under OA conditions (Walther et al. 2009), while other species, such as the swimming crab *Necora puber*, showed a high compensation capability under strong (pH 6.74) OA conditions (Spicer et al. 2006). The high capacity to calcify under OA conditions and even the increased rate of calcification were unexpected results of studies on these organisms (Ries et al. 2009). Overall data on groups of benthic invertebrates from temperate regions show negative yet variable effects on the adults as well as on their reproduction and larval development.

41.3.5 Photosynthesis, respiration and other metabolic processes

With an increase in bicarbonate ions and a decreased pH, the substrate availability and the medium for many fundamental metabolic processes change under OA. Depending on the organism, different effects on these processes are observed.

41.3.5.1 Corals

The increase of CO_2 as a substrate for photosynthesis by coral symbiotic algae resulted in an increased productivity, although CO_2 concentrations above 1000 ppmv resulted in productivity loss (Anthony et al. 2008). Isotopic and physiological measurements showed that, while calcification and zooxanthellae density decreased under OA conditions, coral tissue biomass and chlorophyll density increased (Krief et al. 2010), possibly compensating for the decreased photosynthetic capacity (Crawley et al. 2010). The impact of OA on the coral holobiont (i.e., the community of coral host and associated microorganisms) has just recently been addressed, and the first results suggest a drastic change in microbial composition on the coral mucus, tissue, and skeleton under OA conditions (Meron et al. 2011).

41.3.5.2 Algae

For CCAs, not only their calcification, but also the photosynthetic rate are negatively influenced under OA (Semesi et al. 2009). In contrast to calcifying algae, which are strongly affected, fleshy non calcifying algae and sea grasses flourish under OA conditions (Fabricius et al. 2011; Porzio et al. 2011) as the additional CO_2 acts as substrate for photosynthesis. Moreover, the decline in grazers and in calcifying epiphytes increases algae development (Hall-Spencer et al. 2008). Similar results can be observed for pelagic microalgae from tropical to polar regions, which show higher productivity under OA resulting from a higher uptake of CO_2 and consequently a higher build-up of organic material (Riebesell et al. 2007; Tortell et al. 2008). This leads to a higher organic material transfer to deeper waters, eventually leading to higher oxygen consumption rates and oxygen deficiencies (Hofmann and Schellnhuber 2009; Riebesell et al. 2007). This may in turn affect the biological pump in the open ocean (i.e., the fixation of inorganic carbon and its transport from the productive zone to the ocean interior), which eventually determine the fate of increased atmospheric CO_2 (Garrard et al. 2012).

41.3.5.3 Other benthic invertebrates

Many studies show that echinoderms are affected mainly by an altered acid base regulation. Adult sea urchins of the species *Strongylocentrotus dröebachiensis* and *Psammechinus miliaris* show poor ion regulation under OA conditions and uncompensated respiratory acidosis (Miles et al. 2007; Spicer et al. 2006). The species *Arbacia punctulata* and *Eucidaris tribuloides* showed a negative or no response in calcification to OA, respectively (Ries et al. 2009).

41.3.6 Reproduction and recruitment

41.3.6.2 Corals

Studies on the embryology and juvenile development of corals showed that fertilization success, larval metabolic rates, and settlement rates are inhibited under OA conditions (Albright 2011). Both *Porites asteroides* and *Acropora palmata* suffered from reduced settlement rates and the number of corals settlers was estimated to be reduced to up to 73% (Albright et al. 2010). As revealed by Fabricius et al. (2011), adults of the massive coral of the genus *Porites* are less susceptible to OA than others (such as tabulate corals), although the recruitment of juveniles was low. Another study found a growth rate reduced by up to 78% in the early post settlement stage of *Porites asteroides* (Albright et al. 2008). A delay in the establishment of symbiosis, combined with a reduced growth of *Acroporid* corals, was also observed (Suwa et al. 2009). In addition, a suppressed metamorphosis rate for *Acropora digitifera* was described (Nakamura et al. 2011). These studies demonstrate that juveniles of corals seem to be even more directly affected by OA than their adult stage counterparts, as they suffer from mortality and decreased recruitment rates. Their recruitment success and early developmental stages can therefore act as an indicator of OA. However, adult corals seem to be also heavily affected. When other factors interacting with OA (such as increased nutrients or reduced grazing pressure) are present, this may lead to a transition from a coral- to an algae-dominated reef (Hoegh-Guldberg et al. 2007).

41.3.6.3 Algae

While the recruitment of CCAs was found to be reduced in a mesocosm study (Kuffner et al. 2007), little is known about the impact of OA on the reproduction of macroalgae. OA has not only direct effects on the coralline algae but also indirect negative effects on their interaction with coral larvae, for which they serve as a settlement substrate, eventually resulting in a reduced survival rate of the coral recruits (Doropoulos et al. 2012). On the other hand, in microalgae, higher productivity under OA leads to higher growth rates (Hofmann and Schellnhuber 2009; Tortell et al. 2008). Due to their short generation time, first evidence suggests that microalgae can adapt in a short period of time (Lohbeck et al. 2012).

41.3.6.4 Other benthic invertebrates

Larval development of sea urchins under OA conditions is more intensively investigated than the effects of OA on their adult stage, and shows mainly a reduced fertilisation rate (Byrne et al. 2010; Havenhand et al. 2008; Havenhand and Schlegel 2009). When exposed to OA, sea urchin larvae showed a reduced ability to react to thermal stress (O'Donnell et al. 2008), development delay (Catarino et al. 2011), reduced calcification and growth, and increased metabolic rate (Stumpp et al. 2012). In summary, sea urchins studied so far are negatively impacted by OA during their larval as well as during their adult stages. Impacts of OA include decreased somatic growth and development as well as decreased calcification. Research addressing the effects of OA on sea stars show a conflicting picture as both increased growth and larval survival has been observed under OA conditions (Dupont et al. 2010; Gooding et al. 2009; Schram et al. 2011). Studies focusing on gastropods investigated the effect of OA on the Abalone *Haliotis discus*, *Haliotis kamtschatkana* and the intertidal gastropod *Littorina littorea.* In the Abalone, fertilization, survival, and hatching rate were negatively affected, while the rate of malformation during larval development increased under OA conditions (Crim et al. 2011; Kimura et al. 2011). *Littorina littorea* produced thinner shells when exposed to OA conditions and at the same time showed an increase in predator avoidance behaviour (Bibby et al. 2007). Results comparable with those for *Haliotis sp.* were obtained for the larval development of other mollusc species reared under OA conditions. For example, blue mussels of the genus *Mytilus* showed a higher rate of abnormal development, smaller larval sizes, and a lower hatching rate (Gazeau et al. 2010; Kurihara et al. 2008). Seedlings of the clam *Ruditapes decussates* exhibited reduced feeding rates, clearance, and ingestion rates, as well as respiration rates, under OA conditions (Fernández-Reiriz et al. 2011). A recent study on the oyster *Crassostrea gigas* again revealed similar responses with regard to their larval development (Gazeau et al. 2011), although their sperm motility was not affected (Havenhand and Schlegel 2009). Interestingly, larvae of oysters pre-acclimatized to OA conditions reacted differently. Their size, development rate, and survival rate were similar to those of larvae from adults exposed to ambient pCO_2 (Parker et al. 2011).

Studies available on larvae and adults of crustaceans are also scarce. For the larvae of the lobster *Hommarus americanus*, no reduction in carapace mass, survival, or development rate was observed (Arnold and Findlay 2009). In contrast, larvae of the spider crab *Hyas araneus* reared under OA conditions and elevated temperatures showed delayed metamorphosis, lower survival rates, and a reduction in calcium incorporation as compared to larvae reared at ambient temperature and pH. This effect was more pronounced for larvae of adults living in cold habitats as compared to larvae of adults from warmer habitats (Walther et al. 2011; Walther et al. 2010). In summary, little is known about the effect of OA on crabs and their larvae. It seems that their calcification is little affected; however, comparative measurements of tropical reef species are still missing.

41.3.7 Effects of ocean acidification on the ecosystem level

If we are to understand the potential effects of OA in the global oceans, it is fundamental to scale up the scientific questions to the ecosystem level, therefore taking into consideration a complex array of both biotic and environmental interactions (Garrard et al. 2012).

Mesocosm experiments are used in order to study not only species-specific responses, but also the effects on the community. Data of calcification rates of entire communities reflect well the species-specific and show a decrease of community calcification with increasing OA (Kuffner et al. 2007; Langdon 2003; Leclercq et al. 2002). In contrast to calcification, the net production of the system did not change (Leclercq et al. 2002). Similar observations were made using a natural pH gradient at a field site in the Mediterranean (Hall-Spencer et al. 2008). These findings agree with field observations from another natural volcanic CO_2 vent site in which massive *Porites* colonies dominated the community, with a loss in the 3D structure of the system (Fabricius et al. 2011). At the same time, also bioeroder abundance was elevated, supporting other findings predicting higher bioeroding rates under future OA conditions (Reyes-Nivia et al. 2013; Wisshak et al. 2012). In accordance with the findings for the whole coral community (as named above), also the productivity on the microbial scale did not change under different OA conditions (Witt and Wild 2011). In contrast, the bacterial community did react fast, and an increased abundance of several bacterial species, such as *Alphaproteobacteria* and *Flavobacteriales*, may serve as microbial indicators of OA-induced community changes (Witt and Wild 2011).

In summary, the species-specific response in calcification rate and the high abiotic erosion rates observed under OA conditions (Manzello and Kleypas 2008) suggest that the net ecosystem calcification rate may serve as a good indicator for OA. This indicator, together with measures of pCO_2 and alkalinity, could be used as a monitoring device for community and ecosystem change (Andersson and Gledhill 2013). As for benthic communities, measures of rugosity and cementation rates can be used as convenient indicators of OA impacts. In some cases, such measures already reflect the effects of OA in upwelling areas (Manzello and Kleypas 2008).

Good indicators of OA on the community level in coral reefs are a decreased carbonate accretion rate due to increased erosion, and a loss in biodiversity and structural complexity. In addition, a decrease in hard coral cover, CCAs, calcified invertebrates, and weak framework cementation, as well as an increase in sea grass and non-calcified algae abundance, may serve as biological indicators of increasing OA conditions.

41.4 Outlook

41.4.1 How can acidification interact with other regional or local stressors?

In the future, the world's marine ecosystems will likely be simultaneously affected by a range of global stressors, such as acidification and warming, which will interact with a range of local factors, particularly eutrophication (e.g. Voss et al. 2013).

Literature is lacking with regard to the potential interaction of ocean acidification and eutrophication, but there is some indication that acidification may affect the bioavailability of essential nutrients in the marine realm (Shi et al. 2010). A potentially relevant surplus source of acidification comes from the anthropogenic inputs of nutrients in the coastal waters of the world oceans (Cai et al. 2011). Human activities, such as the use of chemical fertilizers, the discharge of human and animal wastes, and the inputs of oxides of nitrogen (NO_x) from fossil fuels burning, have increased the concentrations of inorganic nutrients and fuelled massive algal blooms in many coastal areas (Howarth et al. 2011). This pronounced marine eutrophication may stimulate ocean acidification via facilitation of CO_2 uptake by phytoplankton. In addition, microbial consumption of the organic matter produced by phytoplankton depletes bottom waters of oxygen (O_2) and releases CO_2, in turn increasing seawater acidity (Sunda and Cai 2012). Therefore, eutrophication and the related increase in bottom water CO_2 concentrations may exacerbate ocean acidification in coastal waters.

Knowledge about the interaction between such global and local factors and their consequences for the ecosystem functioning is scarce, but a few studies indicate cumulative aggravating effects (e.g. Lloret et al. 2008). Future research should, however, concentrate on these aspects.

41.4.2 Recommendation for a system of indicators

A good system of indicators for OA should include a range of indicators of status and process that simultaneously characterize the water chemistry and effects on marine organisms and ecosystems. These indicators may benefit from a combination of measurements of seawater temperature, pH, and alkalinity (status parameters) on the one hand, and quantification of calcification rates and oxygen fluxes (process parameters) of key pelagic (e.g., coccolitophores) and benthic (e.g., corals, sea urchins, and calcifying algae) marine organisms on the other hand. As a supplementation, sedimentary carbonate contents and benthic rugosity (status parameters), along with benthic community changes (process parameter), may be used in order to contribute to the understanding of the consequences of OA on the ecosystem. Such a suggested system of indicators would have a good ratio between sampling effort and information outcome. It should be implemented best in a comparative way using

identical methodology in an appropriate temporal and spatial resolution at several locations of particular interest.

41.4.3 How can management target ocean acidification?

Science-based management of marine coastal ecosystems and their resources considers the interaction of global as well as local factors (refer to section above). This may be achieved through the use of appropriate systems of indicators, as suggested in the preceding section.

An urgent need is to assess the impacts of ocean acidification on the ecosystems. The understanding of the effects of ocean acidification on the interaction among different biotic components and on marine ecosystems is still limited (Fabry et al. 2008; Hall-Spencer et al. 2008). It is particularly important to evaluate possible negative socio-economic impacts that are reflected in decreases in ecosystem services, such as productivity, provisioning of associated biodiversity, and coastal protection (please refer to related publications on coral reefs: Moberg and Folke 1999; Wild et al. 2011).

As for ocean warming, there are no direct management measures for ocean acidification, because it is not feasible to isolate marine ecosystems against these global effects in their medium, the seawater.

However, as ocean acidification is predicted to increase in the mid-term under all IPCC scenarios, conservation priorities should include those areas that exhibit a naturally lower intensity of acidification, such as shallow tropical areas, which at the same time provide many ecosystem services and are among the densest populated areas in the world (for regional differences in ocean acidification please see section 41.2.3). These areas could be protected at least against local stressors, such as overfishing and eutrophication, that act simultaneously with global factors, such as acidification.

Ocean acidification itself may be reduced by all general measures that limit CO_2 emissions. In addition, methods such as carbon capture or sequestration are discussed, but such elaborate and technically expensive measures, which require extensive development and trials, should rather be considered as symptomatic treatment and not as a sustainable management strategy against ocean acidification.

References

Albright R (2011) Effects of Ocean Acidification on Early Life History Stages of Caribbean Scleractinian Corals. Univ. Miami Sch. Repos.

Albright R, Mason B, Langdon C (2008) Effect of aragonite saturation state on settlement and post-settlement growth of *Porites astreoides* larvae. Coral Reefs 27:485–490. doi: 10.1007/s00338-008-0392-5

Albright R, Mason B, Miller MW, Langdon C (2010) Ocean acidification compromises recruitment success of the threatened Caribbean coral *Acropora palmata*. Proc Natl Acad Sci 107:20400-20404. doi: 10.1073/pnas.1007273107

Andersson AJ, Gledhill D (2013) Ocean acidification and coral reefs: effects on breakdown, dissolution, and net ecosystem calcification. Ann Rev Mar Sci 5:321–348. doi: 10.1146/annurev-marine-121211-172241

Anthony KRN, Kline DI, Diaz-Pulido G, Dove SG, Hoegh-Guldberg O (2008) Ocean acidification causes bleaching and productivity loss in coral reef builders. Proc Natl Acad Sci U S A 105:17442–17446. doi: 10.1073/pnas.0804478105

Arnold K, Findlay H (2009) Effect of CO_2-related acidification on aspects of the larval development of the European lobster, *Homarus gammarus* (L.). Biogeosciences 6:1747–1754.

Bates NR, Mathis JT (2009) The Arctic Ocean marine carbon cycle: evaluation of air-sea CO_2 exchanges, ocean acidification impacts and potential feedbacks. Biogeosciences 6:2433–2459. doi: 10.5194/bg-6-2433-2009

Bibby R, Cleall-Harding P, Rundle S, Widdicombe S, Spicer J (2007) Ocean acidification disrupts induced defences in the intertidal gastropod *Littorina littorea*. Biol Lett 3:699–701. doi: 10.1098/rsbl.2007.0457

Byrne M, Soars N, Selvakumaraswamy P, Dworjanyn S a, Davis AR (2010) Sea urchin fertilization in a warm, acidified and high pCO_2 ocean across a range of sperm densities. Mar Environ Res 69:234–239. doi: 10.1016/j.marenvres.2009.10.014

Cai W-J, Hu X, Huang W-J, Murrell MC, Lehrter JC, Lohrenz SE, Chou W-C, Zhai W, Hollibaugh JT, Wang Y, Zhao P, Guo X, Gundersen K, Dai M, Gong G-C (2011) Acidification of subsurface coastal waters enhanced by eutrophication. Nat Geosci 4:1–5. doi: 10.1038/ngeo1297

Catarino AI, Ridder C, Gonzalez M, Gallardo P, Dubois P (2011) Sea urchin *Arbacia dufresnei* (Blainville 1825) larvae response to ocean acidification. Polar Biol. doi: 10.1007/s00300-011-1074-2

Cerrano C, Cardini U, Bianchelli S, Corinaldesi C, Pusceddu A, Danovaro R (2013) Red coral extinction risk enhanced by ocean acidification. Sci Rep 3:1457. doi: 10.1038/srep01457

Coen LD (1988) Herbivory by crabs and the control of algal epibionts on Caribbean host corals. Oecologia 75:198–203. doi: 10.1007/BF00378597

Comeau S, Gattuso J-P, Nisumaa A-M, Orr J (2012) Impact of aragonite saturation state changes on migratory pteropods. Proc Biol Sci 279:732–738. doi: 10.1098/rspb.2011.0910

Crawley A, Kline DI, Dunn S, Anthony KRN, Dove SG (2010) The effect of ocean acidification on symbiont photorespiration and productivity in *Acropora formosa.* Glob Chang Biol 16:851–863. doi: 10.1111/j.1365-2486.2009.01943.x

Crim RN, Sunday JM, Harley CDG (2011) Elevated seawater CO_2 concentrations impair larval development and reduce larval survival in endangered northern abalone (*Haliotis kamtschatkana*). J Exp Mar Bio Ecol 400:272–277. doi: 10.1016/j.jembe.2011.02.002

Crook ED, Cohen AL, Rebolledo-Vieyra M, Hernandez L, Paytan A (2013) Reduced calcification and lack of acclimatization by coral colonies growing in areas of persistent natural acidification. Proc Natl Acad Sci U S A 110:11044–11049. doi: 10.1073/pnas.1301589110

Crook ED, Potts D, Rebolledo-Vieyra M, Hernandez L, Paytan a. (2011) Calcifying coral abundance near low-pH springs: implications for future ocean acidification. Coral Reefs 31:239–245. doi: 10.1007/s00338-011-0839-y

Dickson AG, Sabine CL, Christian JR (2007) *Guide to best practices for ocean CO_2 measurements.* Sidney, British Columbia, North Pacific Marine Science Organization, 176pp. (PICES Special Publication, 3)

Doney SC, Fabry VJ, Feely R a, Kleypas J a. (2009) Ocean acidification: the other CO_2 problem. Ann Rev Mar Sci 1:169–192. doi: 10.1146/annurev.marine.010908.163834

Dore JE, Lukas R, Sadler DW, Church MJ, Karl DM (2009) Physical and biogeochemical modulation of ocean acidification in the central North Pacific. Proc Natl Acad Sci U S A 106:12235–12240. doi: 10.1073/pnas.0906044106

Doropoulos C, Ward S, Diaz-Pulido G, Hoegh-Guldberg O, Mumby PJ (2012) Ocean acidification reduces coral recruitment by disrupting intimate larval-algal settlement interactions. Ecol Lett 338–346. doi: 10.1111/j.1461-0248.2012.01743.x

Drew E (1983) Halimeda biomass, growth rates and sediment generation on reefs in the central Great Barrier Reef Province. Coral Reefs 101–110. doi: 10.1007/BF02395280

Dupont S, Lundve B, Thorndyke MC (2010) Near future ocean acidification increases growth rate of the lecithotrophic larvae and juveniles of the sea star *Crossaster papposus*. J Exp Zool Part B Mol Dev Evol 314:382–389. doi: 10.1002/jezmde.21342

Egleston ES, Sabine CL, Morel FMM (2010) Revelle revisited: Buffer factors that quantify the response of ocean chemistry to changes in DIC and alkalinity. Global Biogeochem Cycles 24: GB1002. doi: 10.1029/2008GB003407

Fabricius KE, Langdon C, Uthicke S, Humphrey C, Noonan S, De'ath G, Okazaki R, Muehllehner N, Glas MS, Lough JM (2011) Losers and winners in coral reefs acclimatized to elevated carbon dioxide concentrations. Nat Clim Chang 1:165–169. doi: 10.1038/nclimate1122

Fabry VJ (2009) Ocean acidification at high latitudes: the bellwether. Oceanography 22:160–171.

Fabry VJ, Seibel B a., Feely R a, Orr JC (2008) Impacts of ocean acidification on marine fauna and ecosystem processes. ICES J Mar Sci 65:414–432. doi: 10.1093/icesjms/fsn048

Feely RA, Sabine CL, Hernandez-Ayon JM, Ianson D, Hales B (2008) Evidence for upwelling of corrosive "acidified" water onto the continental shelf. Science 320:1490–1492. doi: 10.1126/science.1155676

Feely RA, Sabine CL, Lee K, Berelson W, Kleypas J a., Fabry VJ, Millero FJ (2004) Impact of anthropogenic CO_2 on the CaCO3 system in the oceans. Science 305:362–366. doi: 10.1126/science.1097329

Fernández-Reiriz J, Range P, Álvarez-Salgado X, Labarta U (2011) Physiological energetics of juvenile clams (*Ruditapes decussatus*) in a high CO_2 coastal ocean. Mar Ecol Prog Ser 433:97–105. doi: 10.3354/meps09062

Friedrich T, Timmermann A, Abe-Ouchi A, Bates NR, Chikamoto MO, Church MJ, Dore JE, Gledhill DK, González-Dávila M, Heinemann M, Ilyina T, Jungclaus JH, McLeod E, Mouchet A, Santana-Casiano JM (2012) Detecting regional anthropogenic trends in ocean acidification against natural variability. Nat Clim Chang 2:167–171. doi: 10.1038/nclimate1372

Garrard SL, Hunter RC, Frommel a. Y, Lane a. C, Phillips JC, Cooper R, Dineshram R, Cardini U, McCoy SJ, Arnberg M, Rodrigues Alves BG, Annane S, Orte MR, Kumar A, Aguirre-Martínez G V., Maneja RH, Basallote MD, Ape F, Torstensson A, Bjoerk MM (2012) Biological impacts of ocean acidification: a postgraduate perspective on research priorities. Mar Biol 160:1789–1805. doi: 10.1007/s00227-012-2033-3

Gattuso J, Hansson L (2011) Ocean acidification. Oxford University Press, UK. doi: 10.1029/2008EO150004

Gazeau F, Gattuso J-P, Dawber C, Pronker a. E, Peene F, Peene J, Heip CHR, Middelburg JJ (2010) Effect of ocean acidification on the early life stages of the blue mussel (*Mytilus edulis*). Biogeosciences Discuss 7:2927–2947. doi: 10.5194/bgd-7-2927-2010

Gazeau F, Gattuso J-P, Greaves M, Elderfield H, Peene J, Heip CHR, Middelburg JJ (2011) Effect of Carbonate Chemistry Alteration on the Early Embryonic Development of the Pacific Oyster (*Crassostrea gigas*). PLoS One 6:e23010. doi: 10.1371/journal.pone.0023010

Gooding R a, Harley CDG, Tang E (2009) Elevated water temperature and carbon dioxide concentration increase the growth of a keystone echinoderm. Proc Natl Acad Sci U S A 106:9316–9321. doi: 10.1073/pnas.0811143106

Hall-Spencer JM, Rodolfo-Metalpa R, Martin S, Ransome E, Fine M, Turner SM, Rowley SJ, Tedesco D, Buia M-C (2008) Volcanic carbon dioxide vents show ecosystem effects of ocean acidification. Nature 454:96–99. doi: 10.1038/nature07051

Havenhand J, Buttler F, Thorndyke MC, Williamson JE (2008) Near-future levels of ocean acidification reduce fertilization success in a sea urchin. Curr Biol 18:R651–R652. doi: 10.1029/2004JC002671.6.

Havenhand J, Schlegel P (2009) Near-future levels of ocean acidification do not affect sperm motility and fertilization kinetics in the oyster *Crassostrea gigas*. Biogeosciences Discuss 6:4573–4586. doi: 10.5194/bgd-6-4573-2009

Hoegh-Guldberg O, Mumby PJ, Hooten a J, Steneck RS, Greenfield P, Gomez E, Harvell CD, Sale PF, Edwards AJ, Caldeira K, Knowlton N, Eakin CM, Iglesias-Prieto R, Muthiga N, Bradbury RH, Dubi A, Hatziolos ME (2007) Coral reefs under rapid climate change and ocean acidification. Science 318:1737–1742. doi: 10.1126/science.1152509

Hofmann M, Schellnhuber H-J (2009) Oceanic acidification affects marine carbon pump and triggers extended marine oxygen holes. Proc Natl Acad Sci U S A 106:3017–3022. doi: 10.1073/pnas.0813384106

Hönisch B, Ridgwell A, Schmidt DN, Thomas E, Gibbs SJ, Sluijs A, Zeebe R, Kump L, Martindale RC, Greene SE, Kiessling W, Ries J, Zachos JC, Royer DL, Barker S, Marchitto TM, Moyer R, Pelejero C, Ziveri P, Foster GL, Williams B (2012) The geological record of ocean acidification. Science 335:1058–1063. doi: 10.1126/science.1208277

Hoppe CJM, Langer G, Rost B (2011) Emiliania huxleyi shows identical responses to elevated pCO_2 in TA and DIC manipulations. J Exp Mar Bio Ecol 406:54–62. doi: 10.1016/j.jembe.2011.06.008

Howarth R, Chan F, Conley DJ, Garnier J, Doney SC, Marino R, Billen G (2011) Coupled biogeochemical cycles: eutrophication and hypoxia in temperate estuaries and coastal marine ecosystems. Front Ecol Environ 9:18–26. doi: 10.1890/100008

Jantzen C, Häussermann V, Försterra G, Laudien J, Ardelan M, Maier S, Richter C (2013) Occurrence of a cold-water coral along natural pH gradients (Patagonia, Chile). Mar Biol 160:2597–2607. doi: 10.1007/s00227-013-2254-0

Jinendradasa S, Ekaratne S (2002) Composition and monthly variation of fauna inhabiting reef-associated Halimeda. Proc. Ninth Int. Coral Reef Symp. Bali, 23-27 Oct. 2000,. pp 1059–1063

Johnson VR, Russell BD, Fabricius KE, Brownlee C, Hall-Spencer JM (2012) Temperate and tropical brown macroalgae thrive, despite decalcification, along natural CO_2 gradients. Glob Chang Biol 18:2792–2803. doi: 10.1111/j.1365-2486.2012.02716.x

Jokiel PL, Rodgers KS, Kuffner IB, Andersson AJ, Cox EF, Mackenzie FT (2008) Ocean acidification and calcifying reef organisms: a mesocosm investigation. Coral Reefs 27:473–483. doi: 10.1007/s00338-008-0380-9

Kimura R, Takami H, Ono T, Onitsuka T, Nojiri Y (2011) Effects of elevated pCO_2 on the early development of the commercially important gastropod, Ezo abalone *Haliotis discus* hannai. Fish Oceanogr 20: 357–366. doi: 10.1111/j.1365-2419.2011.00589.x

Kleypas J, Anthony KRN, Gattuso J-P (2011) Coral reefs modify their seawater carbon chemistry–case study from a barrier reef (Moorea, French Polynesia). Glob Chang Biol 17:3667–3678. doi: 10.1111/j.1365-2486.2011.02530.x

Krief S, Hendy EJ, Fine M, Yam R, Meibom A, Foster GL, Shemesh A (2010) Physiological and isotopic responses of scleractinian corals to ocean acidification. Geochim Cosmochim Acta 74:4988–5001.

Kuffner IB, Andersson AJ, Jokiel PL, Rodgers KS, Mackenzie FT (2007) Decreased abundance of crustose coralline algae due to ocean acidification. Nat Geosci 1:114–117. doi: 10.1038/ngeo100

Kurihara H, Asai T, Kato S, Ishimatsu A (2008) Effects of elevated pCO_2 on early development in the mussel Mytilus galloprovincialis. Aquat Biol 4:225–233. doi: 10.3354/ab00109

Langdon C, W. S. Broecker, D. E. Hammond, E. Glenn, K. Fitzsimmons, S. G. Nelson, T.-H. Peng, I. Hajdas, and G. Bonani (2003) Effect of elevated CO_2 on the community metabolism of an experimental coral reef. Global Biogeochem Cycles 17:1011. doi: 10.1029/2002gb001941

Langer G, Geisen M, Baumann K-H, Kläs J, Riebesell U, Thoms S, Young JR (2006) Species-specific responses of calcifying algae to changing seawater carbonate chemistry. Geochemistry Geophys Geosystems 7:1–12. doi: 10.1029/2005GC001227

Leclercq N, Gattuso J-P, Jaubert J (2002) Primary production, respiration, and calcification of a coral reef mesocosm under increased CO_2 partial pressure. Limnol Oceanogr 47:558–564. doi: 10.4319/lo.2002.47.2.0558

Lloret J, Marín A, Marín-Guirao L (2008) Is coastal lagoon eutrophication likely to be aggravated by global climate change? Estuar Coast Shelf Sci 78:403–412. doi: 10.1016/j.ecss.2008.01.003

Lohbeck KT, Riebesell U, Reusch TBH (2012) Adaptive evolution of a key phytoplankton species to ocean acidification. Nat Geosci 5:346–351. doi: 10.1038/ngeo1441

Maier C, Watremez P, Taviani M, Weinbauer MG, Gattuso J-P (2012) Calcification rates and the effect of ocean acidification on Mediterranean cold-water corals. Proc Biol Sci 279:1716–1723. doi: 10.1098/rspb.2011.1763

Manzello D, Kleypas J (2008) Poorly cemented coral reefs of the eastern tropical Pacific: Possible insights into reef development in a high-CO_2 world. Proc Natl Acad Sci U S A 105:10450–10455. doi: 10.1073/pnas.0712167105

Martin S, Gattuso J-P (2009) Response of Mediterranean coralline algae to ocean acidification and elevated temperature. Glob Chang Biol 15:2089–2100. doi: 10.1111/j.1365-2486.2009.01874.x

Marubini F, Ferrier-Pagès C, Cuif J-PP, Ferrier-Pages C (2003) Suppression of skeletal growth in scleractinian corals by decreasing ambient carbonate-ion concentration: a cross-family comparison. Proc Biol Sci 270:179–184. doi: 10.1098/rspb.2002.2212

Marubini F, Ferrier-Pagès C, Furla P, Allemand D (2008) Coral calcification responds to seawater acidification: a working hypothesis towards a physiological mechanism. Coral Reefs 27:491–499. doi: 10.1007/s00338-008-0375-6

Meron D, Atias E, Iasur Kruh L, Elifantz H, Minz D, Fine M, Banin E (2011) The impact of reduced pH on the microbial community of the coral *Acropora eurystoma*. ISME J 5:51–60. doi: 10.1038/ismej.2010.102

Miles H, Widdicombe S, Spicer JI, Hall-Spencer J (2007) Effects of anthropogenic seawater acidification on acid-base balance in the sea urchin *Psammechinus miliaris*. Mar Pollut Bull 54:89–96. doi: 10.1016/j.marpolbul.2006.09.021

Millero FJ, Pierrot D, Lee K, Wanninkhof R, Feely R, Sabine CL, Key RM, Takahashi T (2002) Dissociation constants for carbonic acid determined from field measurements. Deep Sea Res Part I Oceanogr Res Pap 49:1705–1723. doi: 10.1016/S0967-0637(02)00093-6

Moberg F, Folke C (1999) Ecological goods and services of coral reef ecosystems. Ecol Econ 29:215–233. doi: 10.1016/S0921-8009(99)00009-9

Mucci A (1983) The solubility of calcite and aragonite in seawater at various salinities, temperatures, and one atmosphere total pressure. Am J Sci 283:780–799. doi: 10.2475/ajs.283.7.780

Mussaka A, Kangwe J, Nyandwi N, Wannäs K, Mtolera M, Björk M (2001) Preliminary results on the sediment sources, grain size distribution and percentage cover of sand-producing Halimeda species and associated flora in Chwaka Bay. In: Richmond MD, Francis J (eds) Mar. Sci. Dev. Tanznaia East. Africa. Marine Science Development in Tanznaia and Eastern Africa. Proceedings of the 20th Anniversary Conference on Advances in Marine Science in Tanzania, Zanzibar, Tanzania. IMS/WIOMSA, pp 51–59

Nakamura M, Ohki S, Suzuki A, Sakai K (2011) Coral larvae under ocean acidification: survival, metabolism, and metamorphosis. PLoS One 6:e14521. doi: 10.1371/journal.pone.0014521

O'Donnell MJ, Hammond LM, Hofmann GE (2008) Predicted impact of ocean acidification on a marine invertebrate: elevated CO_2 alters response to thermal stress in sea urchin larvae. Mar Biol 156:439–446. doi: 10.1007/s00227-008-1097-6

Orr JC, Fabry VJ, Aumont O, Bopp L, Doney SC, Feely RA, Gnanadesikan A, Gruber N, Ishida A, Joos F, Key RM, Lindsay K, Maier-Reimer E, Matear RJ, Monfray P, Mouchet A, Najjar RG, Plattner G-K, Rodgers KB, Sabine CL, Sarmiento JL, Schlitzer R, Slater RD, Totterdell IJ, Weirig M-F, Yamanaka Y, Yool A (2005) Anthropogenic ocean acidification over the twenty-first century and its impact on calcifying organisms. Nature 437:681–686. doi: 10.1038/nature04095

Parker LM, Ross PM, O'Connor W a., Borysko L, Raftos D a., Pörtner H-O (2011) Adult exposure influences offspring response to ocean acidification in oysters. Glob Chang Biol 18: 82–92. doi: 10.1111/j.1365-2486.2011.02520.x

Porzio L, Buia MC, Hall-Spencer JM (2011) Effects of ocean acidification on macroalgal communities. J Exp Mar Bio Ecol 400:278–287. doi: 10.1016/j.jembe.2011.02.011

Price N, Hamilton S, Tootell J, Smith J (2011) Species-specific consequences of ocean acidification for the calcareous tropical green algae Halimeda. Mar Ecol Prog Ser 440:67–78. doi: 10.3354/meps09309

Le Quéré C, Raupach MR, Canadell JG, Marland G, Bopp L, Ciais P, Conway TJ, Doney SC, Feely RA, Foster P, Friedlingstein P, Gurney K, Houghton RA, House JI, Huntingford C, Levy PE, Lomas MR, Majkut J, Metzl N, Ometto JP, Peters GP, Prentice IC, Randerson JT, Running SW, Sarmiento JL, Schuster U, Sitch S, Takahashi T, Viovy N, van der Werf GR, Woodward FI, Marland et al. G, Le Quéré et al. C (2009) Trends in the sources and sinks of carbon dioxide. Nat Geosci 2:831–836. doi: 10.1038/ngeo689

Raven J a., Caldeira K, Elderfield H, Hoegh-Guldberg O, Liss P, Riebesell U, Shepherd J, Turley C, Watson AJ (2005) Ocean acidification due to increasing atmospheric carbon dioxide. The Royal Society, Cardiff, p. 60.

Reyes-Nivia C, Diaz-Pulido G, Kline DI, Guldberg O-H, Dove S (2013) Ocean acidification and warming scenarios increase microbioerosion of coral skeletons. Glob Chang Biol 19:1919–1929. doi: 10.1111/gcb.12158

Ridgwell A, Schmidt DN (2010) Past constraints on the vulnerability of marine calcifiers to massive carbon dioxide release. Nat Geosci 3:196–200. doi: 10.1038/ngeo755

Riebesell U., Fabry V. J., Hansson L. & Gattuso J.-P. (Eds.) (2010) Guide to best practices for ocean acidification research and data reporting, 260 p. Luxembourg: Publications Office of the European Union.

Riebesell U, Schulz KG, Bellerby RGJ, Botros M, Fritsche P, Meyerhöfer M, Neill C, Nondal G, Oschlies A, Wohlers J, Zöllner E (2007) Enhanced biological carbon consumption in a high CO_2 ocean. Nature 450:545–548. doi: 10.1038/nature06267

Ries JB, Cohen AL, McCorkle DC (2009) Marine calcifiers exhibit mixed responses to CO_2-induced ocean acidification. Geology 37:1131–1134. doi: 10.1130/G30210A.1

Robbins LL, Knorr PO, Hallock P (2009) Response of Halimeda to ocean acidification: field and laboratory evidence. Biogeosciences Discuss 6:4895–4918. doi: 10.5194/bgd-6-4895-2009

Sabine CL, Feely RA, Gruber N, Key RM, Lee K, Bullister JL, Wanninkhof R, Wong CS, Wallace DWR, Tilbrook B, Millero FJ, Peng T-H, Kozyr A, Ono T, Rios AF (2004) The oceanic sink for anthropogenic CO_2. Science 305:367–371. doi: 10.1126/science.1097403

Schram JB, McClintock JB, Angus RA, Lawrence JM (2011) Regenerative capacity and biochemical composition of the sea star *Luidia clathrata* (Say) (Echinodermata: Asteroidea) under conditions of near-future ocean acidification. J Exp Mar Bio Ecol 407:266–274. doi: 10.1016/j.jembe.2011.06.024

Semesi IS, Kangwe J, Björk M (2009) Alterations in seawater pH and CO_2 affect calcification and photosynthesis in the tropical coralline alga, *Hydrolithon* sp. (Rhodophyta). Estuar Coast Shelf Sci 84:337–341. doi: 10.1016/j.ecss.2009.03.038

Shaw E, McNeil B, Tilbrook B (2013) Anthropogenic changes to seawater buffer capacity combined with natural reef metabolism induce extreme future coral reef CO_2 conditions. Glob Chang Biol 19:1632–1641. doi: 10.1111/gcb.12154

Shi D, Xu Y, Hopkinson BM, Morel FMM (2010) Effect of ocean acidification on iron availability to marine phytoplankton. Science 327:676–679. doi: 10.1126/science.1183517

Sluijs A, Schouten S, Pagani M, Woltering M, Brinkhuis H, Damsté JSS, Dickens GR, Huber M, Reichart G-J, Stein R, Matthiessen J, Lourens LJ, Pedentchouk N, Backman J, Moran K (2006) Subtropical Arctic Ocean temperatures during the Palaeocene/Eocene thermal maximum. Nature 441:610–613. doi: 10.1038/nature04668

Solomon S, Qin D, Manning M, Chen Z, Marquis M, Averyt K, Tignor M, Miller H.L. (2007) Contribution of Working Group I to the Fourth Assessment Report of the Intergovernmental Panel on Climate Change. Cambridge University Press, Cambridge, United Kingdom and New York, NY, USA.

Spicer JI, Raffo A, Widdicombe S (2006) Influence of CO_2-related seawater acidification on extracellular acid–base balance in the velvet swimming crab *Necora puber*. Mar Biol 151:1117–1125. doi: 10.1007/s00227-006-0551-6

Stachowicz JJ, Hay ME (1999) Reduced mobility is associated with compensatory feeding and increased diet breadth of marine crabs. Mar Ecol Prog Ser 188:169–178. doi: 10.3354/meps188169

Stachowicz JJ, Hay ME (1996) Facultative mutualism between an herbivorous crab and a coralline alga: advantages of eating noxious seaweeds. Oecologia 105:377–387. doi: 10.1007/BF00328741

Steinacher M, Joos F, Frolicher TL, Plattner G-K, Doney SC (2009) Imminent ocean acidification in the Arctic projected with the NCAR global coupled carbon cycle-climate model. Biogeosciences 6:515–533.

Stumpp M, Trübenbach K, Brennecke D, Hu MY, Melzner F (2012) Resource allocation and extracellular acid-base status in the sea urchin *Strongylocentrotus droebachiensis* in response to CO_2 induced seawater acidification. Aquat Toxicol 110-111:194–207. doi: 10.1016/j.aquatox.2011.12.020

Sunda WG, Cai W-J (2012) Eutrophication induced CO_2-acidification of subsurface coastal waters: interactive effects of temperature, salinity, and atmospheric pCO_2. Environ Sci Technol 46:10651–10659. doi: 10.1021/es300626f

Suwa R, Nakamura M, Morita M, Shimada K, Iguchi A, Sakai K, Suzuki A (2009) Effects of acidified seawater on early life stages of scleractinian corals (Genus Acropora). Fish Sci 76:93–99. doi: 10.1007/s12562-009-0189-7

Tans P, Keeling R, (2014) Trends in Atmospheric Carbon Dioxide. National Oceanic and Atmospheric Administration Earth System Research Laboratory Global Monitoring Division; Scripps Institution of Oceanography. http://www.esrl.noaa.gov/gmd/ccgg/trends/ (Accessed 25.02.14).

Tortell PD, Payne CD, Li Y, Trimborn S, Rost B, Smith WO, Riesselman C, Dunbar RB, Sedwick P, DiTullio GR (2008) CO_2 sensitivity of Southern Ocean phytoplankton. Geophys Res Lett 35:L04605. doi: 10.1029/2007GL032583

Uthicke S, Momigliano P, Fabricius KE (2013) High risk of extinction of benthic foraminifera in this century due to ocean acidification. Sci Rep 3:1769. doi: 10.1038/srep01769

Venn A, Tambutte E, Holcomb M, Allemand D, Tambutte S (2011) Live tissue imaging shows reef corals elevate pH under their calcifying tissue relative to seawater. PLoS One 6:e20013. doi: 10.1371/journal.pone.0020013

Vizzini S, Tomasello A, Maida G Di, Pirrotta M, Mazzola A, Calvo S (2010) Effect of explosive shallow hydrothermal vents on δ13C and growth performance in the seagrass *Posidonia oceanica*. J Ecol 98:1284–1291. doi: 10.1111/j.1365-2745.2010.01730.x

Voss M, Bange HW, Dippner JW, Middelburg JJ, Montoya JP, Ward B (2013) The marine nitrogen cycle: recent discoveries, uncertainties and the potential relevance of climate change. Philos Trans R Soc Lond B Biol Sci 368:20130121. doi: 10.1098/rstb.2013.0121

Walther K, Anger K, Pörtner HO (2010) Effects of ocean acidification and warming on the larval development of the spider crab *Hyas araneus* from different latitudes (54° vs. 79°N). Mar Ecol Prog Ser 417:159–170. doi: 10.3354/meps08807

Walther K, Sartoris FJ, Bock C, Pörtner HO (2009) Impact of anthropogenic ocean acidification on thermal tolerance of the spider crab *Hyas araneus*. Biogeosciences Discuss 6:2837–2861. doi: 10.5194/bgd-6-2837-2009

Walther K, Sartoris FJ, Pörtner HO (2011) Impacts of temperature and acidification on larval calcium incorporation of the spider crab *Hyas araneus* from different latitudes (54° vs. 79°N). Mar Biol 158:2043–2053. doi: 10.1007/s00227-011-1711-x

Wild C, Hoegh-Guldberg O, Naumann MS (2011) Climate change impedes scleractinian corals as primary reef ecosystem engineers. Mar Freshw 62:205–215.

Wisshak M, Schönberg CHL, Form A, Freiwald A (2012) Ocean acidification accelerates reef bioerosion. PLoS One 7:e45124. doi: 10.1371/journal.pone.0045124

Witt V, Wild C, Anthony KRN, Diaz-Pulido G, Uthicke S (2011) Effects of ocean acidification on microbial community composition of, and oxygen fluxes through, biofilms from the Great Barrier Reef. Environ Microbiol 13:2976–2989. doi: 10.1111/j.1462-2920.2011.02571.x

Wootton JT, Pfister CA, Forester JD (2008) Dynamic patterns and ecological impacts of declining ocean pH in a high-resolution multi-year dataset. Proc Natl Acad Sci U S A 105:18848–18853. doi: 10.1073/pnas.0810079105

Yamamoto-Kawai M, McLaughlin FA, Carmack EC, Nishino S, Shimada K (2009) Aragonite undersaturation in the Arctic Ocean: effects of ocean acidification and sea ice melt. Science 326:1098–1100. doi: 10.1126/science.1174190

Zachos JC, Röhl U, Schellenberg SA, Sluijs A, Hodell DA, Kelly DC, Thomas E, Nicolo M, Raffi I, Lourens LJ, McCarren H, Kroon D (2005) Rapid acidification of the ocean during the Paleocene-Eocene thermal maximum. Science 308:1611–1615. doi: 10.1126/science.1109004

Zachos JC, Wara MW, Bohaty S, Delaney ML, Petrizzo MR, Brill A, Bralower TJ, Premoli-Silva I (2003) A transient rise in tropical sea surface temperature during the Paleocene-Eocene thermal maximum. Science 302:1551–1554. doi: 10.1126/science.1090110

Zeebe RE, Zachos JC, Dickens GR (2009) Carbon dioxide forcing alone insufficient to explain Palaeocene–Eocene Thermal Maximum warming. Nat Geosci 2:576–580. doi: 10.1038/ngeo578

2 - Effects of high dissolved inorganic and organic carbon availability on the physiology of the hard coral *Acropora millepora* from the Great Barrier Reef

Friedrich W Meyer *[a], Nikolas Vogel [a,b], Karen Diele [a,c], Andreas Kunzmann [a], Sven Uthicke [b], Christian[a] Wild[d]

[a] *Leibniz Center for Tropical Marine Ecology (ZMT), Fahrenheitstraße 6, 28359 Bremen, Germany*

[b] *Australian Institute of Marine Science, PMB 3, Townsville MC, 4810 QLD, Australia*

[c] *Edinburgh Napier University, School of Life, Sport and Social Sciences, Edinburgh, EH11 4BN, UK*

[d] *Faculty of Biology and Chemistry, University of Bremen, Germany*

[*] *Corresponding author*

Phone: +49 (421) 23800 – 118

Fax: +49 (421) 23800 – 30

Email: friedrich.meyer@zmt-bremen.de

URL: http://www.zmt-bremen.de/Friedrich_Meyer.html

This manuscript has been submitted to PLOS ONE

Abstract

Coral reefs are facing major global and local threats through climate change-induced increasing concentrations of dissolved inorganic carbon (DIC) and land-derived increasing inorganic and organic nutrients. Recent research revealed that high availability of labile dissolved organic carbon (DOC) negatively affects scleractinian corals. Studies on the interplay of these factors, however, are lacking, but urgently needed to understand coral reef functioning under present and particularly near future conditions. This experimental study over 16 d thus investigated the single and combined effects of ambient and high DIC (pCO_2 403 µatm/ pH_{Total} 8.2 and 996 µatm/ pH_{Total} 7.8) as well as DOC (added as Glucose 0 and 294 µmol L^{-1}, background DOC concentration of 83 µmol L^{-1}) availability on the physiology (photosynthesis, respiration, dark and light calcification, and growth) of the hard coral *Acropora millepora* (Ehrenberg, 1834) from the Great Barrier Reef. High DIC availability did not affect photosynthesis, respiration and light calcification, but significantly reduced dark calcification and growth by 50 and 23%, respectively. High DOC availability reduced net and gross photosynthesis by 51% and 39%, respectively. DOC addition did not influence calcification, but significantly increased growth by 42%. Combination of high DIC and high DOC availability did not affect photosynthesis, light calcification or growth, but significantly decreased dark calcification when compared to both controls and DIC treatments. On the ecosystem level, high DIC concentrations may lead to reduced accretion and growth of reefs dominated by *Acropora* that in combination with elevated DOC concentrations will likely exhibit reduced primary production rates, ultimately leading to loss of hard substrate and reef erosion. It is therefore important to consider the impacts of elevated DOC and DIC simultaneously to assess real world scenarios, as multiple rather than single factors influence key physiological processes in coral reefs.

Introduction

Concern has recently been raised about the effects of human-induced increases in atmospheric CO_2 that also leads to increases of dissolved inorganic carbon concentration (DIC) in the world ocean, causing ocean acidification (OA) [1]. The rate of increase of DIC seawater concentration is unprecedented for the last 300 million years [2–5] and is expected to rise even further [6]. The resulting reduced pH changes the carbonate system of the seawater by decreasing the saturation state of the different calcium carbonate components [7]. This ultimately affects many coral reef calcifying invertebrates such as hard corals, mollusks, echinoderms and foraminifera [8–13] and may lead to changes in calcification, productivity and benthic community structure of coral reefs (Kuffner et al. 2007, Anthony et al. 2008, Diaz-Pulido et al. 2011, Fabricius et al. 2011, Uthicke & Fabricius 2012). Recent findings suggest that future predictions of pCO_2 levels in seawater are likely a conservative estimate for highly productive areas such as coral reefs in coastal zones, where large natural variability

of the carbonate chemistry [19], coupled with a decrease in buffer capacity, can amplify predicted future pCO_2 concentrations up to three fold [20].

While DIC availability can directly affect coral reef calcifiers, increased dissolved organic carbon (DOC) availability indirectly influences corals by altering coral-associated microbial communities and stimulating microbial activity [21–24]. Main sources of exogenous DOC are sewage waters [25] and terrestrially derived sediments carrying high amounts of particulate organic carbon which are transformed via microbial degradation into dissolved organic material [26]. Inorganic nutrients support micro- and macro-algae growth which in turn leads to increased DOC production (up to 1000 µmol L^{-1}, Kline et al. 2006) during bloom and algae mat formation (up to 130 µmol L^{-1} Hauri et al., 2010). For the Australian Great Barrier Reef (GBR), high inputs of inorganic nutrients and increased sediment loads through human activity have led to so called "phase shifts" and changed some coral reef communities to algae-dominated communities [28–30]. Nutrient and sediment inputs show high spatial and temporal variation. Land-derived inputs are particularly frequent during the wet season when precipitation is higher and storm events are more recurrent, and concentrations high in areas with anthropogenically increased river discharges [26,31,32]. Both, agricultural use and area extent as well as strong storm events and floods are predicted to increase further during the next centuries [33,34] and therefore the contribution of river discharge to DOC availability in the GBR is also likely to rise, as riverine runoff from agricultural influenced areas is one of the main sources of elevated DOC concentrations. In addition, inorganic nutrients may fuel algal growth and ensuing phase shifts which in turn further increases highly bio-available DOC production (Haas et al. 2011, Haas & Wild 2010) and therefore availability to microbial communities [35,37–42]. These compounds may also promote the growth of pathogens leading to coral bleaching and eventually mortality in a period of days only [21–23,43,44]. Finally, high microbial activity and degradation of organic carbon reduces the availability of oxygen for the coral holobiont to potentially critical levels [24,27,35,41].

Given the urgent need for understanding coral reef functioning and vulnerability in the Anthropocene, it is surprising that no studies on the combined effects of the important parameters DOC and DIC have been conducted to date. Moreover, the effects of high DOC availability on corals have so far only been investigated in terms of their survival and in the context of microbial growth. Studies on the effects on coral physiology, i.e. growth, calcification, and photosynthesis, are lacking, but crucial for evaluating the effects of non-lethal exposure to elevated DOC availabilities. In addition, high DOC availability may change the microbial communities associated with the coral holobiont and possibly reduce calcification and photosynthetic rates. This may result in cumulative negative effects in combination with high DIC availability, which has already been demonstrated to reduce calcification of corals [14,45].

Here, we present the results of a laboratory experiment with combined high DIC and DOC exposure to a scleractinian coral. We selected *Acropora millepora* (Ehrenberg, 1834), a common coral species from the GBR of which the response towards elevated DIC has been studied on the gene expression

level [46,47], and effects of elevated DIC on early development and settlement have been described [48]. We monitored photosynthetic performance as well as growth throughout the experiment over 16 d and measured calcification, oxygen and nutrient fluxes as well as chl*a* (chlorophyll a) and protein content at the end of the experiment.

Material and methods

Specimen collection and preparation

Colonies of the coral *Acropora millepora* (Ehrenberg, 1834) were collected from reefs next to Pelorus Island (S 18° 33.001', E 146° 29.304') in 2012 under a GBMPA sampling permit to the Australian Institute of Marine Science (AIMS). The colonies were fragmented, and individual nubbins (3 to 4 cm height) glued onto ceramic stubs with superglue. Nubbins were maintained in natural seawater flow-through aquaria facilities at AIMS under plasma lights (150 µmol photons m^{-2} s^{-1}) in a 12 h/ 12 h light-dark cycle for 3 months until using them for the experiment.

Experimental setup

Two weeks prior to the onset of the manipulative experiment, the nubbins were randomly assigned into 12 experimental tanks (flow-through tanks with 18 l volume each). The experiment itself was conducted over a period of 16 d between 24 July and 9 August 2012 at AIMS. Three replicate tanks for the two treatments with two treatment levels were placed in alternating order. The treatments were pCO_2 in ambient and high availability (403 µatm and 996 µatm, respectively) and DOC in ambient and high availability (83 ± 10 and 294 ± 506 µmol L^{-1} with DOC added as Glucose, D-Glucose, Sigma Aldrich, purity > 99,5% in 0 and 377 µmol L^{-1}). The high DOC treatment was achieved by daily additions of 1170 µmol L^{-1} DOC at 8:00 and 20:00 with pre- weighed Glucose (D-Glucose, Sigma Aldrich), a highly bioavailable short organic carbon molecule. This simulates a sudden increase of DOC and subsequent dissolution as likely to occur in coastal waters, along with sudden increases in river discharges that have been shown to correlate with high amounts of DOC [49–51]. Using stable DOC concentrations would not have adequately reflected natural conditions as production and recycling, especially of high bioavailable DOC occurs on a diurnal basis and even seasonal basis [52]. Dilution by flow through yielded an average concentration of 294 ± 506 µmol L^{-1} determined over the seven sample points (n = 2) while background DOC concentrations remained 83 ± 10 µmol L^{-1} (Fig. 1). The target pCO_2 was 1000 µatm, corresponding to levels reached under the Representative Concentration Pathways (RCP) 6.0 to RCP 8.5 most likely by the year 2100 [53–55]. DOC levels were chosen according to maximum concentrations measured in coral reefs (for summary see Kline et al. 2006) and treatments applied in other studies [21,22,43]. The corals were kept in freshly filtered (0.5 µm) natural seawater at 25 °C, with a salinity of 34.5. Water flow was adjusted to 150 mL min^{-1}. Light

was provided by individually adjustable white and blue light LED (6000 K, Aqua Illumination). Light levels were set to 12 h/ 12 h light-dark cycle with an intensity of 150 µmol photons m^{-2} s^{-1} during the light cycle. Aquaria pumps (AquarWorld, Australia, 250 L h^{-1}) in each specimen tank provided water movement. Target pH levels were achieved by a pH stat system (Aqua Medic, Germany) controlled by potentiometric pH sensors, as described in Vogel and Uthicke (2012). Total alkalinity A_T was determined by gran titration with a Metrohm 855 robotic titrosampler (Metrohm, Switzerland) using 0.5 M HCl (see Uthicke and Fabricius 2012) and certified reference material (CRM Batch 106, A. Dickson, Scripps Oceanographic Institute) for correction. Carbonate system parameters were calculated with CO2calc software [57] utilizing A_T values and pH values obtained with a multiprobe (WTW 3430, Germany). Calculated pCO_2 levels yielded an average of 440 µatm pCO_2 for ambient and 1090 µatm pCO_2 for high treatments (Tab 1).

Maximum quantum efficiency

Maximum quantum efficiency (F_v/F_m) was determined by Pulse Amplitude Modulation (PAM) fluorometry using a diving PAM (Walz, Germany) and a 6 mm diameter fiber optic cable. F_v/F_m measurements were conducted every evening, after dark adaptation, 30 min after the lights turned off automatically.

Coral surface area

The individual surface area of the incubated coral nubbins from 5 to 16 cm² was determined using the advanced geometry method (Naumann et al. 2009). Surface areas were calculated as individual columns, therefore height and width were measured using Image J software.

Light-/ dark calcification, O_2 and nutrient fluxes

After 16 d under experimental conditions, two coral nubbins from each replicate tank were transferred to individual closed plastic chambers (Nalgene 200 mL) and incubated for 60 min in light and 60 min in darkness. PH and DOC concentrations of the seawater in the incubation chambers corresponded to the formerly experienced treatment conditions, and the sea water was pre-filtered some minutes before the start of each incubation in order to remove bacterial background signals from the incubation water. Each incubation run consisted of 12 parallel incubations in 200 mL closed chambers, including two blanks per treatment. A white light LED (4000 K, Megaman, Germany) was installed above each incubation chamber and individually adjusted to meet equal light conditions of the treatment tanks, verified using a quantum sensor (Apogee, USA). To assure constant water temperature during incubation, chambers were placed into a temperature controlled water bath at 25 °C, equal to the temperature during the 16 d incubation. Additionally, glass-coated magnetic stirrer bars ensured water movement within the incubation chambers.

Light- and dark calcification rates were determined by the alkalinity anomaly technique [59]. A subsample of 50 mL was pipetted from the incubation seawater and directly titrated for total alkalinity measurement by a Metrohm855 (as described above). A_T was calculated by non-linear regression fitting between pH 3.5 and pH 3.0. Calcium carbonate precipitation or dissolution in µM C h^{-1} was calculated by half molar of the difference between the post incubation and the blank seawater A_T readings, volume of chamber, time of incubation and organism surface area [60].

O_2 production in light and consumption in darkness were monitored continuously during the incubations by three 4-channel O_2 meters (Firesting, Pyroscience, Germany), connected to each chamber with fiber optic cables. Net photosynthesis, respiration, and resulting gross photosynthesis were determined in µM O_2 h^{-1} and related to organism surface area. In addition, O_2 consumption was corrected to blank readings from empty incubation chambers containing only the respective treatment water.

Nutrient fluxes in the chambers were determined by analyzing subsamples of seawater from light and dark incubations for dissolved inorganic nutrients, DIN (NH_4^+, PO_4^- and NO_2^- + NO_3^- as NO_x) and total organic carbon, TOC (NPOC) directly subsequent to the experimental runs. Samples for DIN were filtered using 0.45 µm syringe filters and kept frozen at -20 °C until measurement by Segmented Flow Analysis (Seal Analytical, USA). Samples for TOC were filtered through 0.45 µm GFF Filters (Whatman), acidified with 150 µL fuming HCl and frozen at -20 °C until analysis on a Shimadzu TOC-5000A (Shimadzu, USA). Nutrient fluxes in µM (DIN) and mg L^{-1} (TOC) were calculated and corrected for the fluxes of the blank incubations and related to organism surface area.

Growth rates

Coral growth was determined using the buoyant weight technique [61]. Individual specimens were weighed (accuracy: 0.1 mg, Mettler Toledo, USA) in a custom-build buoyant weight set-up with water jacket and seawater of constant temperature (25 °C) and salinity (34.5) at the start and end of the experiment. Growth of the organisms was expressed as daily percentage of weight change.

Biological Oxygen Demand (BOD)

To assess effects of elevated organic or inorganic carbon availability on microbial respiration rates, BOD of the treatment water was measured at the end of the experiment for each treatment tank (n = 3). For this purpose, 200 mL of unfiltered seawater were incubated for 24 h in the dark under temperature conditions of the treatments. The O_2 concentration (mg L^{-1} and % saturation) as well as salinity and temperature were recorded before and after the incubation, and O_2 consumption rates were calculated from these two values and related to water volume and time to mg O_2 L^{-1} h^{-1}.

Pigment content

Chl*a* content of *A. millepora* tissue was determined spectrophotometrically. After completion of the incubation experiments, organisms were frozen at -80 °C. In the following, the protocol for Chl*a* measurement described in Vogel and Uthicke (2012) and Schmidt et al. (2011) was used. Coral tissue was separated from the skeleton by stripping with an air gun using fresh, ultra-filtered (0.2 µm) seawater. During several subsequent separation steps, the obtained zooxanthellae pellets were kept on ice for further processing, and the host tissue was frozen at -20 °C for analysis of total protein content (as described below). Pellets were re-suspended in 5 mL of fresh, filtered seawater, and subsamples of 0.5 mL transferred into 2 mL centrifuge tubes. After centrifuging (10.000 x g for 5 min), the supernatant was discarded, and the zooxanthellae pellets were re-suspended in 2 mL of 95% EtOH to extract Chl*a*. Absorbencies were read in 400 µL of the supernatant on a 96-well microtiter plate at 750 and 665 nm wavelengths in a Powerwave microplate reader (BioTek, USA). Chl*a* contents were calculated with equations by Nush (1980) and related to nubbin surface area.

Protein content

Total protein content of *A. millepora* was analyzed with the Bio-Rad protein assay kit (Bio-Rad, USA). Applying the method described in Leuzinger et al. (2003), the coral tissue slurry was digested with 1MNaOH for 60 min at 90 °C in a sealed deep-well plate. Cell-debris was separated from the solution (1500 x g for 10 min). Dilutions of protein standard (bovine serum albumin, BSA) and samples were transferred into a 96-well microtiter plate and protein assay reagents were added. After 15 min, absorbency was read on 750 nm wavelength in a Powerwave microplate reader (BioTek, USA). Total protein content of *A. millepora* was calculated, correlated to protein standard regression and related to nubbin surface area.

Statistical analysis

We tested whether growth rates, light- and dark-calcification rates, photosynthesis, respiration, maximum quantum efficiency, pigment and protein content and nutrient fluxes differed significantly between treatments and control conditions. Data was tested for normality using the Shapiro-Wilk test and for equal variance using the Levene median test. Data of net and gross photosynthesis failed the test for equal variance, but showed equal variances after log10 transformation. A Two Way ANOVA was then performed with the treatments DIC and DOC as fixed factors to test for treatment effects as well as interactions of treatments and “aquarium” as nested factor to test for tank effects. To compare differences between individual treatment combinations, a Pairwise Multiple Comparison Procedure (Holm-Sidak method) was performed when interactions were significant. All statistical analyses were conducted using SigmaPlot 12.0 and NCSS statistical statistical software.

Results

Experimental Treatment Levels

Targeted levels of the manipulated parameters were reached during the experiment. The average control pH was 8.038 ± 0.03 and was reduced under the high DIC treatment to 7.707 ± 0.04 (Tab. 1). Consequently, the aragonite saturation state was also lowered from 4.117 ± 1.2 under control conditions to 2.162 ± 0.6 (Tab. 1). The high DOC treatment (Fig. 1) resulted in an initial Glucose concentration of 1170 µmol L^{-1} which averaged out dueto dilution to a concentration of 294 (± 506 µmol L^{-1}) compared to 0 µmol L^{-1} under control conditions with a background DOC concentration of 83 (± 10) µmol L^{-1}. Alkalinity and oxygen concentrations did not show a difference between the high DIC treatment and the controls. Under the high DOC treatment, oxygen concentrations were 1% lower and pH was reduced by 0.021 compared to the controls.

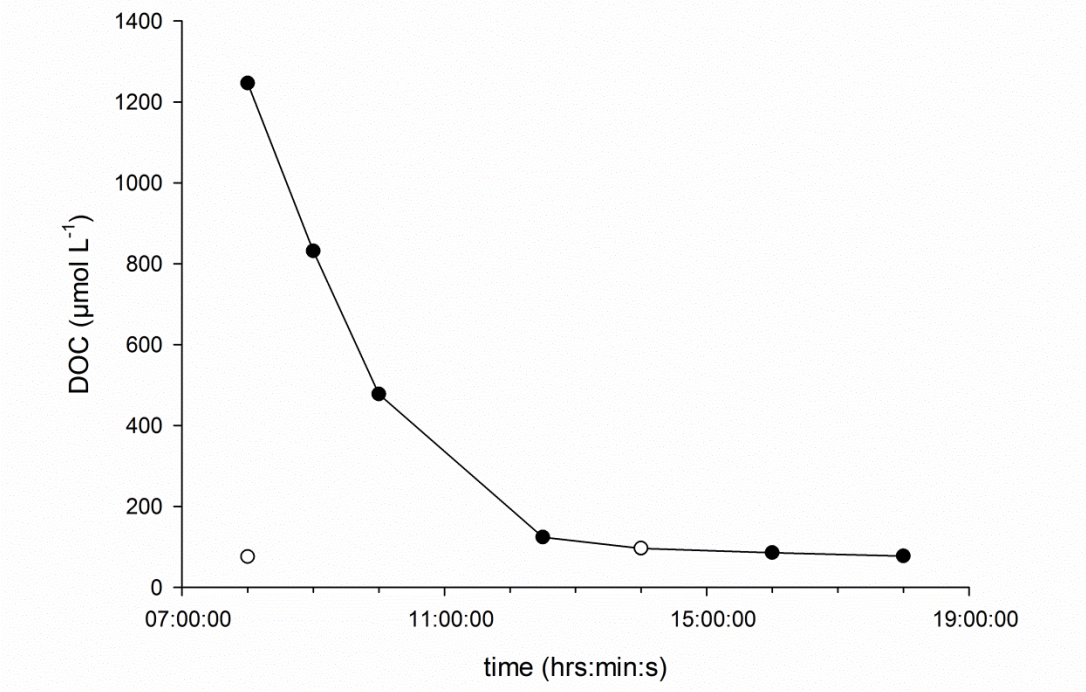

Figure 1. DOC concentrations in the high DOC treatment. Time series (08:00 am until 07:00 pm) after addition of 1170 µmol L^{-1} DOC as glucose and a background concentration (unfilled circles) of 76 and 97 µmol L^{-1} DOC. Filled circles indicate sampling points (n=2) for DOC analysis of the high DOC treatment and unfilled circles of the controls (n = 2 for each point).

Table 1. Carbonate system parameters. Values calculated using CO2Calc with total alkalinity (TA) and pH_{Total} as input parameters (n = 3 for TA, n = 10 for pH, temperature, salinity and O_2). Values are given as average with standard deviation in parentheses

Treatment	pH [Total]	temp [°C]	Salinity [ppt]	% O_2Sat	TA (µmol kgSW^{-1})	pCO_2 (µatm)	HCO_3^- (µmol kgSW^{-1})	ΩAr
Control	8.04	25.4	34.4	105.4	2276.1	402.8	1776.1	4.1
	(0.03)	(0.2)	(0.1)	(4.7)	(13.0)	(10.7)	(15.0)	(1.2)
High DIC	7.71	25.3	34.4	105.9	2281.2	995.9	2011.4	2.2
	(0.04)	(0.1)	(0.1)	(5.7)	(7.3)	(26.2)	(7.6)	(0.6)
High DOC	8.02	25.16	34.4	104.8	2286.4	429,8	1791.6	4.0
	(0.03)	(0.3)	(0.1)	(6.3)	(10.3)	(9.9)	(8.3)	(1.1)
High DIC & High DOC	7.69	25.0	34.4	104.2	2281.7	1080.5	2031.7	2.0
	(0.03)	(0.4)	(0.1)	(5.4)	(16.9)	(15.3)	(12.2)	(0.6)

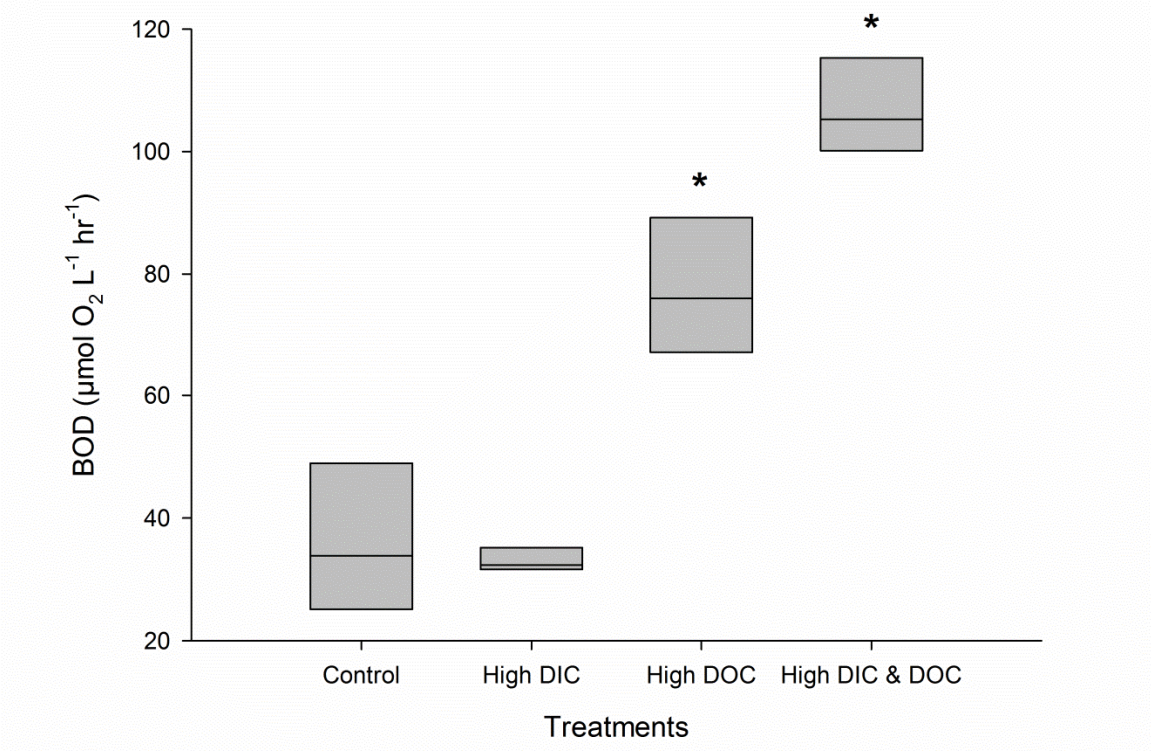

Figure 2. Biological Oxygen Demand (BOD) in the different treatments at the end of the experiment (n=3). Boxplots indicating median (mid of boxplot), 25% and 75% percentile (lower and upper border of boxplot). Significant differences ($p < 0.05$) are marked with an asterisk.

DIC

High DIC availability did not affect the BOD of the treatment water compared to controls (Fig. 2). It significantly reduced dark calcification rates of *A. millepora* by 50% with 0.06 µmol C cm^{-2} h^{-1} compared to 0.13 µmol C cm^{-2} h^{-1} in the control treatments (Fig. 3 c, Tab. 2), but did not affect calcification in light (Fig. 3 b). High DIC also reduced growth of *A. millepora* by 23% with 0.2% bw d^{-1} compared to 0.16% bw d^{-1} in the controls (Fig. 3 a). In contrast, respiration rates as well as net and gross photosynthesis were not affected by high DIC (Fig. 4 a, b, c), although photochemical efficiency was significantly reduced by 6% from 0.58 to 0.55 (Fig. 5 a). Chl*a* and protein (Fig. 5b, c) contents of *A. millepora* were not affected by high DIC availability. High DIC availability did however significantly increase NOx uptake of the coral under light conditions by 21% from 0.017 to 0.021 µmol cm^{-2} h^{-1} (Fig. 6 a), while this was not the case under dark conditions (Fig. 6 b). Neither NH_4^+ nor PO_4^- uptake was influenced by high DIC availability under light or dark conditions (Fig. 6 c, d, e, f). In contrast, DOC release was stimulated through high DIC availability by 141% from 1.75 to 0.75 µmol cm^{-2} h^{-1}, but only in dark conditions (Fig. 6 g, h).

DOC

High DOC availability significantly increased BOD by 115% from 0.81 to 1.73 mg L^{-1} h^{-1} (Fig. 2). It did not affect the calcification rate measured during light or dark incubation (Fig. 3 b, c), but increased growth by 42% from 0.20 to 0.29% bw d^{-1} compared to the controls (Fig. 3 a). The high DOC treatment also reduced net photosynthesis by 5% from 1.24 to 0.63 µmol O_2 cm^{-2} h^{-1} (Fig. 4 b) and gross photosynthesis by 39% from 1.73 to 1.06 µmol O_2 cm^{-2} h^{-1}(Fig. 4 c). High DOC availability did not affect respiration rates of *A. millepora* (Fig. 4 a). Chl a and protein content along with photosynthetic efficiency were unaffected (Fig. 5 a, b, c). The same was observed for NOx fluxes (Fig. 6 a, b). Ammonium uptake however was increased by 36% from 0.007 to 0.009 µmol cm^{-2} h^{-1} (Fig. 6 c) during light conditions, but not during dark conditions. The latter was also true for PO_4^- fluxes (Fig. 6 d, e, f). DOC uptake rates were only, but highly increased in light incubations by 927% from 0.17 to 1.3 µmol cm^{-2} h^{-1} (Fig. 6 g, h).

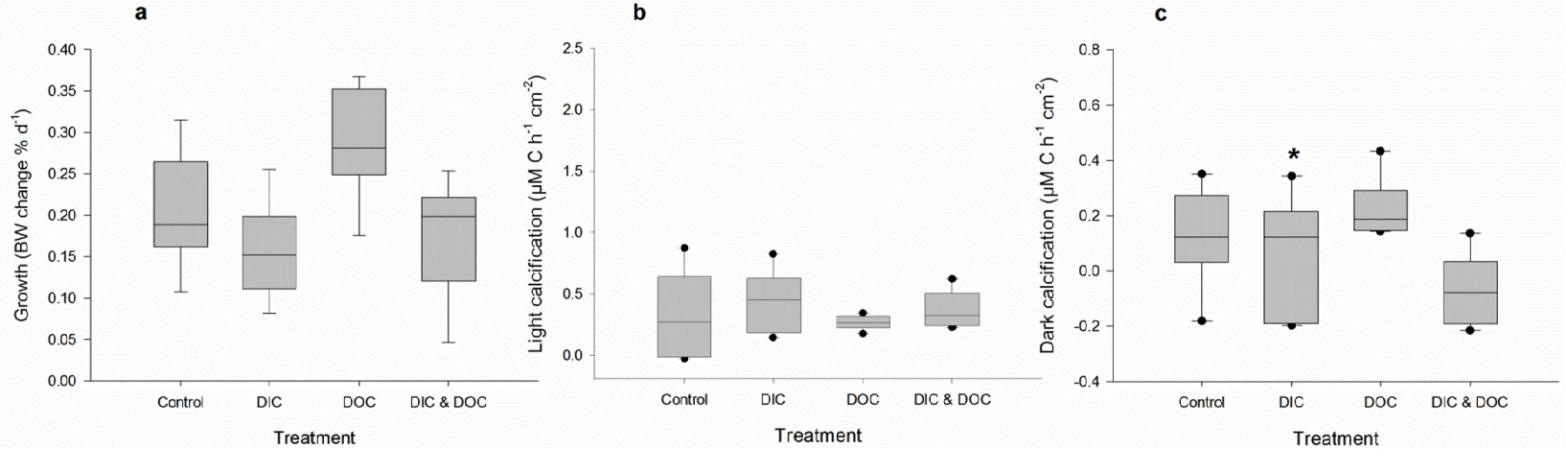

Figure 3. Physiological coral responses to treatments. Growth as (a) % change of buoyant weight (BW) of *Acropora millepora* (Ehrenberg, 1834) (n=12). Calcification during light (b) (150 µmol photons*$m^{-2}s^{-1}$) and dark condition (c) measured via alkalinity anomaly technique and related to surface area. Boxplots indicating median (mid of boxplot), 25% and 75% percentile (lower and upper border of boxplot) and 90 and 10% percentile (whiskers). Significant differences ($p < 0.05$) relative to controls are marked with an asterisk

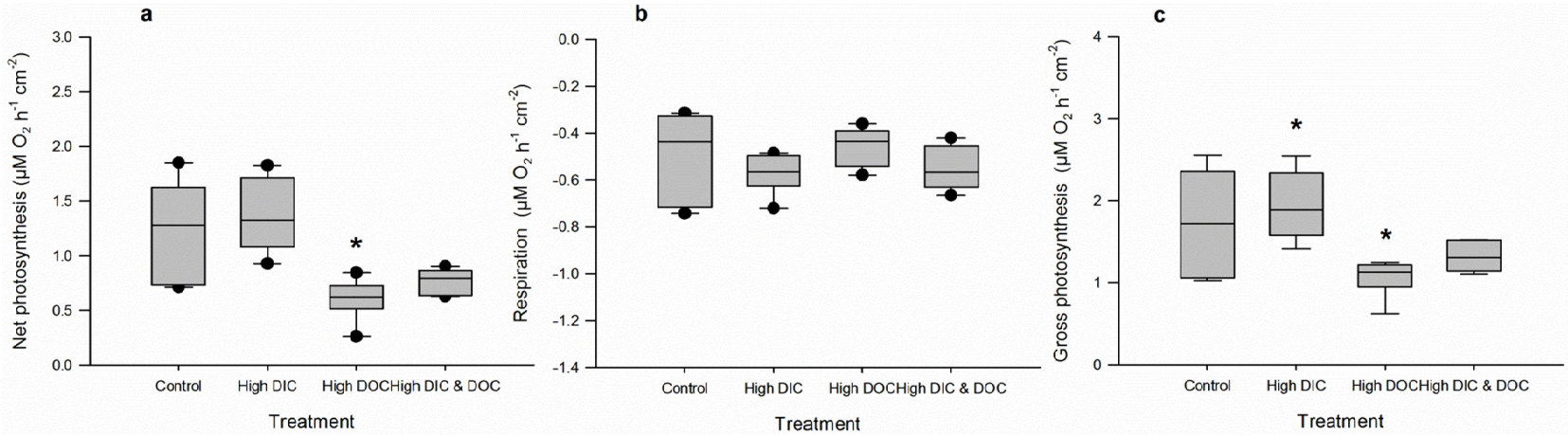

Figure 4. Oxygen fluxes as responses to treatments. Net photosynthesis (a), respiration (b) and gross photosynthesis (c) of *Acropora millepora* (Ehrenberg, 1834) (n=6). Net photosynthesis measured during light (150 µ photons $*m^{-2}s^{-1}$) conditions and respiration during dark condition and related to coral surface area. Significant differences ($p < 0.05$) are marked with an asterisk

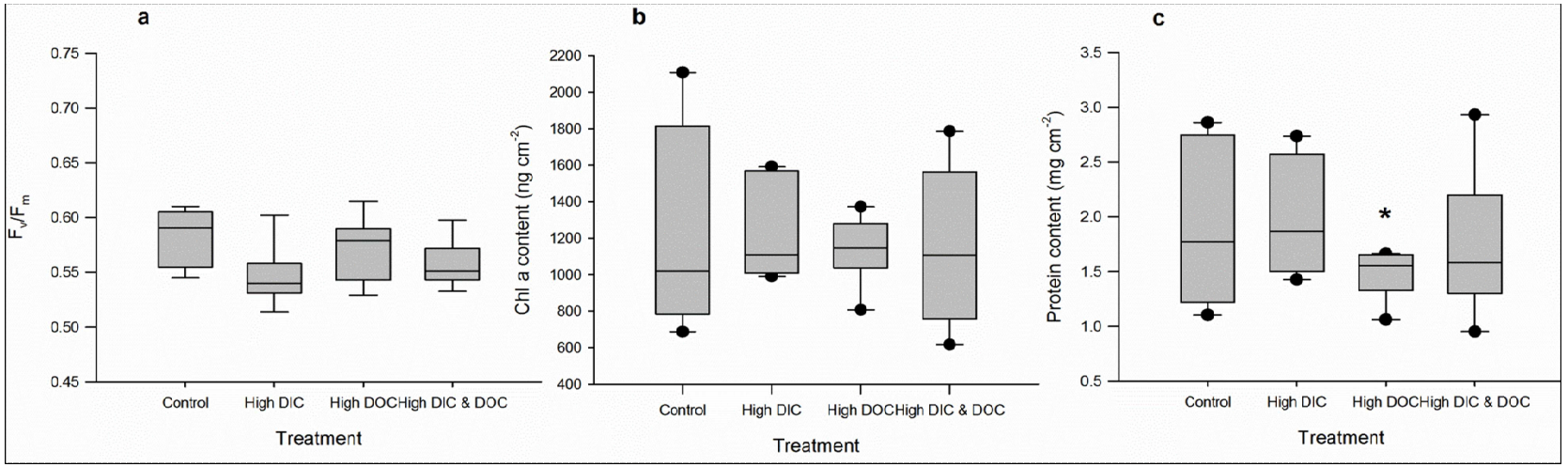

Figure 5. Photosystem parameters as response to treatments. Maximum quantum yield (a) of dark adapted individuals of *Acropora millepora* (Ehrenberg, 1834) (n=12). Chlorophyll content (b) related to fresh weight (n=6). Protein content (c) of *A. millepora* related to surface area (n=6). Significant differences ($p < 0.05$) are marked with an asterisk.

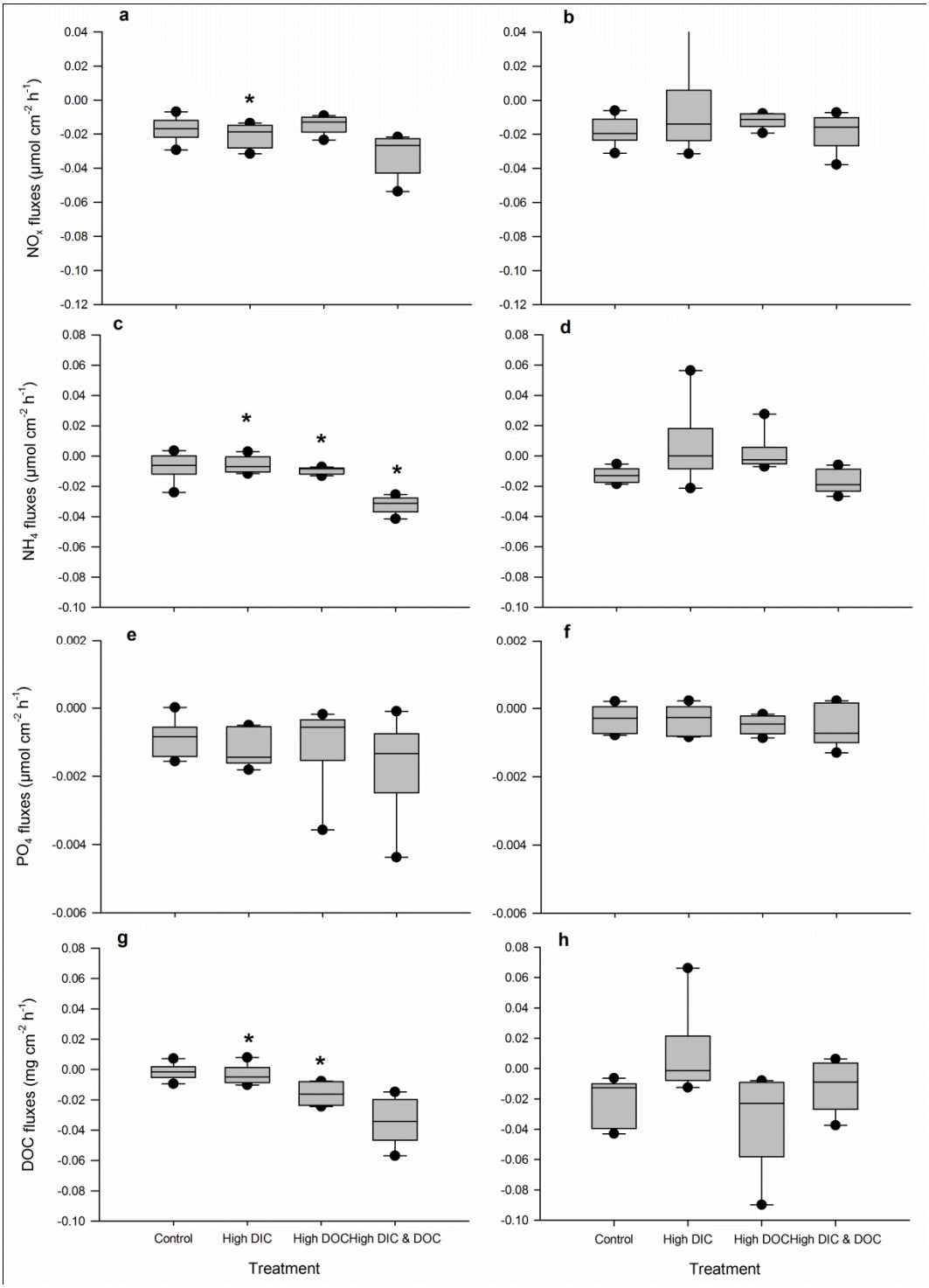

Figure 6. Nutrient fluxes as response to treatments. NO_x fluxes (a, b) , NH_4^+ fluxes (c, d) PO_4^- fluxes (e, f) and DOC fluxes (g, h) calculated from light (150 µmol photons $*m^{-2}s^{-1}$) (graphs on the left) and dark incubations (graphs on the right) of *Acropora millepora* (Ehrenberg, 1834) (n=12). Significant differences ($p < 0.05$) are marked with an asterisk

DIC and DOC

The combined high DIC and high DOC treatments led to additive and interactive effects on some of the variables measured. BOD increased further by another 81% compared to the DOC treatment and 197% compared to the controls, with 2.39 mg L^{-1} h^{-1} (Fig. 2) indicating a synergistic effect.
Coral growth under combined high DOC and DIC availability was similar compared to control conditions, but significantly lower than under high DOC conditions alone and not significantly higher than under high DIC treatment (Fig. 3 a). No significant change was observed for light calcification under the combined treatment (Fig. 3 b). In contrast, dark calcification was reduced by 105% compared to the DIC treatment and 150% compared to the control conditions (Fig. 3 c). High DOC and DIC did not show any combined effects on photosynthesis and respiration (Fig. 4 a, b, c). The same was observed for photosynthetic efficiency, Chl*a* content and protein content (Fig. 5 a, b, c). The uptake rates of NOx in the combined treatment compared to the controls and the DIC treatment were increased in light by 65% and 86%, respectively (Fig. 6 a). In the dark however, no significant differences were observed (Fig. 6 b). For NH_4^+ uptake rates, similar results were observed in both dark and light incubations (Fig. 6 c, d). In light, NH_4^+ uptake rates increased by 330% compared to the DOC treatment and 366% compared to the control. In the dark, NH_4^+ uptake rates increased by 75% compared to the DIC treatment and 100% compared to the controls. No such trend was observed for the uptake rates of PO_4^- (Fig. 6 e, f). However, in light the uptake rates of DOC in the combined treatment were increased by 1163% compared to the DOC treatment and by 2090% compared to the controls (Fig. 6 g). In the dark incubations, DOC uptake rates were not affected by high DOC and DIC concentrations (Fig. 6 h).

Discussion

Treatment conditions

The treatment levels of the high DIC treatment corresponded to set treatment conditions as aimed for [55] and control conditions were close to present levels [65] or below levels observed in inshore reefs with higher natural variability [19]. The pH under the high DOC concentration was further reduced, indicating higher bacterial activity as also shown by a reduction in oxygen saturation, the increase in bicarbonate ions and consequently a reduction of the aragonite saturation state. The addition of glucose twice a day was chosen to mimic natural fluctuation of bioavailable DOC as occurring during periods of heavy rainfall and river input which were found to correlate to high DOC concentrations [49–51]. In addition field concentrations of bioavailable DOC do not only change within season and time of the day [52], but are also readily taken up by e.g. corals themselves and mainly bacteria [41,52,66]. The total level of glucose added is comparable to other studies were monosaccharides as an increase for DOC were added [21,22,43] and was on the higher end of DOC concentrations

described for different reef settings in high DOC environments [21]. In our study we used glucose to experimentally increase DOC to assure reproducibility and due to the ease with which it can be obtained, applied and its concentrations determined. Future studies should now evaluate the effects of combined sugars or different algal exudates in combination with ocean acidification. The latter approach however would need to consider that concentrations of algae derived DOC change under different light conditions and are dependent on the species of algae [42,52].

The effects of high DIC availability

The BOD in the incubation chambers, an indicator of bacterial respiration during the experiment, did not change under high DIC conditions. This is consistent with a study on microbial biofilms from the GBR that also reported constant bacterial background respiration and nutrient fluxes despite different DIC levels [67]. Hence, bacterial communities either did not change during exposure to elevated DIC or rapidly acclimatized as suggested by Witt et al. (2011). High DIC did not affect light calcification and photosynthesis of *A. millepora*, but decreased dark calcification and growth. This contrasts with a previous study on an acroporid coral that reported a reduction of photosynthetic productivity under elevated DIC conditions [14]. However, in the before mentioned study high light dosages of up to 1200 µmol photons m^{-2} s^{-1} were used that reportedly induced bleaching and consecutively productivity loss. In the present experiment, the continuous light dose of 150 µmol photons m^{-2} s^{-1} was comparable to studies under natural light regimes that found no effect of elevated DIC on the productivity of corals [68,69]. We observed carbonate dissolution under dark incubations, which corroborates previous studies that demonstrated negative effects of elevated DIC on coral growth and a net dissolution under similar high pCO_2 levels [9,14,70]. However, in *A. millepora* dissolution occurred mainly under dark conditions. We show that the effect of ocean acidification on calcification becomes most visible when no photosynthetic activity is present in dark conditions. This supports recent findings that show that respiratory processes may enhance the negative effects of elevated DIC concentrations and are the main cause of reduced growth [20]. We found no change in Chl*a* and protein content which explains the stable productivity under elevated DIC concentrations. However, we recorded a significant reduction in photochemical efficiency, eventually also leading to reduced photosynthetic rates. During the 16 d experiment, we could detect the decline of photochemical efficiency, but no acclimation. Long-term experiments need to be conducted in order to determine whether this will cause a reduced productivity or eventual acclimation will lead to constant productivity compared to control conditions.
To our knowledge, the present study is the first to reveal that high DIC stimulates the uptake of NOx and the release of DOC of corals. The uptake rate of NOx under control conditions lies within described uptake rates for the genus *Acropora*, although nitrate concentrations were slightly elevated (1.3 µM, Table 2) compared to other studies (e.g. Bythell 1990, 0.22 - 1.72 µM). The induced NOx

uptake probably resulted from a higher demand for nitrogen to allow keeping productivity stable and on a high level, despite reduced photochemical efficiency. The observed increased DOC release on the other hand may have been caused by high availability of bicarbonate for photosynthesis ensuing increased carbon release when nitrate uptake rates were lower and nitrate becomes limiting [71].

The effects of high DOC availability

In contrast to the high DIC treatment, BOD values in the incubation chambers increased under high DOC. This is in line with other experimental studies investigating the responses of micro-organisms to elevated DOC [21,22,35]. While high DOC reduced photosynthesis of *A. millepora*, it did not affect its light or dark calcification rates, but significantly increased coral net growth. The reduced photosynthesis rates may have been the result of the high microbial respiration on the coral host as already indicated by the BOD values, which could have led to a reduced pH on the coral surface compared to the surrounding water. The observed increased net growth of the coral under high DOC availability was probably caused by heterotrophic compensation of losses in assimilates due to reduced photosynthesis and the surplus of bio-available organic carbon as energy source. This is supported by the finding that bleached corals can survive bleaching through increased heterotrophic feeding [72,73] and are able to maintain photosynthetic quantum yield during thermal stress [74]. Likewise, it was also observed that bleached corals can restore dark calcification when glycerol is added [75], and unbleached corals showed increased calcification rates under glucose addition [76]. The utilization of both ammonia and DOC during light hours under elevated DOC availability may indicate increased microbial activity via ammonia oxidation and carbohydrate metabolism, rather than direct uptake by the coral host itself. This is also supported by the significantly increased BOD. In contrast to other studies, no signs of disease or bleaching were found during the present study. Although the levels of DOC applied were increased by 500 % on average, they were low compared to other studies [21,22,43].

The combined effects of both high DIC and DOC availability

The combination of both high DIC and DOC availability in this study led to an even higher BOD compared to the DOC treatment effect alone, which has not been described before. This synergistic effect [77] was probably caused by altered, heterotrophic bacterial communities due to a higher stress reaction of the coral towards high DIC and DOC, as described for elevated DIC (Meron 2011) or DOC availability alone [21]. The combination of both factors significantly decreased dark calcification, increased ammonia, NOx and DOC uptake rates, but did not affect photosynthesis, light calcification or growth. The present study revealed that high DIC and DOC availability has additive negative effects, and the dark calcification was more reduced under the combined treatment than at high DIC levels alone. This may be due to the elevated bacterial respiration under high DOC conditions which

increased the DIC concentration locally above the level of the DIC treatment condition. Hence, the negative impact of the DIC treatment alone was potentially further enhanced due to respiratory processes as mentioned by other studies on DIC effects alone [20]. Overall growth was similar to the control conditions and may have been affected by the surplus of energy for calcification from the DOC treatment balancing out the DIC treatment effect. The increase in uptake rates of ammonia, NOx and DOC under the combined treatment compared to the individual treatments and the control may have been caused by higher bacterial activity, ammonia oxidation and nitrate uptake, as was already discussed for the effects of the single DIC and DOC treatments. However, it may also be a sign of shifts in microbial community structure due to excess energy derived from high DOC availability. Additionally, the combined effects of both treatments on the coral host may disrupt 'natural' bacterial-host interactions.

Ecological perspective

Our experiment is the first to show that, in addition to the previously described negative influences associated with increased DOC, such as enhanced microbial activity [21,35,39]; higher DOC availability positively impacted coral growth. On the other hand, however, we show that high DIC negatively impacts carbonate production of the investigated coral species, mainly due to increased dissolution rates at night. Finally, our high DIC/DOC combination treatment further amplified this negative effect, leading to even lower carbonate accretion rates. Thus, our results strongly suggest that the simultaneous occurrence of high DIC and DOC in present coastal waters, and likewise even more in future waters as a result of increasing anthropogenic coastal activities, constitutes a serious threat to corals putting their ecological functions and services such as habitat provisioning and coastal protection increasingly at risk.

Our study further demonstrates that BOD increases under high DOC availability, and shows an even stronger increase under combined high DIC/DOC concentrations. It is known that DOC concentrations lower than used in this study can already strongly increase bacterial oxygen consumption in the water, and higher concentrations may even cause local oxygen deficiency and coral death [21,79]. In the context of global change and increasing land-derived pollution, DOC concentrations and BOD are strong first indicators for shifts in bacterial regimes and we strongly advocate that both parameters are considered when assessing reef health in monitoring programs. The control and reduction of labile, highly bio-available DOC from land-derived sources through water management should also be taken into account when mitigating potential effects of riverine inputs on reefs.

Acknowledgements

The authors would like to thank the SeaSim team (especially Craig Humphrey) at AIMS for the provision of the coral nubbins. Furthermore, we would like to thank at Jane Wu Won at AIMS and for the support with the analysis of the TOC samples. In addition, we thank Florita Flores (general assistance) und Michelle Liddy (field + lab assistance).

Reference List

1. Doney SC, Fabry VJ, Feely R a, Kleypas J a. (2009) Ocean Acidification: The Other CO 2 Problem. Ann Rev Mar Sci 1: 169–192. Available: http://arjournals.annualreviews.org/doi/abs/10.1146/annurev.marine.010908.163834.

2. IPCC (2001) The Third assessment report of the Intergovernmental Panel on Climate Change (IPCC). Cambridge Univ Press.

3. Canadell JG, Le Quéré C, Raupach MR, Field CB, Buitenhuis ET, et al. (2007) Contributions to accelerating atmospheric CO2 growth from economic activity, carbon intensity, and efficiency of natural sinks. Proc Natl Acad Sci U S A 104: 18866–18870. Available: http://www.pubmedcentral.nih.gov/articlerender.fcgi?artid=2141868&tool=pmcentrez&rendertype=abstract.

4. Retallack GJ (2001) A 300-million-year record of atmospheric carbon dioxide from fossil plant cuticles. Nature 411: 287–290. Available: http://www.ncbi.nlm.nih.gov/pubmed/11357126.

5. Solomon S (2007) Climate change 2007: contribution of working group I to the fourth assessment report of the intergovernmental panel on climate change. Solomon S, editor Cambridge University Press, Cambridge, United Kingdom and New York, NY,. Available: http://scholar.google.com/scholar?q=Contribution+of+Working+Group+I+to+the+Fourth+Assessment+Report+of+the+Intergovernmental+Panel+on+Climate+Change#1. Accessed 5 August 2011.

6. Peters GP, Marland G, Le Quéré C, Boden T, Canadell JG, et al. (2011) Rapid growth in CO2 emissions after the 2008–2009 global financial crisis. Nat Clim Chang 2: 2009–2011. Available: http://www.nature.com/doifinder/10.1038/nclimate1332. Accessed 4 December 2011.

7. Zeebe RE, Wolf-Gladrow DA (2001) CO2 in seawater: equilibrium, kinetics, isotopes. Elsevier Science. Available: http://books.google.com/books?hl=en&lr=&id=VrumU3XvQ-gC&oi=fnd&pg=PP2&dq=Seawater:+Equilibrium,+Kinetics,+Isotopes,+&ots=0lJD0a2k3_&sig=6G0E8lNEEUyMZQByGa-_CV_RNao. Accessed 5 August 2011.

8. Hoegh-Guldberg O, Mumby PJ, Hooten a J, Steneck RS, Greenfield P, et al. (2007) Coral reefs under rapid climate change and ocean acidification. Science 318: 1737–1742. Available: http://www.ncbi.nlm.nih.gov/pubmed/18079392. Accessed 5 July 2011.

9. Ries JB, Cohen AL, McCorkle DC (2009) Marine calcifiers exhibit mixed responses to CO2-induced ocean acidification. Geology 37: 1131–1134. Available: http://www.unc.edu/~jries/Ries_2010_EARTH_ShellShocked_Biolgical_Effects_of_Ocean_Acidification.pdf. Accessed 6 July 2011.

10. Abbasi T (2011) Ocean Acidification: The Newest Threat to the Global Environment. Crit Rev Environ Sci Technol 41: 1601–1663. Available: http://www.tandfonline.com/doi/abs/10.1080/10643389.2010.481579. Accessed 12 July 2011.

11. Veron JEN (2011) Ocean Acidification and Coral Reefs: An Emerging Big Picture. Diversity 3: 262–274. doi:10.3390/d3020262.

12. Wittmann AC, Pörtner H-O (2013) Sensitivities of extant animal taxa to ocean acidification. Nat Clim Chang 3: 995–1001. Available: http://dx.doi.org/10.1038/nclimate1982. Accessed 14 December 2013.

13. Uthicke S, Momigliano P, Fabricius KE (2013) High risk of extinction of benthic foraminifera in this century due to ocean acidification. Sci Rep 3: 1769. Available: http://www.pubmedcentral.nih.gov/articlerender.fcgi?artid=3642656&tool=pmcentrez&rendertype=abstract. Accessed 27 May 2013.

14. Anthony KRN, Kline DI, Diaz-Pulido G, Dove SG, Hoegh-Guldberg O (2008) Ocean acidification causes bleaching and productivity loss in coral reef builders. Proc Natl Acad Sci U S A 105: 17442–17446. Available: http://www.ncbi.nlm.nih.gov/pubmed/18988740.

15. Diaz-Pulido G, Gouezo M, Tilbrook B, Dove SG, Anthony KRN (2011) High CO2 enhances the competitive strength of seaweeds over corals. Ecol Lett 14: 156–162. Available: http://www.pubmedcentral.nih.gov/articlerender.fcgi?artid=3047711&tool=pmcentrez&rendertype=abstract. Accessed 14 July 2011.

16. Kuffner IB, Andersson AJ, Jokiel PL, Rodgers KS, Mackenzie FT (2007) Decreased abundance of crustose coralline algae due to ocean acidification. Nat Geosci 1: 114–117. Available: http://www.nature.com/doifinder/10.1038/ngeo100. Accessed 9 July 2011.

17. Fabricius KE, Langdon C, Uthicke S, Humphrey C, Noonan S, et al. (2011) Losers and winners in coral reefs acclimatized to elevated carbon dioxide concentrations. Nat Clim Chang 1: 165–169. Available: http://www.nature.com/doifinder/10.1038/nclimate1122. Accessed 10 June 2011.

18. Uthicke S, Fabricius KE (2012) Productivity gains do not compensate for reduced calcification under near-future ocean acidification in the photosynthetic benthic foraminifer species Marginopora vertebralis. Glob Chang Biol 18: 2781–2791. Available: http://doi.wiley.com/10.1111/j.1365-2486.2012.02715.x. Accessed 28 March 2013.

19. Uthicke S, Furnas M, Lønborg C (2014) Coral reefs on the edge? Carbon chemistry on inshore reefs of the great barrier reef. PLoS One 9: e109092. Available: http://www.ncbi.nlm.nih.gov/pubmed/25295864. Accessed 10 October 2014.

20. Shaw EC, McNeil B, Tilbrook B (2013) Anthropogenic changes to seawater buffer capacity combined with natural reef metabolism induce extreme future coral reef CO2 conditions. Glob Chang Biol 19: 1632–1641. Available: http://doi.wiley.com/10.1111/gcb.12154. Accessed 17 January 2014.

21. Kline DI, Kuntz NM, Breitbart M, Knowlton N, Rohwer F (2006) Role of elevated organic carbon levels and microbial activity in coral mortality. Mar Ecol Prog Ser 314: 119–125. Available: http://www.int-res.com/abstracts/meps/v314/p119-125/.

22. Kuntz NM, Kline DI, Sandin SA, Rohwer F (2005) Pathologies and mortality rates caused by organic carbon and nutrient stressors in three Caribbean coral species. Mar Ecol Prog Ser 294: 173–180. Available: http://www.int-res.com/abstracts/meps/v294/p173-180/.

23. Smith JE, Shaw M, Edwards RA, Obura DO, Pantos O, et al. (2006) Indirect effects of algae on coral: algae-mediated, microbe-induced coral mortality. Ecol Lett 9: 835–845. Available: http://www.ncbi.nlm.nih.gov/pubmed/16796574. Accessed 17 January 2014.

24. Haas AF, Nelson CE, Rohwer F, Wegley-Kelly L, Quistad SD, et al. (2013) Influence of coral and algal exudates on microbially mediated reef metabolism. PeerJ 1: e108. Available: http://www.pubmedcentral.nih.gov/articlerender.fcgi?artid=3719129&tool=pmcentrez&rendertype=abstract. Accessed 24 March 2014.

25. Daniel MHB, Montebelo AAA, Bernardes MC, Ometto JPHB, Camargo PB de, et al. (2002) Effects of Urban Sewage on Dissolved Oxygen, Dissolved Inorganic and Organic Carbon, and Electrical Conductivity of Small Streams along a Gradient of Urbanization in the Piracicaba River Basin. Water Air Soil Pollut 136: 189–206. Available: http://link.springer.com/article/10.1023/A:1015287708170. Accessed 17 October 2013.

26. Alongi DM, McKinnon a D (2005) The cycling and fate of terrestrially-derived sediments and nutrients in the coastal zone of the Great Barrier Reef shelf. Mar Pollut Bull 51: 239–252. Available: http://www.ncbi.nlm.nih.gov/pubmed/15757725. Accessed 24 May 2013.

27. Hauri C, Fabricius KE, Schaffelke B, Humphrey C (2010) Chemical and Physical Environmental Conditions Underneath Mat- and Canopy-Forming Macroalgae, and Their Effects on Understorey Corals. PLoS One 5: e12685. Available: http://dx.doi.org/10.1371/journal.pone.0012685.

28. Fabricius KE, De'ath G, De'Ath G (2004) Identifying Ecological Change and Its Causes: A Case Study on Coral Reefs. Ecol Appl 14: 1448–1465. Available: http://www.esajournals.org/doi/abs/10.1890/03-5320. Accessed 27 July 2011.

29. Devantier L, De'ath G, Turak E, Done T, Fabricius KE (2006) Species richness and community structure of reef-building corals on the nearshore Great Barrier Reef. Coral Reefs 25: 329–340. Available: http://dx.doi.org/10.1007/s00338-006-0115-8.

30. Fabricius KE, De'ath G, McCook LJ, Turak E, Williams DM (2005) Changes in algal, coral and fish assemblages along water quality gradients on the inshore Great Barrier Reef. Mar Pollut Bull 51: 384–398. Available: http://www.sciencedirect.com/science/article/pii/S0025326X04003923.

31. Joo M, Raymond M a a, McNeil VH, Huggins R, Turner RDR, et al. (2012) Estimates of sediment and nutrient loads in 10 major catchments draining to the Great Barrier Reef during 2006-2009. Mar Pollut Bull 65: 150–166. Available: http://www.ncbi.nlm.nih.gov/pubmed/22405805. Accessed 3 June 2013.

32. Furnas M, Alongi DM, McKinnon D, Trott L, Skuza M (2011) Regional-scale nitrogen and phosphorus budgets for the northern (14°S) and central (17°S) Great Barrier Reef shelf ecosystem. Cont Shelf Res 31: 1967–1990. Available: http://linkinghub.elsevier.com/retrieve/pii/S0278434311003025. Accessed 17 July 2013.

33. Knutson TR, McBride JL, Chan J, Emanuel K, Holland G, et al. (2010) Tropical cyclones and climate change. Nat Geosci 3: 157–163. Available: http://www.nature.com/doifinder/10.1038/ngeo779. Accessed 24 May 2013.

34. Webster PJ, Holland GJ, Curry J a, Chang H-R (2005) Changes in tropical cyclone number, duration, and intensity in a warming environment. Science 309: 1844–1846. Available: http://www.ncbi.nlm.nih.gov/pubmed/16166514. Accessed 5 June 2013.

35. Haas AF, Nelson C, Kelly L, Carlson C (2011) Effects of coral reef benthic primary producers on dissolved organic carbon and microbial activity. PLoS One 6. Available: http://dx.plos.org/10.1371/journal.pone.0027973. Accessed 17 January 2014.

36. Haas AF, Wild C (2010) Composition analysis of organic matter released by cosmopolitan coral reef-associated green algae. Aquat Biol 10. Available: http://www.int-res.com/abstracts/ab/v10/n2/p131-138/. Accessed 17 January 2014.

37. Rasheed M, Wild C, Jantzen C, Badran M (2006) Mineralization of particulate organic matter derived from coral-reef organisms in reef sediments of the Gulf of Aqaba. Chem Ecol 22: 13–20. doi:10.1080/02757540500456823.

38. Wild C, Naumann MS, Haas AF, Struck U, Mayer FW, et al. (2009) Coral sand O2 uptake and pelagic–benthic coupling in a subtropical fringing reef, Aqaba, Red Sea. Aquat Biol 6: 133–142. doi:10.3354/ab00181.

39. Wild C, Niggl W, Naumann MS, Haas AF (2010) Organic matter release by Red Sea coral reef organisms—potential effects on microbial activity and in situ O2 availability. Mar Ecol Prog Ser 411: 61–71. doi:10.3354/meps08653.

40. Dinsdale E a, Pantos O, Smriga S, Edwards R a, Angly F, et al. (2008) Microbial ecology of four coral atolls in the Northern Line Islands. PLoS One 3: e1584. Available: http://www.pubmedcentral.nih.gov/articlerender.fcgi?artid=2253183&tool=pmcentrez&rendertype=abstract. Accessed 10 July 2014.

41. Gregg A, Hatay M, Haas AF, Robinett N, Barott KL, et al. (2013) Biological oxygen demand optode analysis of coral reef-associated microbial communities exposed to algal exudates. PeerJ 1: e107. Available: http://www.pubmedcentral.nih.gov/articlerender.fcgi?artid=3719127&tool=pmcentrez&rendertype=abstract. Accessed 25 April 2014.

42. Nelson CE, Goldberg SJ, Wegley Kelly L, Haas AF, Smith JE, et al. (2013) Coral and macroalgal exudates vary in neutral sugar composition and differentially enrich reef bacterioplankton lineages. ISME J 7: 962–979. Available: http://www.ncbi.nlm.nih.gov/pubmed/23303369. Accessed 19 November 2013.

43. Haas AF, Al-Zibdah M, Wild C (2009) Effect of inorganic and organic nutrient addition on coral–algae assemblages from the Northern Red Sea. J Exp Mar Bio Ecol 380: 99–105. Available: http://linkinghub.elsevier.com/retrieve/pii/S0022098109003712. Accessed 22 June 2011.

44. Kaczmarsky L, Richardson LL (2010) Do elevated nutrients and organic carbon on Philippine reefs increase the prevalence of coral disease? Coral Reefs 30: 253–257. Available: http://link.springer.com/10.1007/s00338-010-0686-2. Accessed 17 January 2014.

45. Dove SG, Kline DI, Pantos O, Angly FE, Tyson GW, et al. (2013) Future reef decalcification under a business-as-usual CO2 emission scenario. Proc Natl Acad Sci U S A 110: 15342–15347. Available: http://www.pubmedcentral.nih.gov/articlerender.fcgi?artid=3780867&tool=pmcentrez&rendertype=abstract. Accessed 15 November 2013.

46. Moya a, Huisman L, Ball EE, Hayward DC, Grasso LC, et al. (2012) Whole transcriptome analysis of the coral Acropora millepora reveals complex responses to CO_2-driven acidification during the initiation of calcification. Mol Ecol 21: 2440–2454. Available: http://www.ncbi.nlm.nih.gov/pubmed/22490231. Accessed 7 March 2013.

47. Kaniewska P, Campbell PR, Kline DI, Rodriguez-Lanetty M, Miller DJ, et al. (2012) Major cellular and physiological impacts of ocean acidification on a reef building coral. PLoS One 7: e34659. Available: http://www.pubmedcentral.nih.gov/articlerender.fcgi?artid=3324498&tool=pmcentrez&rendertype=abstract. Accessed 6 March 2013.

48. Doropoulos C, Ward S, Diaz-Pulido G, Hoegh-Guldberg O, Mumby PJ (2012) Ocean acidification reduces coral recruitment by disrupting intimate larval-algal settlement interactions. Ecol Lett: 338–346. Available: http://www.ncbi.nlm.nih.gov/pubmed/22321314. Accessed 4 March 2013.

49. Schaffelke B, Carleton J, Skuza M, Zagorskis I, Furnas MJ (2012) Water quality in the inshore Great Barrier Reef lagoon: Implications for long-term monitoring and management. Mar Pollut

Bull 65: 249–260. Available: http://www.ncbi.nlm.nih.gov/pubmed/22142496. Accessed 6 September 2014.

50. Ford P, Tillman P, Robson B, Webster IT (2005) Organic carbon deliveries and their flow related dynamics in the Fitzroy estuary. Mar Pollut Bull 51: 119–127. Available: http://www.ncbi.nlm.nih.gov/pubmed/15757714. Accessed 22 August 2014.

51. Schaffelke B, Thompson A, Carleton J, Cripps E, Davidson J, et al. (2008) Water quality and ecosystem monitoring program: Reef Water Quality Protection Plan: final report. Available: http://elibrary.gbrmpa.gov.au/jspui/handle/11017/406. Accessed 6 September 2014.

52. Mueller B, van der Zande R, van Leent P, Meesters E, Vermeij M, et al. (2014) Effect of light availability on dissolved organic carbon release by Caribbean reef algae and corals. Bull Mar Sci 90: 875–893. Available: http://www.ingentaconnect.com/content/umrsmas/bullmar/2014/00000090/00000003/art00012. Accessed 10 September 2014.

53. Meehl GAG, Stocker TF, Collins WD, Friedlingstein P, Gaye T, et al. (2007) Global climate projections. In: Solomon S, Qin D, Manning M, Chen Z, Marquis M, et al., editors. IPCC, 2007: Climate Change 2007: the physical science basis. contribution of Working Group I to the Fourth Assessment Report of the Intergovernmental Panel on Climate Change. Cambridge University Press, Cambridge, United Kingdom and New York, NY, USA. pp. 747–846. Available: https://publications.csiro.au/rpr/pub?list=BRO&pid=procite:1452cb7a-9f93-44ea-9ac4-fd9f6fd80a07. Accessed 18 July 2013.

54. Rogelj J, Meinshausen M, Knutti R (2012) Global warming under old and new scenarios using IPCC climate sensitivity range estimates. Nat Clim Chang 2: 248–253. Available: http://www.nature.com/doifinder/10.1038/nclimate1385. Accessed 12 March 2012.

55. Vuuren DP, Edmonds J, Kainuma M, Riahi K, Thomson A, et al. (2011) The representative concentration pathways: an overview. Clim Change 109: 5–31. Available: http://link.springer.com/10.1007/s10584-011-0148-z. Accessed 9 January 2014.

56. Vogel N, Uthicke S (2012) Calcification and photobiology in symbiont-bearing benthic foraminifera and responses to a high CO2 environment. J Exp Mar Bio Ecol 424-425: 15–24. Available: http://linkinghub.elsevier.com/retrieve/pii/S0022098112001736. Accessed 8 August 2012.

57. Robbins L, Hansen M, Kleypas J, Meylan S (2010) CO2calc—a user-friendly seawater carbon calculator for Windows, Max OS X, and iOS (iPhone). US Geol Surv Open-File Rep 2010-1280: 17. Available: http://scholar.google.com/scholar?q=CO2calc—A+user-friendly+seawater+carbon+calculator+for+Windows,+Max+OS+X,+and+iOS+(iPhone)#0. Accessed 18 July 2013.

58. Naumann MS, Niggl W, Laforsch C, Glaser C, Wild C (2009) Coral surface area quantification–evaluation of established techniques by comparison with computer tomography. Coral Reefs 28: 109–117. Available: http://www.springerlink.com/index/10.1007/s00338-008-0459-3. Accessed 1 May 2011.

59. Chisholm J, Gattuso J-P (1991) Validation of the alkalinity anomaly technique for investigating calcification and photosynthesis in coral reef communities. Limnol Oceanogr 36: 1232–1239. Available: http://www.jstor.org/stable/10.2307/2837472. Accessed 25 September 2012.

60. Gao K, Zheng Y (2009) Combined effects of ocean acidification and solar UV radiation on photosynthesis, growth, pigmentation and calcification of the coralline alga Corallina sessilis (Rhodophyta). Glob Chang Biol 16: 2388–2398. Available: http://doi.wiley.com/10.1111/j.1365-2486.2009.02113.x. Accessed 22 July 2011.

61. Jokiel P, Maragos J, Franzisket L (1978) Coral growth: buoyant weight technique. Coral reefs Res methods UNESCO, Paris. Available: http://scholar.google.com/scholar?q=Jokiel+P,+Maragos+J,+Franzisket+L+(1978)+Coral+growth:+buoyant+weight+technique&btnG=&hl=en&as_sdt=0,5#0. Accessed 17 January 2014.

62. Schmidt C, Heinz P, Kucera M, Uthicke S (2011) Temperature-induced stress leads to bleaching in larger benthic foraminifera hosting endosymbiotic diatoms. Limnol Oceanogr 56: 1587–1602. Available: http://www.aslo.org/lo/toc/vol_56/issue_5/1587.html. Accessed 7 June 2013.

63. Nush E (1980) Comparison of different methods for chlorophyll and phaeopigment determination. Arch Hydrobiol Beih 14: 14–36. Available: http://bases.bireme.br/cgi-bin/wxislind.exe/iah/online/?IsisScript=iah/iah.xis&src=google&base=REPIDISCA&lang=p&nextAction=lnk&exprSearch=144518&indexSearch=ID. Accessed 18 July 2013.

64. Leuzinger S, Anthony KRN, Willis BL (2003) Reproductive energy investment in corals: scaling with module size. Oecologia 136: 524–531. Available: http://www.ncbi.nlm.nih.gov/pubmed/12802676. Accessed 23 June 2013.

65. Dlugokencky E, Tans P (2013) Trends in Atmospheric Carbon Dioxide: Recent Global CO2. Available: www.esrl.noaa.gov/gmd/ccgg/trends/.

66. Smith JE, Shaw M, Edwards RA, Obura DO, Pantos O, et al. (2006) Indirect effects of algae on coral: algae-mediated, microbe-induced coral mortality. Ecol Lett 9: 835–845. Available: http://dx.doi.org/10.1111/j.1461-0248.2006.00937.x. Accessed 17 January 2014.

67. Witt V, Wild C, Anthony KRN, Diaz-Pulido G, Uthicke S (2011) Effects of ocean acidification on microbial community composition of, and oxygen fluxes through, biofilms from the Great Barrier Reef. Environ Microbiol 13: 2976–2989. Available: http://www.ncbi.nlm.nih.gov/pubmed/21906222. Accessed 17 January 2014.

68. Reynaud S, Leclercq N, Romaine-Lioud S, Ferrier-Pages C, Jaubert J, et al. (2003) Interacting effects of CO2 partial pressure and temperature on photosynthesis and calcification in a scleractinian coral. Glob Chang Biol 9: 1660–1668. Available: http://imars.usf.edu/~cmoses/PDF_Library/Reynaud_et_al_2003.pdf. Accessed 27 July 2011.

69. Schneider K, Erez J (2006) The effect of carbonate chemistry on calcification and photosynthesis in the hermatypic coral Acropora eurystoma. Limnol Ocean 51 1293 51: 1284–1293. Available: http://cat.inist.fr/?aModele=afficheN&cpsidt=17779348. Accessed 17 October 2013.

70. Manzello D, Kleypas J (2008) Poorly cemented coral reefs of the eastern tropical Pacific: Possible insights into reef development in a high-CO2 world. Proc Natl Acad Sci U S A 105: 10450–10455. Available: http://www.pnas.org/content/105/30/10450.abstract. Accessed 10 July 2013.

71. Bythell JC (1990) Nutrient uptake in the reef-building coral Acropora palmata at natural environmental concentrations. Mar Ecol Prog Ser 68: 65–69. Available: http://www.int-res.com/articles/meps/68/m068p065.pdf. Accessed 15 January 2014.

72. Anthony KRN, Hoogenboom MO, Maynard JA, Grottoli AG, Middlebrook R (2009) Energetics approach to predicting mortality risk from environmental stress: a case study of coral bleaching. Funct Ecol 23: 539–550. Available: http://doi.wiley.com/10.1111/j.1365-2435.2008.01531.x. Accessed 13 November 2013.

73. Grottoli AG, Rodrigues LJ, Palardy JE (2006) Heterotrophic plasticity and resilience in bleached corals. Nature 440: 1186–1189. Available: http://dx.doi.org/10.1038/nature04565. Accessed 13 November 2013.

74. Borell EM, Bischof K (2008) Feeding sustains photosynthetic quantum yield of a scleractinian coral during thermal stress. Oecologia 157: 593–601. Available: http://www.ncbi.nlm.nih.gov/pubmed/18618148. Accessed 13 November 2013.

75. Colombo-Pallotta MF, Rodríguez-Román A, Iglesias-Prieto R (2010) Calcification in bleached and unbleached Montastraea faveolata: evaluating the role of oxygen and glycerol. Coral Reefs 29: 899–907. Available: http://link.springer.com/10.1007/s00338-010-0638-x. Accessed 13 August 2013.

76. Cohen A, Holcomb M (2009) Why corals care about ocean acidification: uncovering the mechanism. Oceanography 22: 118–127. Available: http://darchive.mblwhoilibrary.org:8080/handle/1912/3179. Accessed 17 October 2013.

77. Dunne RP (2009) Synergy or antagonism—interactions between stressors on coral reefs. Coral Reefs 29: 145–152. Available: http://link.springer.com/10.1007/s00338-009-0569-6. Accessed 15 November 2013.

78. Meron D, Atias E, Iasur Kruh L, Elifantz H, Minz D, et al. (2011) The impact of reduced pH on the microbial community of the coral Acropora eurystoma. ISME J 5: 51–60. Available: http://www.ncbi.nlm.nih.gov/pubmed/20668489. Accessed 14 July 2011.

79. Weber M, Beer D de (2012) Mechanisms of damage to corals exposed to sedimentation. Proc … 109: E1558–E1567. Available: http://www.pnas.org/cgi/doi/10.1073/pnas.1100715109. Accessed 17 January 2014.

Table S1 Results of Two Way ANOVA for DIC and DOC as fixed factors and "aquarium " as nested factor. Degree of freedom (DF), sum of squares (SS) and mean square (MS) as well as F and P values are given. Data for gross and net photosynthesis were log10 transformed prior to analysis. Significant results are marked bold with an asterisk (*)

Response variable	Source of variation	DF	SS	MS	F-value	P-value
Biological oxygen	DIC	1	0.265	0.265	6.377	**0.036***
demand	DOC	1	5.009	5.009	120.766	**<0.001***
	DIC x DOC	1	0.394	0.394	9.510	0.015
	Residual	9	0.332	0.0415		
	Total	11	6.000	0.545		
Growth	DIC	1	0.0676	0.0676	4.8	0.0598
	DOC	1	0.0289	0.0289	5.07	0.054
	DIC x DOC	1	0.0114	0.0114	0	0.984
	Aquarium	8	0.0760148	0.009501854	2.9	**0.015***
	Residual	31	0.157	0.00412		
	Total	41	0.267	0.00651		
Light calcification	DIC	1	0.0631	0.0631	0.90	0.369
	DOC	1	0.0243	0.0243	0.35	0.571
	DIC x DOC	1	0.000472	0.000472	0.01	0.936
	Aquarium	8	0.5581167	0.06976458	1.65	0.218
	Residual	11	1.024	0.0539		
	Total	22	1.116	0.0507		
Dark calcification	DIC	1	0.191	0.191	8.08	**0.0217***
	DOC	1	0.00201	0.00201	0.08	0.778
	DIC x DOC	1	0.0787	0.0787	3.32	0.106
	Aquarium	8	0.1894387	0.023679	0.83	0.593
	Residual	12	0.532	0.0266		
	Total	23	0.804	0.0350		
Net	DIC	1	0.0496	0.0496	2.567	0.125
photosynthesis	DOC	1	0.453	0.453	23.445	**<0.001***
	DIC x DOC	1	0.00572	0.00572	0.296	0.592
	Aquarium	8	0.1269225	0.0158653	0.73	0.662
	Residual	12	0.387	0.0193		
	Total	23	0.895	0.0389		
Respiration	DIC	1	0.0439	0.0439	2.957	0.101
	DOC	1	0.00527	0.00527	0.355	0.558
	DIC x DOC	1	0.000457	0.000457	0.0308	0.736
	Aquarium	8	0.07187044	0.008983805	0.48	0.849
	Residual	12	0.297	0.0148		
	Total	23	0.346	0.0151		
Gross	DIC	1	0.0419	0.0419	5.68	**0.044***
photosynthesis	DOC	1	0.193	0.193	26.14	**<0.001***
	DIC x DOC	1	0.00158	0.00158	0.21	0.592
	Aquarium	8	0.0590336	0.007379199	0.42	0.886
	Residual	12	0.269	0.0134		
	Total	23	0.505	0.0220		
Maximum quantum yield	DIC	1	0.00699	0.00699	4.67	0.0627
	DOC	1	0.00000307	0.00000307	0.53	0.486
	DIC x DOC	1	0.00146	0.00146	0	0.976

	Aquarium	8	0.02665	0.003332	1.38	0.237
	Residual	36	0.0286	0.000666		
	Total	47	0.0370	0.000804		
Chlorophyll a content	DIC	1	287.783	287.783	0.00187	0.962
	DOC	1	41418.681	41418.681	0.269	0.573
	DIC x DOC	1	204.592	204.592	0.00133	0.968
	Aquarium	8	961368.1	120171	0.68	0.700
	Residual	12	2116668.558	176389		
	Total	23	3119946.614	135649.853		
Protein content	DIC	1	0.164	0.164	1.32	0.283
	DOC	1	0.699	0.699	5.63	**0.045***
	DIC x DOC	1	0.0460	0.0460	0.37	0.559
	Aquarium		0.993662	0.1242077	0.26	0.968
	Residual	20	6.775	0.339		
	Total	23	7.684	0.334		
NO_X fluxes	DIC	1	0.000666	0.000666	21.93	**0.006***
in light	DOC	1	0.000103	0.000103	3.41	0.243
	DIC x DOC	1	0.000289	0.000289	9.46	**0.0152***
	Aquarium	8	0.000243229	0.0000304036	0.31	0.948
	Residual	12	0.00143	0.0000716		
	Total	23	0.00249	0.000108		
NO_X fluxes	DIC	1	0.0000276	0.0000276	5.2	0.051
in dark	DOC	1	0.0000328	0.0000328	6.24	**0.037***
	DIC x DOC	1	0.000456	0.000456	1.99	0.195
	Aquarium	8	0.08068237	0.0100853	0.11	0.997
	Residual	12	0.00430	0.000215		
	Total	23	0.00481	0.000209		
NH_4 fluxes	DIC	1	0.000697	0.000697	17.813	**<0.001***
in light	DOC	1	0.00126	0.00126	32.288	**<0.001***
	DIC x DOC	1	0.000867	0.000867	22.162	**<0.001***
	Aquarium	8	0.0003170658	0.00003963	1.03	0.466
	Residual	12	0.000782	0.0000391		
	Total	23	0.00361	0.000157		
NH_4 fluxes	DIC	1	0.0000000663	0.0000000663	0.000280	0.987
in dark	DOC	1	0.000117	0.000117	0.495	0.490
	DIC x DOC	1	0.00210	0.00210	8.30	**0.0205***
	Aquarium	8	0.002020055	0.000252506	1.13	0.416
	Residual	12	0.00474	0.000237		
	Total	23	0.00695	0.000302		
PO_4 Fluxes	DIC	1	0.00000139	0.00000139	1.278	0.272
in light	DOC	1	0.000000491	0.000000491	0.451	0.509
	DIC x DOC	1	0.000000150	0.000000150	0.138	0.715
	Aquarium	8	0.001739491	0.0002174363	1.06	0.446
	Residual	12	0.0000218	0.0002048563		
	Total	23	0.0000238	0.00000104		
PO_4 Fluxes	DIC	1	0.00000964	0.00000964	0.898	0.355
in dark	DOC	1	0.0000136	0.0000136	1.270	0.273
	DIC x DOC	1	0.0000107	0.0000107	0.75	0.330
	Aquarium	8	2.993147	0.3741434	0.99	0.486
	Residual	12	0.000215	0.0000107		
	Total	23	0.000249	0.0000108		

DOC fluxes	DIC	1	0.000600	0.000600	16.23	**0.003***
in light	DOC	1	0.00303	0.00303	81.93	**<0.001***
	DIC x DOC	1	0.000389	0.000389	10.55	**0.011***
	Aquarium	8	0.0002962058	0.00003702	0.29	0.956
	Residual	12	0.00184	0.0000919		
	Total	23	0.00586	0.000255		
DOC fluxes	DIC	1	0.00393	0.00393	4.63	0.063
in dark	DOC	1	0.00162	0.00162	1.91	0.203
	DIC x DOC	1	0.0000808	0.0000808	0.09	0.767
	Aquarium	8	0.006790499	0.0008488124	2.01	0.133
	Residual	12	0.0119	0.000593		
	Total	23	0.0175	0.000761		

3 - The Physiological Response of Two Green Calcifying Algae From the Great Barrier Reef Towards High Dissolved Inorganic and Organic Carbon (DIC and DOC) Availability

Friedrich Wilhelm Meyer *[1], Nikolas Vogel[1,2], Mirta Teichberg [1], Sven Uthicke [2], Christian Wild [1,31] Department of Ecology, Leibniz Center for Tropical Marine Ecology (ZMT), Bremen, Germany

[2]Australian Institute of Marine Science, Townsville, Queensland, Australia

[3], Faculty of Biology and Chemistry, University of Bremen, Germany

[*] Corresponding author

Email: friedrich.meyer@zmt-bremen.de (FWM)

This manuscript has been accepted for publication in PLOS ONE

Abstract

Increasing dissolved inorganic carbon (DIC) concentrations associated with ocean acidification can affect marine calcifiers, but local factors, such as high dissolved organic carbon (DOC) concentrations through sewage and algal blooms, may interact with this global factor. For calcifying green algae of the genus *Halimeda*, a key tropical carbonate producer that often occurs in coral reefs, no studies on these interactions have been reported. These data are however urgently needed to understand future carbonate production. Thus, we investigated the independent and combined effects of DIC (pCO_2 402 µatm/ pH_{tot} 8.0 and 996 µatm/ pH_{tot} 7.7) and DOC (added as glucose in 0 and 294 µmol L^{-1}) on growth, calcification and photosynthesis of *H. macroloba* and *H. opuntia* from the Great Barrier Reef in an incubation experiment over 16 days. High DIC concentrations significantly reduced dark calcification of *H. opuntia* by 130 % and led to net dissolution, but did not affect *H. macroloba*. High DOC concentrations significantly reduced daily oxygen production of *H. opuntia* and *H. macroloba* by 78 % and 43 %, respectively, and significantly reduced dark calcification of *H. opuntia* by 70%. Combined high DIC and DOC did not show any interactive effects for both algae, but revealed additive effects for *H. opuntia* where the combination of both factors reduced dark calcification by 162 % compared to controls. Such species-specific differences in treatment responses indicate *H. opuntia* is more susceptible to a combination of high DIC and DOC than *H. macroloba*. From an ecological perspective, results further suggest a reduction of primary production for *Halimeda*-dominated benthic reef communities under high DOC concentrations and additional decreases of carbonate accretion under elevated DIC concentrations, where *H. opuntia* dominates the benthic community. This may reduce biogenic carbonate sedimentation rates and hence the buffering capacity against further ocean acidification.

Introduction

Marine calcifiers are facing both global and local threats due to human induced environmental changes. On a global scale, increased emissions from fossil fuel combustion lead to an increased carbon dioxide (CO_2) concentration in the atmosphere [1]. The dissolution of an increased amount of CO_2 in the world's ocean leads to an elevated bicarbonate concentration and a lowered pH of the oceans, causing ocean acidification (OA) and reducing the saturation state (Ω) of carbonates in seawater. Depending on different scenarios, the atmospheric

concentration of CO_2 is predicted to rise from today's level of app. 396 µatm [2] to between 850 and 1370 µatm by the year 2100 [3]. This increase in CO_2 or dissolved inorganic carbon (DIC) in the water affects marine life [4–6], and special focus has been put on the effects on marine calcifiers [7–11] which may exhibit a resulting loss in calcification and a weakened carbonate structure [5,12].

Calcifying green algae of the genus *Halimeda* play a major role in sediment formation and provide habitat for many species [13–16]. Because of their high abundance and fast growth[17], *Halimeda opuntia* (Linnaeus) J.V. Lamouroux, 1816 is one of the most prominent species of its genus, also in the Great Barrier Reef (GBR). *H. opuntia* represents the "sprawler" type, spreading out and growing attached to rock, sand or soft substrate; whereas another species of this genus, *Halimeda macroloba*, Decaisne, 1841, is a typical sand dweller, usual found in lagoon-like environments. Hence, recent studies investigated the effect of OA on the calcification of different species of *Halimeda* and found that calcification was reduced in terms of needle size of the calcium carbonate deposited or reduced inorganic carbon content, while photosynthetic activity was stable or increased by OA compared to controls [7,18–22].

In addition to the global threat OA, marine life is often also facing disturbances on a local scale, such as increased riverine runoff high in inorganic and organic nutrients and sediments. Reefs at inshore locations of the GBR are more exposed to these threats and already undergo changes leading to a shift from coral-dominated to more macro-algae-dominated reefs [23–25]. An often underrepresented chemical parameter in monitoring of water quality is dissolved organic carbon (DOC) which can fuel bacterial and pathogen growth as observed under the addition of labile sugars [26,27] as well as natural DOC sources [28] and thereby has severe effects on corals [29,30], leading to bleaching, disease spread and eventually mortality [29,30]. Average DOC concentrations in the GBR are 66 µmol L^{-1} [31] and can increase in flood plume to over 200 µmol L^{-1} [31] or even 583 µmol L^{-1} (7 mg L^{-1}) [32] or higher in other reef settings [29]. Elevated DOC concentrations, containing highly bioavailable molecules, such as sugars and amino acids, are a result of mostly two processes: increased sewage input connected with river runoff of agricultural land [32–34] and increased release of DOC into the surrounding water by primary producers, mainly benthic and/or planktonic algae [27,35–39]. As the latter is associated with dominance shifts from hard corals to algae during phase shifts, their contribution to the available DOC pool becomes more important [27,38,40]. Climate change and increased storm frequencies with more

pronounced seasons and higher precipitation [41,42] may also cause higher discharge of rivers, very likely resulting in increased DOC inputs into inshore waters of the GBR that have been found to correlate with high water discharge rates of rivers to the GBR [31,43]. Higher river inputs of DOC into marine waters can also carry less labile, refractory material which is not metabolized as fast by bacteria like as labile sugars [28,44], but can be co-metabolized under the presence of additional labile organic carbon [45].

Keeping in mind the known severe effects of DOC on corals, such as increased bacterial growth and disease spread, bleaching and mortality [26,29,40,46], it is surprising that no comparable studies have investigated the effects of elevated DOC on *Halimeda* or other calcifying algae. DOC as a local factor may occur simultaneously with other factors, such as DIC, which occurs on a global scale. Such multi-factor settings may show additive or even synergistic effects of the individual factors. In addition, antagonistic interaction may occur, where one factor reduces the effect of the other, resulting in a decreased organism response. To understand and predict the consequences of multiple factors on key reef species functioning, it is essential to conduct combined manipulation experiments.

Hence, in this study we investigated the independent and combined effect of high DIC and DOC concentrations on the physiology of two key calcifying green algae, *H. opuntia* and *H. macroloba* during a 16 day laboratory experiment.

Under elevated DIC concentration, we expect the calcification of both green algae to decrease and alter the inorganic carbon content of the algae. In addition, photosynthesis and connected photosystem parameters such as F_v/F_m and chlorophyll a content will likely decrease. Nutrient uptake may increase in order to compensate for decreased photosynthetic efficiency. Under elevated DOC concentrations, we hypothesise bacterial growth and connected bacterial respiration to increase and to negatively affect algal fitness, leading to reduced photosynthesis and chlorophyll a contents and ultimately to a reduction of calcification rates. Due to the growing bacterial numbers, we predict nutrient cycling to be enhanced. Hence, uptake rates of organic and inorganic nutrients may increase. Under the combination of both factors, we anticipate additive and synergistic effects leading to further reduced primary production and calcification. In response to both treatments, the physiological parameters measured may show correlation and give indication to what extent the physiology of the whole alga is altered.

Material and Methods

Specimen collection and preparation

Individual thalli of both species *H. opuntia* (50 to 100 segments per thallus) and *H. macroloba* (10 - 30 segments per thallus) were collected from reefs at Orpheus Island (S 18° 36.737', E 146° 29.110') under a GBMPA sampling permit G12/35236.1. Sand dwelling *H. macroloba* were potted into 80 mL plastic containers with ordinary beach sand. Both species were kept in 18 L experimental flow-through aquaria under controlled conditions (LED light, Aqua Illumination, 150 µmol photons m^{-2} s^{-1} at 12h/12h light-dark cycle, temperature 25 °C, salinity 34.3) for two weeks prior to the start of the experimental treatments.

Experimental setup

Prior to the experiment, two thalli of each alga species were randomly re-allocated to each of the experimental treatments, as described in detail below. The experiment was conducted over 16 days between 24 July and 9 August 2012 at the Australian Institute of Marine Science (AIMS). Three replicate open glass tanks of 18 L volume for the two treatments with different treatment levels were placed in alternating order (a total of 12 tanks, 3 controls, 3 high DIC, 3 high DOC and 3 high DIC and DOC). The treatments were pCO_2 in ambient and high availability (403 µatm and 996 µatm, respectively) and DOC in ambient and high availability (83 ± 10 and 294 ± 506 µmol L^{-1} with DOC added as glucose (D-glucose, Sigma Aldrich, purity > 99.5%). The target pCO_2 was 1000 µatm and was reached by pH manipulation via pure CO_2 gas injection by a potentiometric pH sensors controlled pH stat system (Aqua Medic, Germany) as described in Vogel and Uthicke [47]. The pH sensors were calibrated daily using Mettler Toledo NIST-/DIN- pH buffers. The pCO_2 levels corresponded to concentrations likely to be reached under the 'representative concentration pathways' (RCP) 6.0 to RCP 8.5 for the year 2100 [1,48,49]. DOC treatment concentrations were chosen in relation to previously described concentrations for coral reefs [29,40] and treatments applied in other studies [26,29,30]. Glucose, a sugar produced by algae and corals [38] was chosen as DOC enrichment as it is easy obtainable, shows high bacterial availability and also eases replication. Other sources of DOC such as the collection of algal or coral exudates were not feasible for the extent of this study and quantification, as well as qualification of the DOC used for the treatment would be challenging. The DOC treatment was achieved by additions of 1170 µmol L^{-1} DOC (Glucose, D-Glucose, Sigma Aldrich) twice daily at 8:00 and 20:00.

Subsequent dilution resulted in average concentrations of 294 µmol L^{-1} over 12 h. To determine the resulting DOC concentrations due to dilution in the treatments, we measured the DOC concentrations in duplicates from 8:00 after the glucose addition every hour for three hours and then every other hour for eight hours until 18:00. Flow-through rates for the tanks were adjusted to 150 mL min^{-1} using freshly filtered (0.5 µm) natural seawater to avoid accumulation of particles that had not been previously captured by the settlement tanks. To provide additional water movement, aquaria pumps (AquaWorld, Australia, 250 L h^{-1}) were placed in each specimen tank. To determine alkalinity (A_T), a 50 ml water sample of each tank was drawn at the beginning, middle and end of the experiment. It was measured by gran-point titration with a Metrohm 855 autosampler (Metrohm, Switzerland) using 0.5 M HCl [50] and was corrected to certified reference material (CRM Batch 106, A. Dickson, Scripps Oceanographic Institute). Carbonate system parameters were calculated with CO2calc software [51] from A_T in combination with pH readings obtained from a multiprobe (WTW 3430, Germany) calibrated with Mettler Toledo NIST-/DIN- pH buffers.

Measurement of water column Biological Oxygen Demand (BOD)

To assess effects of elevated organic or inorganic carbon availability on microbial respiration rates, BOD of the treatment water was measured at the end of the experiment for each treatment tank (n = 3). For this purpose, 200 mL of unfiltered seawater were incubated for 24 h in the dark under temperature conditions of the treatments in borosilicate bottles. The O_2 concentration (mg L^{-1} and % saturation) as well as salinity and temperature were recorded before and after the incubation, and O_2 consumption rates were calculated from these two values and related to water volume and time to mg O_2 L^{-1} h^{-1}.

Quantification of algae surface area

In order to relate the measured rates of calcification, photosynthesis and nutrient fluxes to individual surface area of the thalli, the surface area was determined using images of the flattened algae and Image J software. Surface area varied for *H. opuntia from* 5 to 35 cm² and for *H. macroloba* from 4 to 30 cm².

Quantification of Light-/ dark calcification and nutrient fluxes

After 16 days under experimental conditions, two algal thalli from each replicate tank were transferred into individual acid-washed nalgene chambers (200 mL) and incubated for 60 min in light and 60 min in darkness. Water for the incubations was taken from the treatments (filtered, 0.5 µm) of the corresponding organisms. Therefore, pH of the incubations corresponded to treatment conditions. DOC in the form of Glucose was added in the concentration of 940 µmol L^{-1} prior to each incubation to assure similar concentrations. The background concentration of DOC was checked before the incubation and was 83 ± 10 µmol L^{-1}. Incubations were performed in 12 parallel incubations including two blanks per treatment. To meet light conditions similar to the treatment tanks, individual white LEDs (4000 K, Megaman, Germany) were installed above each incubation chamber and adjusted individually, using a quantum sensor (Apogee, USA). During the incubation, chambers were placed into a temperature controlled water bath at 25 °C, equal to the temperature during the 16 day incubation. Water movement during the incubation time was maintained using glass-coated magnetic stir bars driven by magnetic stir plates.

Light- and dark calcification rates were determined by the change of A_T during the incubation related to blanks using the alkalinity anomaly technique [52]. To achieve this, a sample of 50 mL incubation water was titrated as described above for the carbonate system parameters. A_T was calculated by non-linear regression fitting between pH 3.5 and pH 3.0. Calcium carbonate precipitation or dissolution expressed in µM C h^{-1} was calculated by half molar of the difference between the post incubation and the blank seawater A_T readings, volume of chamber, time of incubation and organism surface area [53]. For the calculation of daily calcification rates, the data were extrapolated for a 12 h light and 12 h dark cycle using light calcification and dark calcification data obtained from one h incubations.

Nutrient fluxes in the chambers were determined by analysing sub-samples of seawater from light and dark incubations for dissolved inorganic nutrients (DIN) as ammonium (NH_4^+), phosphate (PO^{3-}) and nitrite (NO_2^-) + nitrate (NO_3^-) as NO_x and total organic carbon (TOC as Non Particulate Organic Carbon) directly subsequent to the experimental runs. Samples for DIN were filtered using 0.45 µm syringe filters and kept frozen at -20 °C until measurement by segmented flow analysis (Seal Analytical, USA). Samples for DOC were filtered through 0.45 µm, acidified with 150 µL fuming HCl and frozen at -20 °C until analysis on a Shimadzu TOC-5000A (Shimadzu, USA). Nutrient fluxes were calculated and corrected for the fluxes of the blank incubations, related to organism surface area and expressed as µmol cm^2 h^{-1}.

Measurement of photosynthetic maximum quantum efficiency and oxygen production

Maximum quantum efficiency (F_v/F_m) of dark adapted algae was determined by Pulse Amplitude Modulation (PAM) fluorometry using a diving PAM (Walz, Germany) and a 6 mm diameter fiber optic cable. F_v/F_m measurements were conducted, one hour after the lights turned off automatically. Measurements were taken every evening during the course of the 16d experiment and during the acclimation phase before the experiment,

O_2 concentrations were monitored continuously during the incubations by three 4-channel O_2 meters (Firesting, Pyroscience, Germany), connected to each chamber with fiber optic cables. Net photosynthesis, respiration, and resulting gross photosynthesis were determined in µM O_2 h^{-1} relative to organism surface area. In addition, O_2 consumption was corrected to blank readings from incubation chambers containing only the respective treatment water. For the calculation of daily oxygen evolution rates, the data were extrapolated for a 12 h light and 12 h dark cycle using net photosynthesis and respiration data obtained from one h incubations.

Quantification of growth rates

Growth was determined only for *H. opuntia* as *H. macroloba* (a sand dweller) was kept attached to sediment during the course of the incubation, and this would have interfered with the buoyant weight technique [54]. Individual thalli of *H. opuntia* (n = 6) were weighed (accuracy: 0.1 mg, Mettler Toledo, USA) in a custom-build buoyant weight set-up with water jacket and seawater of constant temperature (25 °C) and salinity (34.5) at the start and end of the experiment. Growth of the organisms was expressed as daily percentage of weight change over the course of the 16 d experiment.

Quantification of algae pigment content

For the determination of chlorophyll *a* (Chl *a*) content, thalli (n = 6) were frozen to -80° C after incubations. Modified from Schmidt et al. [55] and Vogel and Uthicke [47], apical segments of algae were placed in 15 mL Falcon tubes on ice, and 4 mL of cold ethanol (95% EtOH) was added to extract chlorophyll. To break the inner skeleton of the algae, segments were crushed with a homogenizer, and the samples were heat-shocked in a water bath at 78° C for 5 min. Afterwards, samples were put in a fridge at 4 °C for 24 h further extraction, and

absorbencies of the supernatant were read at 750 nm and 664 nm on a Powerwave microplate reader (BioTek, USA). Chl*a* content of algal thalli were calculated after equations by Nusch [56] and standardized to segment fresh weight.

Quantification of carbon and nitrogen contents in algal tissues

Apical segments of *H. opuntia* and *H. macroloba* (n = 6) were dried at 60 °C for 48 h immediately after the incubation. Segments were ground to homogenous powder with a mortar and pestle, and pre-balanced amounts of the homogenate (MX-5 microbalance accuracy: 1µg, Mettler Toledo, Germany) were analysed for total nitrogen and total carbon content on a Euro EA elemental analyser (HEKAtech, Germany). Organic carbon was determined on pre-weighted samples after removing C_{inorg} by acidifying the sample with 300 µL concentrated (37 %) HCl. Inorganic carbon content was calculated by subtracting C_{org} from C_{tot}.

Statistical analyses

All data are given with averages and standard deviation in parentheses. We tested all individual responses for significant differences of the individual and combined treatments using a Two-Way-ANOVA. Data was tested for normality using the Shapiro-Wilk test and for equal variance using the Levene median test. Data of net and gross photosynthesis were $\log_{10}$ transformed to meet the criteria of equal variance. The Two Way ANOVA was performed with the treatments DIC and DOC as fixed factors and "aquarium" as nested factor. In case the interaction term was significant, differences between individual treatment combinations were evaluated, using a Pairwise Multiple Comparison Procedure (Holm-Sidak method). To further elucidate correlations between response variables, a Pearson product moment correlation was performed and a correlation based Principal Component Analysis (PCA) of all grouped response variables was used to identify covariance among response variables. We considered strong correlation (loadings) of the PC and the response variable to be higher than 0.69. In addition the correlation of NO_x fluxes, PO_4 fluxes and DOC fluxes were plotted in relation to the respiration rate for *H. opuntia* and the Pearson product moment correlation was given. All statistical analyses were conducted using SigmaPlot 12.5, NCSS Statistical Software and Statistika 12.0.

Results

Effects of DIC

The biological oxygen demand was relatively low and did not differ between control and high DIC conditions. Elevated DIC conditions (Table 1) did not affect the growth rate of *H. opuntia*, or light calcification of both species, but significantly reduced dark calcification rate of *H. opuntia* by 130 % (Fig. 1, $p < 0.001$, $F = 55.05$) although there was a tank effect ($p = 0.033$, $F = 3.25$). Dark calcification of *H. macroloba,* however, was also not affected by high DIC. High DIC did not affect net and gross photosynthesis and respiration (Fig. 2), which resulted in no effect on the daily photosynthesis rates of both species (Fig. 3). Due to the reduction of dark calcification in *H. opuntia* under high DIC, the daily calcification rate was reduced by 45 % compared to control conditions (Fig. 3) but also showed a tank effect ($p = 0.026$, $F = 3.47$). In contrast, high DIC conditions did not affect daily calcification rate of *H. macroloba.* Maximum quantum yield as F_v/F_m or Chl*a* content along with inorganic carbon, organic carbon and nitrogen content were not affected in either species (Fig. 4, 5).

NO_x uptake under both dark and light conditions were not affected by high DIC for *H. macroloba*, but significantly increased by 45 % for *H. opuntia* under dark conditions (S1 Fig., $p = 0.02$, $F = 12.76$). A similar pattern was observed for NH_4 uptake where high DIC did not affect the uptake of NH_4 by *H. macroloba* under both light and dark conditions, but significantly increased the uptake of NH_4 by *H. opuntia* under light conditions by 25 % (S2 Fig., $p = 0.002$, F 12.68) including a tank effect ($p = 0.007$, $F = 5.02$). Under dark conditions however, NH_4 uptake of *H. opuntia* was reduced by 85 % ($p = 0.003$, $F = 18.44$). Under high DIC conditions, the PO_4 uptake of both species was affected. For *H. macroloba,* PO_4 uptake was reduced under light conditions by 17 % and increased under dark conditions by 27 % compared to the controls (S3 Fig., $p = 0.027$, $F = 7.27$). For *H. opuntia,* PO_4 uptake was significantly increased under light conditions by 93 % ($p = 0.01$, $F = 4.99$) and under dark conditions by 42 % compared to the controls where also a tank effect ($p = 0.048$, $F = 2.89$) was detected. The DOC uptake rates were not significantly affected by DIC for both species and were only slightly reduced for *H. macroloba* by 86% and increased for *H. opuntia* by about one order of magnitude under light conditions (S4 Fig.).

Effects of DOC

The biological oxygen demand increased by 115 % in the high DOC treatment compared to the controls. High DOC concentrations (Table 1) did not affect the growth of *H. opuntia* (Fig. 1). Light calcification of both species was also not affected by high DOC, but the dark calcification rate was reduced for *H. opuntia* by 70 % (Fig. 1, $p < 0.001$, $F = 11.42$) and a tank effect was detected ($p = 0.033$, $F = 3.25$). Net and gross photosynthesis of *H. macroloba* were also reduced under the DOC treatment by 32 and 25 %, respectively ($p = 0.005$, $F = 14.25$ for net photosynthesis, $p = 0.009$, $F = 11.39$ for gross photosynthesis) (Fig. 2). Similar results were observed for *H. opuntia* with a reduction of only net photosynthesis of 45 and 46 %, ($p = 0.002$, $F = 20.5$). Respiration was only affected by the high DOC treatment for *H. opuntia* and resulted in an increased respiration of 37 % ($p = 0.004$, $F = 16.38$). As a result of the reduced photosynthesis rates of both species under high DOC, daily oxygen production rates of both species were significantly reduced by 78 % for *H. macroloba* (p 0.004, $F = 15.85$) and by 32 % from *H. opuntia* (Fig. 3, $p < 0.001$, $F = 57.97$). In contrast, the daily calcification rate of both algal species was not affected (Fig. 3).

Chl *a* content was reduced by 13 %, for *H. opuntia* only (Fig. 4, $p = 0.01$, $F = 8.16$). For the elemental composition no significant effects of the DOC treatment was observed, the C_{org}/N ratio was slightly increased for both species under the high DOC treatment compared to the controls (Fig 5). For *H. macroloba,* C_{org}/N was increased by 28 % from and for *H. opuntia* by 21 % (Fig. 5). NO_x uptake of both algae species was increased only under dark conditions by 51 % for *H. macroloba* ($p = 0.0027$, $F = 18.27$) and by 117 % for *H. opuntia* (S1 Fig., $p = 0.002$, $F = 3.28$). Ammonia uptake rates of both species in light and dark conditions were not affected by elevated DOC concentrations (S2 Fig.). PO_4 fluxes of *H. opuntia* only increased by 45 % during dark (S3 Fig., $p = 0.03$, $F = 7.42$).

DOC uptake rates for *H. macroloba* and *H. opuntia* were affected under both dark and light conditions and increased by 458 % from ($p = 0.032$, $F = 6.76$) in the light and by 369 % ($p = 0.007$, $F = 1.17$) in the dark for *H. macroloba*. For *H. opuntia,* DOC uptake rates were highly increased by 6854 and 331 % ($p < 0.001$, $F = 38.88$ and $p < 0.001$, $F = 35.59$) (S4Fig.) but a tank effect was detected ($p = 0.016$, $F = 4.00$).

Effects of the combined treatment

The biological oxygen demand was significantly increased by the combined treatment compared to the DOC treatment by another 81 %. In the combined treatment, response

variables of the individual treatments showed additive effects as well as synergistic effects. For the dark calcification rate of *H. opuntia,* negative effects of both DOC and DIC treatment alone were additive and resulted in further decrease of dark calcification by another 30 % compared to the DIC and 100 % compared to the DOC treatment (Fig. 1, 3). Similarly, NO_x uptake of *H. opuntia* under dark conditions increased by 90 % compared to the DIC treatment and by 48 % compared to the DOC treatment (S1Fig.). This effect was synergistic, leading to a higher effect as the sum of both individual treatment effects alone. Antagonistic effects and increase of NH_4 uptake was observed for *H. opuntia* under dark conditions where the uptake rate was increased in the presence of both, high DIC and DOC concentrations by 236 % (S2Fig.). PO_4 uptake in the dark showed additive effects of the individual treatments which lead to a higher PO_4 uptake rate of 33 % compared to the DIC treatment and 30 % compared to the DOC treatment alone (S3Fig.). DOC uptake rates of *H. opuntia* in the dark were 390 % higher than in the DIC treatment alone and 90 % higher than in the DOC treatment resulting in an increase of 420 % compared to the control conditions (S4Fig.).

Connection between the different response variables

The correlation of nutrient and DOC fluxes against the respiration rate of *H. opuntia* showed that with increasing respiration rates, NO_x, PO_4 and DOC uptake rates increased under high DOC concentrations (Fig. 6). For the uptake of DOC (Fig. 6 b) as well as PO_4 (Fig. 6 c) no significant correlation to the respiration rate was detected under low DOC conditions but NO_x uptake rates showed that with increasing respiration rates less NO_x is taken up under low DOC conditions compared to high DOC conditions. The PCA of all data from *H. macroloba* combined for the DIC treatment and DOC treatment showed that 29 and 21 % of the total variance among the response variables could be explained by principal component (PC) 1 and PC2, respectively (Table 2, Fig. 7 a). The highest correlations (factor loadings) with PC 1 were found in DOC fluxes in the dark and light, the daily calcification rate and net photosynthesis. On PC 2, only the carbon to nitrogen ratio and the total nitrogen content made a significant contribution. For *H. opuntia,* 21 and 18% of the total variance among the response variables was found in PC1 and PC2, respectively (Table 3, Fig 7 b). The highest factor loadings on PC 1 were found in PO_4 fluxes under dark and light conditions, NO_x fluxes in the dark as well as total nitrogen and organic carbon content and inorganic carbon content and the respiration rate. For PC 2, net photosynthesis and the daily photosynthesis rate made a significant contribution.

Table 1. Carbonate system parameters. Values calculated using CO2Calc with total alkalinity and pH_{tot} as input parameters. (n = 3 for TA measurements, n = 10 for pH, temp, salinity and O_2). Number in parenthesis are standard deviation.

Treatment	pH [Total]	temp [°C]	Salinity [ppt]	% O_2Sat	TA (µmol/kgSW)	pCO_2 (µatm)	HCO_3^- (µmol/kgSW)	Ω_{Ar}
Control	8.038	25.4	34.4	105.4	2276	402	1776	4.12
	(0.031)	(0.2)	(0.1)	(4.7)	(13)	(11)	(15)	(1.2)
High DIC	7.707	25.3	34.4	105.9	2281	996	2011	2.16
	(0.038)	(0.1)	(0.1)	(5.7)	(7)	(26)	(8)	(0.63)
High DOC	8.022	25.2	34.4	104.8	2286	430	1792	3.96
	(0.033)	(0.3)	(0.1)	(6.3)	(10)	(10)	(8)	(1.17)
High DOC & DIC	7.686	25.0	34.4	104.2	2282	1081	2032	2.01
	(0.029)	(0.4)	(0.1)	(5.4)	(17)	(95)	(12)	(0.61)

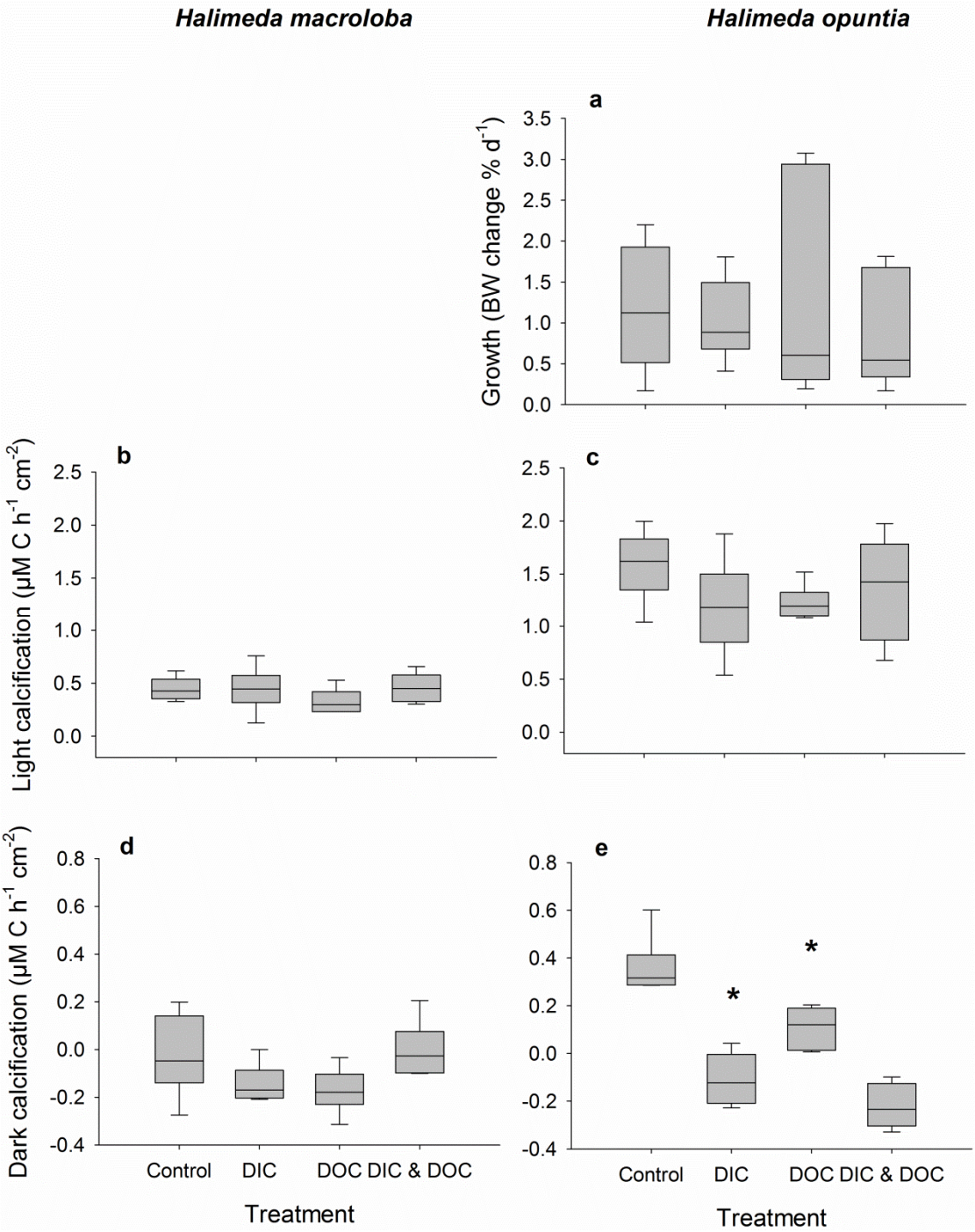

Fig. 1. Growth parameters as treatment response after experimental duration of 16 d. Treatments were controls (ambient DIC and DOC), DIC (high DIC and ambient DOC), DOC (ambient DIC and high DOC) and DIC &DOC. Growth is expressed as % change of buoyant weight (a) of *Halimeda opuntia* (n = 6). Calcification during light (b, c; 150 µE m^{-2} s^{-1}) and dark condition (d, e) of *Halimeda macroloba* (b, d, n = 6) and *Halimeda opuntia* (c, e, n = 6) measured via alkalinity anomaly technique and standardized to surface area. Significant differences compared to controls ($p < 0.05$) are marked with an asterisk. Box plots show the median as well as the upper and lower quartile. Whiskers indicate the 95 percentile.

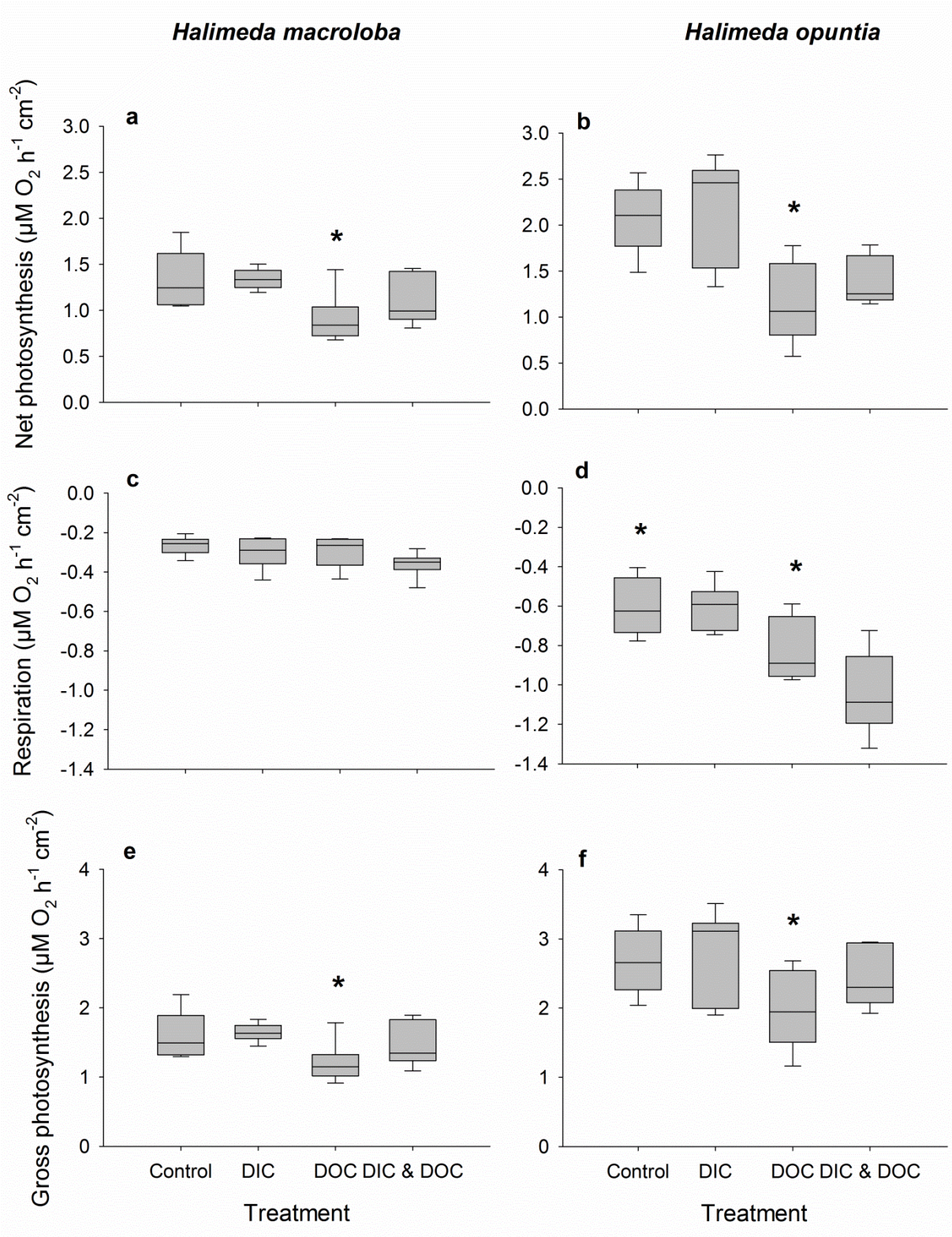

Fig. 2. Oxygen fluxes as treatment response. Oxygen fluxes as net photosynthesis (a, b), respiration (c, d) and growth photosynthesis (e, f) of *Halimeda macroloba* (a, c, e; n = 6) and *Halimeda opuntia* (b, d, f; n = 6). Net photosynthesis measured during light (150 µE m^{-2} s^{-1}) conditions and respiration during dark condition and standardized to surface area. Significant differences compared to control ($p < 0.05$) are marked with an asterisk.

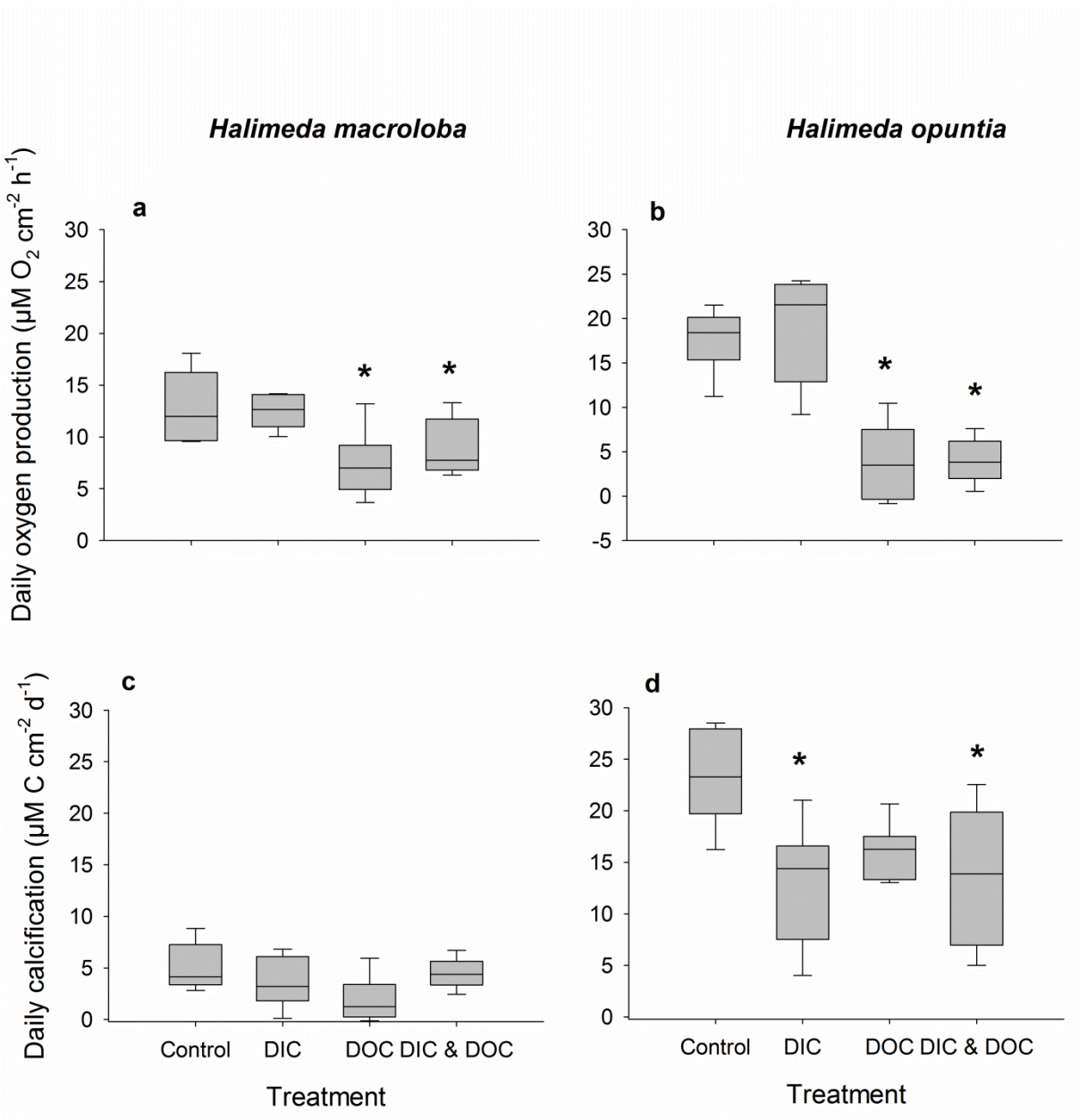

Fig. 3. Oxygen production and calcification as treatment response. Oxygen fluxes are calculated over a 12 hour day (150 µE m^{-2} s^{-1}) and 12 hour night cycle, of *Halimeda macroloba* (a, n = 6) and *Halimeda opuntia* (b, n = 6).Calcification calculated over a 12 hour day (150 µE m^{-2} s^{-1}) and 12 hour night cycle (c, d). Both responses were standardized to surface area. Significant differences compared to control ($p < 0.05$) are marked with an asterisk.

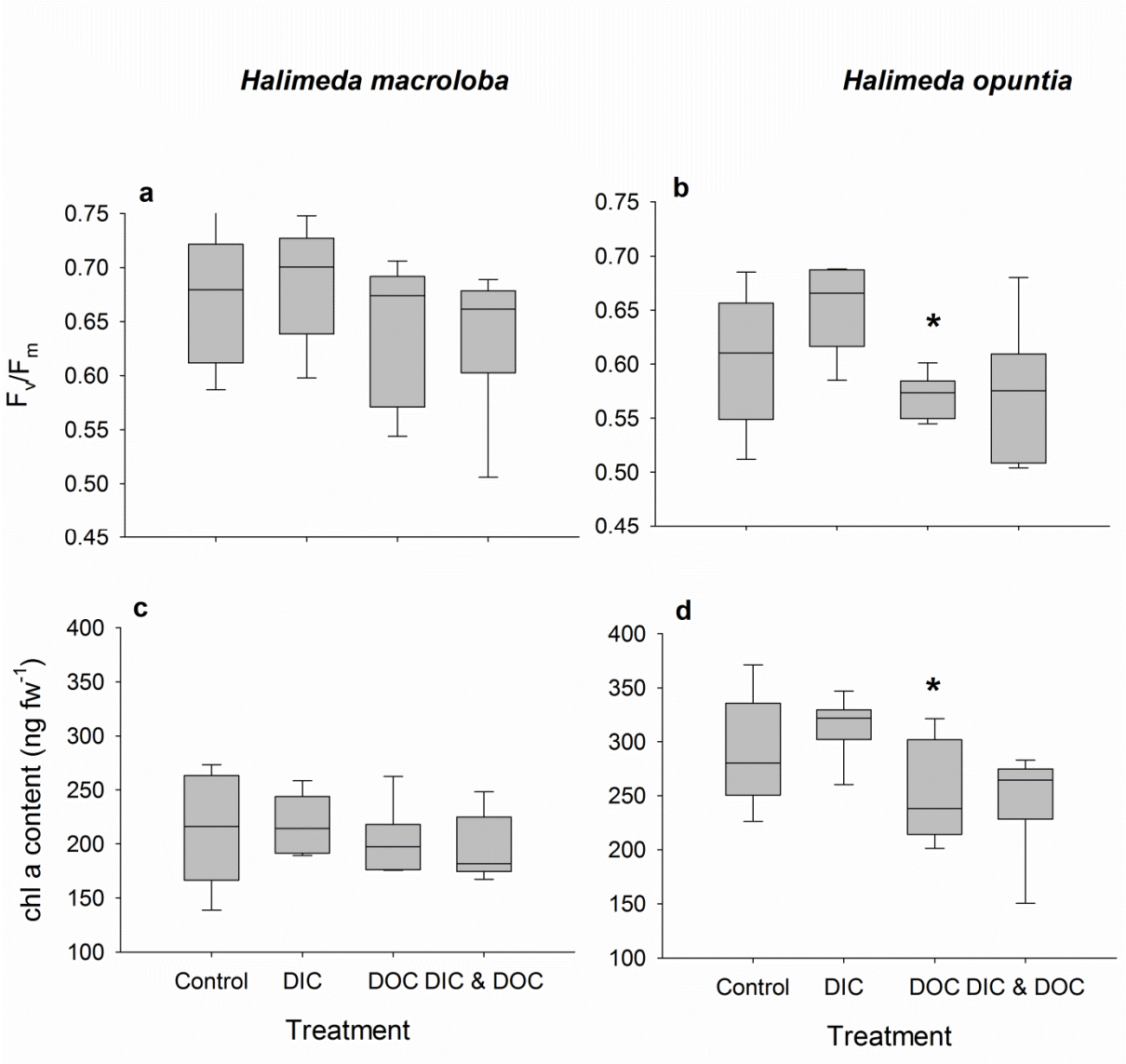

Fig. 4. Photosynthetic efficiency and chlorophyll tissue contents as treatment response. Maximum quantum yield (a, b) of dark- adapted individuals *Halimeda macroloba* (a, c; n = 6) and *Halimeda opuntia* (b, d; n = 6). Chlorophyll content (c, d) of both species are standardized to fresh weight. Significant differences compared to control ($p < 0.05$) are marked with an asterisk.

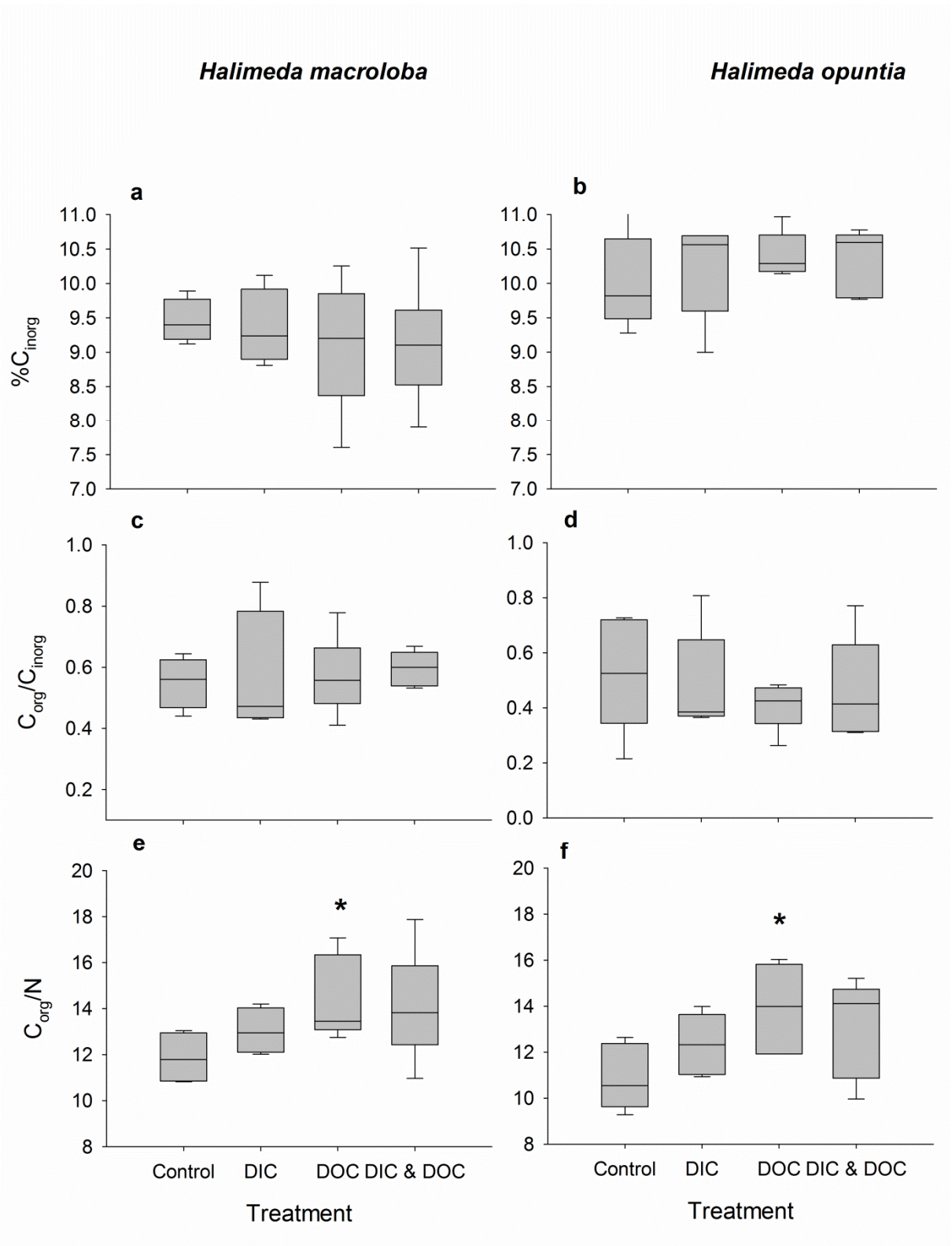

Fig. 5. Inorganic and organic C and N algae tissue contents as treatment response. Percent inorganic carbon content (a, b), ratio of organic and inorganic carbon content (c, d) and ratio of organic carbon content to total nitrogen content (e, f) of *Halimeda macroloba* (a, c, e; n = 6) and *Halimeda opuntia* (b, d, f; n = 6).Significant differences compared to control ($p < 0.05$) are marked with an asterisk.

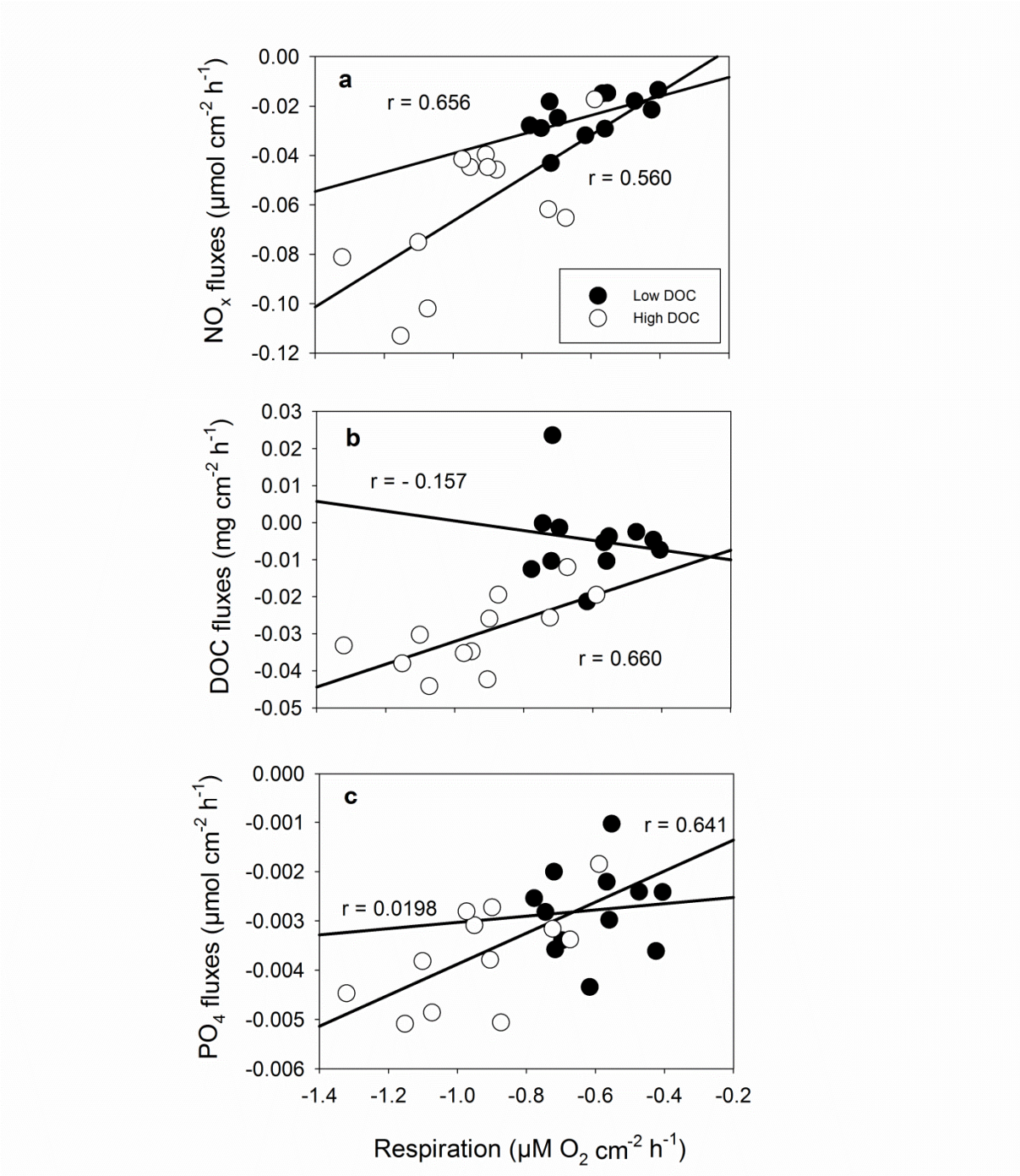

Fig. 6. Correlation of response variables in for different DOC concentrations of *Halimeda opuntia*. (a) NO_x fluxes, (b) DOC fluxes and (c) PO_4 fluxes versus respiration at low (filled circles) and high (empty circles) DOC concentration. Pearson's correlation coefficient (r) is given for each relationship for low and high DOC concentration.

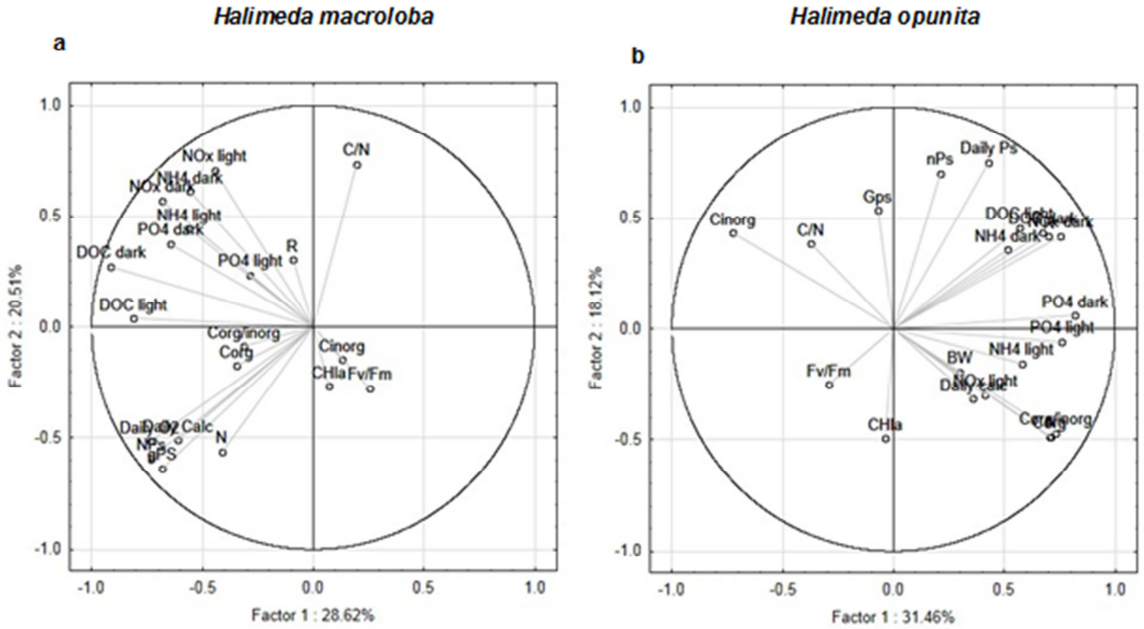

Fig. 7: Principal components (PC) 1 and PC 2 of *Halimeda macroloba* (a) and *H. opuntia* (b) for all response variable measured. Values were obtained using a correlation based PCA and values considered to weigh heavy (>0.69) are marked in bold.

Table 2. Factor loadings of principal components (PC) 1 (28.62 % total variance) and PC 2 (20.51 % total variance) for all response variable measured for *Halimeda macroloba*. Values were obtained using a correlation based PCA and values considered to weigh heavy (>0.69) are marked in bold.

Response variable	PC 1	PC 2
Net photosynthesis	**-0.73**	-0.59
Respiration	-0.09	0.30
Grossphotosynthesis	-0.68	-0.64
Daily photosynthesis rate	-0.61	-0.51
Daily calcification rate	**-0.74**	-0.52
Cinorg	0.13	-0.15
Corg/inorg	-0.31	0.09
C/N	0.19	**0.73**
Corg	0.34	-0.17
N	-0.41	-0.56
NO_x flux light	-0.44	**0.71**
NO_x fluxdark	-0.68	0.57
NH_4 flux light	-0.56	0.44
NH_4 fluxdark	-0.56	0.61
PO_4 flux light	-0.29	0.23
PO_4 fluxdark	-0.65	0.38
DOC flux light	**-0.81**	0.04
DOC fluxdark	**-0.91**	0.27
Photochemical efficiency	0.25	-0.27
Chl *a* content	0.07	-0.27

Table 3. Factor loadings of principal components (PC) 1 (31.46 % of total variance) and PC 2 (18.12 % of total variance) for all response variable measured for *Halimeda opuntia*. Values were obtained using a correlation based PCA and values considered to weigh heavy (> 0.69) are marked in bold

Response variable	PC 1	PC 2
Net photosynthesis	0.21	**0.70**
Respiration	**0.70**	0.42
Gross photosynthesis	-0.07	0.53
Daily photosynthesis rate	0.43	**0.75**
Daily calcification rate	0.36	-0.32
Cinorg	**-0.73**	0.43
Corg/inorg	**0.73**	-0.47
C/N	-0.37	0.38
Corg	**0.71**	-0.48
N	**0.71**	-0.49
NO_x flux light	0.41	-0.30
NO_x flux dark	**0.74**	0.42
NH_4 flux light	0.58	-0.15
NH_4 flux dark	0.52	0.36
PO_4 flux light	**0.76**	-0.06
PO_4 flux dark	**0.82**	0.06
DOC flux light	0.57	0.46
DOC flux dark	0.67	0.43
Photochemical efficiency	-0.29	-0.25
Chl *a* content	-0.04	-0.50
Growth	0.30	-0.19

Discussion

Experimental settings

The treatment values reached during the incubation experiment for both high DIC and DOC, as well as the controls were within natural ranges. For the DIC treatment, the resulting pCO_2 of 996 µatm and 1081 µatm (Table 1) for the combined treatment is well represented in the middle of the most recent RCP's for the year 2100 that predict ranges of 850 (RCP 6.0) to 1370 (RCP 8.5) µatm CO_2 [3]. Due to the use of natural seawater, the resulting natural A_T of 2280 and a saturation of aragonite of 4.1 under the control conditions well represents present day aragonite saturation states in coral reefs. Due to the higher CO_2 content of the DIC treatment, the saturation was reduced by 50 % resulting in Ω_{Arag} = 2.0, well above under-saturated conditions, but below thresholds for projected reef growth [57]. Hence, the manipulated conditions of ocean acidification resemble well the potential OA conditions of the year 2100 in both CO_2 content as well as Ω_{Arag}.

For the DOC treatment, comparable data from other studies are scarce, however the resulting treatment concentration of 294 ± 506 µmol L^{-1} (Table 1) lies within or even below those values reported from other studies that used labile sugars such as glucose and lactose [26,30] and is in the lower range of values already described for natural reef settings [29]. When compared to reported DOC concentrations in the GBR between 66 µmol L^{-1} [31] and 583 µmol L^{-1} (7 mg L^{-1}) [32], the DOC concentration in our study (294 to 800 µmol L^{-1}) are well within described ranges for DOC concentrations. Although in natural reef settings, the DOC pool might be composed of a multitude of substances, the part of labile DOC used in this study reflects upper ranges of concentrations found under disturbed reef conditions [29].. The average treatment level, therefore was low compared to studies and environmental settings named above.

Effects of DIC

Our results show that under elevated DIC conditions, the process of calcification is the most influenced, while primary production and photosynthetic performance stay relatively stable. We could not find an effect of high DIC on the calcification or photosynthesis of *H. macroloba*, but *H. opuntia* showed a decreased daily calcification rate, primarily due to the reduction in the dark calcification rate. This is in line with recent research on *H. opuntia* that showed a reduction in calcification of *H. opuntia* under OA conditions, but no reduction of calcification of a related *Halimeda* species (*Halimeda taenicola)* [22]. Other studies however did not find an effect of OA on the calcification of *H. opuntia* [19], but showed that inorganic carbon content was reduced. This could indicate an effect of reduced calcification. Another study however found high reduction in calcification, photosynthesis, and photochemical efficiency of *H. macroloba* under OA conditions [20]. One explanation for the different responses towards OA we observed for *H. macroloba* and *H. opuntia* could be the different morphology as already discussed for other species comparisons [18,20,22]. In addition we detected a tank effect for this parameter measured which could have altered the effect of DIC and DOC on calcification and reduced or increased the effect we measured. *H. macroloba* exhibits lower photosynthetic and calcification rates compared to *H. opuntia*. The demand for energy to keep the calcification process high is therefore likely higher in *H. opuntia.* Hence, respiration under dark conditions is also likely to be higher which may enhance effects of DIC due to the addition of respiratory CO_2 and thereby explain the observed dissolution under dark conditions. Observations of flume experiments with *Halimeda* showed similar results, where

under ambient CO_2 conditions, calcification during day-time was balanced out during night-time [58]. In order to maintain high photosynthetic activity, more inorganic nutrients may also be taken up. This may explain the higher NO_x as well as NH_4 uptake observed during dark conditions. This effect has not been described before, but evidence from nutrient enrichment experiments suggest a better performance of *H. opuntia* under inorganic nutrient-enriched OA conditions [19].

Effects of DOC

Compared to the more species-specific effect of high DIC, elevated DOC had a negative effect on both algae species. To our knowledge this is the first study that revealed effects of organic carbon enrichment on macroalgae. We were able to show that elevated DOC conditions have a strong negative impact on the photosynthetic performance of both *Halimeda* species and on dark calcification for *H. opuntia*. A species-specific trend appears under elevated DOC conditions as *H. opuntia* also suffers from a reduction in photochemical efficiency and Chl *a* content. Together with the reduction in photosynthesis, the elevated DOC conditions may favor non-beneficial or even harmful bacterial growth on the algae itself as also observed by Kuntz et al. [26] on corals. This is supported by higher uptake rates of DOC by bacteria under the high DOC treatment, which may lead to a reduction of the photosynthetic apparatus via proteolysis from bacterial-derived enzymes and also co-competition for space and nutrients and reduction of the nutrient/gas exchange over the algae tissue [59]. Net uptake of DOC most likely took place by bacteria, as *Halimeda* has been shown to release very little DOC or show net uptake compared to rapid uptake of labile DOC by bacteria [35,36]. The bacteria were introduced with the algae to the experimental tanks, were not removed, and therefore showed a strong treatment response. Less filtration of the flow through water could have increased the overall O_2 consumption, however under high flowthrough rates, accumulation is assumed to be minimal. As different studies have shown, *Halimeda* can also exhibit net release of DOC [27,60] which does not lead to the loss of primary production as observed in the present study. The composition of DOC however is very different from pure glucose as used in this study and my favour its own, beneficial bacterial community [39,61]. The different metabolic rates of the algae may explain the different intensity of reaction towards the treatment in which the more structured morphology of *H. opuntia* may favor more bacterial growth due to higher substrate availability. This is supported by the correlation analysis of the response variables for this species which shows

that as respiration rates increase, the uptake rates of NO_x, PO_4 and also DOC increase under high DIC conditions (Fig. 6). Under a future scenario where elevated DOC from river runoff concentrations are connected to elevated N and P concentration, a N and P surplus may in low concentrations benefit the algal fitness and compensate for a loss in primary productivity. However, nutrient uptake under high N and P conditions also increases [18], which leads to a higher demand for energy which may not be compensated by the negative effect of high DOC concentrations on the primary production of the alga. In addition, elevated P and N concentrations may favour fast growing, turf and fleshy algae that are in direct competition with *Halimeda* [60].

Effects of the combined treatment

Under the combination of both treatments, this study observed additive effects for dark calcification, respiration, and DOC fluxes, indicating that exposure to both factors increases the stress on the algae. As dark calcification further decreased under the presence of both factors compared to the individual factors, it is likely that under future conditions when both factors are present, the investigated algae species will experience loss in total calcification. Over the course of the relatively short experiment, however, we could not observe an interactive negative effect on calcification. The positive interaction, leading to a synergism in NO_x uptake indicates that physiological responses are not always additive, but depend on the level of the other factor present. The observed additive effect on DOC uptake may be explained by DOC-facilitated bacterial growth on the algae [38] which was further enhanced under the high DIC treatment. An increased degradation of polysaccharides has been described under elevated DIC conditions [61] which could explain the increase of DOC uptake rates under the combined treatment compared to the high DOC treatment alone. These changes in microbial degradation processes have been assigned to altered catabolic enzymatic activities [61] while rates of primary productions remain stable [62]. This is also in line with the observations of the biological oxygen demand which also showed an interactive effect of the combined treatment and further increased compared to the high DOC treatment, but did not change under high DIC concentrations alone.

Connection and correlation between the different response variables

We found that many response variables were highly correlated. Daily calcification, photosynthesis, C_{inorg}, C_{org}, Chl *a* content and photochemical efficiency had a high contribution on the principal components (PC) of both algal species, indicating that the responses towards both environmental factors were strongly associated with those variables. This is in line with our observations that the photosynthetic performance under elevated DOC conditions and the calcification process under elevated DIC conditions were primarily affected.

Ecological perspective and outlook

The present study showed that there are strong species-specific responses by macroalgae of the genus *Halimeda* towards both applied environmental factors. Depending on the metabolic activity, expressed as the respiration rates, the effect of high and combined DIC and DOC exposure on *H. opuntia* was much more pronounced than on *H. macroloba*. This is the first study that indicates potential reduction of primary production for algae-dominated benthic communities under high DOC concentrations. Under the presence of both factors, additive as well as synergistic effects further reduced primary production and increased nutrient uptake rates. For further assessment of carbon production rates in coral reefs, not only different factors have to be considered, but also their interactive physiological effects.

Compared to corals, *Halimeda* spp. showed similar reactions towards OA, especially expressed as reduced dark calcification rates. Primary production however was unaffected. Under elevated DOC conditions, no spread of pathogens or bleaching was observed as shown for corals [26,30] but a loss in productivity indicates severe negative effects on their physiology. In the perspective of future phase shift towards algae dominated reefs, the contribution of *Halimeda* towards primary production or carbon accretion may be reduced under the combination of both high DIC and DOC conditions and might provide less carbonate to future buffer capacities of coral reefs, independent of its different morphological structure and different contribution to reef internal carbon cycling [63]. For *Halimeda* dominated reefs [16,64], a future reduction of primary production under elevated DOC concentrations may lead to an additional decrease of carbon accretion where high levels of DIC are present. This might drive a shift of species with heavily calcified (in this case *H. opuntia*) domination to a less calcified, less productive species (in our case *H. macroloba*)

which may have severe impacts on the overall carbon budget of reefs, carbon fixation rates and future buffer capacities against further acidification.

Acknowledgements

The authors would like to thank Jane Wu Won at AIMS for the support with the analysis of the TOC samples. In addition, we thank Florita Flores (general assistance), Michelle Liddy (field + lab assistance), and Dorothea Dasbach for the analysis of the C/N samples.

References

1. Rogelj J, Meinshausen M, Knutti R (2012) Global warming under old and new scenarios using IPCC climate sensitivity range estimates. Nat Clim Chang 2: 248–253. Available: http://www.nature.com/doifinder/10.1038/nclimate1385. Accessed 12 March 2012.

2. Dlugokencky E, Tans P (2013) Trends in Atmospheric Carbon Dioxide: Recent Global CO_2. Available: www.esrl.noaa.gov/gmd/ccgg/trends/.

3. Moss RH, Edmonds JA, Hibbard KA, Manning MR, Rose SK, van Vuuren D,P et al. (2010) The next generation of scenarios for climate change research and assessment. Nature 463: 747–756. Available: http://dx.doi.org/10.1038/nature08823. Accessed 9 January 2014.

4. Fabricius KE, Langdon C, Uthicke S, Humphrey C, Noonan S, De'ath G et al. (2011) Losers and winners in coral reefs acclimatized to elevated carbon dioxide concentrations. Nat Clim Chang 1: 165–169. Available: http://www.nature.com/doifinder/10.1038/nclimate1122. Accessed 10 June 2011.

5. Manzello D, Kleypas J (2008) Poorly cemented coral reefs of the eastern tropical Pacific: Possible insights into reef development in a high-CO_2 world. Proc Natl Acad Sci U S A 105: 10450–10455. Available: http://www.pnas.org/content/105/30/10450.abstract. Accessed 10 July 2013.

6. Crook ED, Cohen AL, Rebolledo-Vieyra M, Hernandez L, Paytan A (2013) Reduced calcification and lack of acclimatization by coral colonies growing in areas of persistent natural acidification. Proc Natl Acad Sci U S A 110: 11044–11049. Available: http://www.ncbi.nlm.nih.gov/pubmed/23776217. Accessed 7 November 2013.

7. Ries JB, Cohen AL, McCorkle DC (2009) Marine calcifiers exhibit mixed responses to CO_2-induced ocean acidification. Geology 37: 1131–1134. Available: http://www.unc.edu/~jries/Ries_2010_EARTH_ShellShocked_Biolgical_Effects_of_Ocean_Acidification.pdf. Accessed 6 July 2011.

8. Fabry VJ, Seibel B a., Feely R a, Orr JC (2008) Impacts of ocean acidification on marine fauna and ecosystem processes. ICES J Mar Sci 65: 414–432. Available: http://icesjms.oxfordjournals.org/cgi/doi/10.1093/icesjms/fsn048.

9. Doney SC, Fabry VJ, Feely RA, Kleypas J a. (2009) Ocean Acidification: The Other CO_2 Problem. Ann Rev Mar Sci 1: 169–192. Available: http://www.annualreviews.org/eprint/QwPqRGcRzQM5ffhPjAdT/full/10.1146/annurev.marine.010908.163834. Accessed 28 April 2014.

10. Dupont S, Ortega-Martínez O, Thorndyke MC (2010) Impact of near-future ocean acidification on echinoderms. Ecotoxicology 19: 449–462. Available: http://www.ncbi.nlm.nih.gov/pubmed/20130988. Accessed 28 June 2011.

11. Anthony KRN, Kline DI, Diaz-Pulido G, Dove SG, Hoegh-Guldberg O (2008) Ocean acidification causes bleaching and productivity loss in coral reef builders. Proc Natl Acad Sci U S A 105: 17442–17446. Available: http://www.ncbi.nlm.nih.gov/pubmed/18988740.

12. Kleypas J a., Feely R, Fabry V, Langdon C (2005) Impacts of ocean acidification on coral reefs and other marine calcifiers: a guide for future research. Rep a Work held 18–20 April 2005, St Petersburg, FL, Spons by NSF, NOAA, US Geol Surv: 88. Available: http://scholar.google.com/scholar?hl=en&btnG=Search&q=intitle:Impacts+of+Ocean+Acidification+on+Coral+Reefs+and+Other+Marine+Calcifiers+:+A+Guide+for#0. Accessed 10 August 2011.

13. Wefer G (1980) Carbonate production by algae *Halimeda*, *Penicillus* and *Padina*. Nature 285: 323–324. Available: http://www.nature.com/nature/journal/v285/n5763/abs/285323a0.html. Accessed 11 November 2011.

14. Multer HG (1988) Growth rate, ultrastructure and sediment contribution of *Halimeda incrassata* and *Halimeda monile*, Nonsuch and Falmouth Bays, Antigua, W.I. Coral Reefs 6: 179–186. Available: http://www.springerlink.com/index/10.1007/BF00302014.

15. Freile D, Milliman JD, Hillis L (1995) Leeward bank margin *Halimeda* meadows and draperies and their sedimentary importance on the western Great Bahama Bank slope. Coral Reefs 14: 27–33. Available: http://link.springer.com/10.1007/BF00304068. Accessed 21 February 2014.

16. Rees S a., Opdyke BN, Wilson P a., Henstock TJ (2006) Significance of *Halimeda* bioherms to the global carbonate budget based on a geological sediment budget for the Northern Great Barrier Reef, Australia. Coral Reefs 26: 177–188. Available: http://link.springer.com/10.1007/s00338-006-0166-x. Accessed 21 February 2014.

17. Vroom PS, Smith CM, Coyer JA, Walters LJ, Hunter CL, Beach KS, et al. (2003) Field biology of *Halimeda tuna* (Bryopsidales, Chlorophyta) across a depth gradient: comparative growth, survivorship, recruitment, and reproduction. Hydrobiologia 501: 149–166 – 166. Available: http://www.springerlink.com/content/vvu7m8162h21736l/. Accessed 15 July 2011.

18. Robbins LL, Knorr PO, Hallock P (2009) Response of *Halimeda* to ocean acidification: field and laboratory evidence. Biogeosciences Discuss 6: 4895–4918. Available: http://www.biogeosciences-discuss.net/6/4895/2009/.

19. Hofmann LC, Heiden J, Bischof K, Teichberg M (2014) Nutrient availability affects the response of the calcifying chlorophyte *Halimeda opuntia* (L.) J.V. Lamouroux to low pH. Planta 239: 231–242. Available: http://www.ncbi.nlm.nih.gov/pubmed/24158465. Accessed 23 January 2014.

20. Sinutok S, Hill R, Doblin MA, Wuhrer R, Ralph PJ (2011) Warmer more acidic conditions cause decreased productivity and calcification in subtropical coral reef sediment-dwelling calcifiers. Limnol Oceanogr 56: 1200–1212. Available: http://cat.inist.fr/?aModele=afficheN&cpsidt=24362064. Accessed 21 February 2014.

21. Sinutok S, Hill R, Doblin MA, Kühl M, Ralph PJ (2012) Microenvironmental changes support evidence of photosynthesis and calcification inhibition in *Halimeda* under ocean acidification and warming. Coral Reefs 31: 1201–1213. Available: http://link.springer.com/10.1007/s00338-012-0952-6. Accessed 21 February 2014.

22. Price N, Hamilton S, Tootell J, Smith J (2011) Species-specific consequences of ocean acidification for the calcareous tropical green algae *Halimeda*. Mar Ecol Prog Ser 440: 67–78. Available: http://www.int-res.com/abstracts/meps/v440/p67-78/. Accessed 31 October 2011.

23. Cooper TF, Uthicke S, Humphrey C, Fabricius KE (2007) Gradients in water column nutrients, sediment parameters, irradiance and coral reef development in the Whitsunday Region, central Great Barrier Reef. Estuar Coast Shelf Sci 74: 458–470. Available: http://www.sciencedirect.com/science/article/pii/S0272771407001412.

24. Fabricius KE, De'ath G, McCook LJ, Turak E, Williams DM (2005) Changes in algal, coral and fish assemblages along water quality gradients on the inshore Great Barrier Reef. Mar Pollut Bull 51: 384–398. Available: http://www.sciencedirect.com/science/article/pii/S0025326X04003923.

25. Fabricius KE, De'ath G, De'Ath G (2004) Identifying ecological change and Its causes: A case study on coral reefs. Ecol Appl 14: 1448–1465. Available: http://www.esajournals.org/doi/abs/10.1890/03-5320. Accessed 27 July 2011.

26. Kuntz NM, Kline DI, Sandin SA, Rohwer F (2005) Pathologies and mortality rates caused by organic carbon and nutrient stressors in three Caribbean coral species. Mar Ecol Prog Ser 294: 173–180. Available: http://www.int-res.com/abstracts/meps/v294/p173-180/.

27. Haas AF, Nelson C, Kelly L, Carlson C (2011) Effects of coral reef benthic primary producers on dissolved organic carbon and microbial activity. PLoS One 6. Available: http://dx.plos.org/10.1371/journal.pone.0027973. Accessed 17 January 2014.

28. Gregg A, Hatay M, Haas AF, Robinett N, Barott KL, Vermeij M, et al. (2013) Biological oxygen demand optode analysis of coral reef-associated microbial communities exposed to algal exudates. PeerJ 1: e107. Available: http://www.pubmedcentral.nih.gov/articlerender.fcgi?artid=3719127&tool=pmcentrez&rendertype=abstract. Accessed 25 April 2014.

29. Kline DI, Kuntz NM, Breitbart M, Knowlton N, Rohwer F (2006) Role of elevated organic carbon levels and microbial activity in coral mortality. Mar Ecol Prog Ser 314: 119–125. Available: http://www.int-res.com/abstracts/meps/v314/p119-125/.

30. Haas AF, Al-Zibdah M, Wild C (2009) Effect of inorganic and organic nutrient addition on coral–algae assemblages from the Northern Red Sea. J Exp Mar Bio Ecol 380: 99–105.

Available: http://linkinghub.elsevier.com/retrieve/pii/S0022098109003712. Accessed 22 June 2011.

31. Schaffelke B, Carleton J, Skuza M, Zagorskis I, Furnas MJ (2012) Water quality in the inshore Great Barrier Reef lagoon: Implications for long-term monitoring and management. Mar Pollut Bull 65: 249–260. Available: http://www.ncbi.nlm.nih.gov/pubmed/22142496. Accessed 6 September 2014.

32. Ford P, Tillman P, Robson B, Webster IT (2005) Organic carbon deliveries and their flow related dynamics in the Fitzroy estuary. Mar Pollut Bull 51: 119–127. Available: http://www.ncbi.nlm.nih.gov/pubmed/15757714. Accessed 22 August 2014.

33. Painter HA, Viney M (1959) Composition of a domestic sewage. J Biochem Microbiol Technol Eng 1: 143–162. Available: http://doi.wiley.com/10.1002/jbmte.390010203. Accessed 28 November 2014.

34. Packett R, Dougall C, Rohde K, Noble R (2009) Agricultural lands are hot-spots for annual runoff polluting the southern Great Barrier Reef lagoon. Mar Pollut Bull 58: 976–986. Available: http://www.ncbi.nlm.nih.gov/pubmed/19303607. Accessed 6 September 2014.

35. Haas AF, Naumann MS, Struck U, Mayr C, El-Zibdah MM, Wild C (2010) Organic matter release by coral reef associated benthic algae in the Northern Red Sea. J Exp Mar Bio Ecol 389: 53–60. Available: http://linkinghub.elsevier.com/retrieve/pii/S0022098110001085. Accessed 14 July 2011.

36. Wild C, Haas AF, Naumann MS, Mayr C, El-Zibdah M (2008) Comparative investigation of organic matter release by corals and benthic reef algae–implications for pelagic and benthic microbial metabolism. 11th International Coral Reef Symposium. pp. 7–11. Available: http://www.nova.edu/ncri/11icrs/proceedings/files/m25-10.pdf. Accessed 20 July 2011.

37. Haas AF, Jantzen C, Naumann MS, Iglesias-Prieto R, Wild C (2010) Organic matter release by the dominant primary producers in a Caribbean reef lagoon: implication for in situ O2 availability. Mar Ecol Prog Ser 409: 27–39. doi:10.3354/meps08631.

38. Nelson CE, Goldberg SJ, Wegley Kelly L, Haas AF, Smith JE, Rohwer F, et al. (2013) Coral and macroalgal exudates vary in neutral sugar composition and differentially enrich reef bacterioplankton lineages. ISME J 7: 962–979. Available: http://www.ncbi.nlm.nih.gov/pubmed/23303369. Accessed 19 November 2013.

39. Haas AF, Wild C (2010) Composition analysis of organic matter released by cosmopolitan coral reef-associated green algae. Aquat Biol 10. Available: http://www.int-res.com/abstracts/ab/v10/n2/p131-138/. Accessed 17 January 2014.

40. Hauri C, Fabricius KE, Schaffelke B, Humphrey C (2010) Chemical and physical environmental conditions underneath mat- and canopy-forming macroalgae, and their effects on understorey corals. PLoS One 5: e12685. Available: http://dx.doi.org/10.1371/journal.pone.0012685.

41. Webster PJ, Holland GJ, Curry J a, Chang H-R (2005) Changes in tropical cyclone number, duration, and intensity in a warming environment. Science 309: 1844–1846. Available: http://www.ncbi.nlm.nih.gov/pubmed/16166514. Accessed 5 June 2013.

42. Knutson TR, McBride JL, Chan J, Emanuel K, Holland G, Landsea C, et al. (2010) Tropical cyclones and climate change. Nat Geosci 3: 157–163. Available: http://www.nature.com/doifinder/10.1038/ngeo779. Accessed 24 May 2013.

43. Schaffelke B, Thompson A, Carleton J, Cripps E, Davidson J, Doyle J, et al. (2008) Water quality and ecosystem monitoring program: Reef Water Quality Protection Plan: final report. Available: http://elibrary.gbrmpa.gov.au/jspui/handle/11017/406. Accessed 6 September 2014.

44. Rusch A, Huettel M, Wild C, Reimers CE (2006) Benthic oxygen consumption and organic matter turnover in organic-poor, permeable shelf sands. Aquat Geochemistry 12: 1–19. doi:10.1007/s10498-005-0784-x.

45. Dinsdale E a, Pantos O, Smriga S, Edwards R a, Angly F, Wegley L, et al. (2008) Microbial ecology of four coral atolls in the Northern Line Islands. PLoS One 3: e1584. Available: http://www.pubmedcentral.nih.gov/articlerender.fcgi?artid=2253183&tool=pmcentrez&rendertype=abstract. Accessed 10 July 2014.

46. Smith JE, Shaw M, Edwards RA, Obura DO, Pantos O, Sala e, et al. (2006) Indirect effects of algae on coral: algae-mediated, microbe-induced coral mortality. Ecol Lett 9: 835–845. Available: http://www.ncbi.nlm.nih.gov/pubmed/16796574. Accessed 17 January 2014.

47. Vogel N, Uthicke S (2012) Calcification and photobiology in symbiont-bearing benthic foraminifera and responses to a high CO_2 environment. J Exp Mar Bio Ecol 424-425: 15–24. Available: http://linkinghub.elsevier.com/retrieve/pii/S0022098112001736. Accessed 8 August 2012.

48. Meehl GAG, Stocker TF, Collins WD, Friedlingstein P, Gaye T, Gregory JM, et al. (2007) Global climate projections. In: Solomon S, Qin D, Manning M, Chen Z, Marquis M, et al., editors. IPCC, 2007: Climate Change 2007: the physical science basis. contribution of Working Group I to the Fourth Assessment Report of the Intergovernmental Panel on Climate Change. Cambridge University Press, Cambridge, United Kingdom and New York, NY, USA. pp. 747–846. Available: https://publications.csiro.au/rpr/pub?list=BRO&pid=procite:1452cb7a-9f93-44ea-9ac4-fd9f6fd80a07. Accessed 18 July 2013.

49. Vuuren DP, Edmonds J, Kainuma M, Riahi K, Thomson A, Hibbard K, et al. (2011) The representative concentration pathways: an overview. Clim Change 109: 5–31. Available: http://link.springer.com/10.1007/s10584-011-0148-z. Accessed 9 January 2014.

50. Uthicke S, Fabricius KE (2012) Productivity gains do not compensate for reduced calcification under near-future ocean acidification in the photosynthetic benthic foraminifer species Marginopora vertebralis. Glob Chang Biol 18: 2781–2791. Available: http://doi.wiley.com/10.1111/j.1365-2486.2012.02715.x. Accessed 28 March 2013.

51. Robbins L, Hansen M, Kleypas J, Meylan S (2010) CO2calc—a user-friendly seawater carbon calculator for Windows, Max OS X, and iOS (iPhone). US Geol Surv Open-File Rep 2010-1280: 17. Available: http://scholar.google.com/scholar?q=CO2calc—A+user-friendly+seawater+carbon+calculator+for+Windows,+Max+OS+X,+and+iOS+(iPhone)#0. Accessed 18 July 2013.

52. Chisholm J, Gattuso J-P (1991) Validation of the alkalinity anomaly technique for investigating calcification and photosynthesis in coral reef communities. Limnol Oceanogr 36: 1232–1239. Available: http://www.jstor.org/stable/10.2307/2837472. Accessed 25 September 2012.

53. Gao K, Zheng Y (2009) Combined effects of ocean acidification and solar UV radiation on photosynthesis, growth, pigmentation and calcification of the coralline alga *Corallina sessilis* (Rhodophyta). Glob Chang Biol 16: 2388–2398. Available: http://doi.wiley.com/10.1111/j.1365-2486.2009.02113.x. Accessed 22 July 2011.

54. Jokiel P, Maragos J, Franzisket L (1978) Coral growth: buoyant weight technique. Coral reefs Res methods UNESCO, Paris. Available: http://scholar.google.com/scholar?q=Jokiel+P,+Maragos+J,+Franzisket+L+(1978)+Coral+growth:+buoyant+weight+technique&btnG=&hl=en&as_sdt=0,5#0. Accessed 17 January 2014.

55. Schmidt C, Heinz P, Kucera M, Uthicke S (2011) Temperature-induced stress leads to bleaching in larger benthic foraminifera hosting endosymbiotic diatoms. Limnol Oceanogr 56:

1587–1602. Available: http://www.aslo.org/lo/toc/vol_56/issue_5/1587.html. Accessed 7 June 2013.

56. Nush E (1980) Comparison of different methods for chlorophyll and phaeopigment determination. Arch Hydrobiol Beih 14: 14–36. Available: http://bases.bireme.br/cgi-bin/wxislind.exe/iah/online/?IsisScript=iah/iah.xis&src=google&base=REPIDISCA&lang=p&nextAction=lnk&exprSearch=144518&indexSearch=ID. Accessed 18 July 2013.

57. Hoegh-Guldberg O, Mumby PJ, Hooten a J, Steneck RS, Greenfield P, Gomez E, et al. (2007) Coral reefs under rapid climate change and ocean acidification. Science 318: 1737–1742. Available: http://www.ncbi.nlm.nih.gov/pubmed/18079392. Accessed 5 July 2011.

58. Anthony KRN, Diaz-Pulido G, Verlinden N, Tilbrook B, Andersson a. J (2013) Benthic buffers and boosters of ocean acidification on coral reefs. Biogeosciences 10: 4897–4909. Available: http://www.biogeosciences.net/10/4897/2013/. Accessed 28 November 2014.

59. Cole J (1982) Interactions between bacteria and algae in aquatic ecosystems. Annu Rev Ecol Syst 13: 291–314. Available: http://www.jstor.org/stable/2097070. Accessed 25 May 2014.

60. Delgado O, Lapointe BE (1994) Nutrient-limited productivity of calcareous versus fleshy macroalgae in a eutrophic, carbonate-rich tropical marine environment. Coral Reefs 13: 151–159. Available: http://link.springer.com/10.1007/BF00301191. Accessed 28 November 2014.

61. Piontek J, Lunau M, Händel N, Borchard C, Wurst M, Engel A (2010) Acidification increases microbial polysaccharide degradation in the ocean. Biogeosciences 7: 1615–1624. Available: http://www.biogeosciences.net/7/1615/2010/. Accessed 26 August 2014.

62. Witt V, Wild C, Anthony KRN, Diaz-Pulido G, Uthicke S (2011) Effects of ocean acidification on microbial community composition of, and oxygen fluxes through, biofilms from the Great Barrier Reef. Environ Microbiol 13: 2976–2989. Available: http://www.ncbi.nlm.nih.gov/pubmed/21906222. Accessed 17 January 2014.

63. Wild C, Woyt H, Huettel M (2005) Influence of coral mucus on nutrient fluxes in carbonate sands. Mar Ecol Prog Ser 287: 87–98. Available: http://www.int-res.com/abstracts/meps/v287/p87-98/.

64. Marshall JF, Davies PJ (1988) *Halimeda* bioherms of the northern Great Barrier Reef. Coral Reefs 6: 139–148. Available: http://link.springer.com/10.1007/BF00302010. Accessed 25 April 2014.

Supplementary Material

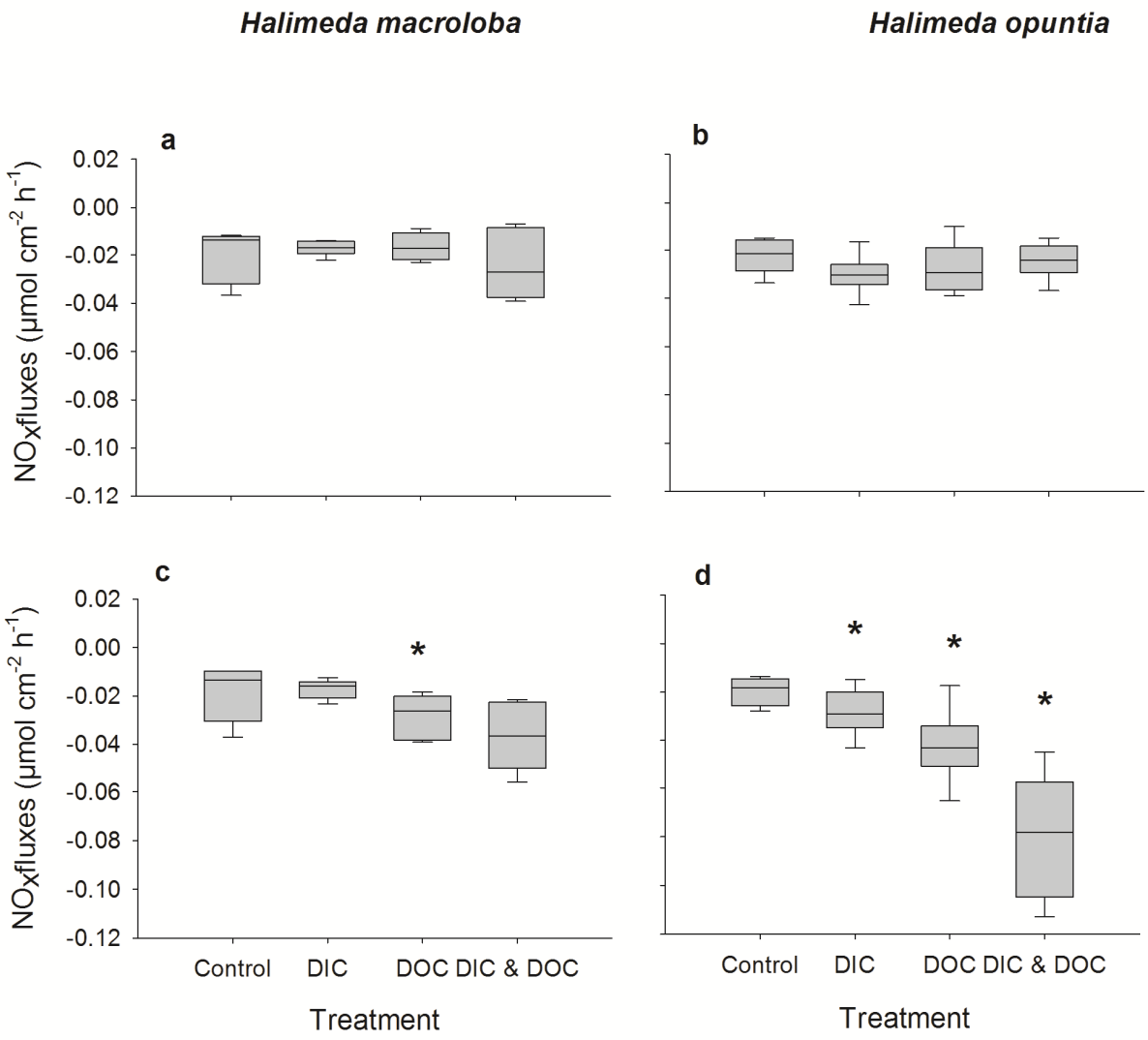

S1 Figure. NO_x fluxes as treatment response. Fluxes are calculated from light (150 µE m^{-2} s^{-1}) (a, b) and dark incubations (c, d) of *Halimeda macroloba* (a, c; n = 6) and *Halimeda opuntia* (a, b; n = 6).Significant differences compared to control ($p < 0.05$) are marked with an asterisk.

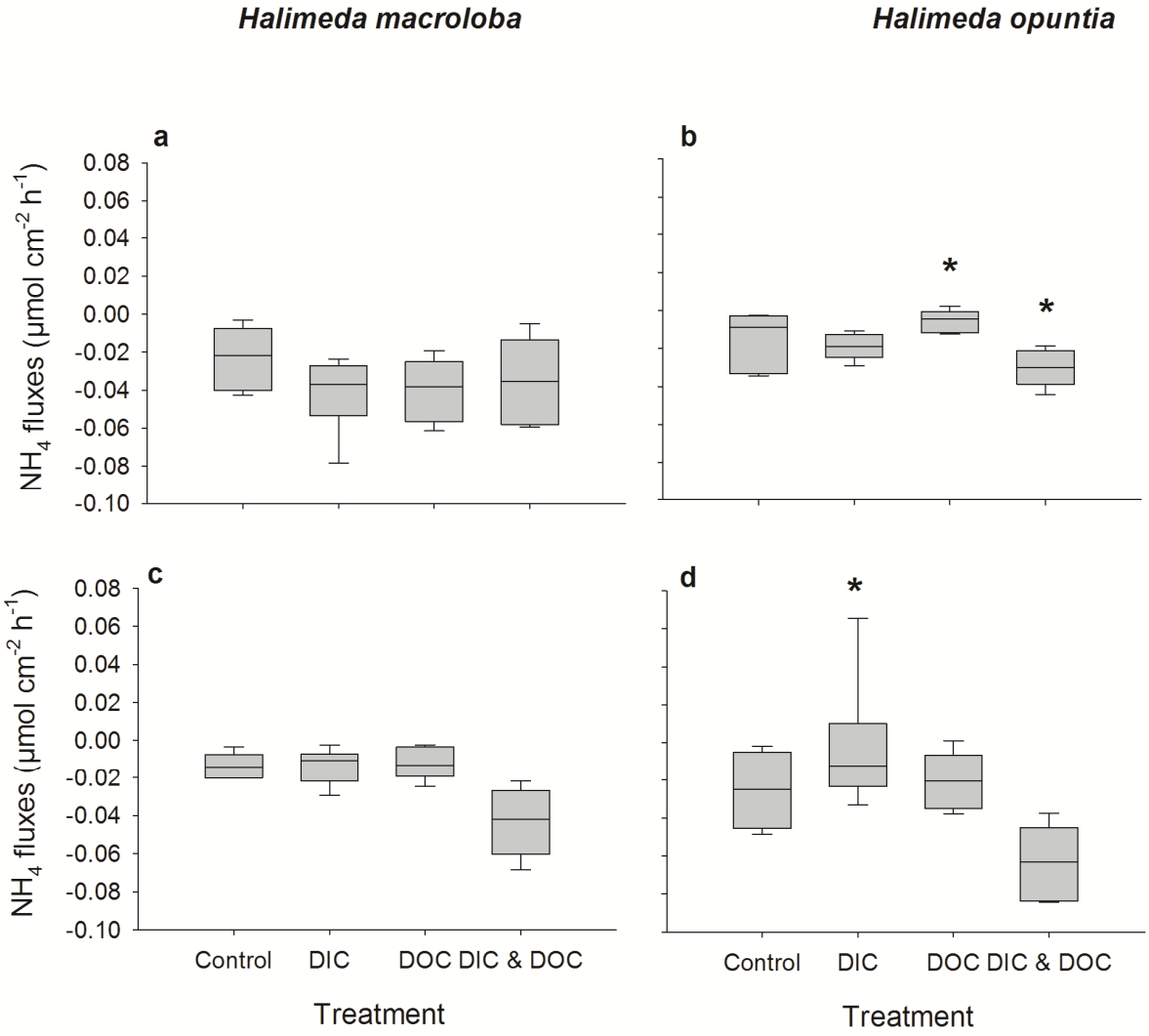

S2 Figure. NH_4 fluxes as treatment response. Fluxes calculated from light (150 µE m^{-2} s^{-1}) (a, b) and dark incubations (c, d) of *Halimeda macroloba* (a, c; n = 6) and *Halimeda opuntia* (a, b; n = 6).Significant differences compared to control ($p < 0.05$) are marked with an asterisk.

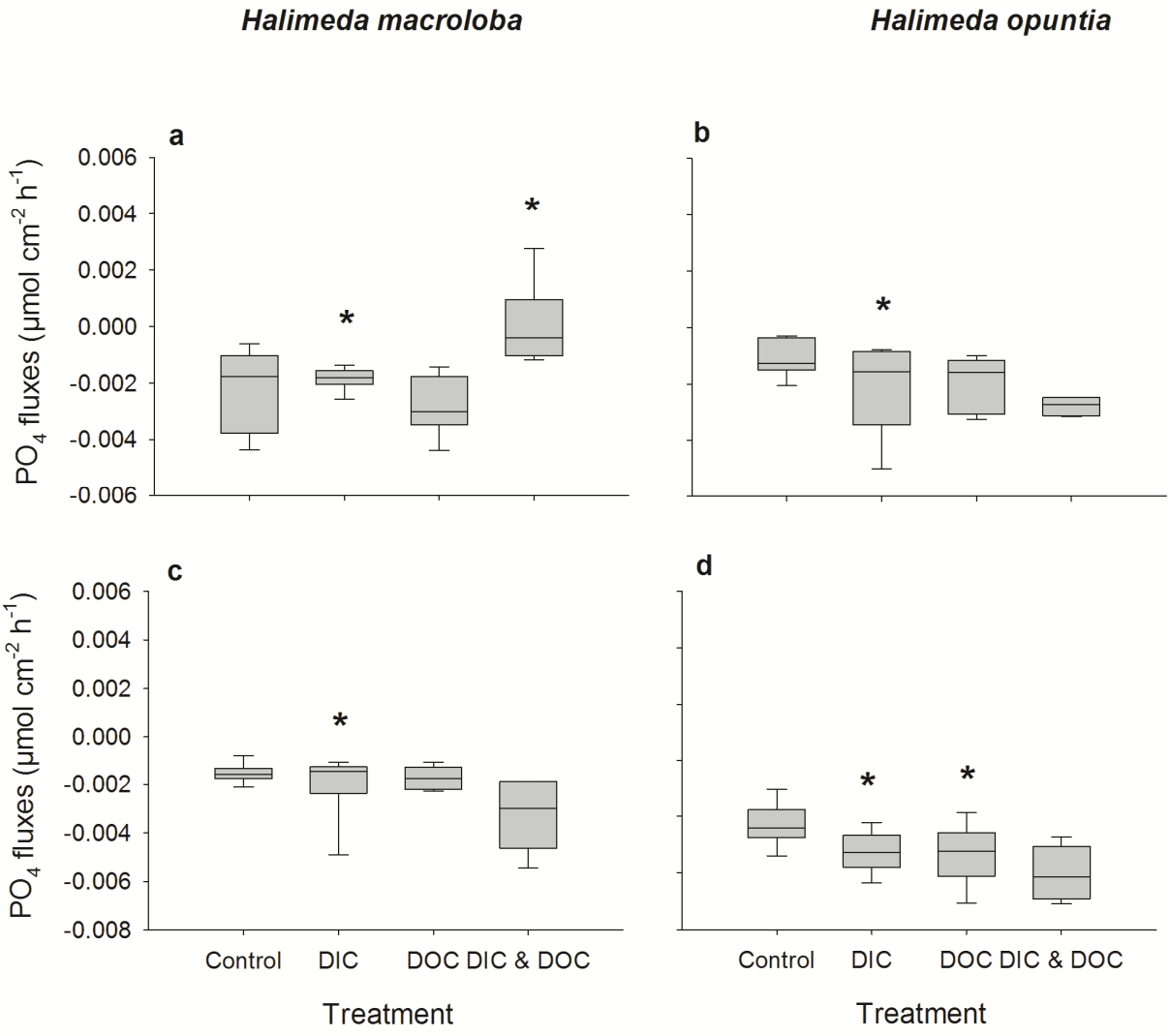

S3 Figure. PO_4 fluxes as treatment response. Fluxes calculated from light (150 µE m^{-2} s^{-1}) (a, b) and dark incubations (c, d) of *Halimeda macroloba* (a, c; n = 6) and *Halimeda opuntia* (b, d; n = 6).Significant differences compared to control ($p < 0.05$) are marked with an asterisk.

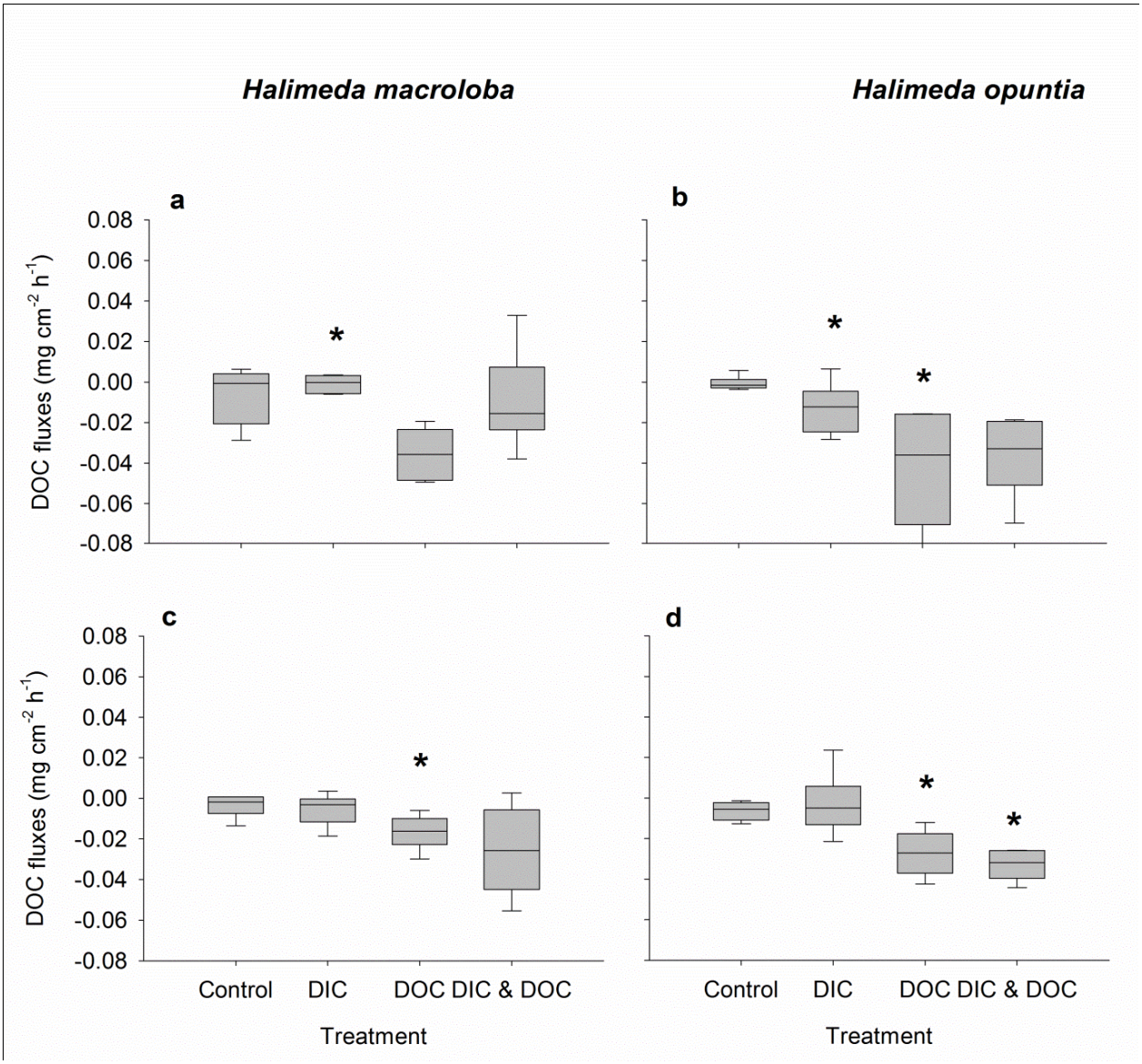

S4 Figure. DOC fluxes as treatment response. Fluxes calculated from light (150 µE m^{-2} s^{-1}) (a, b) and dark incubations (c, d) of *Halimeda macroloba* (a, c; n = 6) and *Halimeda opuntia* (b, d; n = 6).Significant differences compared to control ($p < 0.05$) are marked with an asterisk.

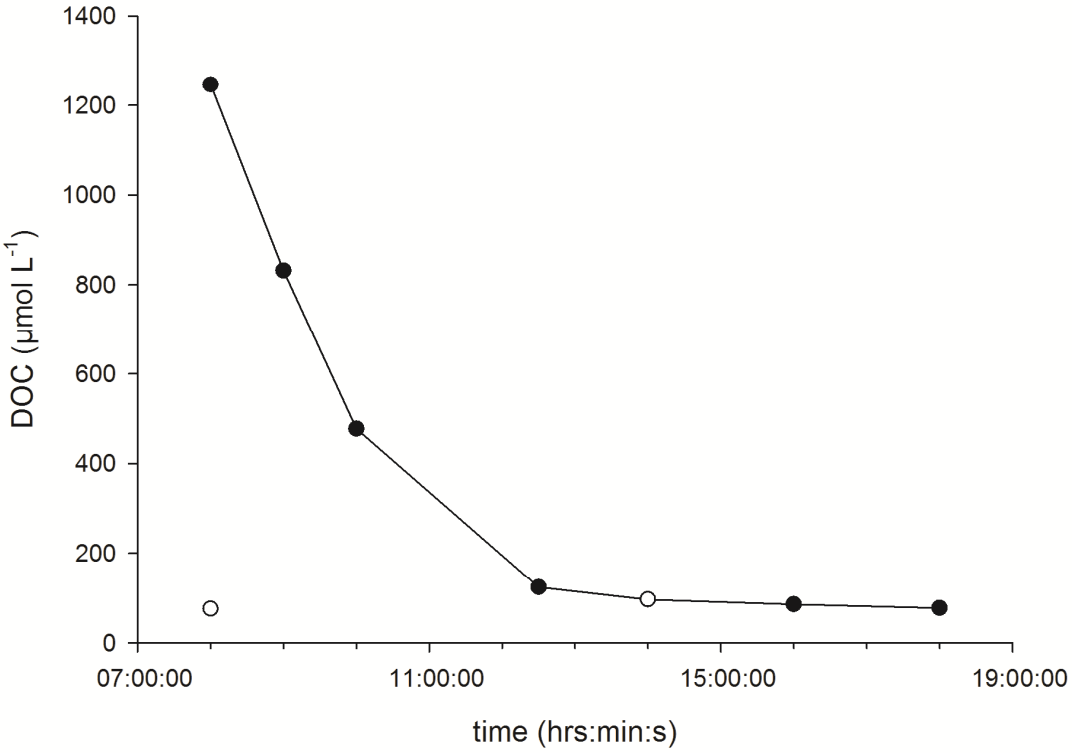

S5 Figure. DOC concentrations over 12 hours in the high DOC treatment. Time series measurement (08:00 am until 07:00 pm) after addition of 1170 µmol L^{-1} DOC as glucose and a background concentration (unfilled circles) of 76 and 97 µmol L^{-1} DOC. Filled circles indicate sampling points (n=2) for DOC analysis of the high DOC treatment and unfilled circles of the controls (n=2 for each point).

S1 Table. Statistical results. Results of Two Way ANOVA for both species: *Halimeda opuntia* and *H. macroloba* with DIC and DOC as fixed factors and aquaria as nested factor. Significant results are marked bold with an asterisk (*).

Response variable	Species	Source of variation	DF	SS	MS	F-value	P-value
Biological oxygen demand	-	DIC	1	0.265	0.265	6.377	**0.036***
		DOC	1	5.009	5.009	120.766	**<0.001***
		DIC x DOC	1	0.394	0.394	9.510	**0.015***
		Residual	9	0.332	0.0415		
		Total	11	6.000	0.545		
Growth	*H. opuntia*	DIC	1	0.525	0.525	0.34	0.575
		DOC	1	0.00722	0.00722	0.00	0.947
		DIC x DOC	1	0.118	0.118	0.08	0.788
		Aquaria	8	12.33405	1.541756	6.16	**0.003***
		Residual	12	15.336	0.767		
		Total	23	15.987			
Light calcification	*H. macroloba*	DIC	1	0.0216	0.0216	1.41	0.269
		DOC	1	0.0173	0.0173	1.12	0.320
		DIC x DOC	1	0.0213	0.0213	1.38	0.273
		Aquaria	8	0.1232182	0.01540228	0.59	0.764
		Residual	11	0.2851351	0.02592138		
		Total	22	0.470			
	H. opuntia	DIC	1	0.106	0.106	0.44	0.524
		DOC	1	0.0512	0.0512	0.21	0.656
		DIC x DOC	1	0.423	0.423	1.76	0.220
		Aquaria	8	1.918423	0.2398028	3.03	**0.041***
		Residual	12	0.9484203	0.07903503		
		Total	23	3.448			
Dark calcification	*H. macroloba*	DIC	1	0.00379	0.00379	0.49	0.504
		DOC	1	0.0000584	0.0000584	0.01	0.933
		DIC x DOC	1	0.126	0.126	16.25	**0.004***
		Aquaria	8	0.062275	0.00778	0.43	0.880
		Residual	11	0.279	0.0140		
		Total	23	0.410			
	H. opuntia	DIC	1	0.955	0.955	55.05	**<0.001***
		DOC	1	0.198	0.198	11.42	**<0.001***
		DIC x DOC	1	0.0288	0.0288	1.66	0.233
		Aquaria	8	0.1387564	0.0173445	3.25	**0.033***
		Residual	12	0.203	0.0101		
		Total	23	1.384			
Daily calcification	*H. macroloba*	DIC	1	2.087715	2.087715	0.5	0.50
		DOC	1	7.900193	7.900193	1.88	0.206
		DIC x DOC	1	24.57278	24.57278	5.89	**0.041***
		Aquaria	8	33.39654	4.174568	0.86	0.57
		Residual	12	57.95209	4.829341		
		Total	23	125.9093			
	H. opuntia	DIC	1	244.6349	244.6349	5.21	**0.0052***
		DOC	1	64.90776	64.90776	1.38	0.273
		DIC x DOC	1	96.85951	96.85951	2.06	0.188
		Aquaria	8	375.6105	46.95132	3.47	**0.026**
		Residual	12	162.4933	13.5411		
		Total	23	944.506			
Net photosynthesis	*H. macroloba*	DIC	1	0.0142	0.0142	1.90	0.205
		DOC	1	0.106	0.106	14.25	**0.005***
		DIC x DOC	1	0.00876	0.00876	1.17	0.311
		Aquaria	8	0.05976	0.00747	0.79	0.620
		Residual	12	0.113	0.00943		
		Total	23	0.302			
	H. opuntia	DIC	1	0.183	0.183	0.82	0.39
		DOC	1	4.558	4.558	20.50	**0.002***
		DIC x DOC	1	0.0193	0.0193	0.09	0.775
		Aquaria	8	1.778866	0.2223582	1.38	0.295
		Residual	12	1.927572	0.160631		
		Total	23	8.467			
Respiration	*H. macroloba*	DIC	1	0.0300	0.0300	3.20	0.111
		DOC	1	0.0232	0.0232	2.48	0.154
		DIC x DOC	1	0.00296	0.00296	0.32	0.59
		Aquaria	8	0.0749	0.00937	1.11	0.420
		Residual	12	0101	0.00884		
		Total	23	0.232			
	H. opuntia	DIC	1	0.0714	0.0714	1.77	0.220
		DOC	1	0.662	0.662	16.38	**0.004***
		DIC x DOC	1	0.0706	0.0706	1.75	0.223
		Aquaria	8	0.3234091	0.040426	2.45	0.078
		Residual	12	0.1977546	0.01.648		
		Total	23	1.325			
Gross	*H. macroloba*	DIC	1	0.0163	0.0163	3.67	0.092

photosynthesis		DOC	1	0.0505	0.0505	11.39	**0.009***
		DIC x DOC	1	0.00680	0.00680	1.53	0.251
		Aquaria	8	0.0354	0.00443	0.53	0.811
		Residual	12	0.101	0.00844		
		Total	23	0.232			
	H. opuntia	DIC	1	0.483	0.483	1.29	0.290
		DOC	1	1.746	1.746	4.65	0.063
		DIC x DOC	1	0.164	0.164	0.44	0.53
		Aquaria	8	3.004597	0.3755747	1.56	0.235
		Residual	12	2.890199	0.2408499		
		Total	23	8.287			
Daily photosynthesis	*H. macroloba*	DIC	1	2.126292	2.126292	0.27	0.615
		DOC	1	123.0113	123.0113	15.85	**0.004***
		DIC x DOC	1	5.284694	5.284694	0.68	0.433
		Aquaria	8	62.08359	7.760448	0.91	0.54
		Residual	12	102.4736	8.53947		
		Total	23	294.9795			
	H. opuntia	DIC	1	3.702061	3.702061	0.17	0.69
		DOC	1	1252.035	1252.035	57.97	**<0.001***
		DIC x DOC	1	2.307144	2.307144	0.11	0.752
		Aquaria	8	172.7754	21.59692	1.32	0.319
		Residual	12	195.868	16.32233		
		Total	23	1626.687			
Maximum quantum yield	*H. macroloba*	DIC	1	0.000122	0.000122	0.02	0.883
		DOC	1	0.00859	0.00859	0.13	0.729
		DIC x DOC	1	0.000683	0.000683	1.63	0.238
		Aquaria	8	0.0422686	0.005283	1.77	0.179
		Residual	12	0.0781	0.00390		
		Total	23	0.0875			
	H. opuntia	DIC	1	0.00375	0.00375	1.510	0.307
		DOC	1	0.0198	0.0198	7.990	0.332
		DIC x DOC	1	0.00336	0.00336	1.354	**0.036***
		Aquaria	8	0.2516267	0.003145333	1.54	0.241
		Residual	12	0.0497	0.00248		
		Total	23	0.0766			
Chlorophyll *a* content	*H. macroloba*	DIC	1	5.960	5.960	0.00	0.946
		DOC	1	1708.899	1708.899	1.42	0.27
		DIC x DOC	1	188.587	188.587	0.16	0.703
		Aquaria	8	9649.605	1206.201	0.84	0.586
		Residual	12	17201.23	1433.436		
		Total	23	28754.283			
	H. opuntia	DIC	1	668.851	668.851	0.331	0.571
		DOC	1	16474.195	16474.195	8.163	**0.010***
		DIC x DOC	1	1278.336	1278.336	0.633	0.435
		Aquaria	8	18151.98	2268.997	1.23	0.362
		Residual	12	40363.234	2018.162		
		Total	23	58784.615			
Inorganic C	*H. macroloba*	DIC	1	0.00974	0.00974	0.02	0.879
		DOC	1	0.416	0.416	1.05	0.335
		DIC x DOC	1	0.0149	0.0149	0.04	0.851
		Aquaria	8	3.168803	0.3961004	0.54	0.8
		Residual	8	9.047	0.565		
		Total	19	9.484			
	H. opuntia	DIC	1	0.0458	0.0458	0.141	0.711
		DOC	1	0.396	0.396	1.223	0.283
		DIC x DOC	1	0.0919	0.0919	0.284	0.601
		Aquaria	8	3.431844	0.4289804	1.79	0.191005
		Residual	10	5.826	0.324		
		Total	21	6.388			
Organic C / Inorganic C	*H. macroloba*	DIC	1	0.00166	0.00166	0.14	0.715
		DOC	1	0.00361	0.00361	0.31	0.592
		DIC x DOC	1	0.000202	0.000202	0.02	0.898
		Aquaria	8	0.009260	0.001576	0.60	0.760
		Residual	8	0.1554698	0.0155		
		Total	19	0.2538606			
	H. opuntia	DIC	1	0.000787	0.000787	0.0265	0.873
		DOC	1	0.0202	0.0202	0.678	0.421
		DIC x DOC	1	0.0107	0.0107	0.360	0.556
		Aquaria	8	0.2579519	0.03224	1.16	0.405
		Residual	10	0.536	0.0298		
		Total	21	0.567			
Organic C / N	*H. macroloba*	DIC	1	1.027	1.027	0.334	0.574
		DOC	1	15.020	15.020	5.01	0.055
		DIC x DOC	1	2.381	2.381	0.79	0.399
		Aquaria	8	23.97476	2.996845	0.89	0.563
		Residual	8	50.876	3.180		
		Total	19	68.796			
	H. opuntia	DIC	1	0.847	0.847	0.279	0.694
		DOC	1	20.905	20.905	6.883	0.077
		DIC x DOC	1	6.586	6.586	2.169	0.288
		Aquaria	8	40.72598	5.090747	3.65	0.03
		Residual	10	54.667	3.037		

		Total	21	83.958			
NO_X fluxes in light	*H. macroloba*	DIC	1	0.0109	0.0109	0.45	0.522
		DOC	1	0.000590	0.000590	0.002	0.880
		DIC x DOC	1	0.0229	0.0229	0.94	0.360
		Aquaria	8	0.194609	0.02432612	0.41	0.897
		Residual	12	0.7206705	0.0458		
		Total	23	0.950			
	H. opuntia	DIC	1	0.0000290	0.0000290	0.404	0.532
		DOC	1	0.000000493	0.000000493	0.00685	0.935
		DIC x DOC	1	0.000173	0.000173	2.400	0.137
		Aquaria	8	0.000828	0.0001034	2.03	0.129
		Residual	12	0.00144	0.0000719		
		Total	23	0.00164			
NO_X fluxes in dark	*H. macroloba*	DIC	1	0.0000778	0.0000778	1.09	0.326
		DOC	1	0.00129	0.00129	18.27	**0.0027***
		DIC x DOC	1	0.000165	0.000165	2.33	0.165
		Aquaria	8	0.000566	0.0000707370	0.58	0.774555
		Residual	12	0.00202	0.000101		
		Total	23	0.00356			
	H. opuntia	DIC	1	0.00317	0.00317	12.761	**0.02***
		DOC	1	0.00827	0.00827	33.281	**0.002***
		DIC x DOC	1	0.00122	0.00122	4.901	0.111
		Aquaria	9	0.003032	0.00037896	2.35	0.088
		Residual	12	0.00497	0.000248		
		Total	23	0.0176			
NH_4 fluxes in light	*H. macroloba*	DIC	1	0.000283	0.000283	0.87	0.377
		DOC	1	0.000160	0.000160	0.49	0.502
		DIC x DOC	1	0.000830	0.000830	2.56	0.148
		Aquaria	8	0.002587	0.00032343	0.78	0.626
		Residual	12	0.00496	0.00042		
		Total	23	0.00881			
	H. opuntia	DIC	1	0.00124	0.00124	12.681	**0.002***
		DOC	1	0.00000393	0.00000393	0.0401	0.843
		DIC x DOC	1	0.000668	0.000668	3.54	0.1
		Aquaria	8	0.00151	0.0001886	5.02	**0.007***
		Residual	12	0.00196	0.0000979		
		Total	23	0.00387			
NH_4 fluxes in dark	*H. macroloba*	DIC	1	0.00143	0.00143	18.44	**0.003***
		DOC	1	0.00124	0.00124	15.99	**0.004***
		DIC x DOC	1	0.00142	0.00142	18.37	**0.003***
		Aquaria	8	0.0006213	0.0000777	0.47	0.855
		Residual	12	0.00198	0.000154		
		Total	23	0.00670			
	H. opuntia	DIC	1	0.0223	0.0223	6.150	0119
		DOC	1	0.0120	0.0120	3.312	0.084
		DIC x DOC	1	0.0201	0.0201	5.541	0.135
		Aquaria	8	0.00587	0.0073	6.18	0.003
		Residual	12	0.0727	0.00363		
		Total	23	0.127			
PO_4 Fluxes in light	*H. macroloba*	DIC	1	0.0000153	0.0000153	7.27	**0.027***
		DOC	1	0.00000236	0.00000236	1.11	0323
		DIC x DOC	1	0.00000911	0.00000911	4.32	0.071
		Aquaria	8	0.0000169	0.00000231	2.28	0.095
		Residual	12	0.0000111	0.00000092		
		Total	23	0.0000549			
	H. opuntia	DIC	1	0.00000511	0.00000511	4.994	**0.01***
		DOC	1	0.00000341	0.00000341	7.42	**0.03***
		DIC x DOC	1	0.0000000523	0.0000000523	0.0511	0.823
		Aquaria	8	0.000003681	0.0000004601	0.33	0.94
		Residual	12	0.0000205	0.00000102		
		Total	23	0.0000290			
PO_4 Fluxes in dark	*H. macroloba*	DIC	1	0.148	0.148	4.54	0.065
		DOC	1	0.140	0.140	4.31	0.071
		DIC x DOC	1	0.0611	0.0611	1.88	0.208
		Aquaria	8	0.2602862	0.0325	1.0	0.482
		Residual	12	0.3897141	0.0325		
		Total	23	0.999			
	H. opuntia	DIC	1	0.00000408	0.00000408	3.10	0.116
		DOC	1	0.00000483	0.00000483	3.68	0.091
		DIC x DOC	1	0.000000107	0.000000107	0.134	0.718
		Aquaria	8	0.00001051	0.00000131	2.89	**0.048***
		Residual	12	0.0000160	0.000000799		
		Total	23	0.0000250			
DOC fluxes in light	*H. macroloba*	DIC	1	0.00151	0.00151	4.80	0.06
		DOC	1	0.00212	0.00212	6.76	**0.032***
		DIC x DOC	1	0.000644	0.000644	2.05	0.190
		Aquaria	8	0.00251	0.000314	1.78	0.177
		Residual	12	0.00211	0.000176		
		Total	23	0.00890			
	H. opuntia	DIC	1	1.039	1.039	5.19	0.052
		DOC	1	4.268	4.268	38.879	**<0.001***
		DIC x DOC	1	1.212	1.212	11.041	0.003*
		Aquaria	8	1.602184	0.200273	4.00	**0.016***

		Residual	12	2.196	0.110		
		Total	23	8.714			
DOC fluxes	*H. macroloba*	DIC	1	0.239	0.239	1.02	0.342
in dark		DOC	1	3.078	3.078	13.17	**0.007***
		DIC x DOC	1	0.0970	0.0970	0.41	0.538
		Aquaria	8	1.87008	0.23376	1.47	0.265
		Residual	12	1.913856	0.159488		
		Total	23	7.197			
	H. opuntia	DIC	1	0.00000840	0.00000840	0.0773	0.784
		DOC	1	0.00387	0.00387	35.592	**<0.001***
		DIC x DOC	1	0.000119	0.000119	1.093	0.308
		Aquaria	8	0.00132	0.000166	2.35	0.087
		Residual	12	0.00217	0.000109		
		Total	23	0.00617			
Fv/Fm	*H. macroloba*	DIC	1	0.0001215	0.0001215	0.02	0.883
		DOC	1	0.000683	0.006827	0.13	0.73
		DIC x DOC	1	0.00859	0.00858	1.63	0.238
		Aquaria	8	0.0423	0.00529	1.77	0.180
		Residual	12	0.035803	0.00298		
		Total	23	0.087464			
	H. opuntia	DIC	1	0.00375	0.00375	1.19	0.307
		DOC	1	0.00336	0.0036	1.07	0.332
		DIC x DOC	1	0.00251	0.0198375	6.31	**0.036***
		Aquaria	8	0.02516	0.0014	1.54	0.241
		Residual	12	0.024491	0.00204		
		Total	23	0.00766			

4 - Effects of high dissolved organic carbon (DOC) and high dissolved inorganic carbon (DIC) on photosynthesis and calcification in two calcifying green algae from a Caribbean reef lagoon

Meyer F W[1], Schubert N[2], Diele K[3], Teichberg M[1], Wild C[1,4], and Enríquez S[2*]

[1] Leibniz Center for Tropical Marine Ecology (ZMT), Fahrenheitstraße 6, Bremen, Germany

[2] Unidad Académica de Sistemas Arrecifales Puerto Morelos, Instituto de Ciencias del Mar y Limnología, Universidad Nacional Autónoma de México, Puerto Morelos, Quintana Roo, Mexico

[3] Edinburgh Napier University, School of Life, Sport and Social Sciences, Edinburgh, UK

[4] Faculty of Biology & Chemistry, University of Bremen, Bibliothekstraße 1, Bremen, Germany

[*] Corresponding author

E-mail: enriquez@cmarl.unam.mx

This manuscript is in preparation for submission to PLOS ONE

Abstract

Because of climate change and coastal eutrophication, coral reefs worldwide are often affected by both increasing dissolved inorganic carbon (DIC) and dissolved organic carbon (DOC) concentrations. Those two stressors can occur simultaneously, particularly in near-shore reef environments under high population pressure. Experimental studies on the interplay of these two stressors are missing, but are needed to understand potential synergistic effects and foresee future changes in reef ecosystem functioning. This manipulative study therefore investigated the impact of DIC (pH_{NBS}: 8.2 and 7.8; pCO_2: 377 and 1076 µatm) and DOC (added as glucose: 0 and 233 µmol L^{-1}) on the two common calcifying green algae *Halimeda incrassata* and *Udotea flabellum* from a Mexican Caribbean reef lagoon. As response parameters calcification, O_2 fluxes and maximum quantum efficiency (F_v/F_m) were quantified during an open mesocosm experiment over 10 days. For the measurements of treatment responses, apical segments of each algal thallus as well as the whole thallus were measured. Findings revealed that under high DIC, F_v/F_m was significantly reduced in the apical segments of *U. flabellum* by 15% compared to the controls. Consequently, gross photosynthesis of the apical segments of *U. flabellum* was reduced by 33%. Calcification of both species was reduced in the apical

segments under high DIC concentrations by 150% for *H. incrassata* and by 13% for *U. flabellum* compared to control conditions. Under high DOC concentrations, F_v/F_m was significantly reduced in the apical segments of *H. incrassata* by 15% and gross photosynthesis was reduced by 41%. Calcification of *H. incrassata* and *U. flabellum* was reduced by 66% and 131% respectively. Respiration of the apical segments of both species was not influenced by any of the treatments. Under the combination of both, high DIC and DOC concentrations, the individual effects of the treatments were reduced leading to a reduction in F_v/F_m for *H. incrassata* only 14% and of 7% for *U. flabellum* compared to the controls. Gross photosynthesis was therefore only reduced by 26% compared to the controls of *H. incrassata* and by 24% compared to the controls of *U. flabellum.* Calcification of *H. incrassata* was reduced by 7% under the combined treatment compared to the controls. For the calcification of *U. flabellum* negative effects were synergistic leading to a further reduction of calcification to 161% compared to the controls. When compared to the whole thallus, gross photosynthesis was reduced only for *H. incrassata* by 35 %, compared to the controls. High DOC concentrations did not affect the O_2 fluxes of the whole thallus. The combined treatment significantly reduced the negative effects of high DIC on photosynthesis of *H. incrassata*.

In comparison to the apical segments measured, fewer effects of the treatments could be detected when measuring the whole algal thallus. Therefore care has to be taken when choosing appropriate measurement techniques and when drawing conclusions. The results thus indicate that high DIC will reduce calcification and primary production of both calcifying green algae species, but this may be mitigated by high DOC availability especially for *H. incrassata*. Species-specific differences towards the combined treatment suggest that under future ocean acidification scenarios, *U. flabellum* could be less successful than *H. incrassata* which may result in overall reduced primary production and carbonate accretion by this dominant sand dweller.

Introduction

During the last decades, many Caribbean coral reefs and their lagoons have suffered from a substantial loss of coral cover and diversity [1] due to the combination of intense warming events, over-exploitation of grazers, pathogen-induced mortality of important grazer species [2], the loss of major reef-building coral species and an increase in storm events [3]. Connected to rising greenhouse gas emission, another threat to coral reefs and marine calcifiers has become evident and is called ocean acidification (OA) [4]. Due to increasing CO_2 concentrations in the atmosphere also the oceans CO_2 partial pressure is rising, leading to an increase in bicarbonate concentrations and a decrease in ocean pH [5]. With this shift in the ocean carbonate system, the saturation state for calcium carbonates is declining, making it harder for marine organisms to calcify and also facilitating dissolution of existing calcium carbonates. Examples of field research and natural low pH sites show that under OA the reef

framework is little stable [6] and reef growth is on the border of erosion. Therefore, reef frameworks may provide less shelter for lagoon ecosystems under future OA scenarios and increased storm intensities [7] which may lead to species shifts in reef lagoons [8]. Lagoon species such as calcifying green algae from the genus *Halimeda* may suffer from reduced carbon accretion rates [9,10] and reduced skeletal density. As these important sediment producers [11–13] show reduce calcium carbonate production rates under OA conditions, future erosion of also lagoon sediments is inevitable under OA conditions. In addition to global threats such as warming and OA, an increase of pollution and the absence of grazers has led already in many parts of the Caribbean and other reefs worldwide to so called "phase shifts" [3,14], resulting in coral depauperate reefs with varying, but persistent high algal cover. One of the main drivers is anthropogenic pollution with agricultural derived inorganic nutrient inputs via rifer runoff and untreated or poorly treated human waste waters. These increased concentrations of organic and inorganic nutrients directly affect reef organisms. Recent studies have shown that an increase of high labile organic matter can negatively affect corals, leading to bleaching [15] and eventually mortality [16] by inducing local oxygen depletion [17–19]. As a result of the shift from a coral to an algae dominated reef, the organic matter cycling changes as corals and algae release different amounts and compositions of organic matter [20–22] that fuel different bacterial lineages [17,22–24]. Under phase shift related algal dominance, bacterial communities may therefore change from autotrophic to heterotrophic communities [22,23]. Source of high concentrations of labile DOC are eventually seagrass beds themselves [20], and human waste water via groundwater discharge [25,26] and seasonal storm events [27].

Surprisingly, no comparable studies are known that investigate the role of elevated dissolved organic matter (DOM) levels on calcifying algae. In addition, OA and elevated organic matter availability may interact and pose an even larger threat to calcifying algae. Hence, studies are needed to assess the individual and combined effect of OA and increased organic matter availability on the physiology of these important carbonate producers. Here we present a laboratory study on the effects of both, DIC and high levels of DOC on the physiology of two calcifying green algae of a typical Caribbean reef lagoon: *Halimeda incrassata* and *Udotea flabellum*. Both algal species make up a significant amount of the calcifying benthic community in a Caribbean reef lagoon [8,28] and produce high amounts of biogenic carbonate sediments that form so called "bioherms" [12,13]. This study aims to increase the understanding of future functioning and role of those two algae species in reef lagoon environments through the measurement of physiological responses towards both, elevated DOC and DIC.

Material and Methods

Algal collection and maintenance

Halimeda incrassata and Udotea flabellum plants were collected in March 2012 (average temperature 27.6 °C ± 0.3) in the Puerto Morelos reef lagoon, at 3-3.5 m water depth using SCUBA and transported in mesh-covered zip log bags to the aquaria facility. To reduce variability due to age differences, thalli of similar sizes of H. incrassata (5-7 segments) and U. flabellum (3-5 cm in height) were collected.

Both species were kept in 50 L experimental seawater flow-through aquaria at constant temperature of 2° C, ambient pH, and a flow rate of 1 L min^{-1} of ~ 50 µm filtered water from the lagoon for 5 days to recover from handling and for acclimation to the tank conditions. The algae were maintained under natural light conditions simulating the irradiance level at collection depth (21% of incident light achieved by shading with mosquito mesh). Light data were continuously logged during experiments using a LI-COR cosine sensor positioned inside the tanks and data were acquired by a LI-COR data logger (LI-COR, Lincoln, U.S.A.).

After the pre-acclimation period, algal thalli of both species (n=12 per tank and species) were transferred to the different treatment tanks.

Experimental treatments

The experiment was conducted over 10 days in March/April 2012 in a flow-through setup which consisted of 12 aquaria of 50 L each. To increase water currents in the tanks, aquaria pumps (pump rate: 500 L h^{-1}) were placed in each tank and connected to a rectangular PVC frame surrounding the tank, with holes facing the inside to create homogenous flow conditions within each tank. The three replicate tanks for the two treatments with two treatment levels were placed in alternating order.

The treatments were simulated OA, as altered pCO_2 in ambient and high availability (329 µatm and 1003 µatm, respectively) and DOC in ambient and high availability (208 µmol L^{-1} and 441 µmol L^{-1} with 233 µmol L^{-1} DOC added as Glucose, D-Glucose, Sigma Aldrich, purity > 99.5 %). The target pCO_2 was 1000 µatm and was achieved through pH manipulation via CO_2 gas injection by a potentiometric pH sensors controlled pH stat system (IKS Aquaritic Products, Karlsbad, Germany). These pCO_2 levels were chosen under consideration of the Representative Concentration Pathways (RCP) with pH of 6.0 to 8.5 for the year 2100 [29–31]. The DOC treatment levels were adjusted to concentrations described for DOC treatments applied in other studies with corals using glucose and lactose as DOC in high concentrations [15,16,19]. The DOC treatment in the form of highly bioavailable DOC was achieved by additions of 833 µmol L^{-1} DOC (Glucose, D-Glucose, Sigma

Aldrich) twice a day at 8:00 a.m. and 8:00 p.m. to each of the six high-DOC treatment tanks. To quantify the resulting DOC treatment conditions, total organic carbon (TOC as Non Particulate Organic Carbon) was measured throughout the experimental duration. Samples for TOC were filtered through 0.45 µm GFF filters (Whatman), acidified with 150 µL fuming HCl and frozen at -20°C until analysis on a Shimadzu TOC-5000A (Shimadzu, USA).

During experiments, salinity and temperature in each tank were monitored twice daily (WTW Multiprobe 3430) and water samples for monitoring total alkalinity (AT) were taken every second day, filtered through 0.45 µm GFF filters and stored with a drop of chloroform at 4°C until analysis. These parameter were used to calculate the carbonate system with the CO2sys excel spreadsheet software [32].

Biological Oxgen Demand (BOD)

To estimate microbial respiration rates of the treatment water, BOD was measured. At the end of the experiment 150 mL of unfiltered seawater were incubated in winkler bottles for 24 h in the dark under temperature conditions of the treatments (n = 3). O_2 concentration (mg L^{-1} and % saturation) as well as salinity and temperature were recorded before and after the incubation, O_2 consumption rates were calculated and related to water volume and time to mg O_2 L^{-1} h^{-1}.

Assessment of maximum photosynthetic quantum efficiency

The maximum quantum efficiency (Fv/Fm) of the algae was determined by using a Pulse Amplitude Modulation (PAM) fluorometer (Diving-PAM, Walz, Germany) with a 6 mm diameter fiber optic cable. Fv/Fm measurements were conducted on the apical algal segments every evening at 8 p.m., thus one hour after sunset, to ensure that the algae were dark acclimated.

Quantification of photosynthesis, respiration and light calcification in algal segments

For the physiological determinations, thallus segments of H. incrassata (4-5 youngest segments) and the uppermost 2 cm of U. flabellum thalli were used in order to avoid variation between replicates due to age differences between plants and artifacts by the presence of epiphytes that increase as older the segments are. The segments were severed from the parent plant (see [33]) at least 2 h before starting measurements to allow wound healing.

Following the 10 days under the different experimental conditions, photosynthesis and calcification rates were determined simultaneously by exposing the thallus segments for 30 min at 2°C to a saturating light intensity (500 µmol quanta m^{-2} s^{-1}). Afterwards, the water was collected to determine

alkalinity changes (see below) and the samples were incubated for another 10-15 min in darkness to determine the post-illuminatory respiration rate. The photosynthetic rates and respiration rates were measured polarographically in 17 mL water-jacked chambers (DW3, Hansatech Instruments Ltd., Norfolk, UK), using Clark-type O_2 electrodes (Hansatech) and a circulating bath with a controlled temperature system (RTE-100/RTE 101LP; Neslab Instruments Inc., Portsmouth, NH, USA). The electrodes were calibrated with air- and N_2-saturated filtered seawater. Freshly filtered seawater (0.45 µm) from the respective treatment tank was used for the incubations. Data were captured with a computer equipped with an analog/digital converter using DATACAN V software (Sable Systems, Inc., Las Vegas, NV, USA).

The calcification rates were measured using the alkalinity anomaly principle based on the ratio of two equivalents of total alkalinity for each mole of $CaCO_3$ precipitation [34]. For alkalinity measurements, a modified spectrophotometer procedure as described by [35] was used. After gently bubbling with N_2 for at least 10 min, Bromocresol Green (BCG; Sigma Aldrich, Steinheim, Germany) was added to the water sample. The changes in the indicator during microtitration with 0.3 N HCl was recorded at 444, 616 and 750 nm using an Ocean Optics USB4000 spectrophotometer (Ocean Optics Inc., Dunedin, USA) with a xenon light source (PX-2, Ocean Optics Inc., Dunedin, USA). The microtitration was performed into a 1 cm cuvette at a rate of 8 µL min^{-1} using a glass syringe (Hamilton Company, Reno, USA) fitted to a syringe pump (Kd Scientific Inc., Holliston, USA). For quality control, a certified reference material of known total alkalinity from the Marine Physical Laboratory (Scripps Institution of Oceanography, USA) was used to calibrate the method.

Quantification of photosynthesis, respiration and light calcification in whole algal thalli

Two algal thalli from each replicate tank were transferred to individual closed acrylic chambers (150 mL) and incubated for 60 min under light-saturated conditions (500 µmol photons m^{-2} s^{-1}) to simultaneously determine photosynthesis and calcification rates. For the incubations, water was taken from the respective treatment tanks and filtered through 0.45 µm GFF filters (Whatman). Therefore, pH and DOC concentrations corresponded to treatment conditions.

Four parallel incubations including one blank per run were performed in a temperature controlled water bath at 28°C, corresponding to the temperature during the 10 days of experiment. To ensure sufficient water movement during the incubation time, magnetic stirrer bars driven by magnetic stir plates were used.

O_2 fluxes were measured by continuous O_2 monitoring using two 4-channel O_2 meters (Firesting, Pyroscience, Germany), connected to each chamber with fiber optic cables. Net photosynthesis, respiration, and resulting gross photosynthesis were then determined in µmol O_2 h^{-1} and related to

organism surface area. In addition, O_2 consumption was corrected to blank readings from empty incubation chambers containing only the respective treatment water.

Light calcification rates were determined through the change of AT during the incubation by application of the alkalinity anomaly technique [36]. AT was measured by end point titration of a 50 ml water sample by a Titroline Alpha plus autosampler (SI Analytics, Germany) using 0.5 M HCl and certified reference material (CRM Batch 111, A. Dickson, Scripps Oceanographic Institute) and calculated by non-linear regression fitting between pH 3.5 and pH 3.0. Calcium carbonate precipitation or dissolution expressed in µM C h-1 was calculated by half molar of the difference between the post incubation and the seawater control [36], and normalized to chamber volume, time of incubation and organism surface area.

Algal surface area quantification

The individual surface area of the algal segments and thalli was determined by either photos taken (Sealife DC1200 without housing) from top in 20 cm distance and using a plastic glass plate to flatten the algae or scanning the algal segments. 2D planar projection and a reference measure in the photos/scans were then used to calculate the surface are with ImageJ software.

Statistical analyses

We tested for significant differences of the individual and combined treatment using a Two-Way-ANOVA. Data were tested for normality using the Shapiro-Wilk test and for equal variance using the Levene median test. The Two Way ANOVA was performed with the treatments DIC and DOC as fixed factors. To evaluate differences between individual treatment combinations, a Pairwise Multiple Comparison Procedure (Holm-Sidak method) was performed. The statistical analyses were conducted using SigmaPlot 12.5 and Statistica 12.0.

Results

Carbonate and water chemistry, BOD

The pH under control conditions was 8.219, and the calculated pCO_2 377 µatm. As a result of the CO_2 addition, the pH dropped to 7.836 in the high DIC treatment and 7.815 in the high DIC high DOC treatment (Table 1). The calculated pCO_2 was 1076 for the high DIC treatment and 1135 for the high DIC high DOC treatment. As a result, the aragonite saturation (Ω_{Arag}) dropped from 4.2 in the controls to 2.0 in the high DIC treatment and the combined treatment (Table 1). In the high DOC treatment, the pH or pCO_2 was slightly lower as the controls with 415 µatm in the DOC treatment and the oxygen

concentration dropped from 208 µmol l^{-1} in the controls to 202 µmol l^{-1} in the high DOC treatment, and to 199 µmol l^{-1} (from 102 % saturation to 99 and 98 % respectively) in the combined treatment. As a result of the elevated organic carbon availability, the BOD only changed significantly in the DOC and the combined treatment from 0.93 µmol O_2 L^{-1} h^{-1} in the control treatment to 1.35 µmol O_2 L^{-1} h^{-1} in the high DOC treatment and 1.62 µmol O_2 L^{-1} h^{-1} in the combined treatment (Fig. 4)

Table 1. Carbonate system parameters. Values calculated using CO2Calc with total alkalinity and pH_{NBS} as input parameters. (n=18).

Treatment	pH [NBS]	temp [°C]	Salinity [ppt]	O_2 conc (µmol l^{-1})	TA (µmol $kgSW^{-1}$)	*p*CO2 (µatm)	HCO_3^- (µmol/kgSW)	ΩAr
Control	8.219 ±0.02	28.1 ±0.1	35.9 ±0.1	208 ±0.4	2414 ±8	377 ±27	1776 ±26	4.2 ±0.2
High DOC	8.186 ±0.03	28.1 ±0.2	35.9 ±0.1	202 ±0.9	2414 ±8	415 ±31	1811 ±31	4.0 ±0.2
High DIC	7.836 ±0.04	28.0 ±0.2	36 ±0.1	208 ±1.7	2409 ±6	1076 ±101	2097 ±24	2.0 ±0.1
High DOC & DIC	7.815 ±0.02	28.0 ±0.1	36 ±0.1	199 ±1.1	2413 ±7	1135 ±55	2114 ±14	2.0 ±0.1

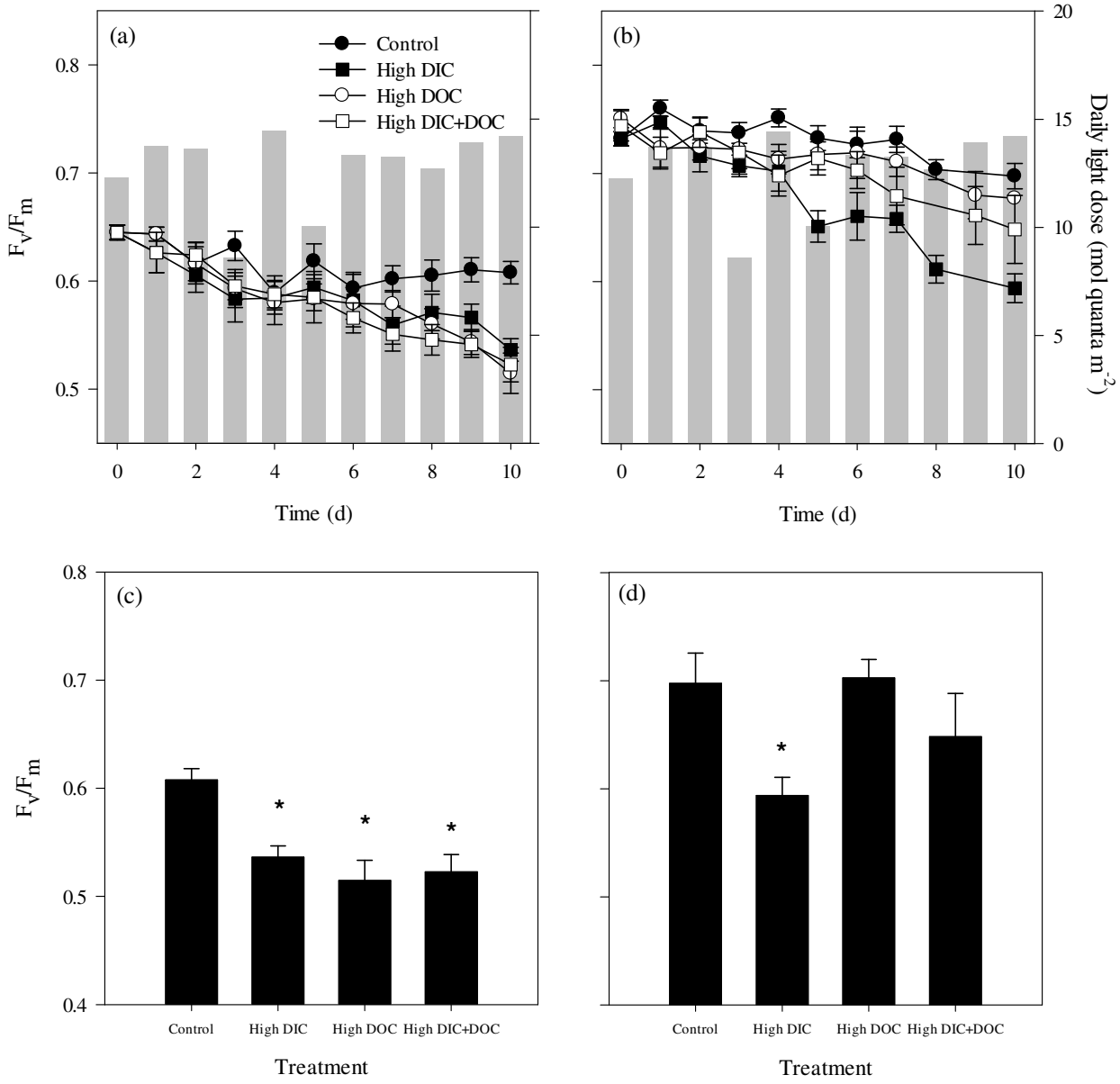

Fig. 1 Photosynthesis parameters of algal segments as responses to treatments. Maximum quantum yield (a, b, c, d) of dark adapted individuals of *Halimeda incrassata* (a, c; n=12) and *Udotea flabellum* (b, d; n=15) over the duration of the experiment (a, b) and at the end of the experiment (c ,d). Light does over each day is given as grey bar (a, b). Bar height represents mean values and error bars standard deviation. Significant differences ($p < 0.05$) are marked with an asterisk.

Effects of high DIC on the algal segments

High DIC conditions reduced the F_v/F_m of *H. incrassata* and *U. flabellum*, by 12 % from 0.61 in the controls to 0.53 in the high DIC treatment for *H. incrassata* and by 15 % from 0.70 in the controls to 0.59 for *U. flabellum* (Fig. 1). Gross photosynthesis of both species was reduced by high DIC concentrations. For *H. incrassata* it was significantly reduced by 28 % from 2.29 to 1.66 µmol O_2 cm^{-2} h^{-1} and for *U. flabellum* by 33 % from 1.1 to 0.75 µmol O_2 cm^{-2} h^{-1} for gross photosynthesis (Fig. 2 a, b). For both species respiration was not affected (Fig. 2). Calcification of both algae species was significantly reduced by the high DIC treatment (Fig. 2 c, d) by 152% from 1.12 to -0.58 µmol C cm^{-2} h^{-1} for *H. incrassata* and by 12.8% from 0.30 to 26 for *U. flabellum*.

Effects of increased DOC availability on the algal segments

Under high DOC availability, F_v/F_m of *H. incrassata* was significantly reduced by 15 % from 0.61 to 0.52 (Fig. 1). The gross photosynthesis of *H. incrassata* was reduced under the high DOC treatment by 51% from 2.29 to 1.36 µmol O_2 cm^{-2} h^{-1}. The respiration rate of both species was not affected (Fig. 2). The calcification rate of both species was significantly decreased under the high DOC treatment and decreased by 67 % from 1.12 to 0.37 µmol C cm^{-2} h^{-1} for *H. incrassata* and by 131 % from 0.3 to -0.1 µmol C cm^{-2} h^{-1} for *U. flabellum* (Fig. 2).

Effects of the combined treatment on the algal segments

The combination of both treatments showed interactive effects on the physiology for both species. For *H. incrassata* DOC and DIC showed antagonistic interactive effects on gross photosynthesis where the combination of high DIC and DOC reduced the effect of DIC compared to the high DIC treatment alone. Hence the gross photosynthesis was significantly reduced by 26 % compared to the controls and was therefore 2 % higher than in the DIC treatment (Fig. 2). The maximum quantum yield of *U. flabellum* also showed an antagonistic effect of the combined treatment, leading to a reduction of F_v/F_m of only 7% compared to the controls and therefore 4% higher than in the DIC treatment. (Fig. 1).

Effects of high DIC on the whole algal thallus

High DIC conditions significantly reduced gross photosynthesis of *H. incrassata* by 35 % from 1.7 to 1.1 µmol O_2 cm^{-2} h^{-1} (Fig. 3). For *U. flabellum*, respiration increased by 159 % from 0.09 to 0.24 µmol cm^{-2} h^{-1}, while respiration of *H. incrassata* was not affected (Fig. 3).

Effects of increased DOC availability

Under high DOC availability the net and gross photosynthesis of both species was not affected, but the respiration rate of *U. flabellum* was significantly reduced by 64 % from 0.38 to 0.14 µmol O_2 cm^{-2} h^{-1} (Fig. 3).

Effects of the combined treatment

The combination of both treatments showed interactive effects on the physiology only for *H. incrassata*. For *H. incrassata* DOC and DIC showed antagonistic interactive effects on gross photosynthesis where the combination of high DIC and DOC reduced the effect of DIC compared to the high DIC treatment alone. Hence the gross photosynthesis was significantly reduced by 11 and 23 % respectively compared to the controls and was therefore 23 % higher than in the DIC treatment (Fig. 3).

Table 2. Comparison of oxygen fluxes in algal segments and thalli. Average values with standard deviation in () are given for *H. incrassata* (upper two rows) and *U. flabellum* (lower two rows) for gross photosynthesis (four left columns) and respiration (four right columns) (n=6).

		Gross Photosynthesis				**Respiration**			
		Control	High DIC	High DOC	High DIC+DOC	Control	High DIC	High DOC	High DIC+DOC
Halimeda	Segment	2.29 (0.3)	1.66 (0.2)	1.36 (0.2)	1.70 (0.4)	0.53 (0.1)	0.50 (0.3)	0.46 (0.1)	0.49 (0.2)
incrassata	Thallus	1.7 (0.3)	1.1 (0.2)	1.3 (0.2)	1.3 (0.3)	0.38 (0.2)	0.37 (0.1)	0.14 (0.1)	0.13 (0.06)
Udotea	Segment	1.11 (0.1)	0.74 (0.2)	1.07 (0.3)	0.84 (0.2)	0.34 (0.1)	0.37 (0.1)	0.38 (0.1)	0.41 (0.1)
flabellum	Thallus	0.96 (0.8)	0.77 (0.1)	0.74 (0.4)	0.76 (0.7)	0.09 (0.1)	0.24 (0.1)	0.19 (0.1)	0.23 (0.2)

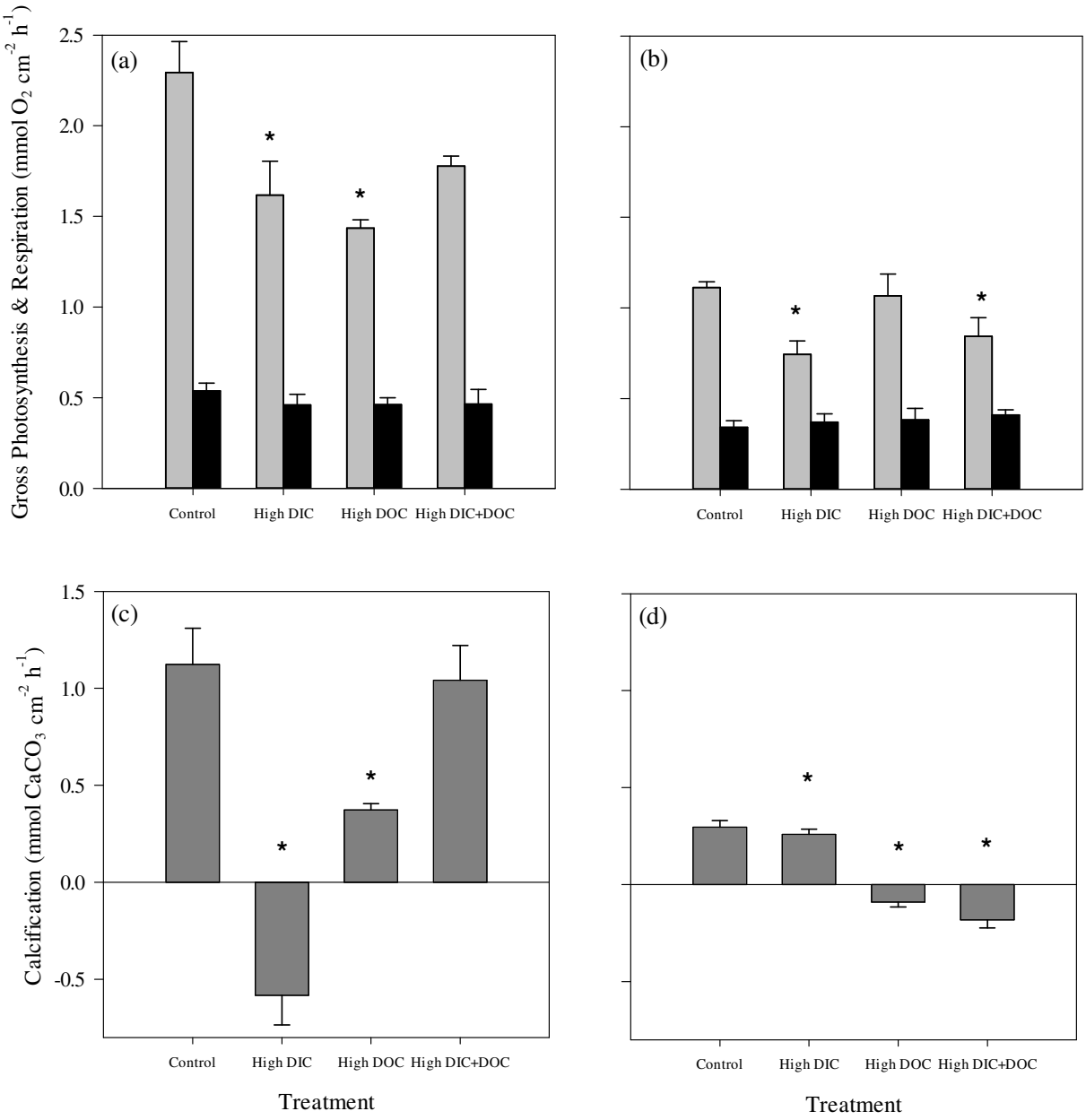

Fig. 2 Oxygen fluxes and calcification of segments of both algae species in responses to treatments. Gross photosynthesis (grey bars, a; b) and respiration (black bars, a; b) of *Halimeda incrassata* (a; n = 6) and *Udotea flabellum* (b; n = 6). Gross photosynthesis measured during light (500 µE m^{-2} s^{-1}) conditions and respiration during dark condition and related to algae surface area. Calcification during light (500 µE m^{-2} s^{-1}) of Halimeda incrassata (c; n= 6) and Udotea flabellum (d; n=6) measured via alkalinity anomaly technique and related to algae surface area. Significant differences ($p < 0.05$) relative to controls are marked with an asterisk

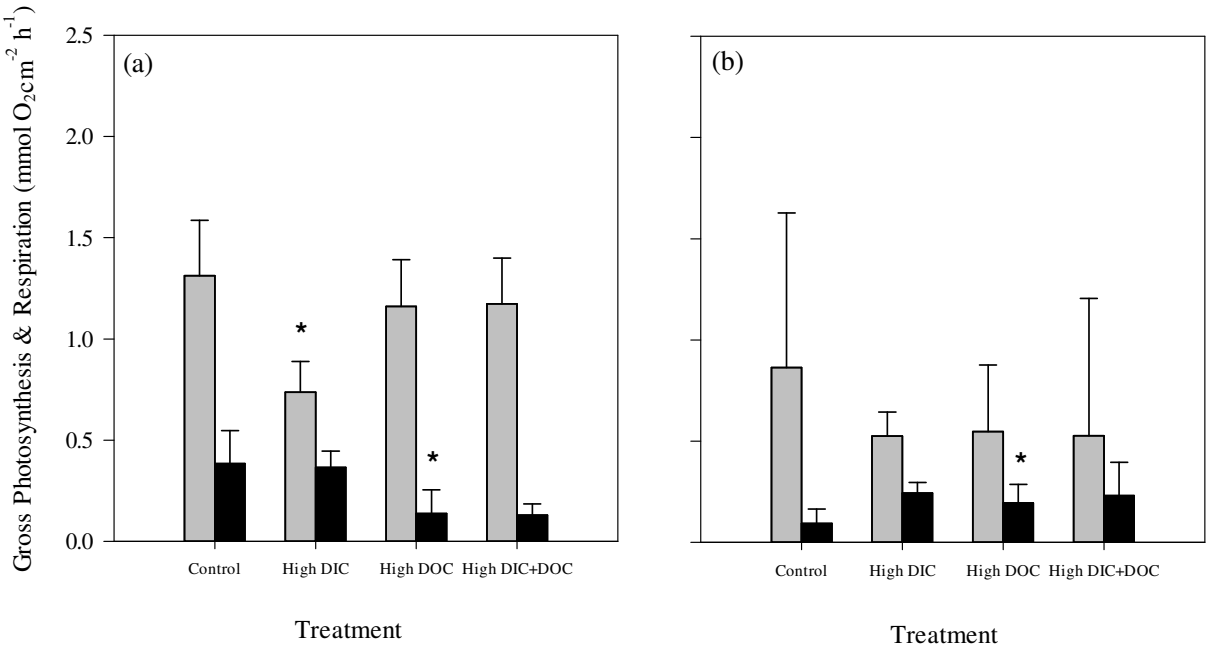

Fig. 3 Oxygen fluxes of algal thalli as responses to treatments. Gross photosynthesis (grey bars, a; b) and respiration (black bars, a; b) of *Halimeda incrassata* (a; n = 6) and *Udotea flabellum* (b; n = 6). Gross photosynthesis measured during light (500 µE m^{-2} s^{-1}) conditions and respiration during dark condition and related to algae surface area. Bar height represents mean values and error bars standard deviation. Significant differences ($p < 0.05$) are marked with an asterisk.

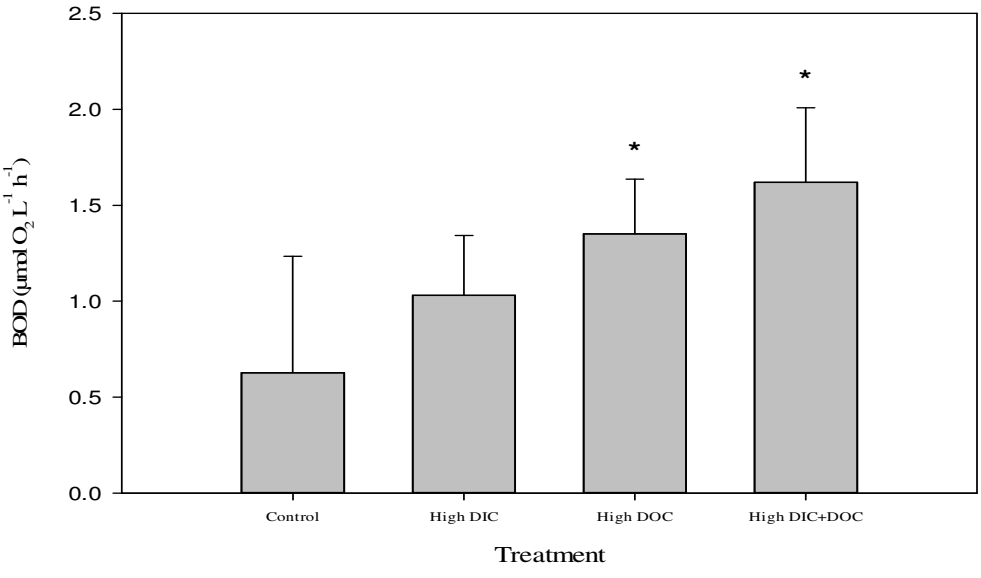

Fig. 4 Biological oxygen demand (BOD) in responses to treatments. Oxygen consumption measured during 24 hour dark incubation and related to water volume (n=3). Significant differences ($p < 0.05$) relative to controls are marked with an asterisk

Table 3. Results of Two Way ANOVA for algal segments of both species: *Halimeda incrassata* and *U. flabellum* with DIC and DOC as fixed factors. Significant results are marked bold with an asterisk (*).

Response variable	Species	Source of variation	DF	SS	MS	F-value	P-value
Light calcification	*H. incrassata*	DIC	1	1.240	1.240	13.882	**0.002***
		DOC	1	0.886	0.886	9.917	**0.007***
		DIC x DOC	1	6.510	6.510	72.867	**<0.001***
		Residual	15	1.340	0.0893		
		Total	18	9.399	0.522		
	U. flabellum	DIC	1	0.0206	0.0206	5.242	**0.036***
		DOC	1	0.836	0.836	212.329	**<0.001***
		DIC x DOC	1	0.00356	0.00356	0.904	0.356
		Residual	16	0.0630	0.00394		
		Total	19	0.902	0.0475		
Gross	*H. incrassata*	DIC	1	0.0997	0.0997	1.116	0.307
photosynthesis		DOC	1	0.903	0.903	10.109	**0.006***
		DIC x DOC	1	1.104	1.104	12.363	**0.003***
		Residual	15	1.339	0.0893		
		Total	18	3.310	0.184		
	U. flabellum	DIC	1	0.500	0.500	11.561	**0.003***
		DOC	1	0.00421	0.00421	0.0973	0.758
		DIC x DOC	1	0.0299	0.0299	0.692	0.416
		Residual	19	0.822	0.0433		
		Total	22	1.352	0.0615		
Respiration	*H. incrassata*	DIC	1	0.00000195	0.00000195	0.0000499	0.994
		DOC	1	0.00675	0.00675	0.173	0.683
		DIC x DOC	1	0.00322	0.00322	0.0825	0.778
		Residual	16	0.625	0.0391		
		Total	19	0.635	0.0334		
	U. flabellum	DIC	1	0.00450	0.00450	0.431	0.519
		DOC	1	0.00989	0.00989	0.947	0.342
		DIC x DOC	1	0.00000840	0.00000840	0.000805	0.978
		Residual	20	0.209	0.0104		
		Total	23	0.223	0.00970		
Maximum quantum yield	*H. incrassata*	DIC	1	1.240	1.240	13.882	**0.002***
		DOC	1	0.886	0.886	9.917	**0.007***
		DIC x DOC	1	6.510	6.510	72.867	**<0.001***
		Residual	15	1.340	0.0893		
		Total	18	9.399	0.522		
	U. flabellum	DIC	1	0.0329	0.0329	6.707	**0.020***
		DOC	1	0.00462	0.00462	0.941	0.346
		DIC x DOC	1	0.00327	0.00327	0.666	0.426
		Residual	16	0.0785	0.00491		
		Total	19	0.121	0.00638		

Table 4. Results of Two Way ANOVA for biological oxygen demand (BOD) and whole thallus of both species: *Halimeda incrassata* and *U. flabellum* with DIC and DOC as fixed factors. Significant results are marked bold with an asterisk (*).

Response variable	Species	Source of variation	DF	SS	MS	F-value	P-value
Gross	*H. incrassata*	DIC	1	0.497	0.497	7.226	**0.014***
photosynthesis		DOC	1	0.0677	0.0677	0.984	0.333
		DIC x DOC	1	0.560	0.560	8.142	**0.010***
		Residual	20	1.376	0.0688		
		Total	23	2.501	0.109		
	U. flabellum	DIC	1	0.00597	0.00597	0.0699	0.794
		DOC	1	0.0294	0.0294	0.344	0.564
		DIC x DOC	1	0.0000894	0.0000894	0.00105	0.975
		Residual	20	1.711	0.0855		
		Total	23	1.746	0.0759		
Respiration	*H. incrassata*	DIC	1	0.000216	0.000216	0.0154	0.902
		DOC	1	0.369	0.369	26.377	**<0.001***
		DIC x DOC	1	0.000861	0.000861	0.0616	0.807
		Residual	20	0.280	0.0140		
		Total	23	0.650	0.0282		
	U. flabellum	DIC	1	0.0525	0.0525	4.844	**0.040***
		DOC	1	0.0117	0.0117	1.079	0.311
		DIC x DOC	1	0.0187	0.0187	1.723	0.204
		Residual	20	0.217	0.0108		
		Total	23	0.300	0.0130		
BOD		DIC	1	0.341	0.341	1.949	0.200
		DOC	1	1.297	1.297	7.412	**0.026***
		DIC x DOC	1	0.0136	0.0136	0.0775	0.788
		Residual	8	1.400	0.175		
		Total	11	3.051	0.277		

Discussion

Carbonate and water chemistry

The resulting values for the manipulated carbonate system for the high DIC treatment matched the value of 1000 µatm CO_2 for RCP 6.0 to 8.5 predicted for the end of the year 2100 [37], and in the combined treatment as well as the high DOC treatment exhibited 50 µatm lower CO_2 values. This would be expected here as high DOC availability serves bacteria as energy source [20,23], increasing respiratory CO_2 release on top of the DIC enrichment [38]. In addition, the present study revealed that

DOC treatment may reduce the photosynthetic performance of both algae species under high DOC conditions, therefore reducing the capacity of the algae to remove CO_2 and increasing the partial pressure of CO_2 in the water.

The average concentration of 441 µmol L^{-1} DOC compared to the controls with 208 µmol L^{-1} calculates to an achieved Glucose concentration as DOC of 233 µmol L^{-1} or 38.85 µmol L^{-1} Glucose. This is comparable low to other studies using values between 2000 [19] and 8000 µmol L^{-1} [15] for experimental studies. The background DOC concentration however was comparably high with 208 µmol L^{-1} compared to pristine areas under undisturbed conditions [19]. During the conduction of the experiment, heavy wind and storm events took place and visibility under water partially went below 1 m. Under these conditions, DOC concentrations can rise up to 166 µmol L^{-1} for this lagoon [27] and are comparable to concentrations measured during this experiment.

Effects of DIC

Under elevated DIC conditions, F_v/F_m of *U. flabellum* and *H. incrassata w*as reduced and the respiration rate of *U. flabellum* was increased. Both responses indicate a negative impact of elevated DIC on the photosynthetic apparatus, ultimately recorded as a reduction in primary production. Other studies revealed similar reduced photosynthetic capacity under high DIC concentrations [9,10]. In addition we could also detect negative effects of high DIC on the calcification of both species. Under future ocean acidification scenarios these algae may thus suffer from reduced carbon accretion rates as well as lowered primary production, but species-specific differences of calcification in response to elevated DIC could lead to more dominant biogenic carbonate production of *U. flabellum* over of *H. incrassata.*

Effects of increased DOC conditions

Elevated DOC/glucose conditions availability did only affect the photosynthesis of *H. incrassata*, but significantly reduced their calcification rates. This is to our knowledge the first study that investigates the impact of elevated DOC concentrations on the physiology of Caribbean reef algae, hence comparable data are scarce. Although, elevated organic carbon levels (added as glycerin) can increase the calcification rates of corals, likely serving as energy supply for this process [39], it also increases bacterial growth [19,22] and may lead to disease spread [16]. As measured by the elevated BOD, increased bacterial respiration increased the seawater pCO_2 and therefore my hinder gas exchange on the algal tissue interface, leading to reduced calcification rates and primary production rates as observed in this study.

Effects of the combined treatment

In the combined treatment, high DOC availability decreased the negative impact of high DIC concentrations on *H. incrassata* but increased the negative effects on the gross photosynthesis and calcification of *U. flabellum*. This might be cause by the different morphology of the agal thallus. As *U. flabellum* has a flat thallus with a high surface area due to the course woven utricles, *H. incrassata* possesses a smoother surface due to strong cementation, therefore giving less space for bacterial growth as *U. flabellum.* This eventually leads to different effects of OA under different levels of high labile, bioavailable DOC, inducing species specific differences of *U. flabellum* and *H. incrassata* where the latter does not show strong effects of OA under high DOC availability.

Comparison of measurements made on agal thallus and segments

Overall rates of photosynthesis and respiration were higher in apical segments as in the whole thallus (Tab. 2). This might be due to the highest activity of the photosynthetic apparatus just after segment formation. In addition, an age gradient [40] increases the variability of the data and also increasing epiphyte growth on the thallus makes measurements of the whole thallus more difficult. As a consequence, a higher variability in the data might be the reason we could not detect as many effects of the treatments on the thallus as we did for the apical segments. For future studies it is therefore important to consider the potential discrepancy the choice of either of the two measurements can cause when answering a specific questions.

Ecological perspective

In this study, we show that high DIC concentrations as expected by the year 2100 [37] can significantly reduce primary production rates and carbon accreation of the important reef lagoon species *Halimeda incrassata* and lead to increased respiration rates of *U. flabellum*. The extreme reduction of primary production of *H. incrassata* by nearlly 30 % may eventually lead to a loss in competitive strength under increasing nutrient loads in the lagoon, which may lead to a loss of an important carbonate sand producer [11–13] and a shift in habitat structure and carbon sequestration rates. These effects however may be alleviated by increased concentrations of high labile DOC, which may reduce species specific differences between *H. incrassata* and *U. flabellum*. Potential source of high labile DOC in this area are the seagrass beds themselves [20], human waste water discharge via groundwater [25,26] and storm events [27] which are all predicted to increase in the future, providing more labile DOC to these ecosystem. For the described carbon budget of this lagoon [28], this may lead to a decrease of the contribution to the overall primary production by calcifying green algae in

favor of sea grasses that may thrive under higher DIC conditions [41]. Similar as corals, calcifying green algae may not succeed under future high DOC and DIC conditions, leading to possible changes in organic matter cycling due to altered contributions to labile DOC pools and minor contributions to POC pools [20]. A consequence of the combination of both, high DOC and high DIC, could be a change in habitat structure with reduced production rates of algal derived sediments, connected changes in sediment porosity and habitat structure.

Acknowledgements

The authors would like to thank the staff of UNAM, Puerto Morelos, especially Román Vásquez and Tim Scheufen, for the field laboratory support. In addition, we would like to thank Matthias Birkicht for the support in TA and TOC analysis. This study was supported by the Leibniz Association.

The experiments performed in this work comply with the current laws of Mexico.

References

1. Wilkinson C, Souter D (2008) Status of Caribbean coral reefs after bleaching and hurricanes in 2005. Global Coral Reef Monitoring Network, and Reef and Rainforest Research Centre, Townsville. Available: http://cmsassets.dev.getunik.net/iucn/downloads/status_carib_corals.pdf. Accessed 30 April 2014.

2. Lessios H (1988) Mass mortality of Diadema antillarum in the Caribbean: what have we learned? Annu Rev Ecol Syst 19: 371–393. Available: http://www.jstor.org/discover/10.2307/2097159?uid=3737864&uid=2&uid=4&purchase-type=article&accessType=RR&sid=21103949425747&showMyJstorPss=false&seq=1&showAccess=true. Accessed 1 May 2014.

3. Hughes T (1994) Catastrophes, phase shifts, and large-scale degradation of a Caribbean coral reef. Sci Pap Ed 265: 1547–1551. Available: http://bio.classes.ucsc.edu/bio160/Bio160readings/Catastrophes, Phase Shifts.pdf. Accessed 30 April 2014.

4. Doney SC, Fabry VJ, Feely RA, Kleypas J a. (2009) Ocean Acidification: The Other CO 2 Problem. Ann Rev Mar Sci 1: 169–192. Available: http://www.annualreviews.org/eprint/QwPqRGcRzQM5ffhPjAdT/full/10.1146/annurev.marine.010908.163834. Accessed 28 April 2014.

5. Zeebe RE, Wolf-Gladrow DA (2001) CO2 in seawater: equilibrium, kinetics, isotopes. Elsevier Science. Available: http://books.google.com/books?hl=en&lr=&id=VrumU3XvQ-gC&oi=fnd&pg=PP2&dq=Seawater:+Equilibrium,+Kinetics,+Isotopes,+&ots=0lJD0a2k3_&sig=6G0E8lNEEUyMZQByGa-_CV_RNao. Accessed 5 August 2011.

6. Manzello D, Kleypas J (2008) Poorly cemented coral reefs of the eastern tropical Pacific: Possible insights into reef development in a high-CO2 world. Proc Natl Acad Sci U S A 105: 10450–10455. Available: http://www.pnas.org/content/105/30/10450.abstract. Accessed 10 July 2013.

7. Knutson TR, McBride JL, Chan J, Emanuel K, Holland G, et al. (2010) Tropical cyclones and climate change. Nat Geosci 3: 157–163. Available: http://www.nature.com/doifinder/10.1038/ngeo779. Accessed 24 May 2013.

8. Cruz-Palacios V, van Tussenbroek BI (2005) Simulation of hurricane-like disturbances on a Caribbean seagrass bed. J Exp Mar Bio Ecol 324: 44–60. Available: http://www.sciencedirect.com/science/article/pii/S002209810500170X. Accessed 1 May 2014.

9. Price N, Hamilton S, Tootell J, Smith J (2011) Species-specific consequences of ocean acidification for the calcareous tropical green algae Halimeda. Mar Ecol Prog Ser 440: 67–78. Available: http://www.int-res.com/abstracts/meps/v440/p67-78/. Accessed 31 October 2011.

10. Sinutok S, Hill R, Doblin MA, WUHRER R, RALPH PJ (2011) Warmer more acidic conditions cause decreased productivity and calcification in subtropical coral reef sediment-dwelling calcifiers. Limnol Oceanogr 56: 1200–1212. Available: http://cat.inist.fr/?aModele=afficheN&cpsidt=24362064. Accessed 21 February 2014.

11. Hine AC, Hallock P, Harris MW, Mullins HT, Belknap DF, et al. (1988) Halimeda bioherms along an open seaway: Miskito Channel, Nicaraguan Rise, SW Caribbean Sea. Coral Reefs 6: 173–178. Available: http://link.springer.com/10.1007/BF00302013. Accessed 1 May 2014.

12. Marshall JF, Davies PJ (1988) Halimeda bioherms of the northern Great Barrier Reef. Coral Reefs 6: 139–148. Available: http://link.springer.com/10.1007/BF00302010. Accessed 25 April 2014.

13. Rees S a., Opdyke BN, Wilson P a., Henstock TJ (2006) Significance of Halimeda bioherms to the global carbonate budget based on a geological sediment budget for the Northern Great Barrier Reef, Australia. Coral Reefs 26: 177–188. Available: http://link.springer.com/10.1007/s00338-006-0166-x. Accessed 21 February 2014.

14. Mumby PJ (2009) Phase shifts and the stability of macroalgal communities on Caribbean coral reefs. Coral Reefs 28: 761–773. Available: http://link.springer.com/10.1007/s00338-009-0506-8. Accessed 1 May 2014.

15. Haas AF, Al-Zibdah M, Wild C (2009) Effect of inorganic and organic nutrient addition on coral–algae assemblages from the Northern Red Sea. J Exp Mar Bio Ecol 380: 99–105. Available: http://linkinghub.elsevier.com/retrieve/pii/S0022098109003712. Accessed 22 June 2011.

16. Kuntz NM, Kline DI, Sandin SA, Rohwer F (2005) Pathologies and mortality rates caused by organic carbon and nutrient stressors in three Caribbean coral species. Mar Ecol Prog Ser 294: 173–180. Available: http://www.int-res.com/abstracts/meps/v294/p173-180/.

17. Gregg A, Hatay M, Haas AF, Robinett N, Barott KL, et al. (2013) Biological oxygen demand optode analysis of coral reef-associated microbial communities exposed to

algal exudates. PeerJ 1: e107. Available: http://www.pubmedcentral.nih.gov/articlerender.fcgi?artid=3719127&tool=pmcentrez&rendertype=abstract. Accessed 25 April 2014.

18. Smith JE, Shaw M, Edwards RA, Obura DO, Pantos O, et al. (2006) Indirect effects of algae on coral: algae-mediated, microbe-induced coral mortality. Ecol Lett 9: 835–845. Available: http://www.ncbi.nlm.nih.gov/pubmed/16796574. Accessed 17 January 2014.

19. Kline DI, Kuntz NM, Breitbart M, Knowlton N, Rohwer F (2006) Role of elevated organic carbon levels and microbial activity in coral mortality. Mar Ecol Prog Ser 314: 119–125. Available: http://www.int-res.com/abstracts/meps/v314/p119-125/.

20. Haas AF, Jantzen C, Naumann MS, Iglesias-Prieto R, Wild C (2010) Organic matter release by the dominant primary producers in a Caribbean reef lagoon: implication for in situ O2 availability. Mar Ecol Prog Ser 409: 27–39. doi:10.3354/meps08631.

21. Haas AF, Wild C (2010) Composition analysis of organic matter released by cosmopolitan coral reef-associated green algae. Aquat Biol 10. Available: http://www.int-res.com/abstracts/ab/v10/n2/p131-138/. Accessed 17 January 2014.

22. Nelson CE, Goldberg SJ, Wegley Kelly L, Haas AF, Smith JE, et al. (2013) Coral and macroalgal exudates vary in neutral sugar composition and differentially enrich reef bacterioplankton lineages. ISME J 7: 962–979. Available: http://www.ncbi.nlm.nih.gov/pubmed/23303369. Accessed 19 November 2013.

23. Haas AF, Nelson CE, Rohwer F, Wegley-Kelly L, Quistad SD, et al. (2013) Influence of coral and algal exudates on microbially mediated reef metabolism. PeerJ 1: e108. Available: http://www.pubmedcentral.nih.gov/articlerender.fcgi?artid=3719129&tool=pmcentrez&rendertype=abstract. Accessed 24 March 2014.

24. Haas AF, Nelson C, Kelly L, Carlson C (2011) Effects of coral reef benthic primary producers on dissolved organic carbon and microbial activity. PLoS One 6. Available: http://dx.plos.org/10.1371/journal.pone.0027973. Accessed 17 January 2014.

25. Null KA, Knee KL, Crook ED, de Sieyes NR, Rebolledo-Vieyra M, et al. (2014) Composition and fluxes of submarine groundwater along the Caribbean coast of the Yucatan Peninsula. Cont Shelf Res 77: 38–50. Available: http://www.sciencedirect.com/science/article/pii/S0278434314000247. Accessed 6 May 2014.

26. Carruthers TJB, van Tussenbroek BI, Dennison WC (2005) Influence of submarine springs and wastewater on nutrient dynamics of Caribbean seagrass meadows. Estuar Coast Shelf Sci 64: 191–199. Available: http://www.sciencedirect.com/science/article/pii/S0272771405000491. Accessed 6 May 2014.

27. Naumann MS, Haas AF, Jantzen C, Iglesias-Prieto R, Wild C (2012) Benthic-pelagic coupling in a Caribbean reef lagoon affected by hurricane" Dolly. Proc 12th Int Coral Reef Symp 12. Available: http://www.icrs2012.com/proceedings/manuscripts/ICRS2012_4C_4.pdf. Accessed 1 May 2014.

28. Naumann MS, Jantzen C, Haas AF, Iglesias-Prieto R, Wild C (2013) Benthic primary production budget of a Caribbean reef lagoon (Puerto Morelos, Mexico). PLoS One 8: e82923. Available: http://www.pubmedcentral.nih.gov/articlerender.fcgi?artid=3867400&tool=pmcentrez&rendertype=abstract. Accessed 1 May 2014.

29. Meehl GAG, Stocker TF, Collins WD, Friedlingstein P, Gaye T, et al. (2007) Global climate projections. In: Solomon S, Qin D, Manning M, Chen Z, Marquis M, et al., editors. IPCC, 2007: Climate Change 2007: the physical science basis. contribution of Working Group I to the Fourth Assessment Report of the Intergovernmental Panel on Climate Change. Cambridge University Press, Cambridge, United Kingdom and New York, NY, USA. pp. 747–846. Available: https://publications.csiro.au/rpr/pub?list=BRO&pid=procite:1452cb7a-9f93-44ea-9ac4-fd9f6fd80a07. Accessed 18 July 2013.

30. Vuuren DP, Edmonds J, Kainuma M, Riahi K, Thomson A, et al. (2011) The representative concentration pathways: an overview. Clim Change 109: 5–31.

Available: http://link.springer.com/10.1007/s10584-011-0148-z. Accessed 9 January 2014.

31. Rogelj J, Meinshausen M, Knutti R (2012) Global warming under old and new scenarios using IPCC climate sensitivity range estimates. Nat Clim Chang 2: 248–253. Available: http://www.nature.com/doifinder/10.1038/nclimate1385. Accessed 12 March 2012.

32. Orr JC, Epitalon J-M, Gattuso J-P (2014) Comparison of seven packages that compute ocean carbonate chemistry. Biogeosciences Discuss 11: 5327–5397. Available: http://www.biogeosciences-discuss.net/11/5327/2014/. Accessed 3 May 2014.

33. Drew EA, Abel KM (1990) Studies on Halimeda. III. A Daily Cycle of Chloroplast Migration within Segments. Bot Mar 33: 31–46. Available: http://www.reference-global.com/doi/abs/10.1515/botm.1990.33.1.31. Accessed 15 July 2011.

34. Smith S, Kinsey D (1978) Calcification and organic carbon metabolism as indicated by carbon dioxide. Coral reefs Res methods. Available: http://scholar.google.com/scholar_lookup?title=Calcification and organic carbon metabolism as indicated by carbon dioxide&author=Smith&publication_year=1978#0. Accessed 26 February 2015.

35. Yao W, Byrne RH (1998) Simplified seawater alkalinity analysis. Deep Sea Res Part I Oceanogr Res Pap 45: 1383–1392. Available: http://www.sciencedirect.com/science/article/pii/S0967063798000181. Accessed 26 February 2015.

36. Chisholm J, Gattuso J-P (1991) Validation of the alkalinity anomaly technique for investigating calcification and photosynthesis in coral reef communities. Limnol Oceanogr 36: 1232–1239. Available: http://www.jstor.org/stable/10.2307/2837472. Accessed 25 September 2012.

37. Meinshausen M, Smith SJ, Calvin K, Daniel JS, Kainuma MLT, et al. (2011) The RCP greenhouse gas concentrations and their extensions from 1765 to 2300. Clim Change 109: 213–241. Available: http://link.springer.com/10.1007/s10584-011-0156-z. Accessed 10 January 2014.

38. Shaw EC, McNeil B, Tilbrook B (2013) Anthropogenic changes to seawater buffer capacity combined with natural reef metabolism induce extreme future coral reef CO2 conditions. Glob Chang Biol 19: 1632–1641. Available: http://doi.wiley.com/10.1111/gcb.12154. Accessed 17 January 2014.

39. Colombo-Pallotta MF, Rodríguez-Román A, Iglesias-Prieto R (2010) Calcification in bleached and unbleached Montastraea faveolata: evaluating the role of oxygen and glycerol. Coral Reefs 29: 899–907. Available: http://link.springer.com/10.1007/s00338-010-0638-x. Accessed 13 August 2013.

40. Enríquez S, Borowitzka MA (2010) The use of the fluorescence signal in studies of seagrasses and macroalgae. Chlorophyll a Fluoresc Aquat …. Available: http://link.springer.com/chapter/10.1007/978-90-481-9268-7_9. Accessed 18 July 2013.

41. Hall-Spencer JM, Rodolfo-Metalpa R, Martin S, Ransome E, Fine M, et al. (2008) Volcanic carbon dioxide vents show ecosystem effects of ocean acidification. Nature 454: 96–99. Available: http://www.ncbi.nlm.nih.gov/pubmed/18536730. Accessed 11 June 2011.

5 - A new model for the calcification of the green macro-alga *Halimeda opuntia* (Lamouroux)

André Wizemann [1,*], Friedrich W. Meyer [1], and Hildegard Westphal [1,2]

[1] Leibniz Center for Tropical Marine Ecology (ZMT), Fahrenheitstraße 6-8, 28359 Bremen (Germany)

[2] University of Bremen, Faculty of Geosciences, Klagenfurter Straße 2, 28359 Bremen (Germany)

[*] Author to whom correspondence should be addressed; E-Mail: andre.wizemann@zmt-bremen.de; Tel.: +49-421-23800-132; Fax: +49-421-23800-30.

This manuscript is published in Coral Reefs

Abstract

Halimeda opuntia is a cosmopolitan marine calcifying green alga in shallow tropical marine environments. Besides *Halimeda*'s contribution to a diverse habitat, the alga is an important sediment producer. Fallen calcareous segments of *Halimeda* spp. are a major component of carbonate sediments in many tropical settings and play an important role in reef framework development and carbonate platform build-up. Consequently the calcification of *H. opuntia* accounts for large portions of the carbonate budget in tropical shallow marine ecosystems.

Earlier studies investigating the calcification processes of *Halimeda* spp. have tended to focus on the microstructure or the physiology of the alga, thus overlooking the interaction of physiological and abiotic processes behind the formation of the skeleton. By analyzing microstructural skeletal features of *Halimeda* segments with the aid of scanning electron microscopy and relating their occurrence to known physiological processes, we have been able to identify the initiation of calcification within an organic matrix and demonstrate that biologically-induced cementation is an important process in calcification. For the first time, we propose a model for the calcification of *Halimeda* spp. that considers both the alga's physiology and the carbon chemistry of the seawater with respect to the development of different skeletal features. The presence of an organic matrix and earlier detected external carbonic anhydrase activity suggest that *Halimeda* spp. exhibits biotic precipitation of calcium carbonate, as many other species of marine organisms do. On the other hand it is the formation of micro-anhedral carbonate through the alga's metabolism that leads to a cementation of

living segments. Precisely this process allows *H. opuntia* to contribute substantial amounts of carbonate sediments to tropical shallow seas.

Introduction

The benthic marine green macro-alga *Halimeda opuntia* (Lamouroux 1816) is a common calcareous alga within tropical shallow marine environments. The alga grows in a branched, segmented habit whereby its numerous calcareous segments function in a leaf-like manner (Fig. 1a). The segments are formed in continuous growth of up to one segment per day and per branch (Vroom et al. 2003). The segmental growth of algae of the genus *Halimeda* is rapid, with a complete turnover of ~30 days or even faster (Hillis-Colinvaux 1980; Wefer 1980; Multer 1988; Tussenbroeck and Dijk 2007). Thus, *Halimeda* segments are a major component of tropical shallow marine sediments (Milliman 1974; Drew 1983; Johns and Moore 1988; Freile et al. 1995). In fact, the contribution of *Halimeda* bioherms to the sediment budget of tropical settings might be equal or even exceed the carbonate sediment production of the corals within the reef (Marshall and Davis 1988; Milliman and Droxler 1996; Rees et al. 2007). *Halimeda* spp. and its sediments play a multitude of ecological roles that range from habitat and substrate provision (Wiman and McKendree 1975; Multer 1988; Payri 1988; Jinendradasa and Ekaratne 2002; Multer and Clavijo 2004) to the significant contribution to island and carbonate platform buildup (Folk and Robles 1964; Neumann and Land 1975; Roberts et al. 1987; Drew and Abel 1988; Hine et al. 1988; Orme and Salama 1988; Phipps and Roberts 1988; Rao et al. 1994; Hillis 1997; Pomar and Kendall 2007). Moreover, calcareous macro-algae take part in the fixation and long-term storage of atmospheric carbon in tropical coral reef environments (Kinsey and Hopley 1991). Consequently, *Halimeda* sediments can be considered as a carbon sink that contribute to the carbonate buffer of tropical shallow seas (Hillis-Colinvaux 1980; Rees et al. 2007). However, without sufficient knowledge of the processes and mechanisms involved it is difficult to predict how *Halimeda*'s calcification will respond to environmental changes such as ocean acidification that have the potential to impact the calcification of marine organisms (Hoegh-Guldberg et al. 2007; Doney et al. 2009; Ries et al. 2009). Our goal is to understand the role of physiological processes and chemical seawater parameters on extracellular $CaCO_3$ biomineralization in *H. opuntia.* As the green macro-alga *H. opuntia* is a rather evolutionarily basal algal species, its calcification can be considered primal, thus making it an ideal model organism to study (Hillis 2001; Kleypas et al. 2006). To investigate the calcification of *H. opuntia*, we reared the alga under controlled conditions and analyzed the internal skeletal microstructure of segments using scanning electron microscopy (SEM). We then relate the formation of observed skeletal features to physiological processes of the alga. Subsequently, we propose a new model of skeletal formation that recognizes the close relationship between precipitation of calcium carbonate and the metabolism of the alga as well as the carbon chemistry of the seawater.

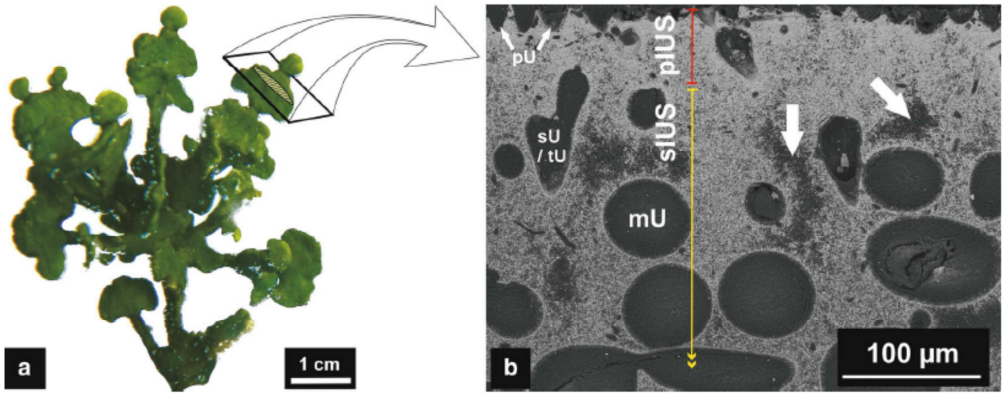

Figure 1 Illustration of the tropical macro-alga *Halimeda opuntia* and its internal calcareous skeletal structure. **(a)** Segmented habit of *H. opuntia*. **(b)** Internal segment microstructure. Scanning Electron Microscope image (via BSE) of a thin section shows utricles and inter-utricular spaces. Large arrows in (b) indicate open areas in the innermost secondary inter-utricular space. pIUS = primary inter-utricular space; sIUS = secondary inter-utricular space; pU / sU / tU / mU = primary / secondary / tertiary / medullary utricle.

Material and methods

Setup of aquaria and seawater parameter measurements

Calcifying green macro-algae of the species *H. opuntia* from reefs of Curaçao (sampled in August 2011 from ~5 m water depth) were acclimatized to laboratory conditions in the marine laboratory facilities of the Leibniz Center for Tropical Marine Ecology (ZMT) in Bremen (Fig. 1a). After acclimatization of several weeks, the algae were individually placed in aquaria (30 L) with pre-installed T5 light bulbs of 150 µE $m^{-2}s^{-1}$ switched in a 12/12 h day/night cycle. During the period of growth UV-sterilized and pre-filtered Atlantic open ocean seawater (SW; unmodified ionic composition) was used. Aeration was provided by an electronically controlled CO_2 gas-mixing system (HTK® Hamburg, Linde® Gas). Fifty percent of the SW was exchanged twice a week. Salinity (S), temperature (T), and pH (NBS scale) were monitored every other day (WTW® Multi 3410, SenTix® ORP 900 pH probe, TetraCon® 925 conductivity probe; Table 1). Total alkalinity (A_T) was measured twice a month by titration of a 50 mL water sample with 0.05N HCL after Dickson (2007) using an automated titrator (SI Analytics®, TitronLine Alpha Plus) and A_T standard provided by A.G. Dickson (batch 111) as certified reference material (Dickson et al. 2003). Mean values of S, T, pH_{NBS}, and A_T were used to calculate the seawater carbon chemistry and the $CaCO_3$ saturation state (Ω) with the program "CO_2SYS" (Pierrot et al. 2006; Table 1).

Sampling

Proto-segments (day = 0) and young apical segments of the first day (day = 1) were collected after one month of experimental duration from selected algae where new segmental growth was observed. Complete algae were collected after three months at the end of the experiment. After sampling, the segments were rinsed with distilled water to remove soluble components and oven-dried at 35° C for 48 h.

Tab. 1 Measured and calculated physical and chemical seawater (SW) parameters (mean ± SD). Salinity (S), temperature (T), total alkalinity (A_T) and pH were measured. These parameters were used to calculate the seawater carbon chemistry with the program CO_2SYS (Pierrot et al. 2006) with the use of K1, K2 constants from Merbach et al. (1973), refit by Dickson and Millero (1978). A_T, TCO_2 and carbon species in µmol kg^{-1}SW, pCO_2 in µatm, pH in NBS scale (mol kg^{-1}SW). Ω = $CaCO_3$ saturation state of the seawater; arag = aragonite, cal = calcite.

S (PSU)	T (C°)	A_T	pH_{NBS}	TCO_2	pCO_2	HCO_3^-	CO_3^{2-}	CO_2	Ω_{arag}	Ω_{cal}
35.5 ± 0.6	26.8 ± 0.5	2104 ± 60	8.14 ± 0.05	1829 ± 57	414 ± 61	1628 ± 62	190 ± 22	11.2 ± 1.7	3.0 ± 0.3	4.6 ± 0.5

Sample preparation and analysis

Thin-sections

To investigate the habit of skeletal features and to get a general overview of the internal microstructure, thin-sections were prepared. For this, segments were embedded in epoxy, cut along the middle plain, and polished to ~35 µm (Fig. 1a,b). Thin-sections were gold sputtered and analyzed with the scanning electron microscope (TESCAN® VEGA3 XMU) at 10 keV using the detector for back-scattered electrons (BSE).

Stub samples

To investigate the topographical morphology of skeletal features in detail, stub samples were prepared for analysis with a scanning electron microscope (SEM). Segments were cut along the middle plain with a razor blade and fixed on a stub with conductive glue with the cut surface facing upwards. The samples were then gold sputtered and analyzed with the SEM at 10 keV using the secondary electron detector (SE).

A total of n > 50 segments of all growing stages (day 1, apical, mid-growth and basal) were analyzed. Details on the segments presented in the results section are shown in Table 2. The organic matter of the segments was not removed in order to allow identification of organic features on the utricle wall. However, organics were lost in some cases due to preparation techniques.

Tab. 2 Details on segments presented in the results section. Shown are the preparation technique, the method of analysis via SEM and the skeletal microstructural features investigated from segments of the first day (day 1), from young, well developed segments (apical) and from mature segments (mid-growth and basal).
IUS = inter-utricular space (p = primary; s = secondary); SE = secondary electrons; BSE = back-scattered electrons.

Figure	Segment age	Preparation	SEM-detector	Feature(s) investigated
1b	mid-growth	thin-section	BSE	microstructural overview
3a	day 1	stub	SE	early needles / organic matrix
3b	apical	stub	SE	short needles
3c	basal	stub	SE	$CaCO_3$ nuclei
3d	basal	stub	SE	short needles / organic matrix
3f	basal	stub	SE	organic matrix
4a	apical	thin-section	BSE	microstructural overview
4b	apical	stub	SE	long needles
4c	mid-growth	stub	SE	micro-anhedral carbonate of pIUS
4d	basal	stub	SE	sIUS with long needles
6	mid-growth	thin-section	BSE	comparison of species

Results

The skeleton of a *Halimeda* segment exhibits several microstructural features that appear in a temporal order as depicted in Figure 2. The subsequent description follows this temporal order. In natural seawater the calcareous skeleton of *Halimeda* spp. is composed of the $CaCO_3$ polymorph aragonite (Macintyre and Reid 1995; Stanley et al. 2010). In SEM analyses (via back-scattered electrons and energy-dispersive X-ray) of samples investigated no evidence for an alteration of the $CaCO_3$ crystal polymorph was found and so here we follow this assumption. Measured parameters and calculated carbon chemistry of the natural seawater in which the algae were grown in the laboratory facilities are shown in Table 1.

Short aragonite needles

Proto-segments (day = 0), identifiable by their whitish color, do not show any $CaCO_3$ crystals. At the onset of photosynthesis in a new segment (day = 1), the earliest needles are formed directly on the

utricle wall in a layer of a dense organic matrix (Fig. 3a). These short aragonite needles, with a length not exceeding 1 µm, have a random orientation (Fig. 3a). The tissue of the utricle wall exhibits a fibrous, scale-like habit (Fig. 3a).

In a mature segment, fully developed short needles on the utricle wall have a roundish shape and a length of up to ~5 µm (Fig. 3b). Likewise newly formed short needles are embedded within an organic matrix (Fig. 3d). The matrix is closely attached to the outer utricle wall. In some samples the matrix is partly disintegrated (Fig. 3e). In other mature segments in which the organic matrix is well-preserved, small roundish nuclei < 1 µm are present on the outer utricle wall (Fig. 3c).

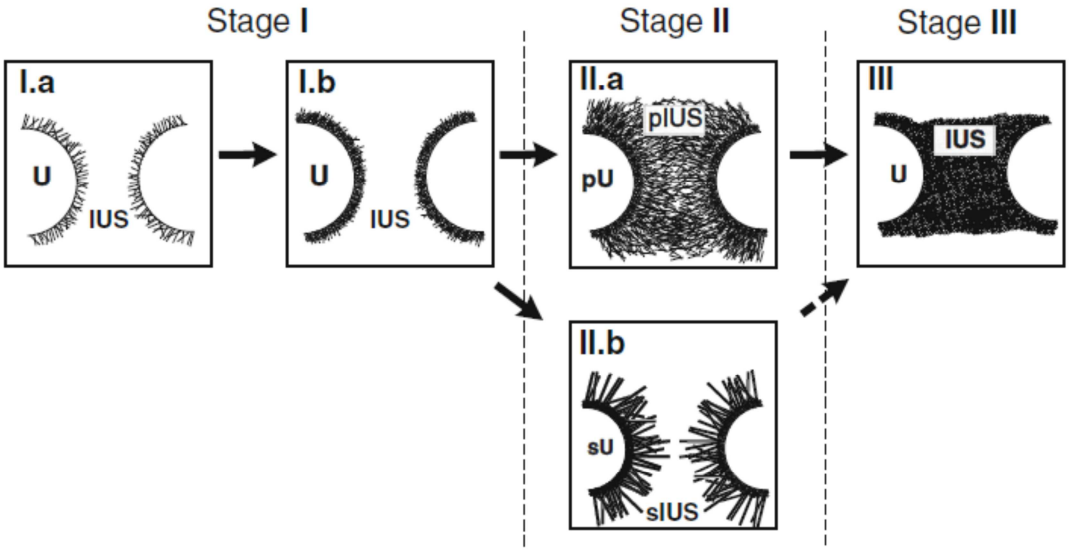

Figure 2 Calcification stages of *Halimeda* spp. (after Macintyre and Reid 1995) **(I.a)** Growth of short skeletal needles on the utricle (U) wall followed by **(I.b)** recrystallization of short needles to micron-sized anhedral crystals. **(II.a)** Primary utricles (pU) / primary inter-utricular space (pIUS) located on the rim of the segment characterized by dense skeletal needles, or **(II.b)** secondary utricles (pU) / secondary inter-utricular space (sIUS) located in the inner part of the segment with long euhedral needles. **(III)** Primary inter-utricular space (pIUS) on the segment rim is filled with micron-sized anhedral crystals, whereas secondary inter-utricular space (sIUS) of the inner part is seldom completely filled (dashed arrow) and remains in stage II (cf. II.b). Calcification stage **III** is not developed in all parts of the segment (cf. Fig. 1b).

Micro-anhedral carbonate (MAC)

Micron-sized anhedral crystals of $CaCO_3$ are observed in the vicinity of the outer utricle walls (Fig. 4a,c,d). In a previous study, $CaCO_3$ crystals < 1 µm of anhedral shape observed within the internal skeletal microstructure of *Halimeda* spp. were described as "mini-micrite" (Macintyre and Reid 1995) and the process of their formation as "micritization" (Alexandersson 1972, Macintyre and Reid 1995). Generally, the term "micrite" (micro-crystalline calcite; Folk 1959) defines all $CaCO_3$ crystals < 4 µm. However, both definitions, "mini-micrite" and "micrite", raise problems of how to distinguish between crystals that have different origins of formation and exhibit different shapes, but are within the same size range. To avoid usage of the term "micrite" and to clearly distinguish between different origins and shapes of the $CaCO_3$ crystals observed in the internal skeletal microstructure of *Halimeda* spp. henceforth we term all non-needle like $CaCO_3$ crystals < 1 µm that exhibit an anhedral shape and are formed in the living *Halimeda* segment, micro-anhedral carbonate (MAC).

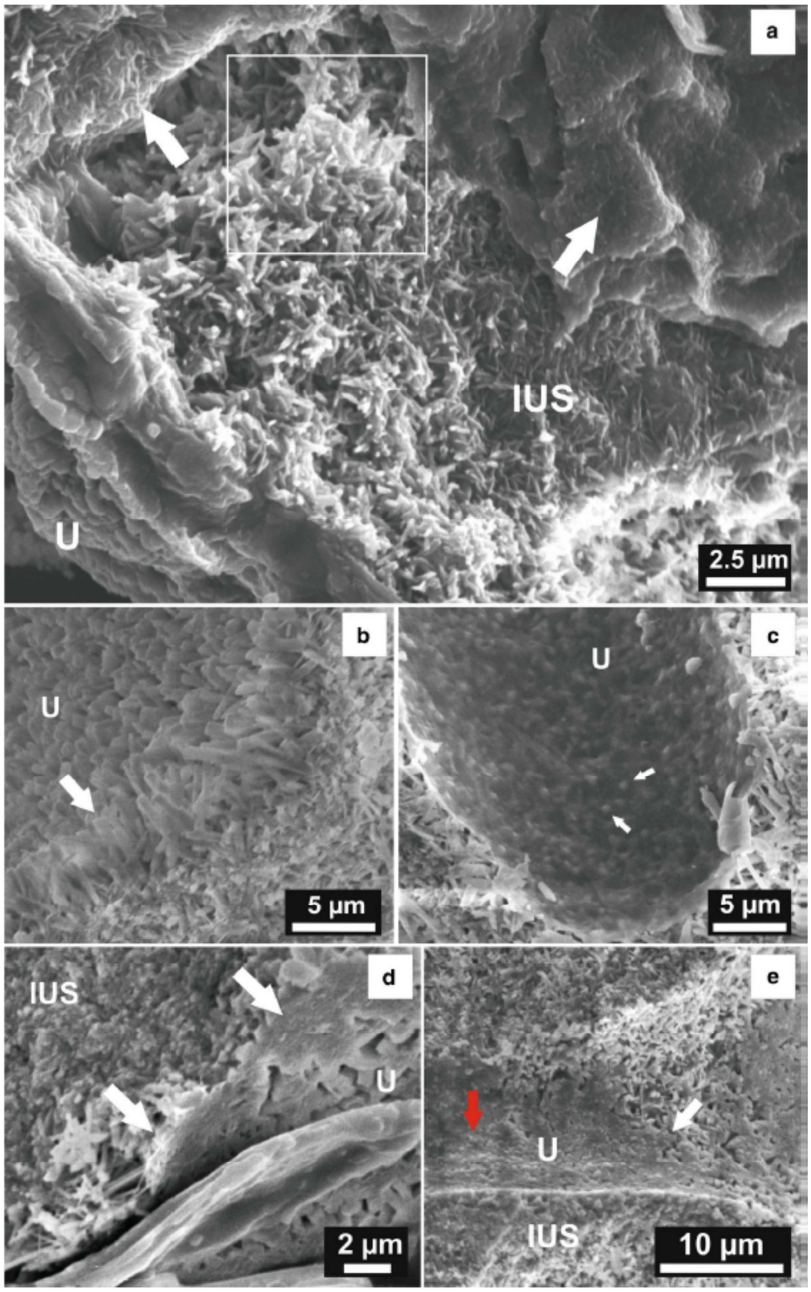

Figure 3 SEM images (via SE) of the internal microstructure of *Halimeda opuntia* from stub samples **(a)** Short needles within the inter-utricular space of a young segment (day = 1) embedded in an organic matrix (white frame). The utricle wall has a fibrous, scale-like habit (white arrows). **(b)** Short needles in a mature segment. Arrow indicates the initialization point of needle crystallization (organics lost). **(c)** Organic utricle wall showing round nuclei of calcium carbonate < 1 µm (arrows). **(d)** Newly formed short needles embedded within an organic matrix (arrows) on the outer utricle wall of a mature segment. **(e)** Disintegrated organic matrix (red arrow) in a mature segment. The white arrow indicates the front of disintegration.

IUS = inter-utricular space; U = utricle.

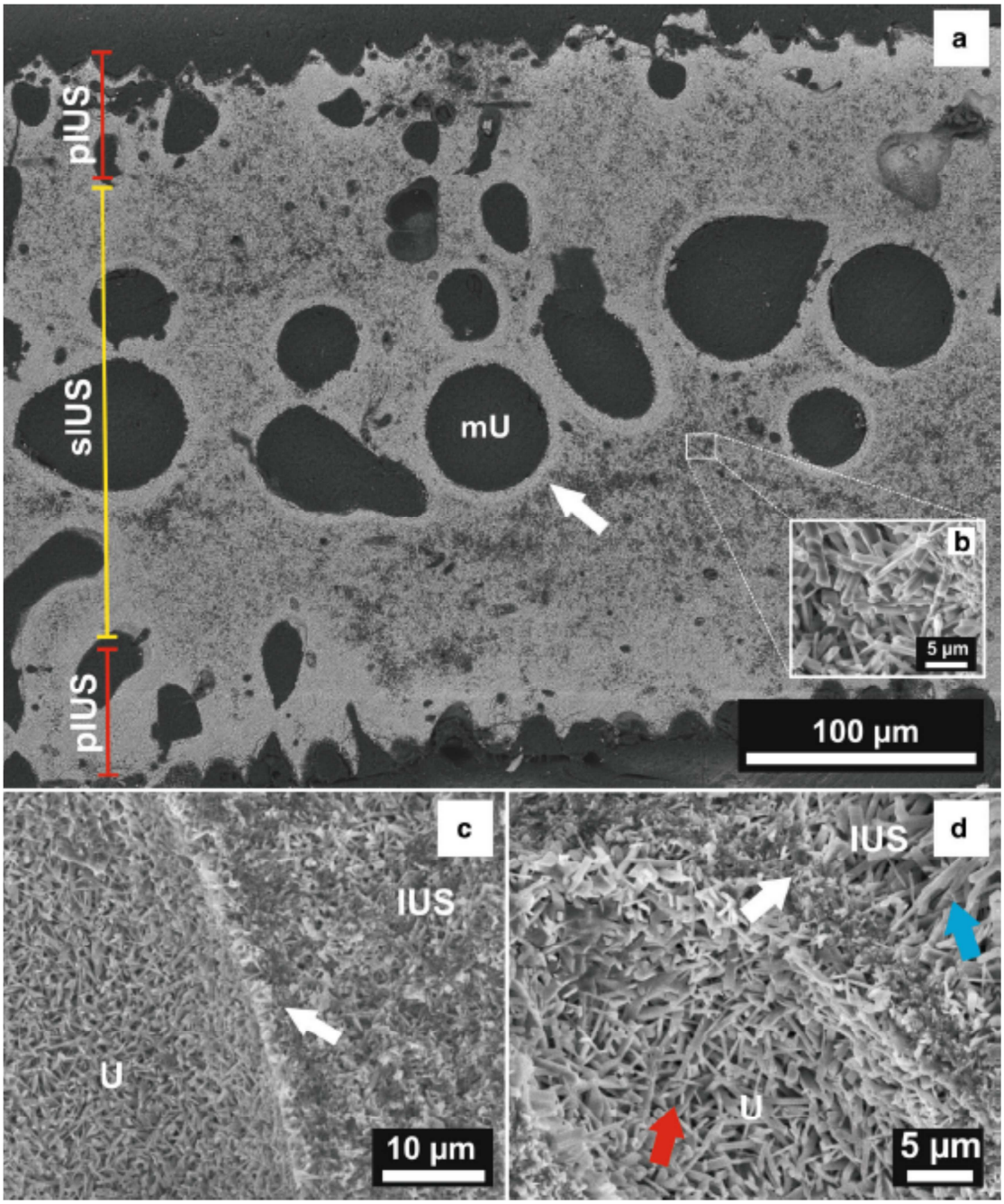

Figure 4 (**a**) SEM image (via BSE) of a thin-section from a mature segment shows rims of micro-anhedral carbonate around utricles (arrow). (**b**) Typical orthorhombic long needles within the inner secondary inter-utricular space. (**c**) Micro-anhedral carbonate filled primary inter-utricular space showing remnants of short needles. A dense meshwork of newly formed needles is present on the utricle wall (organics lost) with micro-anhedral carbonate rim of utricle (arrow). (**d**) Microstructure of the secondary inter-utricular space showing short needles (red arrow) on the utricle wall, micro-anhedral carbonate rim of utricle (white arrow) and long needles (blue arrow) of the inter-utricular space (organics lost).

pIUS = primary inter-utricular space; sIUS = secondary inter-utricular space; U = utricle, mU = medullary utricle.

When short needles are present, the MAC always appears on top of these (Fig. 4c,d). Low amounts of short needles are loosely embedded in the MAC (Fig. 4c). Contrary to the formation process of the short needles, an organic matrix is not observed in the context of MAC formation. MAC is more developed within the inter-utricular space (IUS) of mature segments.

Based on our investigation of the internal microstructure of *H. opuntia*, here we distinguish between two parts of the IUS that are defined as follows. The IUS between the peripheral primary utricles (pU) is defined as the primary inter-utricular space (pIUS). The IUS between the more central secondary, tertiary, and medullary utricles (sU, tU, and mU, respectively) is defined as the secondary inter-utricular space (sIUS) (Fig. 1,2). The pIUS is entirely filled with MAC (Fig. 4c) and forms a dense rim around the segment (Fig. 1, 4a), whereas the sIUS is not as densely packed with MAC. Within the sIUS, MAC is limited in its extent to the outer walls of larger central utricles (Fig. 4a,b).

Long aragonite needles

Euhedral aragonite needles that are elongated along the c-axis point into open space of the IUS. They are found on top of short needles or MAC and are not attached to the organic utricle wall. (Fig. 4a,b,d). In young segments these long needles reach up to 20 µm in length. In contrast to the roundish habit of the short needles, long needles have a prismatic shape and exhibit a blunt end (Fig. 4b). They predominantly radiate out from a specific location (nucleus) in bundles of several aragonite needles. In older mature segments, long needles appear > 20 µm in length as if they continuously extend in length and width congruent to the age of the segment. Where the IUS is filled with MAC, long needles are not observed (Fig. 4c).

Discussion

Our investigations emphasize the relationship between the observed skeletal morphological features and the temporal stage of maturation of a segment. Furthermore, the consecutive and age-related order of appearance of these microstructural features suggest an influence of the physiology of the alga (by its photosynthesis and metabolism) that induces diurnal shifts of seawater carbon chemistry within the inter-utriclular space. The calculated Ω_{arag} ~3.0 of the natural seawater indicates $CaCO_3$ oversaturated water comparable to present day tropical marine conditions (Table 1; Hoegh-Guldberg et al. 2007).

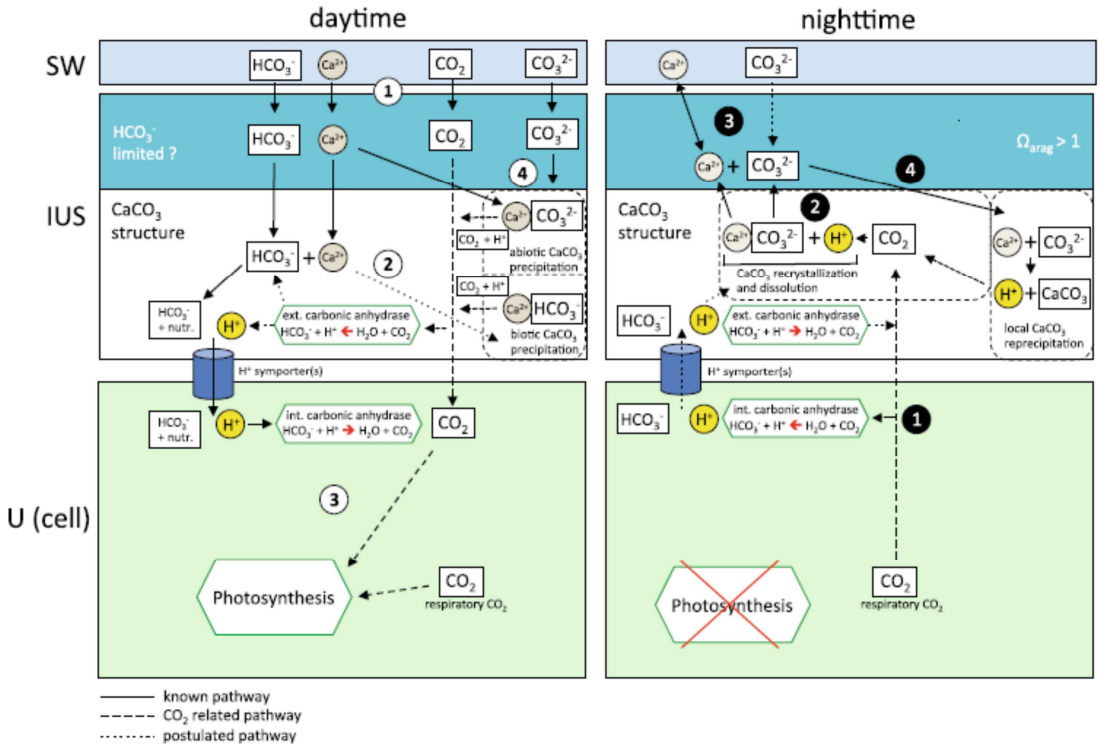

Figure 5 Model of physiological processes related to calcification in *Halimeda* spp. (modified from Comeau et al. 2012)

Photosynthesis at daytime: Ca^{2+} ions and inorganic carbon species enter the inter-utricular space (IUS) (1). Polysaccharides accumulate Ca^{2+} ions on the utricle wall and increase Ca^{2+} saturation. External carbonic anhydrase activity catalyzes $CO_2 + H_2O$ to $HCO_3^- + H^+$. (Unknown) Organic matrix protein(s) / enzyme(s) initiate and control $CaCO_3$ formation out of HCO_3^- and Ca^{2+} = primary calcification (2). Both photosynthesis and external carbonic anhydrase activity extract CO_2 from the IUS. HCO_3^- is cell-imported through H^+ / membrane-bound symporter(s) (3). Subsequently, seawater $CaCO_3$ saturation state within the IUS gets elevated. $CaCO_3$ precipitates abiotically at nucleation sites due to CO_3^{2-} oversaturation = secondary calcification (4).

Respiration at nighttime: Respiratory CO_2 from cell metabolism enters the IUS (1). Rise of seawater pCO_2 lowers seawater $CaCO_3$ saturation state in the IUS. $CaCO_3$, precipitated during daytime, gets partly dissolved and recrystallized (2). Inflow of CO_3^{2-} saturated seawater and dissolution of $CaCO_3$ locally elevate $CaCO_3$ saturation state ($\Omega > 1$) (3). Abiotic re-precipitation of $CaCO_3$ occurs (4).

SW = seawater; IUS = inter-utricular space; U = utricle / cell. Also see text for further explanations.

Primary needles and primary calcification

The onset of calcification in *H. opuntia* is the formation of short aragonite needles (0.5 – 1 µm) on the outer utricle wall in segments that are one day old. Proto-segments (day = 0) do not show any crystal growth even when exposed to light, as chloroplasts for photosynthetic activity are missing (Larkum et

al. 2011). Thus the initiation of calcification seems to be linked to the start of physiological processes. To consider the time-dependent development of the skeletal features here, we define these short needles as “primary needles” and the process of their formation as “primary calcification”.

New primary needles are embedded within an organic matrix. This observation implies that the organic matrix is involved in the development of those needles. An extracellular organic matrix is known to be involved in the process of calcification in a variety of marine organisms, such as mollusks, echinoderms, corals, protozoa, and bacteria (Simkiss 1965; Isenberg et al. 1966; Wheeler and Sikes 1984; Simkiss and Wilbur 1989; Mann 2001; Bonucci 2007; Weiss and Marin 2008; Cuif et al. 2012). Nakahara and Bevelander (1978) observed an organic coating on initial needles that precipitated in *Halimeda incrassata*. An organic matrix consists of molecules, such as polysaccharides, proteins, and enzymes, which have major steering functions in the process of calcification (Weiss and Marin 2008; Falini et al. 2013). One of the essential functions of organic matrix molecules is their ability to adsorb and accumulate ions. For example extracellular acidic polysaccharides or proteoglycans with glycosaminoglycan (GAG) chains exhibit high cation affinity (Bonucci 2007; Arias and Fernández 2008; Salgado et al. 2011). Fibrous elements, presumably organic pectin-hemicellulose fibers (Sikes 1978; Arnott 1982) that are observed in the vicinity of early primary needles on the outer utricle wall suggest that these fibers are involved in the $CaCO_3$ nucleation process. Indeed, Böhm 1973 observed that these fibrous filaments on the utricle wall are acidic (sulfated) polysaccharides with Ca^{2+} affinity. However observations of primary needles in *Halimeda* growing in a random orientation rules out the possibility that these polysaccharides are directly involved in crystal development or acting as a template (Wilbur et al. 1969). This is supported by findings from Böhm and Goreau (1973) that the polysaccharides exhibit, despite a high Ca^{2+} affinity, only a weak Ca^{2+} binding strength and thus likely function as an intermediate Ca^{2+} pool for calcification. Thus they might attract Ca^{2+} ions for binding sites (e.g., aspartic ß-pleated sites) of calcifying proteins to promote crystallization (Böhm 1973; Mann 2001).

Roundly shaped nuclei < 1 µm, presumably of $CaCO_3$, are located directly on the utricle wall. Their appearance might indicate the start of a calcification event. We propose that these roundish nuclei seen at the utricle wall might (partly) consist of amorphous $CaCO_3$ as indicated by their morphology (Faatz et al. 2004). Acidic polysaccharides on the utricle wall might provide nucleation sites for amorphous $CaCO_3$ that in turn is stabilized by macromolecules (e.g., proteins) within the organic matrix to form aragonite crystals (Zhong and Chu 2010). The initiation of crystallization (nucleation) in biological systems investigated so far was shown to start in vivo and in vitro with a precursor phase of amorphous $CaCO_3$ (Mann 2001; Addadi et al. 2003, 2006).

In the segments investigated, the organic matrix seems to be in a stage of disintegration when primary needle growth on the utricle wall is observed. Borowitzka (1982b) proposed that early needle formation in *Halimeda* spp. may be associated with a matrix that disintegrates soon after crystal formation. Studies on the calcification of vertebrate bone or dentinogenesis (enamel) show that the

organic molecules stabilizing the early crystals have to disintegrate to allow crystallization to proceed (Robinson 1998; Watanabe et al. 2003; Bonucci 2007). Liebezeit and Dawson (1981) postulate a degradation of organic matrix components in mature segments of *Halimeda incrassata* after calcification has reached a certain stage. Primary needle growth and remnants of the organic matrix are also observed in mature, basal segments. This leads to the conclusion that the development of the matrix and its disintegration is most likely happening at the initiation and for the progression of every calcification event respectively, as long as the segment is part of the living alga. However, primary calcification in mature segments seems to be limited. Overall thinner and smaller primary needles (< 3 µm) are found in a mature segment, which might be due to the insufficient space remaining between the micro-anhedral carbonate and the utricle wall, and thus a consequently restricted exchange of ions with the seawater.

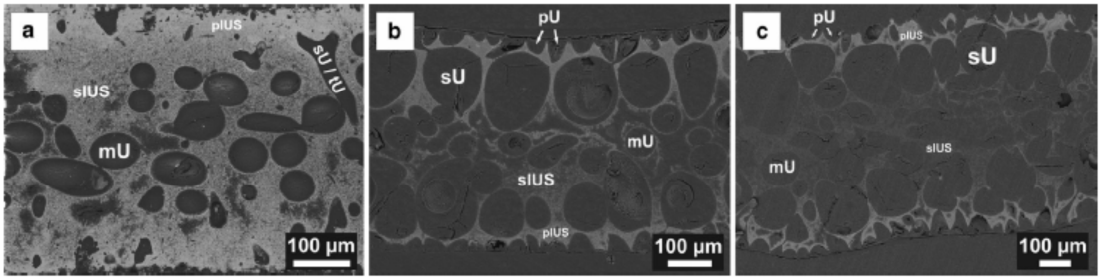

Figure 6 Comparison of the internal skeletal microstructure of segments from different *Halimeda* species. SEM images (via BSE) of thin-sections from mature segments of **(a)** *Halimeda opuntia*, **(b)** *Halimeda copiosa* and **(c)** *Halimeda cuneata*. Note the difference in dimensions of secondary, medullary utricles and the respective volume of inter-utricular space that is available for segment calcification. Also note the species-specific thickness of the peripheral primary inter-utricular space that resembles the micro-anhedral carbonate rim of the segment.
U = utricle (p = primary, s = secondary, t = tertiary, m = medullary); IUS = inter-utricular space (p = primary, s = secondary).

Primary cementation by micro-anhedral carbonate (MAC) formation

Micro-anhedral carbonate (MAC) is precipitated along the outer utricle walls. As suggested by Macintyre and Reid (1995), we propose this MAC to consist mainly of recrystallized $CaCO_3$ from primary calcification. This is supported by the fact that remnants of primary needles are identified within the MAC. The recrystallization and breakdown of the primary needles to anhedral crystals (< 1 µm) is most likely induced by the nightly metabolic respiratory activity of the alga exhaling CO_2 into the IUS, which decreases seawater pH and thereby $CaCO_3$ saturation state within the IUS. This hypothesis is likely for two reasons. First, the initial precipitation of MAC is observed primarily close to the utricle wall, e.g. at the rims of larger central medullary utricles (mU). If this MAC formation was simply intra-granular cementation (Milliman 1974), it is unclear why there was no precipitation of

MAC along the abundant long needles in the innermost parts of the IUS. Second, a dense rim that consists of MAC is observed surrounding the segment, which forms within the pIUS. Nightly CO_2 evolution might be highest along the segment rim, where the metabolically derived CO_2 from all algal cells is released into the environment. In addition, the close contact of the segment's surface with the surrounding $CaCO_3$ oversaturated seawater (Ω_{arag} ~3.0) may have a buffer effect that allows $CaCO_3$ re-precipitation. Analyses of segments of different age show that first the peripheral primary IUS is filled with MAC until secondly, the more central secondary IUS gains density in MAC. In a young segment, the pIUS is rapidly filled with primary needles, which in turn get recrystallized. Thus, similar to Macintyre and Reid (1995) we observe that the peripheral pIUS between primary utricles (pU) can completely fill with MAC during the lifetime of a segment.

The process of MAC formation during the lifetime of a segment can be considered important for the accumulation of *Halimeda* segments in the sediment as the extent of MAC is a key parameter for the later preservation of a segment in the sediment. A thick stabilizing rim of MAC build-up around the segment during its lifetime is a requirement for later intra-granular cementation. Less MAC filled segments rapidly break apart forming carbonate (needle) mud. Thus it seems opportune to name this biologically-induced early cementation process consistently the "primary cementation" of the segment. It is important to distinguish primary cementation from the subsequent intra-granular cementation of the dead segment. Henceforth we term this succeeding process the "secondary cementation" of the *Halimeda* segment. Secondary cementation also infills the inner sIUS of the segment that remained open during its lifetime and the utricles, after the organics have disintegrated. Additionally, secondary cements may exhibit a different $CaCO_3$ polymorph than aragonite, namely (low or high) Mg-calcite (Milliman 1974; Alexandersson and Milliman 1981; Reid and Macintyre 1998). As secondary cementation mainly takes place within a dropped segment, no physiological processes of the alga are involved. However, the initiation of secondary cementation is possible in dead segments that are still attached to the living alga (Milliman 1974).

Secondary needles and secondary calcification

Long euhedral needles are observed in the innermost parts of the IUS (especially within the sIUS), extending into available open space. These needles grow more than 20 µm in size on top of the primary needles or the MAC. That indicates formation after that of the primary needles. To describe the time-dependent development and the different location of these long needles, we define them as "secondary needles" and the process of their formation as "secondary calcification".

Secondary needles are elongated in the c-axis and have a typical prismatic aragonite crystal shape with a rather blunt end. Thus, it is assumed that they are precipitated abiotically during daytime photosynthesis. This implies that the seawater pH in the innermost parts of the IUS does not rise above pH ~9, as at higher seawater pH aragonite is usually precipitated in a granular crystal shape (De Beer and Larkum 2001; Holcomb et al. 2009). In addition, an organic matrix associated with secondary

needles was not detected. In most cases, secondary needles radiated out in bundles from distinct nuclei on top of the MAC layer. Similar observations can be made by the investigation of SEM images of former studies (e.g., Weiner and Lowenstam 1986; Multer 1988; Macintyre and Reid 1995). Therefore, it seems likely that remnants of primary needles on top of the MAC may act as nucleation sites and secondary needles are simply the result of continued crystal growth (Macintyre and Reid 1995). Crystal morphology suggests that $CaCO_3$ oversaturation in the IUS during photosynthesis is not high enough for spontaneous abiotic crystal nucleation, thus it seems rather unlikely that these long needles crystallize on the surface of organic utricle walls without any nuclei of $CaCO_3$ present (Holcomb et al. 2009). That might explain why the secondary needles are never found attached to the utricle wall between primary needles or remnants of them within the MAC.

The role of external carbonic anhydrase activity in calcification

In a previous study, external carbonic anhydrase activity was detected within the IUS of *Halimeda* spp. (Borowitzka and Larkum 1976b). External carbonic anhydrase activity is one of the essential enzymatic activities recognized within the organic matrix of most marine calcifying organisms (Mitsunaga et al. 1986; Miyamoto et al. 1996, 2005; Tambutté et al. 2007; Moya 2008; Rahman 2008). Studies on the calcification mechanism of marine algae and plants argue that the product of external carbonic anhydrase activity is CO_2 for photosynthesis, by the use of HCO_3^- as a substrate (Simkiss 1965; Borowitzka 1982a). Although for non-calcifying aquatic algae and plants this seems to be most likely the case (reviewed by Tsuzuki and Miyachi 1989), our observation of an organic matrix in *H. opuntia* and other recent analyses on the response of external carbonic anhydrase activity to elevated seawater pCO_2 question this view for calcifying macro-algae (Hofmann et al. 2013, 2014). Generally it is accepted that external carbonic anhydrase activity catalyzes the hydration of CO_2 to HCO_3^- when present in the calcifying matrix of marine organisms (e.g., in corals, Bertucci et al. 2013). Subsequently, enzymes use HCO_3^- for $CaCO_3$ formation (Weiss and Marin 2008). Although carbonic anhydrase activity may take part in the cell-uptake of HCO_3^- by representing a functional domain in a transport-metabolon of HCO_3^- / H^+ symporters, the occurrence of several coexisting isoforms of carbonic anhydrase domains (e.g., catalytic sites in the tertiary or quarterly structure of calcifying proteins within the organic matrix) is not uncommon (e.g., Marin and Luquet 2004; Bertucci et al. 2013).

Combining our observation of an organic matrix with the previous results of Böhm (1973) on the presence of acidic polysaccharides on the utricle wall and of Borowitzka and Larkum (1976b) and Hofmann et al. (2014) on external carbonic anhydrase activity within the IUS, we conclude that calcification mechanisms similar to those of other marine calcifying organisms are present. Testing this hypothesis exceeds the scope of the current study. However, our study considers external carbonic anhydrase activity as a key feature in the calcification of *Halimeda* spp. Whether this is correct needs to be investigated in future work.

A new model for the calcification in *Halimeda* spp.

To place the findings of this study in the context of the present knowledge of $CaCO_3$ biomineralization and of the physiology of the alga, we propose a new model for the calcification in *Halimeda* spp. (Fig. 5). The model is based on Alexandersson (1974) and his work on the skeleton of living coralline red algae. He suggested that it is primarily the metabolism of the alga that contributes to the abiotic formation of "non-biogenic" carbonate crystals within the skeleton. In addition the model is influenced by the work of Comeau et al. (2012), who proposed a new model for calcification in crustose coralline red algae with the evidence that abiotic re-precipitation of $CaCO_3$ during nighttime should be considered as a common process in skeletal formation.

Daytime processes

Physiological processes that are important for daytime calcification involve photosynthesis, external carbonic anhydrase activity, and cell-uptake of ions. These processes modify seawater parameters like carbon chemistry and ion availability within the inter-utricular space (IUS). HCO_3^- from the seawater is used in the physiology of *Halimeda* spp. for both photosynthesis and calcification. External carbonic anhydrase activity catalyzes H_2O and CO_2 to HCO_3^- and protons (H^+), necessary for nutrient and HCO_3^- / H^+ (proton-driven trans-membrane) symport into the cell. Removal of CO_2 via trans-membrane diffusion and external carbonic anhydrase activity elevates seawater CO_3^{2-} saturation in the IUS. Resulting CO_3^{2-} oversaturation supports biotic primary needle formation, and especially maintains abiotic secondary needle formation. To counteract the decrease in HCO_3^- / CO_2 availability in the IUS, as they are used up in photosynthesis and as a substrate of external carbonic anhydrase activity, calcification might be a "byproduct" to replenish CO_2 for its use in photosynthesis and also for its use in external carbonic anhydrase activity to gain HCO_3^-. In addition, calcification generates H^+ for nutrient trans-membrane symport. In particular HCO_3^- concentration may drop in the IUS due to biotically driven calcification and active cell import. Thus, we propose here that the primary calcification in *Halimeda* spp. may be HCO_3^- limited. However, Borowitzka and Larkum (1976a) note that in *Halimeda* spp. the use of HCO_3^- in photosynthesis, catalysed to CO_2 via cell-internal carbonic anhydrase activity, is less efficient compared to the direct use of CO_2.

Other physiological daytime processes not shown in the model

Not included in the model is a light-induced membrane-bound proton pump (presumably a H^+-ATPase; De Beer and Larkum 2001) from the cell to the IUS, as in our view it is not directly involved in the process of calcification and might rather play a role in balancing the internal cell pH. Furthermore, it can be safely assumed that protons discharged to the IUS are (re)used for nutrient symport back into the cell. Nevertheless, a proton efflux during the daytime supports the assumption of a matrix-driven primary calcification, as the pH in the microenvironment at the utricular site of

calcification is likely to be comparably low (pH < 9) to allow abiotic precipitation of $CaCO_3$. Likewise not considered is a postulated OH^- efflux from the cell into the IUS during daytime photosynthesis (Borowitzka and Larkum 1976a), as no mechanism and thus no evidence regarding the process was found yet.

Nighttime processes

Physiological cell processes shift during the nighttime from photosynthesis to metabolic respiration. This change affects the seawater carbon chemistry within the inter-utricular space (IUS). Metabolic respiration elevates CO_2 concentration and thus decreases CO_3^{2-} saturation within the IUS. As a consequence, aragonite needles precipitated during the daytime become partially dissolved, recrystallized, and break down to micro-anhedral crystals (< 1µm). $CaCO_3$ saturated seawater that enters the IUS might be sufficient to sustain local abiotic re-precipitation of previously dissolved $CaCO_3$ along possible nucleation sites (e.g., remnants of primary needles) on the utricle wall. Both processes lead to the formation of MAC.

The role of calcification in *H. opuntia*

Calcification has a range of functions for marine organisms (Kleypas et al. 2006). Nevertheless, at first glance it is not obvious why a marine macro-alga invests energy into the formation of a rigid calcium carbonate skeletal structure, when other marine algae and plants do not. Hence, it is important to consider the species-specific habitat of *H. opuntia* and its environmental conditions to provide answers to this enigma.

H. opuntia calcifies not solely to gain CO_2 or protons for photosynthesis or nutrient up-take. The skeleton also plays a major structural role in the alga's ecology making it less susceptible to breakage in high-energy regimes (DeWreede 2006; Ries 2009). Additionally, a calcareous skeleton is an efficient method of protection from grazing. Heavily calcified *Halimeda* species are grazed to a lesser extent than less calcified ones (Littler 1976; Paul and Hay 1986; Schupp and Paul 1994). *H. opuntia* is primarily located in the high-energy regimes of the reef crest, fore reef, and deep reef of tropical coral reefs (Johns and Moore 1988). *Halimeda* species that grow in these habitats possess smaller, but much heavier calcified segments, which presumably is an adaption to environmental conditions (Multer 1988; Kooistra and Verbruggen 2005). The enhanced stage of the segment's primary cementation (MAC formation) might derive from their smaller but higher number of utricles and accordingly smaller but higher total volume of IUS (Fig. 6; Macintyre and Reid 1995; Verbruggen and Kooistra 2004), the given seawater parameters (e.g., light conditions, pCO_2) of the environment in which these species grow and also species-specific metabolism, i.e. respiratory activity. Strong primarily cemented segments are less susceptible to breakage or disintegration, especially when shed into the sediment. Together these characteristics may explain why *H. opuntia* is one of the main macro carbonate sediment producers (> 1 cm) in the tropics. In fact, it is these small and heavily cemented segments by

Halimeda species of the sections (or lineages) Opuntia and Micronesicae (Drew and Abel 1988; Freile et al. 1995; Hillis 2001; Verbruggen et al. 2005, 2007) that are responsible for the build-up of carbonate platforms characterized by *Halimeda* sediments and thus might contribute crucially to island formation as they get transported over long distances, from their origin on the fore reef and reef crest, down the slope, onto the reef flat and up to the beach or into the lagoon (Jindrich 1969; Moore et al. 1976; Drew and Abel 1988; Hine et al. 1988; Johns and Moore 1988; Freile et al. 1995; Wienberg et al. 2010).

Based on the observation of *H. opuntia's* specific microstructural features, the calcification in *Halimeda* spp. obviously cannot be considered as simple abiotic $CaCO_3$ precipitation. The features that are present, namely acidic polysaccharides on the utricle walls, external carbonic anhydrase activity within the inter-utricular space, and an organic matrix in which the early primary needles are embedded, strongly suggest active calcification or at least the active initiation of crystal growth as in many other marine calcifying organisms. However, biologically-induced calcification (i.e., secondary calcification) is present but restricted to parts of the inter-utricular space that are not in direct contact with the cell wall. Thus, formation of the distinct skeletal microstructure seen in *H. opuntia* is more complex than previously thought. Here we propose that it is the interplay of biological processes with biochemical parameters of the seawater, which act in parallel to form this distinct $CaCO_3$ skeletal microstructure. Our model for calcification in *Halimeda* spp. considers both the biotic driven calcification and the abiotic driven precipitation of $CaCO_3$ depending on seawater carbonate chemistry influenced by the physiology of the alga. The model explains the formation of skeletal features in the living alga, as well as the first sedimentary processes already starting during the segments lifetime. Our investigations show that it is necessary to combine insights from fields of biology and physiology with biogeochemistry and sedimentology to gain a better understanding of processes influencing each other in a biological system.

Further investigations are needed to test the postulated model and the explanations given for the development of the skeletal morphological features seen in the skeletal microstructure of *H. opuntia*. Beyond the detection of an organic matrix, some deeper insights may come from microsensor studies dealing with diurnal changes of the seawater parameters within the IUS including a high-resolution mineralogical analysis of the different skeletal features, as well as the role of external carbonic anhydrase activity in calcification, its molecular characterization and whether or not other extracellular matrix proteins are present and involved in the process of calcification. However, the development of the most prominent microstructural feature in the skeleton of *H. opuntia*, the micro-anhedral carbonate, is not biologically controlled and may depend directly on seawater carbon chemistry. The process of micro-anhedral carbonate formation that causes cementation of the segment during its lifetime has implications for the alga and for its environment. Reduced segment cementation may result directly in a loss of segments in the sediment with an impact on ecosystem functioning and shoreline and island stability.

Acknowledgments

Sebastian Flotow (ZMT-Bremen) is thanked for preparing thin-sections and help with the SEM. Achim Meyer (ZMT-Bremen) provided help in conducting experiments and maintaining the aquaria. Claire Reymond and Julien Michel (ZMT-Bremen) thoughtfully reviewed the manuscript. We are grateful for the funding of this study by the ZMT-Bremen. We sincerely thank the associate editor and two reviewers for the helpful comments that greatly improved the manuscript.

References

Addadi L, Raz S, Weiner S (2003) Taking advantage of disorder: amorphous calcium carbonate and its roles in biomineralization. Adv Mater 15:959–970

Addadi L, Joester D, Nudelman F, Weiner S (2006) Mollusk shell formation: a source of new concepts for understanding biomineralization processes. Chemistry 12:980–987

Alexandersson ET (1972) Intragranular growth of marine aragonite and Mg-calcite; evidence of precipitation from supersaturated seawater. J Sediment Res 42:441–460

Alexandersson ET (1974) Carbonate cementation in coralline algal nodules in the Skagerrak, North Sea; biochemical precipitation in undersaturated waters. J Sediment Res 1:7–26

Alexandersson ET, Milliman JD (1981) Intragranular Mg-calcite cement in *Halimeda* plates from the Brazilian continental shelf. J Sediment Res 51:1309–1314

Arias JL, Fernández MS (2008) Polysaccharides and proteoglycans in calcium carbonate-based biomineralization. Chem Rev 108:4475–82

Arnott HJ (1982) Three systems of biomineralization in plants with comments on the associated organic matrix. In: Nancollas GH (ed) Biological mineralization and demineralization., Springer, Berlin Heidelberg, pp 199–218

Bertucci A, Moya A, Tambutté S, Allemand D, Supuran CT, Zoccola D (2013) Carbonic anhydrases in anthozoan corals–a review. Bioorg Med Chem 21:1437–50

Böhm EL (1973) Composition and calcium binding properties of the water soluble polysaccharides in the calcareous alga *Halimeda opuntia* (L.) (Chlorophyta, Udoteaceae). Internationale Revue der gesamten Hydrobiologie und Hydrogeographie 58:117–126

Böhm EL, Goreau T (1973) Rates of turnover and net accretion of calcium and the role of calcium binding polysaccharides during calcification in the calcareous alga *Halimeda opuntia* (L.). Internationale Revue der gesamten Hydrobiologie und Hydrogeographie 58:723–740

Bonucci E (2007) Main suggested calcification mechanisms: extracellular matrix. In: Schreck S (ed) Biological calcification: normal and pathological processes in the early stages. Springer, Heidelberg, pp 507–558

Borowitzka MA (1982a) Morphological and cytological aspects of algal calcification. Int Rev Cytol 74:127–162

Borowitzka MA (1982b) Mechanism in algal calcification. Progr Phycol Res 1:137–177

Borowitzka MA, Larkum AWD (1976a) Calcification in the green alga *Halimeda*. III. The sources of inorganic carbon for photosynthesis and calcification and a model of the mechanism of calcification. J Exp Bot 27:879–893

Borowitzka MA, Larkum AWD (1976b) Calcification in the green alga *Halimeda* IV. The action of metabolic inhibitors on photosynthesis and calcification. J Exp Bot 27:894–907

Comeau S, Carpenter R, Edmunds PJ (2012) Coral reef calcifiers buffer their response to ocean acidification using both bicarbonate and carbonate. Proc R Soc B Biol Sci 280:1753

Cuif JP, Dauphin Y, Nehrke G, Nouet J, Perez-Huerta A (2012) Layered growth and crystallization in calcareous biominerals: impact of structural and chemical evidence on two major concepts in invertebrate biomineralization studies. Minerals 2:11–39

De Beer D, Larkum AWD (2001) Photosynthesis and calcification in the calcifying algae *Halimeda discoidea* studied with microsensors. Plant Cell Environ 24:1209–1217

DeWreede R (2006) Biomechanical properties of coenocytic algae (Chlorophyta, Caulerpales). Sci Asia Suppl 1:57–62

Dickson AG, Millero FJ (1987) A comparison of the equilibrium constants for the dissociation of carbonic acid in seawater media. Deep Sea Res 34:1733-1743.

Dickson AG, Afghan JD, Anderson GC (2003) Reference materials for oceanic CO_2 analysis: a method for the certification of total alkalinity. Mar Chem 80.2:185-197

Dickson AG, Sabine CL, Christopher JR (2007) Guide to best practices for ocean CO_2 measurements. Sidney, British Columbia, North Pacific Marine Science Organization Special Publication 3, pp 176

Doney SC, Balch WM, Fabry VJ, Feely RA (2009) Ocean acidification: a critical emerging problem for the ocean sciences. North 22: 16–25

Drew EEA (1983) *Halimeda* biomass, growth rates and sediment generation on reefs in the central Great Barrier Reef province. Coral Reefs 2:101–110

Drew E, Abel K (1988) Studies on *Halimeda* I. The distribution and species composition of *Halimeda* meadows throughout the Great Barrier Reef Province. Coral Reefs 6:195–205

Faatz M, Gröhn F, Wegner G (2004) Amorphous calcium carbonate: synthesis and potential intermediate in biomineralization. Adv Mater 16:996–1000

Falini G, Reggi M, Fermani S, Sparla F, Goffredo S, Dubinsky Z, Levi O, Dauphin Y, Cuif JP (2013) Control of aragonite deposition in colonial corals by intra-skeletal macromolecules. J Struct Biol 183: 226–238

Folk RL (1959) Practical petrographic classification of limestones. Am Assoc Pet Geol Bull 43.1:1–38

Folk R, Robles R (1964) Carbonate sands of isla perez, alacran reef complex, Yucatan. J Geol 75:412–437

Freile D, Milliman J, Hillis L (1995) Leeward bank margin *Halimeda* meadows and draperies and their sedimentary importance on the western Great Bahama Bank slope. Coral Reefs 14: 27–33

Hillis, L (1997) Coralgal reefs from a calcareous green alga perspective and a first carbonate budget. Proc 8th Int Coral Reef Symp 1:761–766

Hillis L (2001) The calcareous reef alga *Halimeda* (Chlorophyta, Byropsidales): a cretaceous genus that diversified in the Cenozoic. Palaeogeogr Palaeoclimatol Palaeoecol 166:89–100

Hillis-Colinvaux L (1980) Ecology and taxonomy of *Halimeda*: primary producer of coral reefs. Adv Mar Biol 17:1–327

Hine AC, Hallock P, Harris MW, Mullins HT, Belknap DF, Jaap WC (1988) *Halimeda* bioherms along an open seaway: Miskito Channel, Nicaraguan Rise, SW Caribbean Sea. Coral Reefs 6:173–178

Hoegh-Guldberg O, Mumby PJ, Hooten AJ, Steneck RS, Greenfield P, Gomez E, Harvell CD, Sale PF, Edwards AJ, Caldeira K, Knowlton N, Eakin CM, Iglesias-Prieto R, Muthiga N, Bradbury RH, Dubi A, Hatziolos ME (2007) Coral reefs under rapid climate change and ocean acidification. Science 318:1737–1742

Hofmann LC, Straub S, Bischof K (2013) Elevated CO_2 levels affect the activity of nitrate reductase and carbonic anhydrase in the calcifying rhodophyte *Corallina officinalis*. J Exp Bot 64.4:899–908

Hofmann LC, Heiden J, Bischof K, Teichberg M (2014) Nutrient availability affects the response of the calcifying chlorophyte *Halimeda opuntia* (L.) J.V. Lamouroux to low pH. Planta 239:231–242.

Holcomb M, Cohen AL, Gabitov RI, Hutter JL (2009) Compositional and morphological features of aragonite precipitated experimentally from seawater and biogenically by corals. Geochim Cosmochim Acta 73:4166–4179

Isenberg H, Douglas S, Lavine L, Spicer S, Weissfeller H (1966) A protozoan model of hard tissue formation. Ann NY Acad Sci

Jindrich V (1969) Recent carbonate sedimentation by tidal channels in the Lower Florida Keys. J Sediment Res 39:531–553

Jinendradasa S, Ekaratne S (2002) Composition and monthly variation of fauna inhabiting reef-associated *Halimeda*. Proc 9th Int Coral Reef Symp 2:1059–1063

Johns H, Moore C (1988) Reef to basin sediment transport using *Halimeda* as a sediment tracer, Grand Cayman Island, West Indies. Coral Reefs 6:187–193

Kinsey D, Hopley D (1991) The significance of coral reefs as global carbon sinks–response to greenhouse. Palaeogeogr Palaeoclimatol Palaeoecol 89:363–377

Kleypas JA, Feely RA, Fabry VJ, Langdon C, Sabine CL, Robbins LL (2006) Impacts of ocean acidification on coral reefs and other marine calcifiers. A guide for future research. Report of a workshop sponsored by NSF, NOAA and USGS.

Kooistra WHCF, Verbruggen H (2005) Genetic patterns in the calcified tropical seaweeds *Halimeda opuntia, H. distorta, H. hederacea*, and *H. minima* (Bryopsidales, Chlorophyta) provide insights in species boundaries and interoceanic dispersal. J Phycol 41:177–187

Larkum AWD, Salih A, Kühl M (2011) Rapid mass movement of chloroplasts during segment formation of the calcifying siphonalean green alga *Halimeda macroloba*. Plos One 6:e20841

Liebezeit G, Dawson R (1981) Changes in the polysaccharide matrix of calcareous green algae during growth. Indices biochemiques et milieux marins. Journées du GABIM 14:147–154

Littler M (1976) Calcification and its role among the macroalgae. Micronesica 12:27–41

Macintyre I, Reid RP (1995) Crystal alteration in a living calcareous alga (*Halimeda*): implications for studies in skeletal diagenesis. J Sediment Res A Sediment Petrol Process 65:143–153

Mann S (2001) Biomineralization: principles and concepts in bioinorganic materials chemistry. Oxford University Press Vol. 5

Marin F, Luquet G (2004) Molluscan shell proteins. Cr Acad Sci II A 3:469–492

Marshall JF, Davies PJ (1988) *Halimeda* bioherms of the northern Great Barrier Reef. Coral Reefs 6:139–148

Merbach C, Culberson CH, Hawley JE, Pytkowicz RM (1973) Measurements of the apparent dissociation constants of carbonic acid in seawater at atmospheric pressure. Limnol Oceanogr 18:897–907

Milliman JD (1974) Recent sedimentary carbonates, part 1. Marine carbonates. Springer, Heidelberg

Milliman JD, Droxler AW (1996) Neritic and pelagic carbonate sedimentation in the marine environment: ignorance is not bliss. Geol Rundsch 85:496–504

Mitsunaga K, Akasaka K, Shimada H, Fujino Y, Yasumasu I, Numanoi H (1986) Carbonic anhydrase activity in developing sea urchin embryos with special reference to calcification of spicules. Cell Differ 18:257–62

Miyamoto H, Miyoshi F, Kohno J (2005) The carbonic anhydrase domain protein nacrein is expressed in the epithelial cells of the mantle and acts as a negative regulator in calcification in the mollusc *Pinctada fucata*. Zool Sci 22:311–5

Miyamoto H, Miyashita T, Okushima M, Nakano S, Morita T, Matsushiro A (1996) A carbonic anhydrase from the nacreous layer in oyster pearls. Proc Natl Acad Sci USA 93:9657–60

Moore CH, Graham EA, Land LS (1976) Sediment transport and dispersal across the deep fore-reef and island slope (-55 m to -305 m), Discovery Bay, Jamaica. J Sediment Petrol 46:174–187

Moya A, Tambutté S, Bertucci A, Tambutté E, Lotto S, Vullo D, Supuran C, Allemand D, Zoccola D (2008) Carbonic anhydrase in the scleractinian coral *Stylophora pistillata*: characterization, localization, and role in biomineralization. J Biol Chem 283:25475–84

Multer HG (1988) Growth rate, ultrastructure and sediment contribution of *Halimeda incrassata* and *Halimeda monile*, Nonsuch and Falmouth Bays, Antigua, W.I. Coral Reefs 6:179–186

Multer HG, Clavijo I (2004) *Halimeda* investigations: progress and problems. NOAA/RSMAS

Nakahara H, Bevelander G (1978) The formation of calcium carbonate crystals in *Halimeda incrassata* with special reference to the role of the organic matrix. Jap J Phycol 26: 9–12

Neumann AC, Land LS (1975) Lime mud deposition and calcareous algae in the Bight of Abaco, Bahamas; a budget. J Sediment Res 45:763–786

Orme GR, Salama MS (1988) Form and seismic stratigraphy of *Halimeda* banks in part of the northern Great Barrier Reef Province. Coral Reefs 6:131–137

Paul V, Hay M (1986) Seaweed susceptibility to herbivory: chemical and morphological correlates. Mar Ecol Prog Ser 33:255–264

Payri CE (1988) Halimeda contribution to organic and inorganic production in a Tahitian reef system. Coral Reefs 6:251–262

Phipps C, Roberts HH (1988) Seismic characteristics and accretion history of *Halimeda* bioherms on Kalukalukuang Bank, eastern Java Sea (Indonesia). Coral Reefs 6:149–159

Pierrot D, Lewis E, Wallace DWR (2006) CO_2SYS DOS Program developed for CO_2 system calculations. ORNL/CDIAC-105. Carbon Dioxide Information Analysis Center, Oak Ridge National Laboratory, US Department of Energy, Oak Ridge, TN

Pomar L, Kendall CGSC (2007) Architecture of carbonate platforms: a response to hydrodynamics and evolving ecology. In: Lukasik J, Simo JA (eds) Controls on carbonate platform and reef development. SEPM 89:187–216

Rahman MA, Oomori T, Uehara T (2008) Carbonic anhydrase in calcified endoskeleton: novel activity in biocalcification in alcyonarian. Mar Biotechnol 10:31–8

Rao VP, Veerayya M, Nair RR, Dupeuble PA, Lamboy M (1994) Late Quaternary *Halimeda* bioherms and aragonitic faecal pellet-dominated sediments on the carbonate platform of the western continental shelf of India. Mar Geol 121:293–315

Rees SA, Opdyke BN, Wilson PA, Henstock TJ (2007) Significance of *Halimeda* bioherms to the global carbonate budget based on a geological sediment budget for the Northern Great Barrier Reef, Australia. Coral Reefs 26:177–188

Reid RP, Macintyre GI (1998) Carbonate recrystallization in shallow marine environments: a widespread diagenetic process forming micritized grains. J Sediment Res 68: 928–946

Ries JB (2009) Effects of secular variation in seawater Mg/Ca ratio (calcite-aragonite seas) on $CaCO_3$ sediment production by the calcareous algae *Halimeda* , *Penicillus* and *Udotea* - evidence from recent experiments and the geological record. Terra Nova 21:323–339

Ries JB, Cohen AL, McCorkle DC (2009) Marine calcifiers exhibit mixed responses to CO_2-induced ocean acidification. Geology 37:1131–1134

Roberts H, Phipps C, Effendi L (1987) *Halimeda* bioherms of the eastern Java Sea, Indonesia. Geology 15:371–374

Robinson C, Brooks SJ, Shore RC, Kirkham J (1998) The developing enamel matrix: nature and function. Eur J Oral Sci 106:282–291

Salgado LT, Amado Filho GM, Fernandez MS, Arias JL, Farina M (2011) The effect of alginates, fucans and phenolic substances from the brown seaweed *Padina gymnospora* in calcium carbonate mineralization in vitro. J Cryst Growth 321:65–71

Schupp PJ, Paul VJ (1994) Calcium carbonate and secondary metabolites in tropical seaweeds: variable effects on herbivorous fishes. Ecology 75:1172–1185

Sikes CS (1978) Calcification and cation sorption of *Cladophoha glomerata* (chlorophyta) 1, 2. J Phycol 14.3:325–329

Simkiss K (1965) The organic matrix of the oyster shell. Comp Biochem Phys 16:427–35

Simkiss K, Wilbur KM (1989) Biomineralization. Academic Press, San Diego, California 92101

Stanley SM, Ries JB, Hardie LA (2010) Increased production of calcite and slower growth for the major sediment-producing alga *Halimeda* as the Mg/Ca ratio of seawater is lowered to a "Calcite Sea" level. J Sediment Res 80:6–16

Tambutté S, Tambutté E, Zoccola D, Caminiti N, Lotto S, Moya A, Allemand D, Adkins J (2007) Characterization and role of carbonic anhydrase in the calcification process of the azooxanthellate coral *Tubastrea aurea*. Mar Biol 151:71–83

Tussenbroek BI, van Dijk JK (2007) Spatial and temporal variability in biomass and production of psammophytic *Halimeda incrassata* (Bryopsidales, Chlorophyta) in a Caribbean reef lagoon. J Phycol 43:69–77

Tsuzuki M, Miyachi S (1989) The function of carbonic anhydrase in aquatic photosynthesis. Aquat Bot 34:85–104Verbruggen H, Littler DS, Littler MM (2007) *Halimeda pygmaea* and *Halimeda pumila* (Bryopsidales, Chlorophyta): two new dwarf species from fore reef slopes in Fiji and the Bahamas. Phycologia 46:513–520

Verbruggen H, De Clerck O, Cocquyt E, Kooistra WHCF, Coppejans E (2005) Morphometric taxonomy of siphonous green algae: a methodological study within the genus *Halimeda* (Bryopsidales). J Phycol 41:126–139

Verbruggen H, Kooistra W (2004) Morphological characterization of lineages within the calcified tropical seaweed genus *Halimeda* (Bryopsidales, Chlorophyta). Eur J Phycol 39:213–228

Vroom PS, Smith CM, Coyer JA, Walters LJ, Hunter CL, Beach KS, Smith JE (2003) Field biology of *Halimeda tuna* (Bryopsidales, Chlorophyta) across a depth gradient: comparative growth, survivorship, recruitment, and reproduction. Hydrobiologia 501:149–166

Watanabe T, Fukuda I, China K, Isa Y (2003) Molecular analyses of protein components of the organic matrix in the exoskeleton of two scleractinian coral species. Comp Biochem Physiol B Biochem Mol Biol 136:767–774

Wefer G (1980) Carbonate production by algae *Halimeda, Penicillus* and *Padina*. Nature 285:323–324

Weiner S, Lowenstam H (1986) Organization of extracellularly mineralized tissues: a comparative study of biological crystal growth. Crit Rev Biochem Mol Biol 20:365–408

Weiss IM, Marin F (2008) The role of enzymes in biomineralization processes. In: Sigel A, Sigel H, Sigel RKO (eds) Biomineralization: from nature to application. Wiley, West Sussex, pp 71–126

Wheeler AP, Sikes CS (1984) Regulation of carbonate calcification by organic matrix. Integr Comp Biol 24:933–944

Wienberg C, Westphal H, Kwoll E, Hebbeln D (2010) An isolated carbonate knoll in the Timor Sea (Sahul Shelf, NW Australia): facies zonation and sediment composition. Facies 56:179–193

Wilbur KM, Hillis-Colinvaux L, Watabe N (1969) Electron microscope study of calcification in the alga *Halimeda* (order Siphonales) 1. Phycologia 8:27–35

Wiman SK, McKendree WG (1975) Distribution of *Halimeda* plants and sediments on and around a patch reef near Old Rhodes Key, Florida. J Sediment Res 45:415–421

Zhong C, Chu CC (2010) On the origin of amorphous cores in biomimetic $CaCO_3$ spherulites: new insights into spherulitic crystallization. Cryst Growth Des 10:5043–5049

6 - Decreased light availability can amplify negative impacts of ocean acidification on calcifying coral reef organisms

N. Vogel[1,2,3*], F. W. Meyer[2,3], C. Wild[2,3], S. Uthicke[1]

[1]Australian Institute of Marine Science, PMB 3, Townsville MC, 4810 QLD, Australia

[2]Leibniz Center for Tropical Marine Ecology, Fahrenheitstraße 6, 28359 Bremen, Germany

[3]Faculty of Biology and Chemistry (FB 2), University of Bremen, 28359 Bremen, Germany

*Corresponding author, n.vogel@aims.gov.au

This mansuscirpt is published in MEPS

Abstract: Coral reef organisms are increasingly and simultaneously affected by global and local stressors, such as ocean acidification (OA) and reduced light availability. However, knowledge of the interplay between OA and light availability is scarce. We exposed two calcifying coral reef species (the scleractinian coral *Acropora millepora* and the green alga *Halimeda opuntia*) to combinations of ambient and increased pCO_2 (427 and 1073 µatm, respectively), and two light intensities (35 and 150 µmol photons m^{-2} s^{-1}) for 16 days. We evaluated the individual and combined effects of these two stressors on weight increase, calcification rates, O_2 fluxes and chlorophyll content for the species investigated. Weight increase of *A. millepora* was significantly reduced by OA (48%) and low light intensity (96%) compared to controls. While OA did not affect coral calcification in the light, it decreased calcification in the dark by 155%, leading to dissolution of the skeleton. *H. opuntia* weight increase was not affected by OA, but decreased (40%) at low light. OA did not affect algae calcification in the light, but decreased calcification in the dark by 164%, leading to dissolution. Low light significantly reduced gross photosynthesis (56% and 57%), net photosynthesis (62% and 60%) and respiration (43% and 48%) of *A. millepora* and *H. opuntia*, respectively. In contrast to *A. millepora*, *H. opuntia* significantly increased chlorophyll content by 15% over the course of the experiment. No interactive effects of OA and low light intensity were found on any response variable for either organism. However, *A. millepora* exhibited additive effects of OA and low light, while *H. opuntia* was only affected by low light. Thus, this study suggests that negative effects of low light and OA are additive on corals, which may have implications for management of river discharge into coastal coral reefs.

Introduction

Anthropogenically increased carbon dioxide (CO_2) introduced to the atmosphere is changing the earth's climate. In addition to aggravating the greenhouse effect and thus driving global warming, approximately one third of the atmospheric CO_2 is taken up by the oceans [1]. Carbon dioxide, which is added to the oceanic carbonate system increases hydrogen ion concentrations and thus leads to a reduction of seawater pH (ocean acidification, OA) [2,3]. Depending on the 'representative concentration pathways' (RCP) followed, atmospheric CO_2 is predicted to rise from present day, ~395 µatm [4], to between 850 and 1370 µatm by the year 2100 (RCP6.0 and RCP8.5, respectively), which is correlated with a further decrease in ocean pH, unless drastic reductions and carbon capture are achieved (RCP 2.6 and 4.5) [5]. In turn, a reduction of pH leads to a shift in the oceanic carbonate system, which results in a decreased calcium carbonate ($CaCO_3$) saturation state (Ω) of seawater. Recent studies revealed negative effects of decreased Ω on growth/ calcification of a vast range of coral reef organisms, projecting shifts in community structures, loss of framework builders and loss of coral reef biodiversity under predicted future conditions [6-12].

In addition to increasing sea surface temperature (SST) and OA, often local disturbances, such as elevated organic and inorganic nutrients, increased turbidity or decreased salinity present additional pressures on coral reef organisms at inshore reefs exposed to land-runoff [13-17]. Water quality is known to affect inshore reef communities leading to declined hard coral diversity and increased macroalgae richness [18-20]. Decrease in water quality on the Great Barrier Reef has been linked to anthropogenic activities associated with land-use, and has been declined since European settlement [21,22]. Predominantly during summer months, enhanced precipitation leads to increased riverine runoff and its associated implications on near-shore reef communities become more severe. Combinations of global and local stressors may have additive or synergistic effects and may push organisms closer to tolerance thresholds. For instance, interactive effects of OA and irradiance, OA and eutrophication, ocean warming (OW) and herbicides, or OW and eutrophication have been shown to have impacts on several coral reef organisms [17,23-26].

For many calcareous reef organisms photosynthesis is essential for energy supply, calcification and/ or survival, either because they are autotrophic primary producers or exhibit mixotrophic carbon acquisition. Scleractinian corals host photosynthetically active dinoflagellates as endosymbionts, which provide important energy to the host [27,28]. Moreover, by fixing CO_2 from the environment in the light, they increase cellular, surface and boundary layer pH levels and therefore facilitate the precipitation of $CaCO_3$, by elevating the aragonite saturation state, Ω_{ar} [27,29]. For the calcifying green alga genus *Halimeda*, photosynthesis is important for calcification, since some species do not possess active calcification mechanisms. In fact, in some *Halimeda* species, calcification is a byproduct of increased intracellular pH from photosynthesis, which results in abiotic precipitation of

aragonite needles [30]. By increasing the pH levels in the environment, photosynthesis may even protect organisms against OA, as long as sufficient light is available [29,31].

At reefs susceptible to land-runoff, increased turbidity leads to reduced light availability and therefore decreased photosynthetically available radiation (PAR) for photosynthesizing organisms. While sediment from rivers and dredging activities directly increase turbidity, elevated nutrient levels from agricultural land-runoff increase turbidity indirectly. Inshore eutrophication can enhance the abundance of chlorophyll, phytoplankton and microalgae blooms in the water column [13,32], which in turn leads to a reduction of PAR. Consequently, reduced PAR due to increased turbidity with increasing OA may have additional negative effects on growth, calcification and other responses of coral reef organisms. As shown in previous studies, calcification and photosynthesis in corals decrease with increasing turbidity [33,34] and decreasing light intensity [35,36]. However, knowledge of the interaction between OA and low light conditions is scarce but acknowledging the interplay between those stressors is crucial. Keeping in mind that photosynthesis plays a crucial role in calcification and OA has impacts on calcification of many organisms, it is surprising that the present study is one of the first to investigate this interaction. Local stressors are generally easier to manage than global stressors and therefore it is of high interest, to understand their interactions. Findings from respective manipulative experiments can be used to take actions in environmental management plans aiming to reduce the pressure on coral reef organisms.

The aim of the present study was to investigate the individual and interactive effects of OA and decreased PAR on two different coral reef taxa, the scleractinian coral *Acropora millepora* and the calcifying green alga *Halimeda opuntia*. *A. millepora* is common and widespread over tropical coral reefs and contributes to primary productivity, carbonate production and reef development. *H. opuntia* is a major, fast growing primary producer, commonly found on tropical coral reefs. *Halimeda* spp. considerably contribute to carbonate production, sediment formation and play an important role in the benthic community by providing habitat for many invertebrate species [37-40]. Thus, we conducted a laboratory experiment at controlled conditions and determined the response parameters, growth rates (measured by buoyant weight), calcification rates in light and in dark (measured by alkalinity anomaly), O_2 fluxes (productivity and respiration) and chlorophyll *a* content.

Methods

Specimen collection and preparation

Colonies of the coral *Acropora millepora* were collected from a fringing reef next to Pelorus Island (S 18° 33.001', E 146° 29.304') between 2 to 4 m below lowest astronomical tide (LAT) in the central section of the GBR. After fragmenting, individual coral nubbins were glued on stubs and kept at the

Australian Institute of Marine Science (AIMS, Townsville) in flow-through (recirculating flow ~1200 L h^{-1}) aquaria facilities under plasma light (150 µmol photons m^{-2} s^{-1}) for more than three months. Two weeks prior to the start of experiment, nubbins were transferred into experimental tanks and acclimated to experimental control conditions. Specimens of the calcifying green alga *Halimeda opuntia* were collected from a fringing reef next to Orpheus Island (S 18° 36.737', E 146° 29.110') between 0.5 to 1.0 m below LAT. Algae fragments (each with 50-100 phylloids) were acclimated in experimental aquaria under control conditions for two weeks until the start of the experiment.

Both sites of collection, Pelorus Island and Orpheus Island are considered inshore locations. Light regimes at the collection site of *A. millepora* were similar as control light conditions in the experiment. *H. opuntia* was subjected to lower light conditions in the experiment than found in the field, due to collection from shallower depths. However, both organisms were acclimated to the same 'control light' conditions for two weeks before the start of the experiment. Light levels chosen as control and low light condition were well within average ranges found between 3 to 6 m below LAT at mid-shelf and inshore reefs on the GBR, respectively [41]. Moreover, light data was collected with light loggers (Odyssey, New Zealand) simultaneously at mid-shelf location Rib Reef (S 18° 28.785', E 146° 52.256') and inshore location Orpheus Island (S 18° 38.949', E 146° 29.183') in 5 m below LAT over a period of 18 days in February 2013. At Rib Reef, daily light sums averaged 10.45 mol photons m^{-2} d^{-1} ranging from 4.58 to 13.35 mol photons m^{-2} d^{-1}. Daily light sums at Orpheus Island averaged 1.95 mol photons m^{-2} d^{-1} ranging from 0.22 to 4.66 mol photons m^{-2} d^{-1}. Comparing field data to present experimental conditions with daily light sums of 6.48 mol photons m^{-2} d^{-1} for controls and 1.51 mol photons m^{-2} d^{-1} for low light regimes, experimental light levels were well within naturally available light intensities at ~5 m below LAT at mid-shelf and inshore locations of the GBR.

Experimental setup

The manipulative aquaria experiment was carried out in flow-through conditions over a period of 16 days between July and August 2012 at AIMS. After two weeks acclimation, four nubbins of *A. millepora* and two fragments of *H. opuntia* were allocated to each of the twelve experimental aquaria. Four treatments with three replicate tanks (working volume 17.5 L) were placed in alternating order. Treatments consisted of combinations of ambient pCO_2 (427 µatm), high pCO_2 (1073 µatm), low light (35 µmol photons m^{-2} s^{-1}) and control light (150 µmol photons m^{-2} s^{-1}). High pCO_2 conditions corresponded to projections between the RCP 6.0 and RCP 8.5 scenario for the year 2100 [5]. Light intensities were chosen from average PAR readings from an inshore and mid-shelf reef at ~5 m below LAT, present during the summer months. Water flow was provided with fresh filtered (0.5 µm) seawater at 25 °C, with a salinity of 34.5, at a flow-rate of 150 mL min^{-1}. Irradiance was delivered by white light LED (6000 K, Aqua Illumination), covering the full color spectrum. Light levels were set to 12 h/ 12 h light-dark cycle. Additional aquaria pumps (AquarWorld, Australia, 250 L h^{-1}) were fitted into each tank to assure water movement. Target pH levels were achieved by an automatic CO_2

injection system (Aqua Medic, Germany) controlled by potentiometric pH sensors, as described in Vogel and Uthicke [42].

Carbonate system parameters

Total alkalinity (TA) was determined by gran titration with a Metrohm 855 robotic titrosampler (Metrohm, Switzerland) using 0.5 M HCl [see also 11]. Total alkalinity was calculated by non-linear regression fitting between pH 3.5 and pH 3.0 and was corrected to certified reference material (CRM Batch 106, A. Dickson, Scripps Oceanographic Institute). Seawater pH, temperature and millivolts (mV) were measured daily (including early morning and evening measurements to incorporate diurnal fluctuations) with a temperature corrected, hand-held pH meter (WTW, Germany), calibrated on NIST (National Institute of Standards and Technology, USA) scale. Millivolt and temperature readings were utilized to calculate pH on total (pH_{total}) scale. Carbonate system parameters (Table 1) were calculated with CO2calc software [43] utilizing TA and pH_{total} values and CO_2 constants from Lueker et al. [44]. Carbonate system parameters were calculated from measurements in each aquarium and three sampling events over the course of the experiment. Calculated pCO_2 levels yielded averages of 427 µatm for controls and 1073 µatm for future scenario conditions (Table 1). Aragonite saturation state yielded averages of $\Omega_{ar} = 3.3$ and $\Omega_{ar} = 1.7$ for controls and high pCO_2 treatments, respectively.

Growth rates

Growth of organisms was determined by the buoyant weight technique. Individual specimens were single-weighted (accuracy: 0.1 mg, Mettler Toledo, USA) in a custom build buoyant weight set-up with water jacket and seawater of constant temperature (25 °C) and salinity (34.5 ppt) at the start and at the end of the experiment. Growth of organisms was expressed as daily percentage of change.

Calcification in light and dark, net photosynthesis and respiration

After 16 days in experimental conditions, two individuals of each species and replicate tank were incubated for 1 h in the light and thereafter 1 h in the dark to determine calcification and photosynthetic rates. Light intensity and seawater pH of incubations corresponded to treatment condition of each organism. One experimental run consisted of 12 parallel incubations in 200 mL incubation chambers, including two blanks per treatment. To assure constant water temperature during incubation, chambers were placed into a flow-through water bath at 25 °C. Additionally, magnetic stirrer bars ensured water movement within the incubation chambers.

Calcification rates in light and dark were determined by the alkalinity anomaly technique [45]. A subsample of 50 mL was pipetted from the incubation seawater and directly titrated for A_T on a Metrohm 855 (as described above). Calcium carbonate precipitation or dissolution in µM C h^{-1} was calculated following Gao and Zheng [46] and standardized to organisms surface area (*A. millepora*) or

buoyant weight (*H. opuntia*). Daily net calcification was calculated by 12 h of daylight and 12 h of darkness. We determined surface areas of coral nubbins using the wax-weight method [47] and chose buoyant weight as standardization for the algae due to their highly three dimensional structures and lowest variability in data.

Net photosynthesis in the light or dark respiration were monitored consecutively during the incubations by three Firesting 4-channel oxygen meters (Pyroscience, Germany), which were connected to each chamber with fiber optic cables. Gross photosynthesis, net photosynthesis and respiration rates were expressed as $\mu M\ O_2\ h^{-1}$ and standardized to organism surface area (*A. millepora*) or buoyant weight (*H. opuntia*).

Pigment content

Chlorophyll *a* (Chl *a*) content of algae tissue was determined spectrophotometrically. Organisms were frozen to -80° C after incubations. Similar to the Chl *a* extraction described in Schmidt et al. [48] and Vogel and Uthicke [42], apical segments of algae were placed in 15 mL Falcon tubes on ice and 4 mL of cold ethanol (95% EtOH) was added. After crushing the segments with a homogenizer, extracts were heat-shocked in a water bath (78° C for 5 min), and left in a fridge for 24 h extraction. Absorbencies on 750 nm and 664 nm were read on a Powerwave microplate reader (BioTek, USA). Chlorophyll *a* content was calculated with equations by Nusch [49] and standardized to segment fresh weight.

Chlorophyll *a* content of coral *A. millepora* was determined after coral tissue was stripped from the skeleton with an air gun utilizing fresh, ultra-filtered (0.2 µm) seawater. Zooxanthellae were isolated from the host tissue and re-suspended in 2 mL of ethanol (EtOH 95%), heat shocked and extracted for 24h in the cold. Absorbencies were read (as described above) and Chl *a* contents were calculated standardized to nubbin surface area.

Statistical analysis

We statistically tested growth rates, net-, light- and dark-calcification rates, gross photosynthesis, net photosynthesis, respiration, and Chl *a* content for significant differences between experimental treatment conditions. Levene's tests for equal variances were performed on datasets with the R software [50]. If necessary response variables were $\log_{10}$ transformed prior to analyses, to fulfill assumptions of equal of variances. Mixed effect ANOVA's were conducted on datasets with NCSS software [51] with pH and light treatment as fixed factors. Replicate tanks were considered as nested (random) factor. To distinguish significantly differing groups we conducted Tukey-Kramer Multiple-Comparison tests.

Table 1 Carbonate system parameters of experimental conditions. Data is given as means and standard deviations.

Treatment	pH_{total}	Temp [°C]	TA [µmol $kgSW^{-1}$]	DIC [µmol $kgSW^{-1}$]	pCO_2 [µatm]	HCO_3^-[µmol $kgSW^{-1}$]	CO_3^{2-}[µmol $kgSW^{-1}$]	CO_2[µmol $kgSW^{-1}$]	Ω_{ar}
control pCO_2 + control light	8.038 (0.031)	25.4 (0.2)	2276 (13)	1990 (17)	421 (19)	1774 (21)	203 (5)	12 (1)	3.2 (0.1)
high pCO_2 + control light	7.707 (0.038)	25.3 (0.1)	2281 (7)	2160 (5)	1069 (71)	2026 (8)	104 (6)	30 (2)	1.7 (0.1)
control pCO_2 + low light	8.008 (0.015)	25.7 (0.8)	2278 (7)	1983 (11)	433 (15)	1762 (17)	209 (7)	12 (1)	3.4 (0.1)
high pCO_2 + low light	7.693 (0.016)	25.5 (0.3)	2288 (5)	2164 (8)	1076 (18)	2029 (9)	106 (2)	30 (1)	1.7 (0.0)

Results

For none of the parameters the interaction term between pCO_2 and light intensity was significant (Table 2). However, coral *A. millepora* exhibited additive negative effects of high pCO_2 and low light conditions on growth rates and calcification rates in the dark (Table 3).

Mean growth rates (Fig. 1) of *A. millepora* was significantly ($p = 0.032$) reduced in high pCO_2 (Table 2 and Table 3) by 48% compared to controls, while growth rate of *H. opuntia* was not impacted by high pCO_2. Low light significantly ($p < 0.0001$) reduced growth rates of *A. millepora* by 96% compared to controls, while growth of *H. opuntia* was not significantly reduced (Table 2, $p = 0.069$).

Net calcification rates (Fig. 1) of *A. millepora* and *H. opuntia* (measured by alkalinity anomaly) followed similar trends as growth rates measured by buoyant weight (Table 2 and Table 3). Both methods, buoyant weight integrated over long term and alkalinity anomaly determined in short-term, agreed well and showed similar pattern for treatment effects.

Elevated pCO_2 had no effect on organisms' calcification in the light (Fig. 1). While low light significantly (Table 2, $p = 0.006$) reduced light calcification of *A. millepora* by 83%, *H. opuntia* light calcification was not reduced in low light conditions.

The most distinct effect of elevated pCO_2 however, was observed in dark incubations (Fig .1). Elevated pCO_2 significantly reduced calcification of *A. millepora* and *H. opuntia* (Table 2, $p = 0.002$ and < 0.001, respectively) by 155% and 164%, respectively with decalcification of their skeleton in high pCO_2 conditions. Please note that reduction of calcification by more than 100% indicates decalcification. Moreover, low light conditions significantly (Table 2, $p = 0.002$) reduced dark calcification of *A. millepora* in darkness by 155% compared to controls.

High pCO_2 did not show any effect on gross photosynthesis, net photosynthesis or respiration of *A.millepora* and *H. opuntia* (Fig. 2). However, low light levels significantly reduced gross photosynthesis (Table 2, $p < 0.001$ and $p < 0.001$, respectively), net photosynthesis (Table 2, $p < 0.001$ and $p < 0.001$, respectively) and respiration (Table 2, $p = 0.001$ and $p = 0.001$, respectively), by 56% and 57%, 62% and 60%, as well as 43% and 48% for *A. millepora* and *H. opuntia*, respectively.

Chlorophyll *a* content (Fig. 2) of *H. opuntia* was significantly (Table 2, $p = 0.032$) increased by 15% in low light conditions compared to controls.

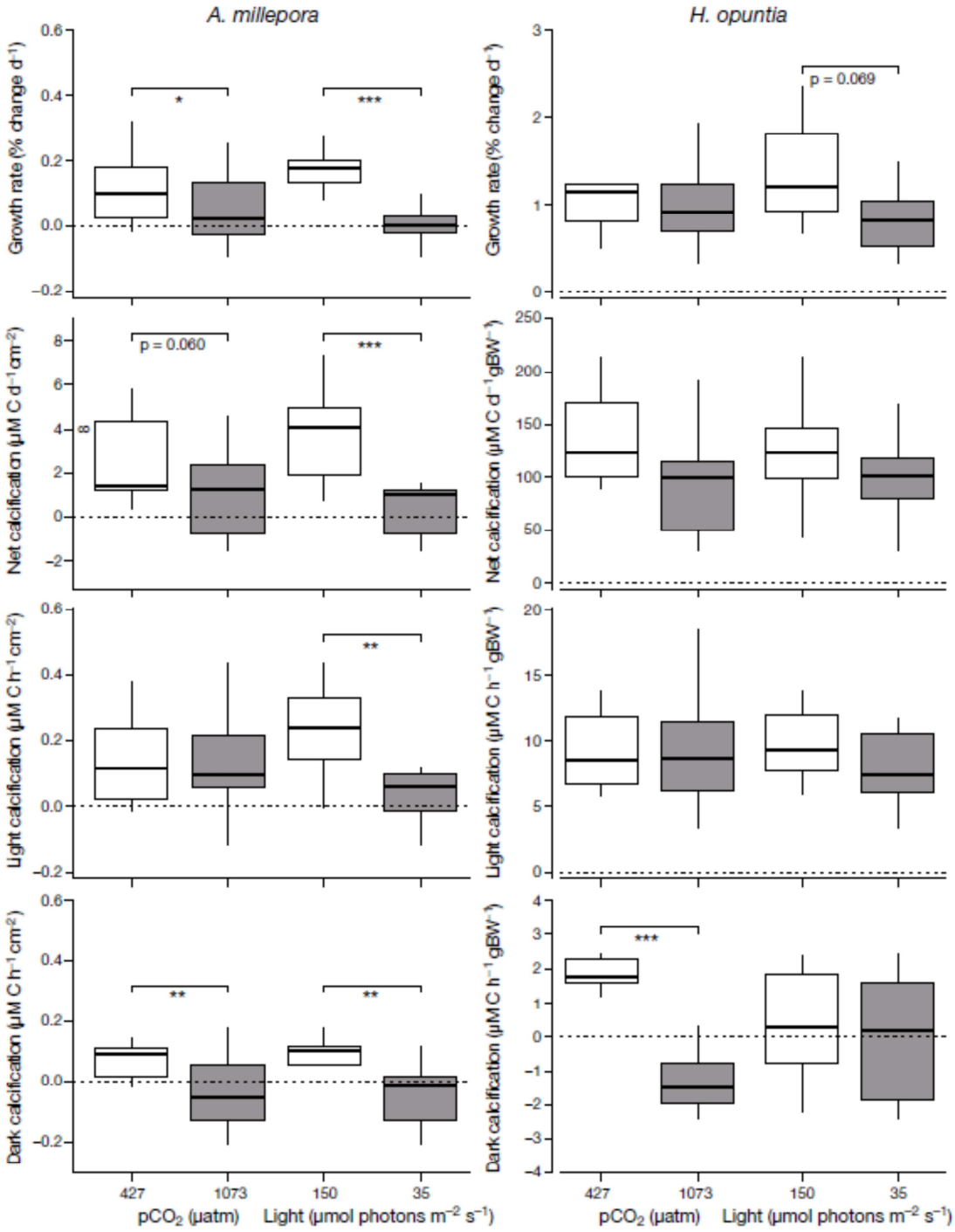

Fig. 1 Growth rates, net-, light- and dark calcification rates of *A. millepora* and *H. opuntia* after 16 days exposure to experimental conditions. Data was pooled across pCO_2 and light treatment because there was no significant interaction. X-axes represent OA treatments in µatm pCO_2 and light treatments in µmol photons $m^{-2}s^{-1}$. Whiskers represent lower and upper extremes. Brackets indicate significant differences in ANOVA's, with significance levels * $p < 0.05$, ** $p < 0.001$, *** $p < 0.0001$.

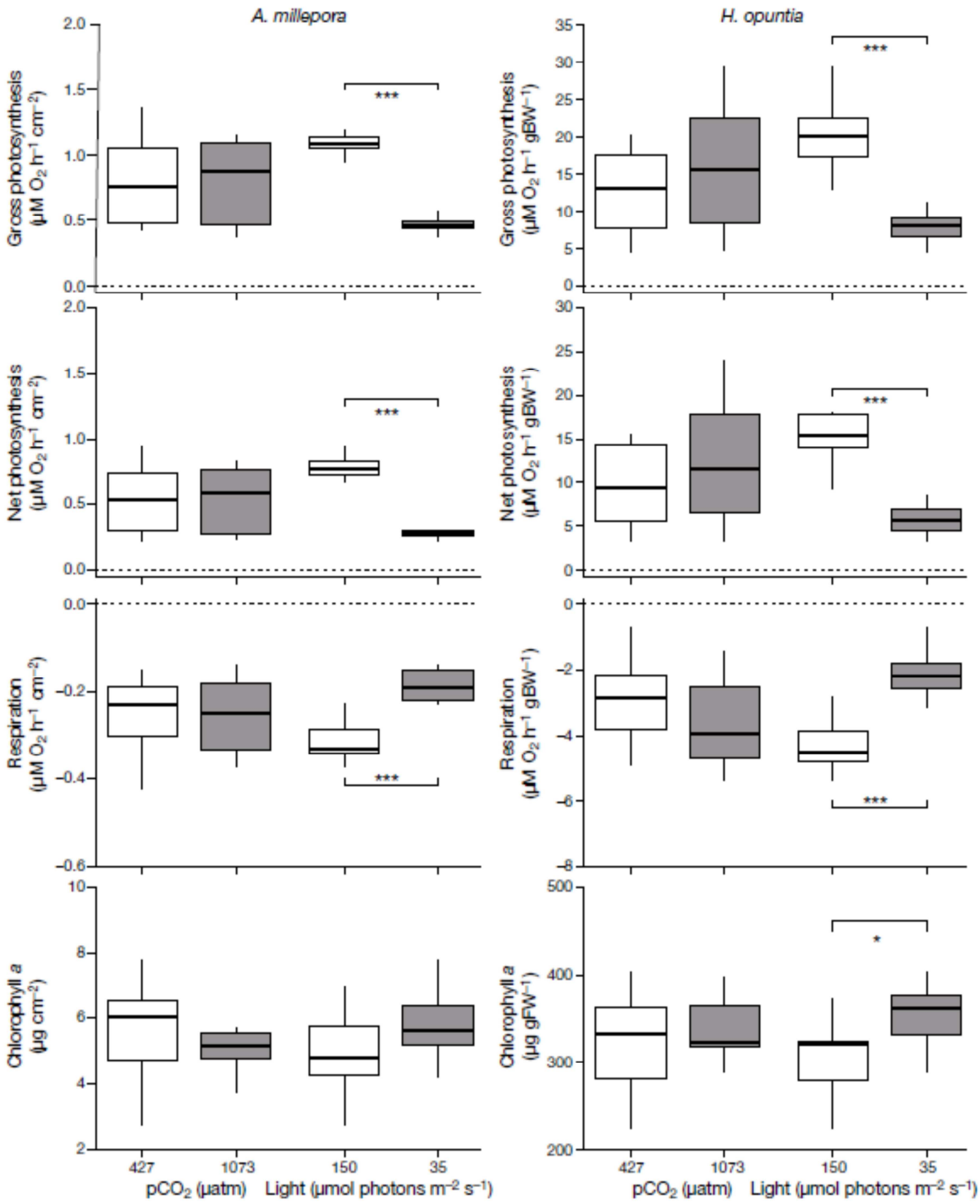

Fig. 2 Gross-, net photosynthesis, respiration and Chl *a* content of *A. millepora* and *H. opuntia* after 16 days exposure to experimental conditions. Data was pooled across pCO_2 and light treatment because there was no significant interaction. X-axes represent OA treatments in µatm pCO_2 and light treatments in µmol photons $m^{-2}s^{-1}$. Whiskers represent lower and upper extremes. Brackets indicate significant differences in ANOVA's, with significance levels * $p < 0.05$, ** $p < 0.001$, *** $p < 0.0001$.

Discussion

Negative effects of ocean acidification on a range of marine calcifying organisms has been well documented [e.g. 10,12,52,53-55]. The present study demonstrated that especially *A. millepora* was negatively affected by elevated pCO_2 and that decreased light availability can have an additional impact on both organisms. Although, the factors were not synergistic (i.e. higher than the effect of individual stressors added, see Table 3), additive effects on some response parameters clearly suggest

that some coral may better cope with global OA if PAR is not reduced at the same time. With increasing OA many corals will experience lower growth rates in future. If PAR is reduced at the same time, both inhibitors (elevated pCO_2 and reduced PAR) add up [56] and growth rates of corals impacted by reduced PAR at inshore reefs will be more compromised than of corals on mid-shelf reefs. Therefore, by improving water quality the additional stressor of low light availability for inshore corals can be reduced.

Table 3 Summary of effects of treatment variables on response parameters for *A. millepora* and *H. opuntia*. Decreases > 100% are possible due to decalcification.

Response parameter	Species	pCO_2	Light	Predicted additive effect	Measured additive effect
Growth	*A. millepora*	- 48%	- 96%	- 144%	- 114%
	H. opuntia	ns	ns	ns	ns
Net calcification	*A. millepora*	-57%	- 99%	- 156%	- 127%
	H. opuntia	ns	ns	ns	ns
Light calcification	*A. millepora*	ns	- 83%	ns	ns
	H. opuntia	ns	ns	ns	ns
Dark calcification	*A. millepora*	- 155%	- 155%	- 310%	- 204%
	H. opuntia	- 164%	ns	ns	ns
Gross photosynthesis	*A. millepora*	ns	- 56%	ns	ns
	H. opuntia	ns	- 57%	ns	ns
Net photosynthesis	*A. millepora*	ns	- 62%	ns	ns
	H. opuntia	ns	- 60%	ns	ns
Respiration	*A. millepora*	ns	- 43%	ns	ns
	H. opuntia	ns	- 48%	ns	ns
Chlorophyll *a* content	*A. millepora*	ns	ns	ns	ns
	H. opuntia	ns	- 15%	ns	ns

(ns) indicates no significant treatment effect, "measured additive effects" represent differences of means between the control pCO_2/ high light and high pCO_2/ low light treatment

In the present study we observed a significant reduction of growth rates for *A. millepora* in high pCO_2 conditions after 16 days in experimental conditions. To date, experiments revealed mixed responses of coral reef calcifiers towards altered pCO_2 conditions, showing decreased growth/ calcification in elevated pCO_2, or no effect at all [e.g. 8,57]. Yet, the present study revealed that *A. millepora* belongs

to the group which is likely to experience negative impacts in future environmental conditions. Presumably, reduced Ω_{ar} is the driving factor of decreased calcification of corals in a high pCO_2 environment [58,59]. Due to a decrease of Ω_{ar} in OA conditions, many organisms become impaired in building $CaCO_3$ skeletons [3,60,61]. In contrast, *H. opuntia* showed no significant trend on growth rates in relation to Ω_{ar}/ pCO_2. Some previous studies suggest that *Halimeda* spp. may be impacted in future OA conditions, showing reduced growth in elevated pCO_2 [8,62,63]. However, similar to corals, *Halimeda* spp. exhibits different growth forms with associated morphological distinctions. *Halimeda* spp. occur as heavily calcified and less calcified species, sand-dwellers and rock-anchored species as well as species with different sizes and shapes of phylloids. *Halimeda* spp. with smaller phylloids have a higher surface to volume ratio than with larger phylloids and hence are subjected to a higher exposure of their physical environment. As shown by Comeau et al. [57] *H. macroloba* showed no impact of increased pCO_2 on calcification, but *H. minima* showed reduced calcification in elevated pCO_2. However, different outcomes may also arise from different methodologies implemented such as flow conditions, nutrient availability, size of organisms, level of pCO_2 condition implemented, or combinations of different stressors (e.g. OA and OW). The impact of elevated pCO_2 on growth of *H. opuntia* in Price et al. [62] compared to the lack of response to elevated pCO_2 in the present study is unclear. We propose that different results mainly arose due to different methodologies implemented. The present study used flow-through conditions with constant supply of fresh filtered seawater and associated nutrients, while in Price et al. [62] 0.7 L tanks were utilized with water exchange every 48 h, not accounting for nutrient depletion. Moreover, daily light sums of control light in the present study were considerably higher and closer to natural light conditions than reduced natural light regimes in Price et al. [62], where light maxima at mid-day averaged 150 µmol photons $m^{-2}s^{-1}$. In the present study we chose a pCO_2 level which is likely to be reached by the year 2100 under projections between the RCP 6.0 and RCP 8.5 scenario [5], the experimental set-up provided flow-through conditions with continuous supply of nutrients and light regimes naturally found on mid-shelf and inshore locations of the GBR, at 5 m below LAT. One potential explanation that *H. opuntia* is still capable to grow in a high pCO_2 environment while *A. millepora* is not, may be that calcification rates in *Halimeda* spp. are generally higher than in corals when both standardized either to surface area or buoyant weight. For *H. opuntia* daytime calcification rates were approximately one order of magnitude higher than dissolution rates in the dark under elevated pCO_2 conditions. Thus, even when some dissolution is taking place in the dark, higher light calcification rates sum up to positive net calcification rates. In contrast, for *A. millepora* dark dissolution and light calcification rate were in a similar range, indicating net dissolution if impacts of future OA and low light conditions become additive (Table 3).

Notably, light calcification rates, determined by alkalinity anomaly technique, of both organisms were unaffected by increased pCO_2. To our knowledge, this is the first study to show that calcification of *A. millepora* and *H. opuntia* in elevated pCO_2 is not impacted in the light and supports the assumption

that in the light, photosynthetic activity can counteract negative impacts of OA by increasing intracellular, surface and boundary-layer pH. By utilizing CO_2, photosynthesis increases pH and Ω_{ar} [30,31,64]. As shown by Al-Horani et al. [29], pH increases under the calcioblastic layer of corals in light, which elevated the super saturation of Ω_{ar} from 3.2 up to 25, facilitating deposition of $CaCO_3$ [27,29].

However, the present study also suggested that for dark calcification rates, the opposite effect is the case. During respiration in the dark, additional CO_2 reduces pH and Ω_{ar}, once more than already reduced by OA, impeding deposition of $CaCO_3$. Hence, in the present study we also showed that in the absence of light, both organisms were strongly negatively impacted by high pCO_2 conditions, leading to dissolution of their skeleton. Therefore, the present study shows that the impact of OA on calcification rates of *A. millepora* and *H. opuntia* is not taking place in the light, however a fortiori in the dark. In contrast, under present day conditions both organisms can still calcify in the dark, thus in the absence of photosynthesis. This observation is in agreement with a previous study, showing decalcification of *A. eurystoma* in high pCO_2 and darkness, while $CaCO_3$ was still deposited under control conditions or in high pCO_2 in the light [58]. Previous studies have also shown that reef communities can change the diurnal local seawater carbonate chemistry by photosynthesis, respiration, calcification and dissolution and that $CaCO_3$ dissolution is primarily taking place in the dark [25,65-67]. While respiration is taking place in the dark, additional CO_2 is added to the carbonate system and already lowered pH levels from OA are further reduced, leading to an additional reduction of Ω_{ar} as already provoked by OA. Consequently, *A. millepora* and *H. opuntia* were not only incapable to deposit $CaCO_3$, yet even experienced dissolution of their skeleton in the dark.

Considering the negative impacts of OA in darkness, we demonstrated low light conditions may likewise result in additional negative implications on organisms, once PAR is reduced below a level, at which photosynthesis cannot buffer reduced pH by OA. Presumably, this threshold level is below 35 µmol photons m^{-2} s^{-1} as tested in the present study. As shown in the present study by measurements in the light, OA showed no impact on calcification rates of either organism. Thus, the availability of sufficient light, associated with photosynthetic activity and apparent buffer capacity, mitigated negative effects of OA in light incubations. However, turbidity decreases PAR and therefore reduces the capability of the organisms' photosynthesis to buffer the negative impacts of OA, even during the day. As shown by our O_2 flux measurements, low light regimes significantly decreased gross- and net photosynthesis of both organisms. This enhances negative impacts of OA during the day, especially at inshore reefs, where riverine runoff leads to reduced PAR [32]. As shown by light data from mid-shelf and inshore reefs at 5 m below LAT at the GBR, light availability can be extremely reduced at inshore reefs, considerably impacting organisms' photosynthetic capacities. Moreover, reduced photosynthetic activity of organisms in reduced light availability may also change DIC/ carbonate chemistry on inshore reefs, compared to mid-shelf locations. At low light conditions, mean growth rates of both,

coral and algae were reduced compared to higher light. Light enhanced photosynthesis and calcification of coral and algae is a well-documented phenomenon [27,30,31,68,69]. With increasing OA and the additive negative effects of low light on coral growth, as demonstrated in the present study, the mechanism of light enhanced calcification may gain in importance. Moreover, at lower light conditions, when photosynthetic activity is reduced, organisms obtain less energy supply, thus reducing the scope for growth.

Photosynthesis of algae and coral can be limited by dissolved inorganic carbon (DIC) availability [26,30,59,70,71]. Carbonic anhydrase can utilize elevated bicarbonate availability to increase the CO_2 pool available for photosynthetic activity. Thus we assumed that photosynthesis could be enhanced under higher pCO_2. However, photosynthesis of organisms investigated here could not benefit from increased DIC concentrations. This may have two different reasons; the first is that organisms were not DIC limited in present experimental control conditions. The second reason may be that under present light conditions photosynthesis/ calcification of organisms was not saturated and hence, there was no detectable benefit from increased DIC availability. Former studies conducted by Marubini et al. [59] and Crawley et al. [70] indicating DIC limitation, both utilized higher light intensities than the present study (~300 and ~1000 µmol photons m^{-2} s^{-1}, respectively). This suggests that under present experimental conditions (i.e. present light intensities) calcification and photosynthesis were not DIC limited.

Moreover, we showed that in decreased PAR, *H. opuntia* increased its tissue Chl *a* content in order to compensate for less light availability, while the coral was not able to do so over the period of the experiment. By adjusting its Chl *a* content the alga might acclimate to reduced light availability in short term, and increase its photosynthetic capacity in low light. Increased productivity changes the carbonate chemistry to the advantage of the algae, by facilitating deposition of $CaCO_3$. In contrast, *A. millepora* did not have this advantage because it could not increase Chl *a* over the short experimental period and thus may not be able to acclimate in short-term to decreased light availability inshore. As shown by previous studies, corals can alter their Chl *a* content by either, increasing zooxanthellae per unit area, or by an increase of Chl *a* content in zooxanthellae [26,72]. Field data suggests that *A. millepora* show increased pigmentation with decreasing water clarity from mid-shelf to inshore [73]. However, this might also be a response towards a more chronic exposure to low light conditions and other water quality parameters (i.e. increased nutrient availability at inshore reefs). Therefore, the algae may show more immediate responses towards changing light regimes and thus have an advantage in acclimation compared to the coral.

Organisms investigated did not exhibit significant interactive effects on response parameters measured, which is an indication that effects were not synergistic [56]. Similar, Comeau et al. [74] and Comeau et al. [23] found no interactive effects of OA and irradiance on calcification rates of *Porites rus* and *Acropora pulchra*, respectively, after three weeks exposure to experimental conditions. In

contrast, a study on *Pocillopora damicornis* recruits presented interactive effects of OA and light after 5 days of experimentation [75]. However, the responses were non-linear and impacts of OA on calcification rates were only found at intermediate light intensities (70 µmol photons m^{-2} s^{-1}) and not at lower or higher light levels (31, 41, 122 and 226 µmol photons m^{-2} s^{-1}). Moreover, a study on *Acropora horrida* and *Porites cylindrica* showed impacts of OA on calcification were greatest in light calcification of corals grown in lower light conditions (100 µmol photons m^{-2} s^{-1}) compared to corals grown in higher light (400 µmol photons m^{-2} s^{-1}) after 5 weeks of experimentation [76]. This is unexpected and in contrast to the present study, where the impact of OA on calcification of organisms was not occurring in the light, however was strongly impacted in the dark. In the present study *A. millepora* did not show interactive effects of OA and light, however exhibited additive effects of both stressors because it showed reduced growth rates (-48%) when exposed to high pCO_2 conditions and it showed reduced growth rates when exposed to low light regimes (-96%). Thus, both factors add up negative effects (-144%) and lead to a stronger negative impact on *A. millepora* growth (Table 3). This may also have an ecological implication for corals inhabiting inshore reefs susceptible to land-runoff and thus decreased light availability. Turbidity changes the attenuation of light penetrating the water column decreasing PAR by depth more rapidly than in clear water conditions. This in turn, may lead to a stronger depth limitation for corals and thus to potential habitat decline in future OA conditions, because they gain less light with lower water depth, compared to clear water habitats.

In the present experiment, it was confirmed that the marine calcifiers investigated are negatively impacted by ocean acidification, with *A. millepora* showing more negative impacts than *H. opuntia*. As long as sufficient light is available during the day, photosynthesis aids organisms to counteract negative impacts of OA. However, if there is not sufficient light available (e.g. due to high turbidity), there may be impacts of OA on calcification also during the day. Thus, low light conditions inshore remove this advantage from photosynthesizing organisms. As suggested by the dark incubations, respiration potentially aggravates the impacts of OA on the organisms, leading to dissolution of their skeleton. This highlights the importance to consider light-dependent impacts of OA on photosynthesizing calcifiers. Moreover, we showed that decreased light availability is an additive stressor with OA, particularly for the coral *A. millepora*, because the coral exhibits reduced calcification in OA conditions as well as in low light conditions. *H. opuntia*, on the other hand, grows marginally less in low light, but was not negatively impacted by OA in its overall growth. Consequently, the combination of OA and low light conditions may contribute to a changing coral reef ecosystem with even less hard corals as framework builders and more macroalgae on inshore reefs of the future. Potential acclimatization to environmental stressors in long term could lead to different responses of organisms. Therefore, further investigations are needed to test the effects of OA in combination with light availability on coral reef organisms. However, by improving water clarity on inshore reefs, the additional stressor of low light availability for corals will be reduced.

Acknowledgements

The authors would like to thank the SeaSim team at AIMS for providing the coral nubbins and their general assistance. We thank Michelle Liddy for her assistance in the field and laboratory. Many thanks for general assistance from Florita Flores. We would like to acknowledge the National Environmental Research Program, which provided the stipend for Nikolas Vogel. This study was conducted with the support of funding from the Australian Government's National Environmental Research Program and an Australian Research Council Discovery Grant.

References

1. Bindoff NL, Willebrand J, Artale V, Cazenave A, Gregory JM, et al. (2007) Observations: oceanic climate change and sea level. Cambridge, United Kingdom and New York, NY, USA: Cambridge University Press. 0521880092 0521880092. 385-432 p.
2. Golubik S, Krumbein W, Schneider K (1979) The Carbon Cycle In: Trudinger PA, Swaine DJ, editors. Biogeochemical Cycling of Mineral-Forming Elements Amsterdam, The Netherlands: Elsevier.
3. Kleypas JA, Langdon C (2006) Coral reefs and changing seawater carbonate chemistry. Coastal and Estuarine Studies: Coral Reefs and Climate Change Science and Management Coastal JT Phinney, OH Guldberg, J Kleypas, W Skirving and A Strong Washington DC, American Geophysical Union: 73-110.
4. Tans P, Keeling R (2015) Trends in Atmospheric Carbon Dioxide: Recent Global CO_2. NOAA/ESRL.
5. Moss RH, Edmonds JA, Hibbard KA, Manning MR, Rose SK, et al. (2010) The next generation of scenarios for climate change research and assessment. Nature 463: 747-756.
6. Gattuso JP, Frankignoulle M, Bourge I, Romaine S, Buddemeier RW (1998) Effect of calcium carbonate saturation of seawater on coral calcification. Global and Planetary Change 18: 37-46.
7. Langdon C, Takahashi T, Sweeney C, Chipman D, Goddard J, et al. (2000) Effect of calcium carbonate saturation state on the calcification rate of an experimental coral reef. Global Biogeochemical Cycles 14: 639-654.
8. Ries JB, Cohen AL, McCorkle DC (2009) Marine calcifiers exhibit mixed responses to CO_2-induced ocean acidification. Geology 37: 1131-1134.
9. Fabricius KE, Langdon C, Uthicke S, Humphrey C, Noonan S, et al. (2011) Losers and winners in coral reefs acclimatized to elevated carbon dioxide concentrations. Nature Climate Change.

10. Orr JC, Fabry VJ, Aumont O, Bopp L, Doney SC, et al. (2005) Anthropogenic ocean acidification over the twenty-first century and its impact on calcifying organisms. Nature 437: 681-686.
11. Uthicke S, Fabricius KE (2012) Productivity gains do not compensate for reduced calcification under near-future ocean acidification in the photosynthetic benthic foraminifer species *Marginopora vertebralis*. Global Change Biology 18: 2781–2791.
12. Fabricius KE, De'ath G, Noonan S, Uthicke S (2014) Ecological effects of ocean acidification and habitat complexity on reef-associated macroinvertebrate communities. Proceedings of the Royal Society B: Biological Sciences 281: 20132479.
13. Bell PRF (1992) Eutrophication and coral reefs - some examples in the Great Barrier Reef lagoon. Water Research 26: 553-568.
14. Fabricius KE (2005) Effects of terrestrial runoff on the ecology of corals and coral reefs: review and synthesis. Marine Pollution Bulletin 50: 125-146.
15. Fabricius KE (2011) Factors determining the resilience of coral reefs to eutrophication: a review and conceptual model. Coral Reefs: An Ecosystem in Transition: 493-505.
16. Wooldridge S, Brodie J, Furnas M (2006) Exposure of inner-shelf reefs to nutrient enriched runoff entering the Great Barrier Reef Lagoon: Post-European changes and the design of water quality targets. Marine Pollution Bulletin 52: 1467-1479.
17. Uthicke S, Vogel N, Doyle J, Schmidt C, Humphrey C (2011) Interactive effects of climate change and eutrophication on the dinoflagellate-bearing benthic foraminifer *Marginopora vertebralis*. Coral Reefs: 1-14.
18. De'ath G, Fabricius KE (2010) Water quality as a regional driver of coral biodiversity and macroalgae on the Great Barrier Reef. Ecological Applications 20: 840-850.
19. Fabricius KE, De'ath G, McCook L, Turak E, Williams DE (2005) Changes in algal, coral and fish assemblages along water quality gradients on the inshore Great Barrier Reef. Marine Pollution Bulletin 51: 384-398.
20. Schaffelke B, Mellors J, Duke NC (2005) Water quality in the Great Barrier Reef region: responses of mangrove, seagrass and macroalgal communities. Marine Pollution Bulletin 51: 279-296.
21. McCulloch M, Fallon S, Wyndham T, Hendy E, Lough J, et al. (2003) Coral record of increased sediment flux to the inner Great Barrier Reef since European settlement. Nature 421: 727-730.
22. Roff G, Clark TR, Reymond CE, Zhao J-x, Feng Y, et al. (2013) Palaeoecological evidence of a historical collapse of corals at Pelorus Island, inshore Great Barrier Reef, following European settlement. Proceedings of the Royal Society B: Biological Sciences 280.
23. Comeau S, Carpenter RC, Edmunds PJ (2014) Effects of irradiance on the response of the coral *Acropora pulchra* and the calcifying alga *Hydrolithon reinboldii* to temperature elevation and ocean acidification. Journal of Experimental Marine Biology and Ecology 453: 28-35.

24. Negri AP, Flores F, Roethig T, Uthicke S (2011) Herbicides increase the vulnerability of corals to rising sea surface temperature. Limnology and Oceanography 56: 471-485.

25. Langdon C, Atkinson MJ (2005) Effect of elevated pCO_2 on photosynthesis and calcification of corals and interactions with seasonal change in temperature/irradiance and nutrient enrichment. Journal of Geophysical Research 110: C09S07.

26. Chauvin A, Denis V, Cuet P (2011) Is the response of coral calcification to seawater acidification related to nutrient loading? Coral reefs: 1-13.

27. Goreau TF (1959) The physiology of skeleton formation in corals. I. A method for measuring the rate of calcium deposition by corals under different conditions. Biological Bulletin: 59-75.

28. Wainwright SA (1963) Skeletal organization in the coral, *Pocillopora damicornis*. Quarterly Journal of Microscopical Science 3: 169-183.

29. Al-Horani FA, Al-Moghrabi SM, de Beer D (2003) The mechanism of calcification and its relation to photosynthesis and respiration in the scleractinian coral *Galaxea fascicularis*. Marine Biology 142: 419-426.

30. de Beer D, Larkum AWD (2001) Photosynthesis and calcification in the calcifying algae *Halimeda discoidea* studied with microsensors. Plant Cell and Environment 24: 1209-1217.

31. de Beer D, Kühl M, Stambler N, Vaki L (2000) A microsensor study of light enhanced Ca^{2+} uptake and photosynthesis in the reef-building hermatypic coral *Favia sp*. Marine ecology Progress series 194: 75-85.

32. Devlin M, Schaffelke B (2009) Spatial extent of riverine flood plumes and exposure of marine ecosystems in the Tully coastal region, Great Barrier Reef. Marine and Freshwater Research 60: 1109-1122.

33. Kendall Jr JJ, Powell EN, Connor SJ, Bright TJ, Zastrow CE (1985) Effects of turbidity on calcification rate, protein concentration and the free amino acid pool of the coral *Acropora cervicornis*. Marine Biology 87: 33-46.

34. Kendall Jr JJ, Powell EN, Connor SJ, Bright TJ (1983) The effects of drilling fluids (muds) and turbidity on the growth and metabolic state of the coral *Acropora cervicornis*, with comments on methods of normalization for coral data. Bulletin of Marine Science 33: 336-352.

35. Mass T, Einbinder S, Brokovich E, Shashar N, Vago R, et al. (2007) Photoacclimation of *Stylophora pistillata* to light extremes: metabolism and calcification. Marine Ecology Progress Series 334: 93-102.

36. Marubini F, Barnett H, Langdon C, Atkinson MJ (2001) Dependence of calcification on light and carbonate ion concentration for the hermatypic coral *Porites compressa*. Marine Ecology Progress Series 220: 153-162.

37. Rees SA, Opdyke BN, Wilson PA, Henstock TJ (2007) Significance of *Halimeda* bioherms to the global carbonate budget based on a geological sediment budget for the Northern Great Barrier Reef, Australia. Coral reefs 26: 177-188.

38. Wefer G (1980) Carbonate production by algae *Halimeda*, *Penicillus* and *Padina*. Nature 285: 323-324.

39. Freile D, Milliman J, Hillis L (1995) Leeward bank margin *Halimeda* meadows and draperies and their sedimentary importance on the western Great Bahama Bank slope. Coral Reefs 14: 27-33.

40. Fukunaga A (2008) Invertebrate community associated with the macroalga *Halimeda kanaloana* meadow in Maui, Hawaii. International Review of Hydrobiology 93: 328-341.

41. Uthicke S, Altenrath C (2010) Water column nutrients control growth and C: N ratios of symbiont-bearing benthic foraminifera on the Great Barrier Reef, Australia. Limnol Oceanogr 55: 1681-1696.

42. Vogel N, Uthicke S (2012) Calcification and photobiology in symbiont-bearing benthic foraminifera and responses to a high CO_2 environment. Journal of Experimental Marine Biology and Ecology 424-425: 15-24.

43. Robbins LL, Hansen ME, Kleypas JA, Meylan SC (2010) CO2calc—A user-friendly seawater carbon calculator for Windows, Max OS X, and iOS (iPhone). Geological Survey Open-File Report 2010-1280: 17.

44. Lueker TJ, Dickson AG, Keeling CD (2000) Ocean pCO_2 calculated from dissolved inorganic carbon, alkalinity, and equations for K1 and K2: validation based on laboratory measurements of CO_2 in gas and seawater at equilibrium. Marine Chemistry 70: 105-119.

45. Chisholm JRM, Gattuso JP (1991) Validation of the alkalinity anomaly technique for investigating calcification and photosynthesis in coral-reef communities. Limnology and Oceanography 36: 1232-1239.

46. Gao K, Zheng Y (2010) Combined effects of ocean acidification and solar UV radiation on photosynthesis, growth, pigmentation and calcification of the coralline alga *Corallina sessilis* (Rhodophyta). Global Change Biology 16: 2388-2398.

47. Veal C, Carmi M, Fine M, Hoegh-Guldberg O (2010) Increasing the accuracy of surface area estimation using single wax dipping of coral fragments. Coral Reefs 29: 893-897.

48. Schmidt C, Heinz P, Kucera M, Uthicke S (2011) Temperature-induced stress leads to bleaching in larger benthic foraminifera hosting endosymbiotic diatoms. Limnol Oceanogr 56: 1587-1602.

49. Nush EA (1980) Comparison of different methods for chlorophyll and phaeopigment determination. Arch Hydrobiol Beih 14: 14-36.

50. R Development Core Team (2014) R: A language and environment for statistical computing. Vienna, Austria: R Foundation for Statistical Computing.

51. Hintze J (2007) NCSS. Kaysville, Utah: NCSS, LCC.

52. Kleypas JA, Yates KK (2009) Coral Reefs and Ocean Acidification. Oceanography 22: 108-117.

53. Guinotte JM, Fabry VJ (2008) Ocean acidification and its potential effects on marine ecosystems. Annals of the New York Academy of Sciences 1134: 320-342.

54. Hendriks IE, Duarte CM, Álvarez M (2010) Vulnerability of marine biodiversity to ocean acidification: a meta-analysis. Estuarine, Coastal and Shelf Science 86: 157-164.

55. Pandolfi JM, Connolly SR, Marshall DJ, Cohen AL (2011) Projecting coral reef futures under global warming and ocean acidification. Science 333: 418-422.

56. Dunne RP (2010) Synergy or antagonism—interactions between stressors on coral reefs. Coral Reefs 29: 145-152.

57. Comeau S, Edmunds PJ, Spindel NB, Carpenter RC (2013) The responses of eight coral reef calcifiers to increasing partial pressure of CO_2 do not exhibit a tipping point. Limnol Oceanogr 58: 388-398.

58. Schneider K, Erez J (2006) The effect of carbonate chemistry on calcification and photosynthesis in the hermatypic coral *Acropora eurystoma*. Limnology and Oceanography: 1284-1293.

59. Marubini F, Ferrier-Pages C, Furla P, Allemand D (2008) Coral calcification responds to seawater acidification: a working hypothesis towards a physiological mechanism. Coral Reefs 27: 491-499.

60. Hoegh-Guldberg O, Mumby PJ, Hooten AJ, Steneck RS, Greenfield P, et al. (2007) Coral reefs under rapid climate change and ocean acidification. Science 318: 17371742.

61. Raven J, Caldeira K, Elderfield H, Hoegh-Guldberg O, Liss P, et al. (2005) Ocean acidification due to increasing atmospheric carbon dioxide.

62. Price NN, Hamilton SL, Tootell JS, Smith JE (2011) Species-specific consequences of ocean acidification for the calcareous tropical green algae *Halimeda*. Mar Ecol Prog Ser 440: 67-78.

63. Sinutok S, Hill R, Doblin MA, Wuhrer R, Ralph PJ (2011) Warmer more acidic conditions cause decreased productivity and calcification in subtropical coral reef sediment-dwelling calcifiers. Limnology and Oceanography 56: 1200-1212.

64. Glas MS, Fabricius KE, de Beer D, Uthicke S (2012) The O_2, pH and Ca^{2+} Microenvironment of Benthic Foraminifera in a High CO_2 World. PloS one 7: e50010.

65. Anthony KRN, Diaz-Pulido G, Verlinden N, Tilbrook B, Andersson AJ (2013) Benthic buffers and boosters of ocean acidification on coral reefs. Biogeosciences Discussions 10: 1831-1865.

66. Chisholm JRM (2000) Calcification by crustose coralline algae on the northern Great Barrier Reef, Australia. Limnology and Oceanography 45: 1476-1484.

67. Kleypas JA, Anthony K, Gattuso JP (2011) Coral reefs modify their seawater carbon chemistry–case study from a barrier reef (Moorea, French Polynesia). Global Change Biology 17: 3667-3678.

68. Chalker BE (1981) Simulating light-saturation curves for photosynthesis and calcification by reef-building corals. Marine Biology 63: 135-141.

69. Chalker BE, Taylor DL (1975) Light-enhanced calcification, and the role of oxidative phosphorylation in calcification of the coral *Acropora cervicornis*. Proceedings of the Royal Society of London Series B Biological Sciences 190: 323-331.

70. Crawley A, Kline DI, Dunn S, Anthony K, Dove S (2010) The effect of ocean acidification on symbiont photorespiration and productivity in *Acropora formosa*. Global Change Biology 16: 851-863.

71. Borowitzka MA, Larkum AWD (1976) Calcification in the green alga *Halimeda* III. The sources of inorganic carbon for photosynthesis and calcification and a model of the mechanism of calcification. Journal of Experimental Botany 27: 879-893.

72. Coles S, Jokiel P (1978) Synergistic effects of temperature, salinity and light on the hermatypic coral *Montipora verrucosa*. Marine Biology 49: 187-195.

73. Fabricius KE (2006) Effects of irradiance, flow, and colony pigmentation on the temperature microenvironment around corals: Implications for coral bleaching? Limnology and Oceanography 51: 30-37.

74. Comeau S, Carpenter RC, Edmunds PJ (2013) Effects of feeding and light intensity on the response of the coral *Porites rus* to ocean acidification. Marine Biology 160: 1127-1134.

75. Dufault AM, Ninokawa A, Bramanti L, Cumbo VR, Fan T-Y, et al. (2013) The role of light in mediating the effects of ocean acidification on coral calcification. The Journal of experimental biology 216: 1570-1577.

76. Suggett DJ, Dong LF, Lawson T, Lawrenz E, Torres L, et al. (2013) Light availability determines susceptibility of reef building corals to ocean acidification. Coral Reefs 32: 327-337.

Supplementrary Table 2 Mixed effect ANOVA's results for *A. millepora* and *H. opuntia*.

Response variable	Species	Source of variation	df	*F*-value	*p*-value
Growth	*A. millepora*	pCO_2	1	6.78	0.032*
		Light	1	64.98	< 0.001*
		pCO_2:Light	1	0.17	0.692
		Tank	8	2.44	0.037*
		Residual	29		
	H. opuntia	pCO_2	1	0.60	0.460
		Light	1	4.41	0.069
		pCO_2:Light	1	0.05	0.833
		Tank	8	1.71	0.231
		Residual	8		
Net calcification	*A. millepora*	pCO_2	1	4.78	0.060
		Light	1	25.95	0.001*
		pCO_2:Light	1	1.02	0.342
		Tank	8	1.09	0.434
		Residual	11		
	H. opuntia	pCO_2	1	3.59	0.095
		Light	1	1.09	0.328
		pCO_2:Light	1	0.31	0.594
		Tank	8	2.26	0.098
		Residual	12		
Light calcification	*A. millepora*	pCO_2	1	0.14	0.722
		Light	1	13.72	0.006*
		pCO_2:Light	1	0.18	0.684
		Tank	8	1.61	0.227
		Residual	11		
	H. opuntia	pCO_2	1	0.01	0.910
		Light	1	0.48	0.509
		pCO_2:Light	1	0.45	0.523
		Tank	8	2.14	0.113
		Residual	12		
Dark calcification	*A. millepora*	pCO_2	1	21.45	0.002*
		Light	1	21.36	0.002*
		pCO_2:Light	1	2.54	0.150
		Tank	8	0.41	0.892
		Residual	11		
	H. opuntia	pCO_2	1	57.53	< 0.001*
		Light	1	2.81	0.132
		pCO_2:Light	1	0.09	0.772

		Tank	8	4.15	0.014*
		Residual	12		
Gross	*A. millepora*	pCO_2	1	0.00	1.000
photosynthesis		Light	1	208.60	<0.001*
		pCO_2:Light	1	0.00	1.000
		Tank	8	1.07	0.441
		Residual	12		
	H. opuntia	pCO_2	1	3.51	0.098
		Light	1	38.76	0.003*
		pCO_2:Light	1	0.41	0.542
		Tank	8	1.53	0.252
		Residual	11		

Continuation **Table 2**

Response variable	Species	Source of variation	df	*F*-value	*p*-value
Net photosynthesis	*A. millepora*	pCO_2	1	0.00	1.000
		Light	1	267.99	< 0.001*
		pCO_2:Light	1	0.21	0.661
		Tank	8	0.77	0.636
		Residual	12		
	H. opuntia	pCO_2	1	3.08	0.117
		Light	1	35.85	< 0.001*
		pCO_2:Light	1	0.47	0.512
		Tank	8	1.40	0.297
		Residual	11		
Respiration	*A. millepora*	pCO_2	1	0.0	0.947
		Light	1	31.31	0.001*
		pCO_2:Light	1	0.23	0.646
		Tank	8	4.13	0.014*
		Residual	12		
	H. opuntia	pCO_2	1	2.85	0.130
		Light	1	25.38	0.001*
		pCO_2:Light	1	0.06	0.817
		Tank	8	3.89	0.020*
		Residual	11		
Chlorophyll *a*	*A. millepora*	pCO_2	1	0.34	0.577
		Light	1	2.23	0.174
		pCO_2:Light	1	0.02	0.895
		Tank	8	3.17	0.035*
		Residual	12		
	H. opuntia	pCO_2	1	1.09	0.326
		Light	1	6.69	0.032*
		pCO_2:Light	1	1.10	0.324
		Tank	8	1.16	0.398
		Residual	12		

7 - Ocean acidification alters the calcareous microstructure of the green macro-alga *Halimeda opuntia*

André Wizemann[1,*], Friedrich W. Meyer[1], Laurie C. Hofmann[2], Christian Wild[1,2] and, Hildegard Westphal[1,3]

[1] Leibniz Center for Tropical Marine Ecology (ZMT), Fahrenheitstraße 6, 28359 Bremen (Germany)

[2] University of Bremen, Faculty of Biology and Chemistry, Leobener Straße NW2, 28359 Bremen (Germany)

[3] University of Bremen, Faculty of Geosciences, Klagenfurter Straße 2, 28359 Bremen (Germany)

* Author to whom correspondence should be addressed; E-Mail: andre.wizemann@zmt-bremen.de; Tel.: +49-421-23800-132; Fax: +49-421-23800-30.

This manuscript is acceptes in Coral Reefs

Abstract

Decreases in seawater pH and carbonate saturation state (Ω) following the continuous increase in atmospheric CO_2 represent a process termed ocean acidification, which is predicted to become a main threat to marine calcifiers in the near future. Segmented, tropical, marine green macro-algae of the genus *Halimeda* form a calcareous skeleton that involves biotically-initiated and -induced calcification processes influenced by cell physiology. As *Halimeda* is an important habitat provider and major carbonate sediment producer in tropical shallow areas, alterations of these processes due to ocean acidification may cause changes in the skeletal microstructure that have major consequences for the alga and its environment, but related knowledge is scarce. This study used scanning electron microscopy to examine changes of the $CaCO_3$ segment microstructure of *Halimeda opuntia* specimens that had been exposed to artificially elevated seawater pCO_2 of ~650 µatm for 45 days. In spite of elevated seawater pCO_2, the calcification of needles, located at the former utricle walls, was not reduced as frequent initiation of new needle-shaped crystals was observed. Abundance of the needles was ~22 % μm^{-2} higher and needle crystal dimensions ~14 % longer. However, those needles were ~42 % thinner compared to the control treatment. Moreover, lifetime cementation of the segments

decreased under elevated seawater pCO_2 due to a loss in micro-anhedral carbonate as indicated by significantly thinner calcified rims of central utricles (35 - 173 % compared to the control treatment). Decreased micro-anhedral carbonate suggests that seawater within the inter-utricular space becomes $CaCO_3$ undersaturated ($\Omega < 1$) during nighttime under conditions of elevated seawater pCO_2 thereby favoring $CaCO_3$ dissolution over micro-anhedral carbonate accretion. Less cemented segments of *H. opuntia* may impair the environmental success of the alga, its carbonate sediment contribution, and the temporal storage of atmospheric CO_2 within *Halimeda*-derived sediments.

Introduction

Atmospheric greenhouse gases, such as CO_2, rapidly equilibrate in the ocean. An increase in the atmospheric CO_2 concentration thus leads to an increase in the CO_2 concentration of seawater, causing a process known as ocean acidification (Caldeira and Wikett 2003). Progressive ocean acidification reduces seawater pH and shifts seawater carbon chemistry, thereby decreasing seawater carbonate ion (CO_3^{2-}) saturation (Feely et al. 2004; Orr et al. 2005). The seawater carbonate saturation state (Ω) is an important parameter for the formation of calcium carbonate structures, as it determines whether calcium carbonate ($CaCO_3$) precipitation or dissolution is favored (Kleypas et al. 1999). Calcifying organisms in the ocean thus may face severe consequences when the carbonate saturation state is lowered (Doney et al. 2009). However, calcification processes of most marine organisms are not well understood. For example, elevated seawater pCO_2 experiments on the calcification of marine micro-algae such as coccolithophores revealed species-specific responses of $CaCO_3$ structure formation (Riebesell 2004; Langer et al. 2006). Generally, $CaCO_3$ biomineralization in most, if not all, marine organisms is an enzyme-driven process, whereby the use of bicarbonate (HCO_3^-) is predominant (Bonucci 2007; Weiss and Marin 2008; Jury et al. 2010). As an increase in seawater pCO_2 shifts the equilibrium towards a higher availability of HCO_3^-, $CaCO_3$ biomineralization may be enhanced by moderate ocean acidification in organisms where the ionic composition of the extracellular calcifying matrix or fluid is influenced by seawater. In contrast, abiotic $CaCO_3$ precipitation is negatively affected by elevation of seawater pCO_2 as seawater $CaCO_3$ saturation is consequently reduced (e.g., Morse et al. 2007; Stanley 2008).

Tropical marine calcifying green macro-algae of the genus *Halimeda* likely exhibit biotic induction of calcification, as external carbonic anhydrase activity is present (Borowitzka and Larkum 1976; Hofmann et al. 2014). Nevertheless, the formation of the algal calcareous skeleton of the $CaCO_3$ polymorph aragonite is also influenced by its physiology, which causes diurnal shifts in the seawater carbon chemistry in the inter-utricular space (Macintyre and Reid 1995; De Beer and Larkum 2001). Thereby, the extracellular calcareous microstructure is formed in semi-enclosed open spaces in-between the algal cells, i.e., tube-like filaments called utricles. The open space in between these

utricles is thus referred to as inter-utricular space. The formation of the $CaCO_3$ segment microstructure involves several time-dependent steps described by Macintyre and Reid (1995) and refined by Wizemann et al. (2014). The occurrence of different skeletal features (i.e., primary needles, micro-anhedral carbonate, secondary needles) is the result of complex interactions between physiological processes (i.e., photosynthesis and metabolism) and environmental parameters (e.g., seawater carbon chemistry, light availability, temperature).

With the formation of the extracellular calcareous skeleton likely driven by a combination of biotic and abiotic calcification processes, influenced by both cell physiology and seawater parameters, *Halimeda* is a model organism for studying the effects of ocean acidification on calcification in its entirety. Thus, the distinct formation of the calcareous skeletal microstructure and the importance of the genus *Halimeda* as a major carbonate sediment producer and bioherm builder have lead to several studies that assessed effects of ocean acidification on its calcification (Robbins et al. 2009; Ries et al. 2009, Ries 2011; Sinutok et al. 2011, 2012; Price et al. 2011; Hofmann et al. 2014). Whereas most studies have focused on the physiological response and the subsequent change of total calcification (total algal $CaCO_3$ content), little is known regarding alterations of the skeletal microstructure of *Halimeda* due to shifts in seawater carbon chemistry. The focus of this study is to identify alterations of the internal skeletal $CaCO_3$ microstructure of the species *Halimeda opuntia* that result from an elevation of seawater pCO_2.

Study organism

Halimeda opuntia (Lamouroux 1816) is a cosmopolitan marine macro-alga of tropical shallow seas. Macro-algae of the genus *Halimeda* exhibit a segmented, branched growth habit whereby the algae form calcareous segments of the $CaCO_3$ polymorph aragonite (Hillis-Colinvaux 1980; Macintyre and Reid 1995; Stanley et al. 2010; Fig. 1a). Because of a rapid growth rate of up to one segment per day on each branch, the genus *Halimeda* is one important $CaCO_3$ sediment producer in tropical coral reef environments (Wefer 1980; Drew 1983; Hine et al. 1988; Multer 1988; Freile et al. 1995; Rees et al. 2007; Wienberg et al. 2010). Within the genus of *Halimeda* the species *H. opuntia* morphologically defines the lineage Opuntia (Hillis 2001; Verbruggen and Kooistra 2004). Generally, taxa of this lineage are characterized by the absence of a bulbous holdfast, but possess thin root-like filaments with which they are able to attach primarily to hard substrates. Thus, *Halimeda* species of the lineage Opuntia are often found in coral reef environments (Hillis-Colinvaux 1980; Johns and Moore 1988).

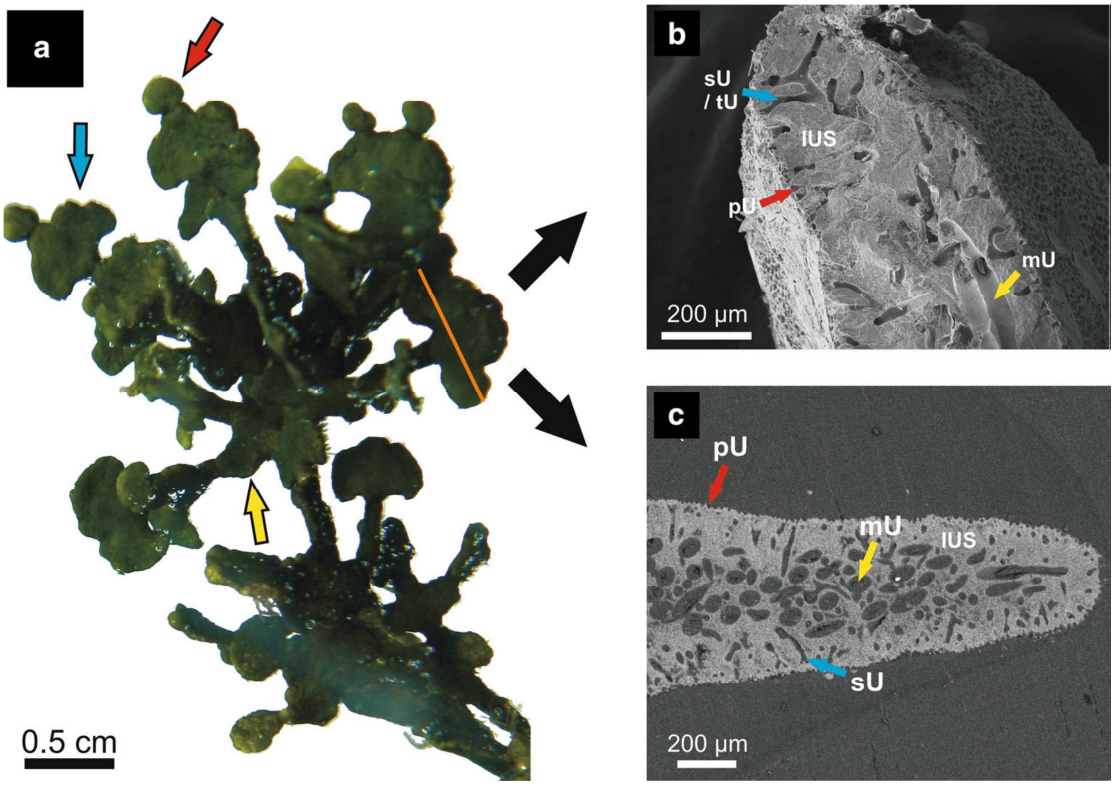

Figure 1 The segmented green macro-alga *Halimeda opuntia*. **(a)** Growing alga with young segments (< 2 d; red arrow), mature apical segments (2 – 7 d; blue arrow) and mature mid-growth segments (> 7 d; yellow arrow). The orange line indicates the cutting plane of a segment when prepared for scanning electron microscope (SEM) analyses. **(b)** SEM image (via SE) of a stub-sample from a segment cut in the middle plain. **(c)** SEM image (via BSE) of a thin-section from a segment cut in the middle plane.

U = utricle (p = primary, s = secondary, t = tertiary, m = medullary); IUS = inter-utricular space.

Material and methods

Experimental setup

Macro-algae of the species *H. opuntia* from reefs off Cebu (Philippines, purchased from Marina Fauna Inc.®) were brought to the marine experimental facility of the Leibniz-Center for Tropical Marine Ecology (ZMT) in Bremen (Germany). The algae were acclimatized for one month to laboratory seawater conditions (approx. temperature 27 °C, salinity 35 PSU, light regime 150 µmol photons m^{-2} s^{-1}). After acclimatization, the algae were placed into mesocosms (265-l) with carbonate live sand (Ocean Direct®) as substrate. A total of five algae were placed in each of six mesocosms. The mesocosms were fully closed (however with an open water-filtering system) and equipped with an electronically controlled gas-mixing system (HTK® Hamburg; pure CO_2 provided by Linde® Gas) that premixes air with pure CO_2 to adjust the pCO_2 concentration of the outflow air. On the gas-mix

system, the pCO_2 level of the outflow air was set to 400 ppm (ambient air pCO_2) for three mesocosms of the control treatment and to max output provided by the system of > 1500 ppm (elevated air pCO_2) for the three mesocosms of the high pCO_2 treatment. The premixed air was directly bubbled into the mesocosms; no negative feedback mechanism regarding the actual equilibrated seawater pCO_2 was implemented (i.e., no stat-system was used). T5 light bulbs switched in a 12/12 h day/night cycle provided a moderate light-regime of 150 µmol photons m^{-2} s^{-1}. Artificial seawater (SW) was used both for acclimatization and the experiment in the mesocosms.

Artificial seawater preparation

The artificial SW was prepared in a 35,000-l tank with tap water pre-filtered and UV-sterilized using reverse-osmosis purification technique prior to filling the mesocosms. The salinity of the water in the tank was then adjusted to 35 (PSU). As the sea salt (custom made; Electronic Supplementary Materials (ESM) Table S1) that was used for artificial seawater preparation exhibited an unnatural high total alkalinity (A_T) of > 3000 µmol kg^{-1}SW, the A_T of the artificial seawater in the tank was initially reduced to 2200 ± 100 µmol kg^{-1}SW with HCl (1N) i.e., to an A_T range typical for tropical surface ocean waters in the Pacific region (e.g., Takahashi et al. 1981). The water was given adequate residual time of more than two weeks in the 35,000-l tank for proton/pH equilibration through outgassing of CO_2 prior to the start of the experiment (Riebesell et al. 2010).

Measurements of chemical and physical seawater parameters

During the experiment, seawater A_T of the mesocosms was measured twice per week with an automated titrator (SI Analytics®, TitronLine Alpha Plus) with an A_T standard provided by A.G. Dickson (batch 111) as certified reference material (Dickson et al. 2003, 2007). Seawater A_T in the mesocosms was re-adjusted to 2200 ± 100 µmol kg^{-1} SW by the addition of $NaHCO_3$ solution with a peristaltic pump during the experiment, when required. Temperature (T), salinity (S), and pH (NBS-scale) were monitored multiple times a day, during daylight, with a multi-probe (WTW® Multi 3410, SenTix® ORP 900 pH probe, TetraCon® 925 conductivity probe). The pH probe was calibrated using two-point calibration with standard NBS buffer solutions (WTW®) for pH 4.01 and 7.

Seawater carbon chemistry

Measured seawater parameters (T, S, A_T, and pH_{NBS}) were used to calculate carbon chemistry and the respective $CaCO_3$ saturation state (Ω) of the seawater in the mesocosms with the program CO_2SYS (Pierrot et al. 2006; Table 1). Based on calculations, seawater in the three mesocosms of the control treatment and the three mesocosms of the high pCO_2 treatment reached a mean equilibrated pCO_2 in the range of 400 ± 50 µatm (ambient pCO_2; daylight) and 650 ± 50 µatm (elevated pCO_2; daylight), respectively. Natural fluctuations of the equilibrated seawater pCO_2 and seawater carbon chemistry are likely due to outgassing of CO_2 (10 % water exchange per week and open water-filtering system), photosynthesis (daytime) / respiration (nighttime) cycle of the mesocosm community (sediment, algae, epibionts) and absence of a negative feedback mechanism to the gas-mix system. Calculated seawater pCO_2 and carbon species concentrations for the seawater in the mesocosms may be slightly off, as pH_{NBS} measurements used for calculations of seawater carbon chemistry are especially subject to drift (e.g., Riebesell et al. 2010). Direct measurements of the equilibrated seawater pCO_2 were not conducted.

Sampling

The algae were collected from the mesocosms after 45 d of growth, briefly rinsed with distilled water, and oven-dried at 35 °C for 48 h. Afterwards, young segments (< 2 d; n = 9), well developed apical segments (2 – 7 d; n = 9), and mature mid-growth segments (> 7 d; n = 9) were collected randomly from algae in each mesocosm for further analyses (Fig. 1a; ESM Table S2). The approximate segment age was visually determined from growing "branches" of the algae as illustrated in Fig. 1a. Due to the experimental duration (45 d) and the visually observed segment growth rate of the algae (2 - 3 segments per week on each branch), sampling of older, preexisting segments was excluded. Segments were not stained, as staining may affect algae growth performance and probably disturb the mesocosm microbial sediments and epibiont communities, which would hamper the mesocosm approach (i.e., natural shifts in seawater carbon chemistry due to community respiration and photosynthesis; cf. alizarin and corals, Dodge et al. 1984). Additionally, all mature segments sampled (2 – 7 d and > 7 d) showed the sun-leaf segment morphotype of *H. opuntia* (i.e., "butterfly-" or "fan-like" segment shape; cf. Fig. 1a), as light intensity (i.e., photosynthesis vs. respiration rate) influences the segments grade in $CaCO_3$ density (i.e., micro-anhedral carbonate content; Macintyre and Reid 1995; pers. obs.).

Sample preparation for SEM analyses

Stub samples

Segments were cut in the middle plane with a razor blade and mounted on a stub with conductive glue, fractured surface facing upwards (Fig. 1a). They were gold-sputtered and analyzed with a scanning electron microscope (TESCAN® VEGA3 XMU) with the secondary electron (SE) detector at 2.5, 6, and 10 keV (Fig. 1b).

Thin-sections

Segments were embedded in epoxy and cut in the middle plane. Afterwards they were polished to ~35 µm, gold-sputtered, and analyzed with an SEM with the detector for back-scattered electrons (BSE) at 10 keV (Fig. 1c). Organics were not removed in order to allow identification of internal microstructural features. Organics were lost in some cases due to the preparation technique.

Microstructural analyses

Primary needle abundance and dimensions

Primary needle abundance and dimensions within central medullary utricles were obtained from SEM images with ImageJ. To measure needle abundance, a 100-μm^2 area was defined randomly and further subdivided into 16 squares of 6.25 μm^2 each. All needles within the squares were point-counted and the mean crystal density per μm^2 was calculated. This was carried out for three independent segments of each mesocosm from the control treatment and the high pCO_2 treatment. Several medullary utricles (> 5) within each segment were screened to ensure that areas counted showed needle densities representative of the whole segment.

To obtain needle dimension, the length and width were measured for 20 randomly and independently selected primary needles of central medullary utricles within a randomly selected area of 200 μm^2 of four independent apical segments (= different alga and/or mesocosm) from the control treatment and the high pCO_2 treatment. Mean values and standard deviations were calculated. Only needles were measured whose extents and especially termini (for width determination) were mostly visible in the SEM images. In case crystals exhibited a polygonal shape, the longer axis of the crystal blunt end (terminus) was measured to determine needle width. However, the line of view to determine crystal extents on the SEM images often was not parallel due to individual needle growth direction; thus measurements of crystal dimension are biased to some degree. To make sure that other medullary utricles showed a similar crystal habit, numerous areas of each segment were screened (> 5).

Thickness of micro-anhedral carbonate utricle rims

The thickness of micro-anhedral carbonate rims around central medullary utricles from three segments at three consecutive maturation stages (< 2 d, 2 – 7 d, > 7 d; Fig. 1a; ESM Table S1) from both treatments was measured from SEM images of thin-sections using ImageJ. Therefore, ten measurements distributed randomly but radially around each utricle were obtained. Visual screening of numerous utricles (> 5) of each segment ensured that representative areas were chosen.

Statistical analyses

All statistical calculations were carried out with the program Sigma Plot® from raw measurement data. Between-group differences in primary needle abundance per μm^2 between control treatment and high pCO_2 treatment algae were tested using a one-way ANOVA. Additionally, a pairwise multi comparison analysis (Holm-Sidak method) was run to analyze significant in-group differences between the control treatment and the high pCO_2 treatment groups. To check for significant differences in primary needle width and length and to compare the thickness of MAC utricle rims of all stages of segment maturation (< 2 d, 2 – 7 d, > 7 d; Fig. 1a) between the control treatment and the high pCO_2 treatment, a paired t-test was done. As the normality test failed with the data obtained from the early segment stages (< 2 d) a Wilcoxon-Signed rank test was performed for this group instead.

Table 1 Measured seawater (SW) parameters (mean ± SD) and calculated SW carbon chemistry (via CO_2SYS; Pierrot et al. 2006) of control treatment (ambient pCO_2) and high pCO_2 treatment (elevated pCO_2) mesocosms (n = 3). Temperature (T), salinity (S), pH_{NBS} and, total alkalinity (A_T) were measured (at daytime). Carbon chemistry was calculated using K1, K2 constants from Mehrbach et al. (1973) refit by Dickson and Millero (1987). A_T and carbon species are given in µmol kg^{-1}SW, seawater pCO_2 in µatm. Ω = calculated $CaCO_3$ saturation state (arag = aragonite; cal = calcite).

Mesocosm	T (C°)	S (PSU)	pH_{NBS}	A_T	pCO_2	CO_2	HCO_3^-	CO_3^{2-}	Ω_{arag}	Ω_{cal}
1 (ambient)	25.9 ± 0.4	35.6 ± 0.2	8.15 ± 0.04	2053 ± 125	385 ± 28	11 ± 0.5	1587± 65	185 ± 35	2.9 ± 0.4	4.4 ± 0.6
2 (ambient)	26.4 ± 0.4	35.3 ± 0.1	8.15 ± 0.04	2287 ± 160	434 ± 15	12 ± 0.6	1775 ± 92	208 ± 31	3.3 ± 0.5	5.0 ± 0.7
3 (ambient)	26.3 ± 0.4	35.1 ± 0.5	8.15 ± 0.02	2208 ± 54	418 ± 15	12 ± 0.3	1714 ± 19	199 ± 15	3.2 ± 0.2	4.8 ± 0.3
1 (elevated)	26.3 ± 0.3	35.4 ± 0.3	8.01 ± 0.04	2159 ± 121	600 ± 31	16 ± 0.5	1782 ± 73	152 ± 22	2.4 ± 0.3	3.6 ± 0.5
2 (elevated)	26.2 ± 0.2	35.3 ± 0.2	7.98 ± 0.01	2119 ± 143	638 ± 18	17 ± 0.5	1770 ± 114	140 ± 14	2.2 ± 0.2	3.4 ± 0.4
3 (elevated)	26.2 ± 0.1	35.6 ± 0.3	7.97 ±0.03	2280 ± 79	705 ± 34	20 ± 0.3	1914± 44	149 ± 15	2.4 ± 0.3	3.6 ± 0.4

Results

The terms used for the description of the $CaCO_3$ segment microstructure follow Macintyre and Reid (1995) as refined by Wizemann et al. (2014).

Primary needles

Primary needles form directly at the external cell walls of utricles facing into the inter-utricular space and are the first $CaCO_3$ precipitated by the alga. They are up to 5 µm in length, often exhibit smooth edges with a roundish tip when newly formed, and may completely fill-up the primary inter-utricular space of younger segments.

In apical segments grown under ambient seawater pCO_2, the inter-utricular space was densely filled with $CaCO_3$ (Fig. 2a). Especially within the primary inter-utricular space, but also to some extent within the secondary inter-utricular space, primary needles were abundant and the dominant needle type (Fig. 2b, c, d). In apical segments from algae of the high pCO_2 treatment, the observation of primary needles was limited to an appearance on the utricle walls and partially to the primary inter-utricular space (Fig. 3b, c). In these segments the $CaCO_3$ density of the inter-utricular space was not as pronounced as in segments of the control treatment (cf. Fig. 2a and 3a). Under elevated seawater pCO_2, apical segments are characterized by open inter-utricular space (Fig. 3b, d). On primary utricle walls of young segments (< 2 d) grown under elevated pCO_2, a high abundance and density of $CaCO_3$ nuclei was observed (ESM Fig. S2a).

Primary needle abundance and dimensions

Apical segments of the control treatment and the high pCO_2 treatment showed differences in primary needle abundance and dimensions (width and length; Fig. 4a, b and ESM Fig. S1a, b). In segments from the high pCO_2 treatment, primary needle abundance measured per μm^2 was significantly higher (22 ± 7 %; $p < 0.001$; ESM Table S3). In segments of the high pCO_2 treatment, primary needles investigated were 42 % (± 21 %) thinner and 14 % (± 6 %) longer (paired t-test, $p < 0.001$ and $p < 0.05$, respectively; Fig. 4a, b; ESM Table S3). There was no significant in-group difference of needle abundance (pairwise multiple comparison test, $p > 0.05$) within the control treatment or the high pCO_2 treatment group.

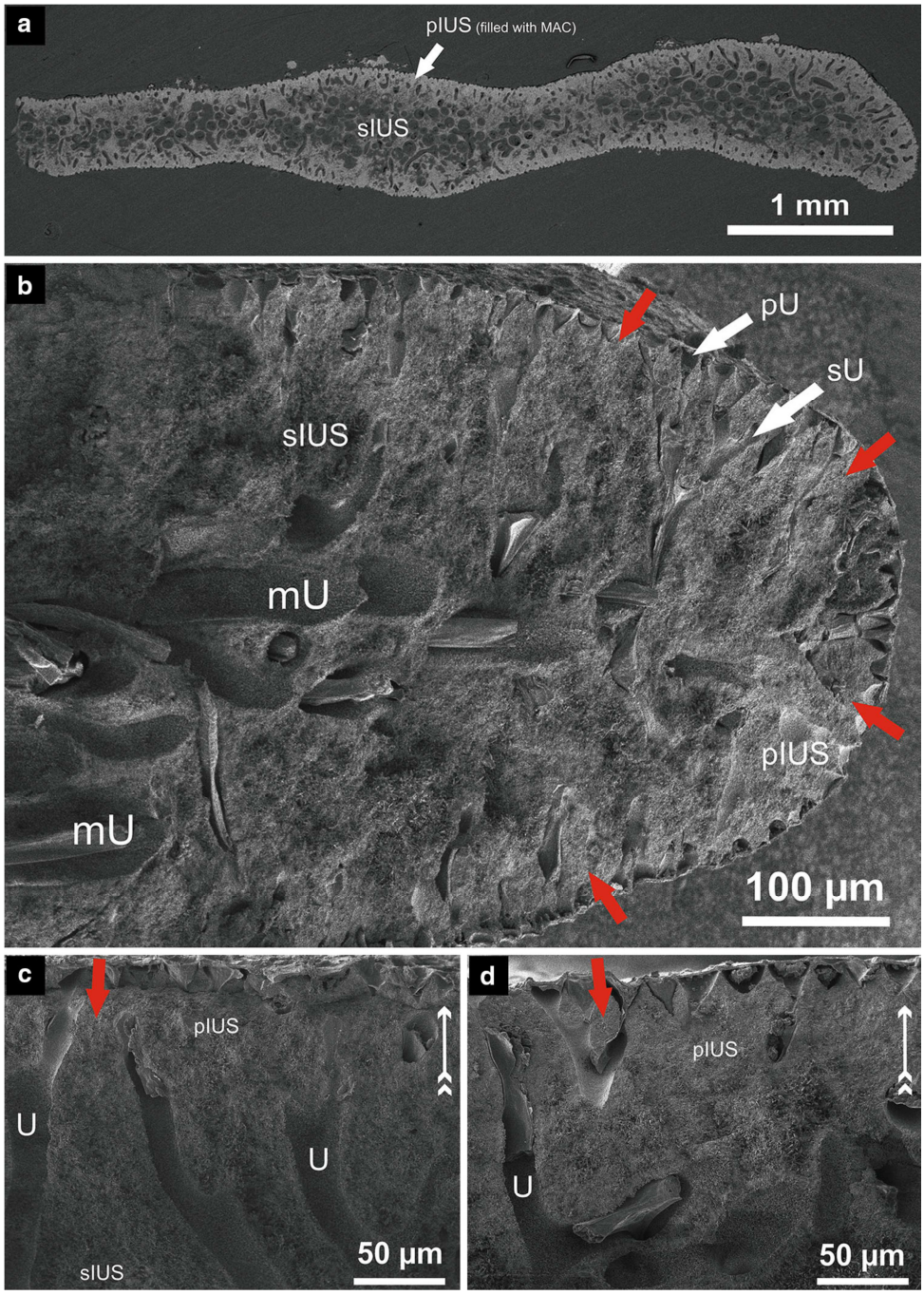

Figure 2 SEM-analyses of the $CaCO_3$ microstructure of an apical segment at ambient seawater pCO_2 (control treatment). **(a)** Cross-section overview of the microstructure of a complete segment (thin-section via BSE). **(b)** Magnification from the tip of a segment showing the location of inter-utricular space (IUS) and utricles (U). Note the early stage of micro-anhedral carbonate formation (e.g., red arrows). **(c + d)** Detailed analyses of the primary inter-utricular space (pIUS) to illustrate stage of micro-anhedral carbonate density (= primary cementation; e.g., red arrows). White arrows indicate direction to segment surface.

U = utricle (p = primary, s = secondary, m = medullary); IUS = inter-utricular space (p = primary, s = secondary).

Primary cementation (micro-anhedral carbonate formation)

The grade of segment lifetime cementation (i.e., primary cementation) that is caused by the formation of MAC is an indicator for the overall calcification of the alga (Wizemann et al. 2014). Thus, the more micro-anhedral carbonate that is formed, the more heavily calcified is the carbonate skeleton of the algal segment. Generally, micro-anhedral carbonate is most pronounced in the primary inter-utricular space and at the central utricle rims. As the name indicates, micro-anhedral $CaCO_3$ crystals are micron-sized and of anhedral shape.

The primary inter-utricular space of apical segments from the control treatment was completely filled with micro-anhedral carbonate (Fig. 2a, b). The secondary inter-utricular space of these segments was partly filled with micro-anhedral carbonate (Fig. 2b, c, d). Micro-anhedral carbonate within the inter-utricular space of apical segments grown under elevated seawater pCO_2 was less developed than in apical segments from the control (Fig. 3a, b). The secondary inter-utricular space was not densely filled with $CaCO_3$ in segments of algae grown under elevated seawater pCO_2 (Fig. 3c, d).

Growth-time series

In a growth-time series, segments sampled in consecutive order from a "branch" in the control treatment seemed to gain overall density in $CaCO_3$ with increasing segment age (Fig. 5a-f). In segments from the high pCO_2 treatment, the secondary inter-utricular space was gradually less filled with micro-anhedral carbonate equivalent to an increase in segment size and thus increase in segment age (Fig. 5g-l).

Cementation of central utricle rims (Growth-time series)

Central medullary utricles (mU) within the secondary inter-utricular space of segments from the control treatment showed thick $CaCO_3$ rims of micro-anhedral carbonate. The rim of micro-anhedral carbonate gains thickness with segment age, as seen in SEM images of the growth-time series (Fig. 5a, c, e). The micro-anhedral carbonate rims of central medullary utricles within the secondary inter-utricular space in segments of the high pCO_2 treatment were thinner when segments of similar age were compared (Fig. 5). In young segments (< 2 d) micro-anhedral carbonate thickness of utricle rims from segments in the control treatment was 35 % ± 6 % higher than in segments from the high pCO_2 treatment (Wilcoxon-Signed rank test, $p < 0.05$). In older, mature segments (2 – 7 d, > 7 d), the difference in micro-anhedral carbonate thickness was significant (paired t-test, $p < 0.001$). The micro-anhedral carbonate utricle rim was 152 % ± 12 % (2 – 7 d) to 173 % ± 27 % (> 7 d) thicker in mature segments from the control treatment than from the high pCO_2 treatment. Medullary utricle rims of

mature segments from the high pCO_2 treatment did not show thicker layers of micro-anhedral carbonate than young apical segments (Fig. 5g, i, k).

Cementation of segment rims (Growth-time series)

In segments from the control treatment, segment rims of micro-anhedral carbonate seemed to extend in dimension with proceeding segment maturation (Fig. 5b, d, f). Additionally, an extensive area of the secondary inter-utricular space was filled with micro-anhedral carbonate in mature mid-growth segments (Fig. 5f). In segments of the treatment, the micro-anhedral carbonate rim was well developed in young segments (< 2 d; Fig. 5h), but did not seem to increase in its extent when compared to apical (2 – 7 d) and mature mid-growth segments (> 7 d; Fig. 5j, l).

Secondary needles

Secondary needles are long euhedral orthorhombic $CaCO_3$ crystals (typically of more than 20 µm length) that face and grow into the inner inter-utricular space.

Within the inter-utricular space of segments from the control treatment, secondary needles were less abundant, shorter, and only observed within the secondary inter-utricular space (Fig. 2b, c, d). In apical segments from the high pCO_2 treatment, a high abundance of long secondary needles was observed within the secondary inter-utricular space (Fig. 3b). Moreover, secondary needles were also observed within parts of the primary inter-utricular space (Fig. 3d). In some cases, secondary needles were found directly on top of primary needles; no layer of micro-anhedral carbonate was visible (ESM Fig. S3a). Additionally, thin-sections showed that secondary needles form a major part of the calcified skeleton of segments from the high pCO_2 treatment (ESM Fig. S3b).

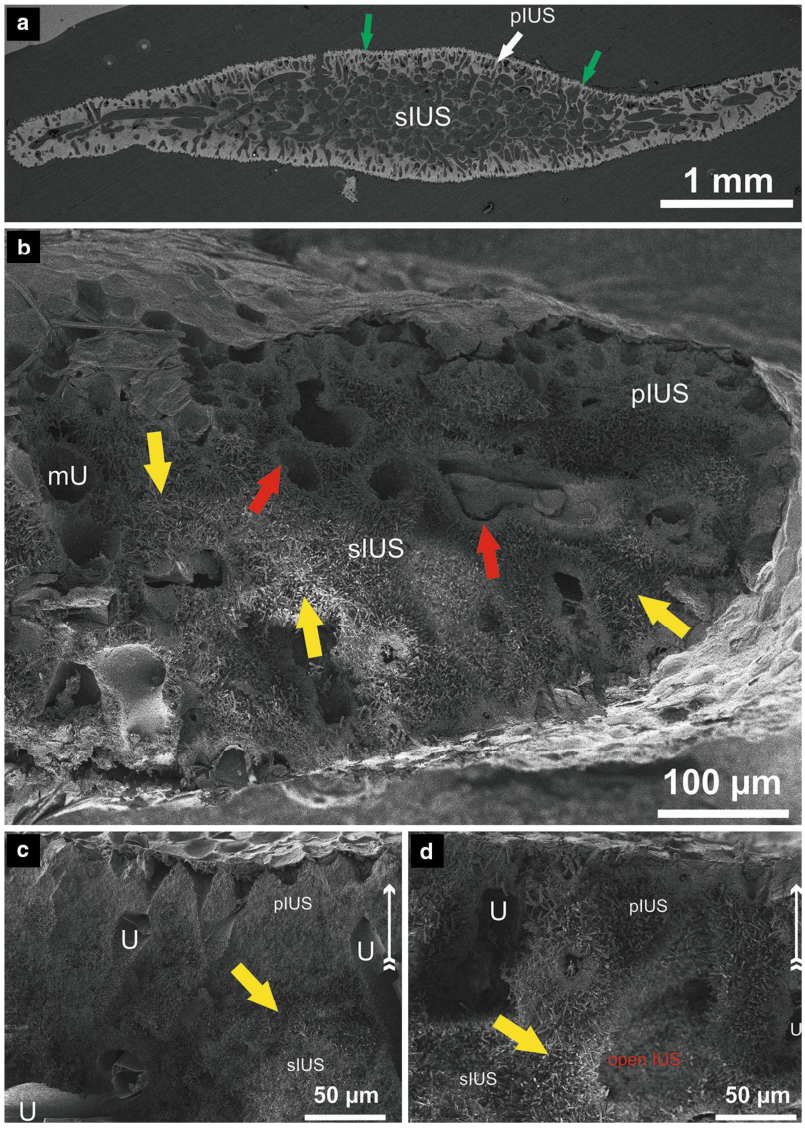

Figure 3 SEM-analyses of the $CaCO_3$ microstructure of an apical segment under elevated seawater pCO_2 (high pCO_2 treatment). **(a)** Cross-section overview of the microstructure of a complete segment (thin-section via BSE). Note the thin calcified segment rim (green arrows; cf. Fig. 2a) **(b)** Magnification from the tip of a segment showing the location of utricles (U) and inter-utricular space (IUS). Note that micro-anhedral carbonate (MAC) is mostly limited to utricle rims (e.g., red arrows) and the high abundance of secondary needles (e.g., yellow arrows; cf. Fig. 2b) in the inter-utricular space. **(c + d)** Detailed analyses of the primary inter-utricular space (pIUS) illustrate a lack of micro-anhedral carbonate density (= primary cementation; cf., Fig. 2c + d). Note the high abundance of secondary needles within the primary inter-utricular space (pIUS) and the open space within the secondary inter-utricular space (sIUS) observed in **(d)** (e.g., yellow arrows). White arrows indicate direction to segment surface.

U = utricle (m = medullary); IUS = inter-utricular space (p = primary, s = secondary).

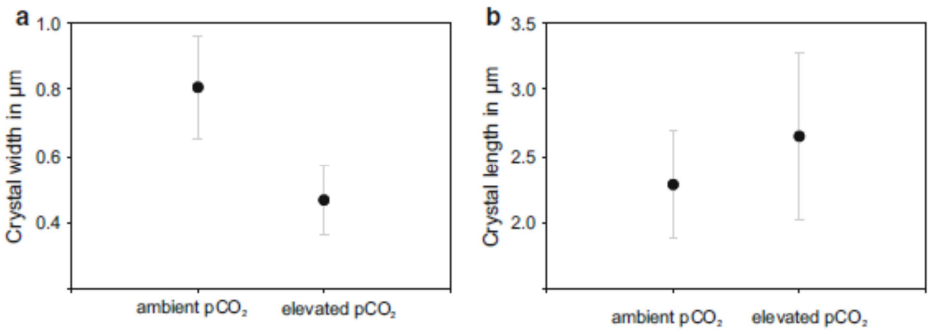

Figure 4 Dimensions of primary needle single crystals that formed on the external cell wall (organics lost) of medullary utricles of segments from the control treatment (ambient pCO_2) and the high pCO_2 treatment (elevated pCO_2). Shown in **(a)** is the mean (± SD) crystal width and in **(b)** the mean (± SD) crystal length.

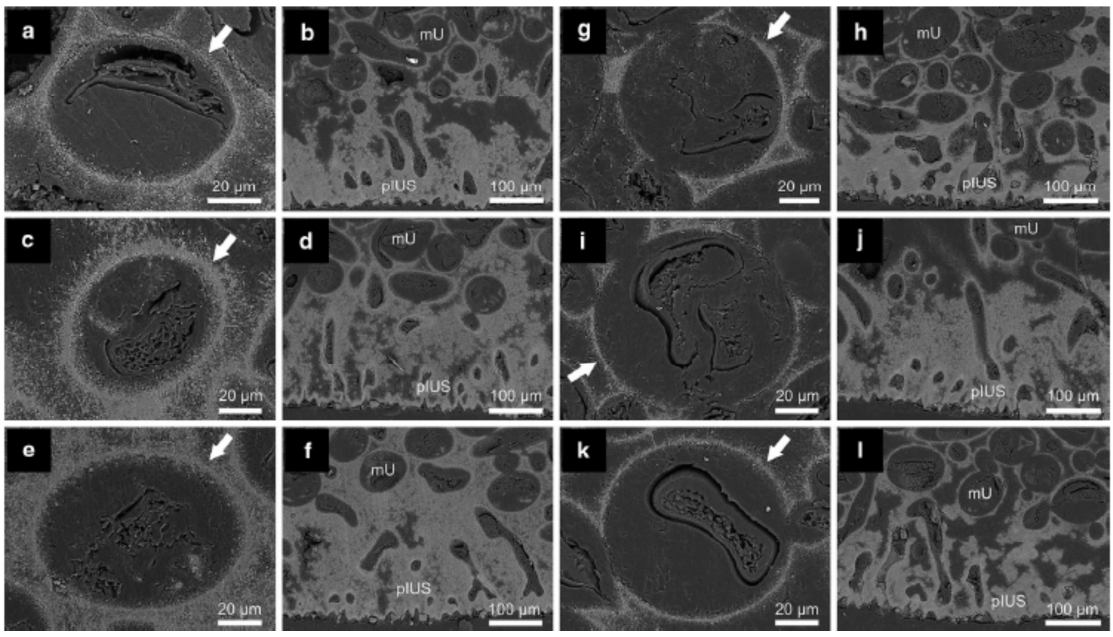

Figure 5 SEM thin-section analyses (via BSE) of segments sampled in consecutive order from a "branch" grown under **(a-f)** ambient seawater pCO_2 and **(g-l)** elevated seawater pCO_2. Segment age for **(a** and **b, g** and **h)** < 2 d, **(c** and **d, i** and **j)** 2 – 7 d, **(e** and **f, k** and **l)** > 7 d (cf., ESM Table S2). **(a, c, e)** Micro-anhedral carbonate rims of central medullary utricles (mU) from segments of increasing maturation and **(b, d, f)** corresponding primary inter-utricular space (pIUS). Same order for **(g, i, k)** and **(h, j, l)** for the elevated seawater pCO_2 respectively. White arrows in **(a, c, e, g, i**, **k)** indicate micro-anhedral carbonate rims of medullary utricles. Note the decreasing $CaCO_3$ density of the inter-utricular space and the low accumulation of micro-anhedral carbonate at the rims of utricles with increasing segment maturation as shown in segments grown under elevated seawater pCO_2 **(g-l)**.

mU = medullary utricle; pIUS = primary inter-utricular space.

Discussion

Strong shifts in seawater pH and $CaCO_3$ saturation (Ω) naturally occur within the inter-utricular space as a result of physiological day and night cycles of the algal cell metabolism and influence the formation of the segment $CaCO_3$ microstructure (Macintyre and Reid 1995; De Beer and Larkum 2001). In the following paragraphs, the additional effect of elevated seawater pCO_2 on the development of each microstructural feature in the segment is discussed separately.

Primary calcification under elevated seawater pCO_2

Our observations of a high abundance of small, thin primary needles and numerous nuclei within the organic matrix of a primary utricle are consistent with previously reported effects of elevated seawater pCO_2 on *Halimeda* (Robbins et al. 2009; Sinutok et al. 2011). Primary calcification may be driven by organic matrix components and involve external carbonic anhydrase activity (Wizemann et al. 2014). Hofmann et al. (2014) showed that an increase in seawater pCO_2 leads to an elevation of external carbonic anhydrase activity in *H. opuntia*. If the product of external carbonic anhydrase is HCO_3^- that is used by calcifying proteins in $CaCO_3$ biomineralization (Bonucci 2007; Weiss and Marin 2008; Bertucci et al. 2013), it is likely that primary needle formation is actively enhanced. Additionally, the fast removal of CO_2 from the inter-utricular space through external carbonic anhydrase activity elevates the seawater $CaCO_3$ saturation (Ω) and the pH sufficiently to sustain daytime calcification under moderately elevated seawater pCO_2.

Primary cementation (micro-anhedral carbonate formation) under elevated seawater pCO_2

Less micro-anhedral carbonate was observed within the inter-utricular space of apical and mature segments, as well as along utricle walls of segments grown under elevated seawater pCO_2 when compared to segments from the control treatment. Primary needle recrystallization and $CaCO_3$ re-precipitation that both cause micro-anhedral carbonate formation are most likely initiated and driven by exhaled respiratory CO_2 (Macintyre and Reid 1995; Wizemann et al. 2014). Micro-anhedral carbonate formation may strongly depend on the carbonate saturation state (Ω) of the seawater that enters the inter-utricular space. Presented results suggest that $CaCO_3$ oversaturation ($\Omega_{arag} > 1$) necessary for significant nighttime micro-anhedral carbonate accretion is no longer reached when seawater pCO_2 is elevated > 650 µatm (cf., Vogel et al. 2015a, b). Thereby, the onset of $CaCO_3$ dissolution likely is caused by seawater $CaCO_3$ undersaturation ($\Omega_{arag} < 1$) inside the inter-utricular space, due to the fact that the combination of seawater pCO_2 and CO_2 from metabolism determines the $CaCO_3$ saturation state within the inter-utricular space. Additionally, species-specific respiratory

activity of *H. opuntia* is significantly higher than of other *Halimeda* species (ESM Table S4). That may cause onset of $CaCO_3$ dissolution and negative effects on micro-anhedral carbonate formation in *H. opuntia* even at moderately elevated seawater pCO_2. However, the extent to which seawater pCO_2 affects micro-anhedral carbonate formation depends on the respiratory activity of each individual alga and naturally differs under varying environmental conditions (e.g., water depth / light regime) and with other environmental stressors (e.g., seawater temperature). Furthermore, endolithic microbes are likely present within the inter-utricular space and the $CaCO_3$ skeletal structure (Macintyre and Reid 1995; Reyes-Nivia et al. 2014). These most certainly play an additional role in the add-up of metabolic derived CO_2 and thus are an important steering factor for micro-anhedral carbonate formation to consider. Thus, a very complex multifactorial system influences the seawater $CaCO_3$ saturation (Ω) within the inter-utricular space that determines if micro-anhedral carbonate accretion or $CaCO_3$ dissolution occurs.

Secondary calcification under elevated seawater pCO_2

High abundance of euhedral secondary needles was observed within the inter-utricular space in apical segments grown under elevated seawater pCO_2. Comparison between secondary needle dimensions in apical segments from both treatments indicates that under elevated seawater pCO_2 secondary needles are larger in size. Even so, this is likely caused by higher availability of open space within the inter-utricular space under elevated seawater pCO_2; it also emphasizes that despite elevated seawater pCO_2 the $CaCO_3$ saturation of the seawater in the inter-utricular space is sufficient for crystallization during photosynthesis. In some cases, secondary needles were observed initiating on top of primary needles without a micro-anhedral carbonate layer present, which deviates from identified calcification patterns of different *Halimeda* species that grew in unmodified seawater carbon chemistry (e.g., Weiner and Lowenstam 1986; Multer 1988; Macintyre and Reid 1995; Wizemann et al. 2014). However, discussed impacts of elevated seawater pCO_2 on micro-anhedral carbonate formation may explain this observation.

Alteration of the *Halimeda* segment $CaCO_3$ microstructure under ocean acidification

Wizemann et al. (2014) shows a schematic drawing of the development of the calcareous microstructure in the *Halimeda* segment that is based on Macintyre and Reid (1995). Here it is modified to illustrate and compare the formation of the $CaCO_3$ segment microstructure with alterations observed under elevated seawater pCO_2 and lowered $CaCO_3$ saturation (Fig. 6).

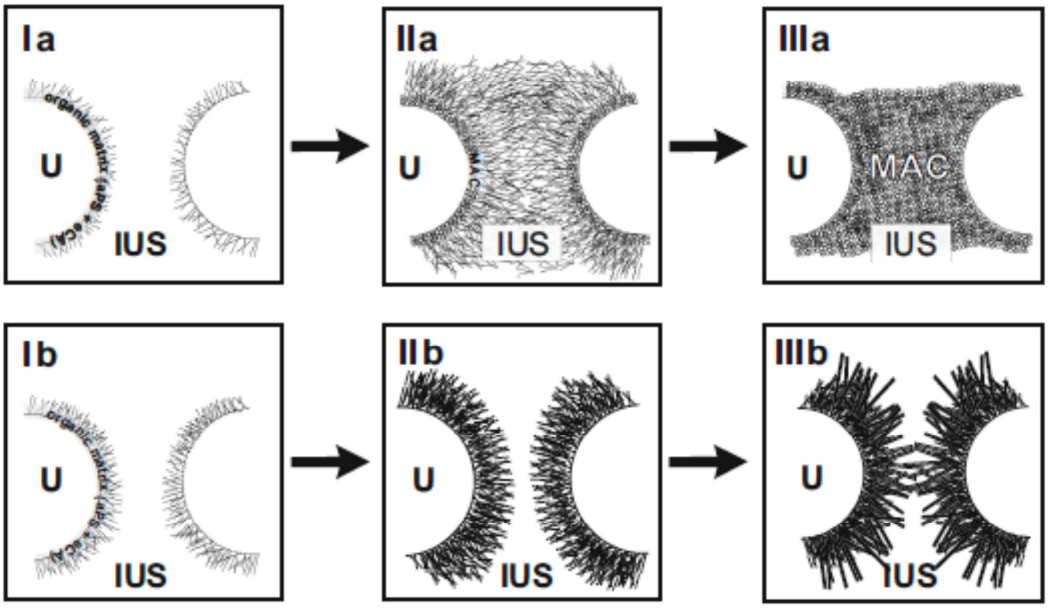

Figure 6 Schematic drawing of the $CaCO_3$ microstructural segment development in the genus *Halimeda* lineage Opuntia; **(Ia to IIIa)** under ambient conditions and **(Ib to IIIb)** when altered under elevated seawater pCO_2 (modified from Wizemann et al. 2014 and references therein).

(Ia) Primary needles form actively in an organic matrix at the external utricle wall. **(IIa)** Primary needles may completely fill in open inter-utricular space. Micro-anhedral carbonate (MAC) forms in vicinity of utricle walls out of recrystallized primary needles. **(IIIa)** Inter-utricular space (IUS) may become completely filled up with micro-anhedral carbonate (MAC), leading to a primary cementation of the segment. Potential formation of secondary needles in innermost secondary inter-utricular space (sIUS), which is in strong dependency to the availability of open space, is not shown in this illustration (cf., Wizemann et al. 2014).

(Ib) Abundant and longer primary needles form actively in an organic matrix at the external utricle wall. **(IIb)** Proceeding active calcification fills inter-utricular space (IUS) with primary needles. Note that naturally extensive formation of micro-anhedral carbonate at external utricle walls is hampered by elevated seawater pCO_2 as it causes $CaCO_3$ undersaturation ($\Omega < 1$). **(IIIb)** Abundant and large secondary needles, which may nucleate directly on top of primary needles, form during daytime in inner inter-utricular space (IUS); no layer of micro-anhedral carbonate is present. Due to the availability of open space, inter-utricular space (IUS) is largely dominated by secondary needle growth, as extensive primary cementation does not occur (cf., Wizemann et al. 2014). Also see text for further explanation.

U = utricle; IUS = inter-utricular space; aPS = acidic polysaccharides; eCA = external carbonic anhydrase; MAC = micro-anhedral carbonate.

Microstructural daytime processes in the segment under elevated pCO_2

During daytime, the formation of primary needles in an organic matrix at the external utricle wall represents the onset of segment calcification (Fig. 6 Ia, Ib). Under elevated pCO_2 a higher density of needles and longer needles are observed (Fig. 6 Ib; cf., ESM Figs. S1, S2a). Thus, the process of their formation might be stimulated by the shift in seawater carbon chemistry that enhances active primary calcification. CO_2 is a substrate for external carbonic anhydrase (eCA). It has been shown that external carbonic anhydrase activity in several calcifying macro-algae, including *H. opuntia*, increases under elevated seawater pCO_2 (Hofmann et al. 2013, 2014). The use of CO_2 via external carbonic anhydrase activity and CO_2 cell-uptake allow the $CaCO_3$ saturation state in the inter-utricular space to reach a similar level as under ambient seawater pCO_2. Consequently, abundant growth of secondary needles is observed in segments grown under elevated pCO_2 (Fig. 6 IIIb, cf. Fig. 3).

Microstructural nighttime processes in the segment under elevated pCO_2

At nighttime, respiratory CO_2 and presumably CO_2 as a product of cell-internal carbonic anhydrase activity are exhaled into the inter-utricular space. Under ambient seawater pCO_2 (< 400 µatm) this leads to the formation of micro-anhedral carbonate and thus to an advancing cementation of the segment (Fig. 6 IIa, IIIa). However, if CO_2 from cell-metabolism equilibrates in seawater that is already enriched in CO_2, this results in a lower seawater pH in the inter-utricular space. The shift in seawater carbon chemistry may drive the seawater in the inter-utricular space to a state of $CaCO_3$ undersaturation ($\Omega_{arag} < 1$). Subsequently, $CaCO_3$ that is precipitated during daytime starts to dissolve and does not become recrystallized to and/or re-precipitated as micro-anhedral carbonate (Fig. 6 IIb). Micro-anhedral carbonate formation during nighttime is affected, which ultimately results in a less cemented inter-utricular space. This is observed in segments grown under elevated seawater pCO_2 when secondary needles are partially initiating directly on top of primary needles without a layer of micro-anhedral carbonate present (Fig. 6 IIIb; cf. ESM Fig. S3a). Large secondary needles fan out into the available inter-utricular space where, in contrast, under ambient conditions micro-anhedral carbonate may fill out most of that open space (cf. Fig. 6 IIIa).

Consequences of the impact of elevated seawater pCO_2 on micro-anhedral carbonate formation

The strong species-specific micro-anhedral carbonate density of the segments protects *H. opuntia* from grazing and from physical stress in high-energy regimes (Paul and Hay 1986; Johns and Moore 1988). Any impact on the segmental skeleton density may cause it to be accessible to a wider range of grazing organisms that normally avoid the segments because of their high $CaCO_3$ content. With a less

solid calcified internal microstructure, the environmental niche of *H. opuntia* may shift to lower energetic regimes whereby breakage of "branches" and an effect on upright growth is less likely. However, species competition is at its highest in habitats that exhibit high biodiversity, such as tropical coral reefs, thus rapid niche turnover may not be an option (Verbruggen et al. 2009; Hoegh-Guldberg and Bruno 2010). Albeit moderately elevated seawater pCO_2 is supposed to have a positive effect on algal growth rate (total biomass) as it is supposed to enhance photosynthesis (e.g., Cornwall et al. 2012), non-calcifying species (i.e., fleshy algae) exhibit a faster response to higher availability of CO_2 and may easily be able to outcompete calcifying species like *H. opuntia* (Sinutok et al. 2011; Hofmann et al. 2012; Koch et al. 2013; Johnson et al. 2014).

Segments with high micro-anhedral carbonate content also are relevant for the sediment budget in reef ecosystems. The process of micro-anhedral carbonate formation leads to a lifetime cementation of the segment (i.e., primary cementation; Wizemann et al. 2014). Primary cementation is a precondition for subsequent intra-granular secondary cementation of the segment that takes place in the sediment after the organics have disintegrated (Milliman 1974; Reid and Macintyre 1998). Specifically primary cementation of segments enables certain lithophytic *Halimeda* species (mainly of the lineages Opuntia and Micronesicae; Hillis 2001; Verbruggen and Kooistra 2004) to contribute significant amounts of macroscopic *Halimeda* segments to tropical shallow settings (Drew 1983; Drew and Abel 1988; Milliman 1993; Rees et al. 2007). Segments of *H. opuntia* with a low grade of primary cementation may share the fate of segments from other, lesser-calcified *Halimeda* species that are prone to disintegrate rapidly and particularly contribute to the formation of carbonate (needle) mud (< 63 µm; Neumann and Land 1975; Macintyre and Reid 1992). Thus, impacts on the process of micro-anhedral carbonate formation may have major consequences for the carbonate sediment budget and grain-size structure of tropical shallow-water environments and sedimentary settings. Negative effects of ocean acidification observed on the primary cementation of *Halimeda* segments will lead to a fining of shallow-water sediments over the long-term, when structures become less dense (cemented) and more susceptible to fragmentation (Guinotte and Fabry 2008; Manzello et al. 2008). Subsequently, segment contribution of heavily calcified *Halimeda* species to tropical carbonate sediments, to the buildup of tropical islands and carbonate platforms, may significantly decrease in the future.

Acknowledgments

Sebastian Flotow (ZMT-Bremen) is acknowledged for the preparation of thin-sections and support with the SEM analyses. Nils Rädecker and Florian Roth (ZMT-Bremen, University of Bremen) provided help in the setup of mesocosms, sample collection and water parameter measurements. Achim Meyer (ZMT-Bremen) helped to maintain the mesocosms and the gas-mixing system during the experiment. This research was funded by the Leibniz-Center for

Tropical Marine Ecology. Contribution of L.C. Hofmann was funded by the German Federal Ministry of Education and Research (BMBF) project Biological Impacts of Ocean Acidification (BIOACID). Helpful comments and suggestions from reviewers and the associate editor highly improved the manuscript.

Conflict of Interest

The authors declare no conflict of interest.

References

Bertucci A, Moya A, Tambutté S, Allemand D, Supuran CT, Zoccola D (2013) Carbonic anhydrases in anthozoan corals–a review. Bioorg Med Chem 21:1437–50

Bonucci E (2007) Main suggested calcification mechanisms: extracellular matrix. In: Schreck S (ed) Biological calcification: normal and pathological processes in the early stages. Springer, Heidelberg, pp 507–558

Borowitzka MA, Larkum AWD (1976) Calcification in the green alga *Halimeda* IV. the action of metabolic inhibitors on photosynthesis and calcification. J Exp Bot 27:894–907

Caldeira K, Wickett ME (2003) Oceanography: anthropogenic carbon and ocean pH. Nature 425:365–365

Cornwall CE, Hepburn CD, Pritchard D, Currie KI, McGraw CM, Hunter KA, Hurd CL (2012) Carbon-use strategies in macroalgae: differential responses to lowered pH and implications for ocean acidification. J Phycol 48:137–144

De Beer D, Larkum AWD (2001) Photosynthesis and calcification in the calcifying algae *Halimeda discoidea* studied with microsensors. Plant Cell Environ 24:1209–1217

Dickson AG, Millero FJ (1987) A comparison of the equilibrium constants for the dissociation of carbonic acid in seawater media. Deep Sea Res 34:1733–1743

Dickson AG, Afghan JD, Anderson GC (2003) Reference materials for oceanic CO_2 analysis: a method for the certification of total alkalinity. Mar Chem 80.2:185–197

Dickson AG, Sabine CL, Christopher JR (2007) Guide to best practices for ocean CO_2 measurements. North Pacific Marine Science Organization Special Publication 3, Sidney, British Columbia, pp 176

Dodge RE, Wyers SC, Frith HR, Knap AH, Smith SR, Cook CB, Sleeter TD (1984) Coral calcification rates by the buoyant weight technique: effects of alizarin staining. J Exp Mar Biol Ecol 75:217–232

Doney SC, Balch WM, Fabry VJ, Feely RA (2009) Ocean acidification: a critical emerging problem for the ocean sciences. North 22:16–25

Drew EEA (1983) *Halimeda* biomass, growth rates and sediment generation on reefs in the central Great Barrier Reef province. Coral Reefs 2:101–110

Drew EEA, Abel KM (1988) Studies on Halimeda I. The distribution and species composition of *Halimeda* meadows throughout the Great Barrier Reef Province. Coral Reefs 6:195–205

Feely RA, Sabine CL, Lee K, Berelson W, Kleypas J, Fabry VJ, Millero FJ (2004) Impact of anthropogenic CO_2 on the $CaCO_3$ system in the oceans. Science 305:362–366

Freile D, Milliman J, Hillis L (1995) Leeward bank margin *Halimeda* meadows and draperies and their sedimentary importance on the western Great Bahama Bank slope. Coral Reefs 14: 27–33

Guinotte JM, Fabry VJ (2008) Ocean acidification and its potential effects on marine ecosystems. Ann NY Acad Sci 1134:320–342

Hillis L (2001) The calcareous reef alga *Halimeda* (Chlorophyta, Byropsidales): a cretaceous genus that diversified in the Cenozoic. Palaeogeogr Palaeocl 166:89–100

Hillis-Colinvaux L (1980) Ecology and taxonomy of *Halimeda*: primary producer of coral reefs. Adv Mar Biol 17:1–327

Hine AC, Hallock P, Harris MW, Mullins HT, Belknap DF, Jaap WC (1988) *Halimeda* bioherms along an open seaway: Miskito Channel, Nicaraguan Rise, SW Caribbean Sea. Coral Reefs 6:173–178

Hoegh-Guldberg O, Bruno JF (2010) The impact of climate change on the world's marine ecosystems. Science 328:1523–1528

Hofmann LC, Straub S, Bischof K (2012) Competition between calcifying and noncalcifying temperate marine macroalgae under elevated CO_2 levels. Mar Ecol Prog Ser 464:89–105

Hofmann LC, Straub S, Bischof K (2013) Elevated CO_2 levels affect the activity of nitrate reductase and carbonic anhydrase in the calcifying rhodophyte *Corallina officials*. J Exp Bot 64:899–908

Hofmann LC, Heiden J, Bischof K, Teichberg M (2014) Nutrient availability affects the response of the calcifying chlorophyte *Halimeda opuntia* (L.) J.V. Lamouroux to low pH. Planta 239:231–242

Johns H, Moore C (1988) Reef to basin sediment transport using *Halimeda* as a sediment tracer, Grand Cayman Island, West Indies. Coral Reefs 6:187–193

Johnson MD, Price NN, Smith JE (2014) Contrasting effects of ocean acidification on tropical fleshy and calcareous algae. PeerJ 2:e411

Jury CP, Whitehead RF, Szmant AM (2010) Effects of variations in carbonate chemistry on the calcification rates of *Madracis auretenra* (= *Madracis mirabilis* sensu Wells, 1973): bicarbonate concentrations best predict calcification rates. Glob Change Biol 16:1632–1644

Kleypas JA, Buddemeier RW, Archer D, Gattuso JP, Langdon C, Opdyke BN (1999) Geochemical consequences of increased atmospheric carbon dioxide on coral reefs. Science 284:118–120

Koch M, Bowes G, Ross C, Zhang XH (2013) Climate change and ocean acidification effects on seagrasses and marine macroalgae. Glob Change Biol 19:103–132

Langer G, Geisen M, Baumann KH, Kläs J, Riebesell U, Thoms S, Young JR (2006) Species-specific responses of calcifying algae to changing seawater carbonate chemistry. Geochem Geophy Geosy 7

Macintyre IG, Reid RP (1992) Comment on the origin of aragonite needle mud: a picture is worth a thousand words. J Sediment Res 62

Macintyre IG, Reid RP (1995) Crystal alteration in a living calcareous alga (*Halimeda*): implications for studies in skeletal diagenesis. J Sediment Res A65:143–153

Manzello DP, Kleypas JA, Budd DA, Eakin CM, Glynn PW, Langdon C (2008) Poorly cemented coral reefs of the eastern tropical Pacific: possible insights into reef development in a high-CO_2 world. P Natl A Sci 105:10450–10455

Merbach C, Culberson CH, Hawley JE, Pytkowicz RM (1973) Measurements of the apparent dissociation constants of carbonic acid in seawater at atmospheric pressure. Limnol Oceanogr 18:897–907

Milliman JD (1993) Production and accumulation of calcium carbonate in the ocean: Budget of a nonsteady state. Global Biogeochem Cy 7:927–957

Milliman JD (1974) Recent sedimentary carbonates, part 1. Marine carbonates. Springer, Heidelberg

Morse JW, Arvidson RS, Lüttge A (2007) Calcium carbonate formation and dissolution. Chem Rev 107:342–381

Multer HG (1988) Growth rate, ultrastructure and sediment contribution of *Halimeda incrassata* and *Halimeda monile*, Nonsuch and Falmouth Bays, Antigua, W.I. Coral Reefs 6:179–186

Neumann AC, Land LS (1975) Lime mud deposition and calcareous algae in the Bight of Abaco, Bahamas; a budget. J Sediment Res 45:763–786

Orr JC Fabry VJ, Aumont O, Bopp L, Doney SC, Feely RA, Gnanadesikan A, Gruber N, Ishida A, Joos F, Key RM, Lindsay K, Maier-Reimer E, Matear R, Monfray P, Mouchet A, Najjar RG, Platter GK, Rodgers KB, Sabine CL, Sarmiento JL, Schlitzer R, Slater RD, Totterdell IJ, Weirig MF, Yamanaka Y, Yool A (2005) Anthropogenic ocean acidification over the twenty-first century and its impact on calcifying organisms. Nature 437:681–686

Paul V, Hay M (1986) Seaweed susceptibility to herbivory: chemical and morphological correlates. Mar Ecol-Prog Ser 33:255–264

Pierrot D, Lewis E, Wallace DWR (2006) CO_2SYS DOS Program developed for CO_2 system calculations. ORNL/CDIAC-105. Carbon Dioxide Information Analysis Center, Oak Ridge National Laboratory, US Department of Energy, Oak Ridge, TN

Price NN, Hamilton SL, Tootell JS, Smith JE (2011) Species-specific consequences of ocean acidification for the calcareous tropical green algae *Halimeda*. Mar Ecol-Prog Ser 440:67–78

Rees SA, Opdyke BN, Wilson PA, Henstock TJ (2007) Significance of *Halimeda* bioherms to the global carbonate budget based on a geological sediment budget for the Northern Great Barrier Reef, Australia. Coral Reefs 26:177–188

Reid RP, Macintyre IG (1998) Carbonate recrystallization in shallow marine environments: a widespread diagenetic process forming micritized grains. J Sediment Res 68:928–946

Reyes-Nivia C, Diaz-Pulido G, Dove S (2014) Relative roles of endolithic algae and carbonate chemistry variability in the skeletal dissolution of crustose coralline algae. Biogeosciences Discuss 11:2993–3021

Riebesell U (2004) Effects of CO_2 enrichment on marine phytoplankton. J Oceanogr 60:719–729

Riebesell U, Fabry VJ, Hansson L, Gattuso JP (2010) Guide to best practices for ocean acidification research and data reporting. Luxembourg: Publications Office of the European Union, pp 260

Ries JB, Cohen AL, McCorkle DC (2009) Marine calcifiers exhibit mixed responses to CO_2-induced ocean acidification. Geology 37:1131–1134

Ries JB (2011) Skeletal mineralogy in a high-CO_2 world. J Exp Mar Biol Ecol 403:54–64

Robbins LL, Knorr PO, Hallock P (2009) Response of *Halimeda* to ocean acidification: field and laboratory evidence. Biogeosciences Discuss 6

Stanley SM (2008) Effects of global seawater chemistry on biomineralization: past, present, and future. Chem Rev 108:4483–4498

Stanley SM, Ries JB, Hardie LA (2010) Increased production of calcite and slower growth for the major sediment-producing alga *Halimeda* as the Mg/Ca ratio of seawater is lowered to a "Calcite Sea" level. J Sediment Res 80:6–16

Sinutok S, Hill R, Doblin MA, Wuhrer R, Ralph PJ (2011) Warmer more acidic conditions cause decreased productivity and calcification in subtropical coral reef sediment-dwelling calcifiers. Limnol Oceanogr 56:1200–1212

Sinutok S, Hill R, Doblin MA, Kühl M, Ralph PJ (2012) Microenvironmental changes support evidence of photosynthesis and calcification inhibition in Halimeda under ocean acidification and warming. Coral Reefs 31:1201–1213

Takahashi T, Broecker WS, Bainbridge AE (1981) The alkalinity and total carbon dioxide concentration in the world oceans. Carbon Cycle Modelling, SCOPE, 16:271–286

Verbruggen H, Kooistra W (2004) Morphological characterization of lineages within the calcified tropical seaweed genus *Halimeda* (Bryopsidales, Chlorophyta). Eur J Phycol 39:213–228

Verbruggen H, Tyberghein L, Pauly K, Vlaeminck C, Nieuwenhuyze KV, Kooistra WH, Leliaert F, Clerck OD (2009) Macroecology meets macroevolution: evolutionary niche dynamics in the seaweed *Halimeda*. Global Ecol Biogeogr 18:393–405

Vogel N, Fabricius KE, Strahl J, Noonan SHC, Wild C, Uthicke S (2015a) Calcareous green alga *Halimeda* tolerates ocean acidification conditions at tropical carbon dioxide seeps. Limnol Oceanogr 60:263–275

Vogel N, Meyer F, Wild C, Uthicke S (2015b) Decreased light availability can amplify negative impacts of ocean acidification on calcifying coral reef organisms. Mar Ecol Prog Ser 521:49–61

Wefer G (1980) Carbonate production by algae *Halimeda, Penicillus* and *Padina*. Nature 285:323–324

Weiner S, Lowenstam H (1986) Organization of extracellularly mineralized tissues: a comparative study of biological crystal growth. Crit Rev Biochem Mol 20:365–408

Weiss IM, Marin F (2008) The role of enzymes in biomineralization processes. In: Sigel A, Sigel H, Sigel RKO (eds) Biomineralization: From nature to application. Wiley, West Sussex, pp 71–126

Wienberg C, Westphal H, Kwoll E, Hebbeln D (2010) An isolated carbonate knoll in the Timor Sea (Sahul Shelf, NW Australia): facies zonation and sediment composition. Facies 56:179–193

Wizemann A, Meyer FW, Westphal H (2014) A new model for the calcification of the green macro-alga *Halimeda opuntia* (Lamouroux). Coral Reefs 33:1–14

8 - Ocean acidification rapidly decreases dinitrogen fixation associated with the hermatypic coral *Seriatopora hystrix*

Running head: Ocean acidification reduces N_2 fixation associated with a hard coral

Nils Rädecker[1,2], Friedrich W. Meyer[1], Vanessa N. Bednarz[1], UlisseCardini[1], Christian Wild[1,2]

[1]Leibniz Center for Tropical Marine Ecology (ZMT), Fahrenheitstr. 6, D-28359 Bremen, Germany

[2]Faculty of Biology and Chemistry (FB2), University of Bremen, Germany

The manuscript has been published in Marine Ecology Progress Series, DOI:10.3354/meps10912

Abstract

Since productivity and growth of coral associated dinoflagellate algae is nitrogen (N)-limited, dinitrogen (N_2) fixation by coral-associated microbes is likely crucial for maintaining the coral-dinoflagellate symbiosis. It is thus essential to understand the effects future climate change will have on N_2 fixation by the coral holobiont. This laboratory study is the first to investigate short-term effects of ocean acidification on N_2 fixation activity associated with the tropical, hermatypic coral *Seriatopora hystrix* using the acetylene reduction assay in combination with calcification measurements. Findings reveal that simulated ocean acidification (pCO_2 1080 µatm) caused a rapid and significant decrease (53 %) in N_2 fixation rates associated with *S. hystrix* compared to the present day scenario (pCO_2 486 µatm). In addition, N_2 fixation associated with the coral holobiont showed a positive exponential relationship with its calcification rates. This suggests that even small declines in calcification rates of hermatypic corals under high CO_2 conditions may result in decreased N_2 fixation activity, since these two processes may compete for energy in the coral holobiont. Ultimately, an intensified N limitation in combination with a decline in skeletal growth may trigger a negative feedback loop on coral productivity exacerbating the negative long-term effects of ocean acidification.

Introduction

Hermatypic corals are highly adapted to the oligotrophic waters in which they occur by forming a mutualistic symbiosis with dinoflagellate algae of the genus *Symbiodinium* [1]. Although this symbiosis enables an efficient internal recycling of nutrients, new nutrients (particularly bioavailable nitrogen) are needed to sustain net productivity and to compensate the loss of nutrients. New nitrogen (N) is acquired by the coral holobiont via capture of prey, assimilation of inorganic and organic N from the water column, and dinitrogen (N_2) fixation [2,3]. In this context, Lesser *et al.* [4] for the first time detected endosymbiotic cyanobacteria in the coral *Montastraea cavernosa.* Recent research revealed that diazotrophs (N_2 fixing bacteria and archaea) are ubiquitous members of coral-associated microbial communities and form species-specific associations with their hosts [5–7]. N_2 fixation activity has also been detected for several coral species, suggesting a high importance of this process in fulfilling the N demand of corals (reviewed in Fiore *et al.* [8] and Cardini *et al.* [9]).

Since growth of *Symbiodinium* spp. is N limited, low DIN availability may be essential to maintain the stability of this symbiosis [10]. On the other hand, *Symbiodinium* spp. is efficient in the uptake of fixed N [11], and cell division rates are faster in corals that show high N_2 fixation activity [2]. Hence, N_2 fixation may play a key role in regulating the coral-dinoflagellate symbiosis. The effects of environmental changes, such as ocean acidification, on N_2 fixation associated with hermatypic corals have yet to be resolved. Several studies reported reduced calcification rates under high CO_2 conditions and reduced aragonite saturation [12–14]. Even though positive as well as negative effects of ocean acidification on N_2 fixation activity by planktonic diazotrophs have been reported [15–17] there are no studies up to now investigating the effects of ocean acidification on N_2 fixation associated with hermatypic corals. Thus, in the present study we experimentally investigated the short-term response of N_2 fixation and calcification (light/dark) in the exemplary coral holobiont, *Seriatopora hystrix*, exposed to high CO_2 conditions as they may occur before 2100 according to the IPCC scenario RCP 8.5 [18].

Material and Methods

Model organism and sample preparation. The hermatypic coral *S. hystrix* was selected as model organism for this study as it is abundant, occurs in a wide range of habitats, and is frequently used in physiological studies [19–21]. The coral used for the experiment was acquired from the company De Jong Marinelife, Netherlands and originated from the Indo-Pacific region. One individual colony was fragmented into 30 smaller colonies of an average size of 11.75 ± 1.12 cm² (mean ± SE) to remove genetic variability. All fragments were kept in a mesocosm holding tank (2000L) in the laboratory facilities of the Leibniz Centre for Tropical Marine Ecology (ZMT, Bremen) for two months prior to the measurements.

Experimental incubations. The seawater used for the CO_2 treatment was taken from the coral holding tank, filtered (0.1 µm, AcroPak™) and equilibrated with gas of defined CO_2 concentrations of either 486 ppmv (ambient) or 1080 ppmv (high). The resulting changes in seawater carbonate chemistry were calculated from pH (NBS) and total alkalinity (TA) using the CO_2 Sys Excel Macro) [22]. pH (NBS) reading was obtained from a multiprobe (WTW 3430, Germany) and TA was measured by end-point titration with TW alpha plus (SI Analytic, Germany) using 0.5 M HCl. Corals were exposed to the CO_2 treatment in holding tanks for 20 h prior to the first incubations and for 24 h in between the first and the second incubation (salinity = 34‰, temperature = 26 ± 1 °C, PAR = 110 ± 5 quanta µmol s^{-1} m^{-2}). Additionally seawater at ambient or high CO_2 was used during the incubations, respective to the treatment.Calcification, photosynthesis, respiration and N_2 fixation rates were measured in two consecutive incubations. A total of 30 fragments were incubated with n = 15 for each CO_2 treatment level (ambient and high). Firstly, O_2 fluxes and calcification rates under treatment conditions (seawater of ambient or high CO_2) were quantified during the same incubation. Oxygen fluxes of the coral fragments were measured during light (PAR = 110 ± 5 quanta µmol s^{-1} m^{-2}) and dark incubations (less than 2 h each to avoid supersaturation of O_2) in 250 mL glass chambers by constant logging of O_2 concentrations using O_2 optodes (Firesting, PyroScience Sensor Technology, Germany). Water samples of 50 ml were collected from each chamber before and after each incubation (light/dark) to measure calcification rates. All coral fragments were returned to the treatment aquaria of high or ambient CO_2, according to the treatment, for 24 h before start of the second incubation.

In the second incubation, the acetylene reduction technique was used to quantify N_2 fixation rates of the coral fragments [23,24]. Coral fragments were incubated in 1 L glass chambers filled with 800 mL of treatment water (ambient or high CO_2 respectively), of which 10 % (80 mL) were previously saturated with acetylene (C_2H_2) to improve equilibration in the chamber. Also, 10 % (20 mL) of the 200 ml headspace were replaced with C_2H_2 gas after the chambers were sealed gastight. The incubation lasted for 22 h, starting with a 12 h dark phase followed by a 10 h light phase. During incubation, chambers were kept at constant temperature of 26.0 ± 0.3 °C. Gas samples of 1 mL were taken from the headspace after time intervals of 0, 4, 12 and 22 h, and collected in 2 mL glass vials previously filled with deionized water. Vials were stored frozen upside down until analysis to prevent any leakage from the septa.

Sample Analyses. Respiration and gross photosynthesis rates were calculated from the incubation periods which showed linear changes in O_2 concentration. Changes in the total alkalinity of the water samples before and after the incubations were converted into calcification rates using the alkalinity anomaly technique [25]. Nitrogen fixation rates were calculated as ethylene (C_2H_4) evolution rates and not converted into actual fixation rates of N_2, as we acknowledge that there is an ongoing discussion about the correct conversion factor in the scientific community [26,24]. C_2H_4 concentrations in the gas samples were quantified by gas chromatography (Varian 3800 with AL203/KCL 50x0.53 column and

FID detector). Changes in C_2H_4 concentration were converted into C_2H_4 evolution rates according to Breitbarth *et al.* [27]. N_2 fixation rates showed a distinct initial lag phase during the first 4 h of incubation. This is a common phenomenon during acetylene reduction assays [28–30]. Hence, N_2 fixation rates for the dark were calculated based on C_2H_4 concentration differences during the second time interval (4 to 12 h) without considering the first 4 h of incubation. Light N_2 fixation rates were calculated based on concentration differences between 12 and 22 h of incubation time.

Photosynthesis, respiration, calcification and N_2 fixation rates were corrected for seawater control (n = 6) signals and normalized to incubation time and coral surface area, which was quantified by advanced geometry [31].

Data Analysis. All statistical analyses were conducted with R version 3.0.2. Differences in N_2 fixation rates were analysed using generalized mixed effect linear models (GLMM) with gamma distribution and an inverse link function taking into account minor fluctuations in water temperatures during the incubations to increase the fit of the model. O_2 fluxes, calcification rates and the relationship of calcification with N_2 fixation rates were also analysed with generalized linear models (GLM) with gamma distribution and an inverse link function. To meet the assumptions of gamma distribution, O_2 fluxes, calcification and N_2 fixation rates were (x+1) transformed. All data were corrected for outliers using the Dixon test.

Results

The seawater carbonate system following the manipulation of CO_2 concentrations showed significant differences. At a total alkalinity of 1784 ± 36 µmol kg seawater^{-1} ambient CO_2 concentrations resulted in an aragonite saturation state (Ω Ar) of 1.9 ± 0.1 at a pH of 8.02, whereas high CO_2 concentrations showed an Ω Ar of 1.0 ± 0 at a pH of 7.71.

Short-term exposure to high CO_2 concentrations revealed strong effects on the physiology of fragments of *S. hystrix* compared to the fragments incubated under ambient CO_2 concentrations. N_2 fixation activity (acetylene reduction) was variable, but measurable in all coral fragments. Rates were higher (3-4 times) in the light than in the dark independently of the treatment applied ($\chi^2_{(1,\ N=30)}$ = 22.839, p << 0.001). N_2 fixation rates ranged from 0.04 to 1.98 nmol C_2H_4 cm^{-2} h^{-1} during the light period and from 0.00 to 0.56 nmol C_2H_4 cm^{-2} h^{-1} during the dark period (Fig 1a,b). High CO_2 levels caused a significant decline (53%) in the N_2 fixation rates of the coral holobiont in the light ($\chi^2_{(1,\ N=30)}$ = 6.8271,p<0.01), but not in the dark, because rates were too low to indicate any significant differences ($\chi^2_{(1,\ N=30)}$ = 0.8311, p=0.36). N_2 fixation rates of the coral nubbins in the light were 0.83 ± 0.16 nmol C_2H_4 cm^{-2} h^{-1} (means ± SE) under ambient CO_2 concentrations compared to 0.39 ± 0.09 nmol C_2H_4 cm^{-2} h^{-1} under high CO_2 concentrations.

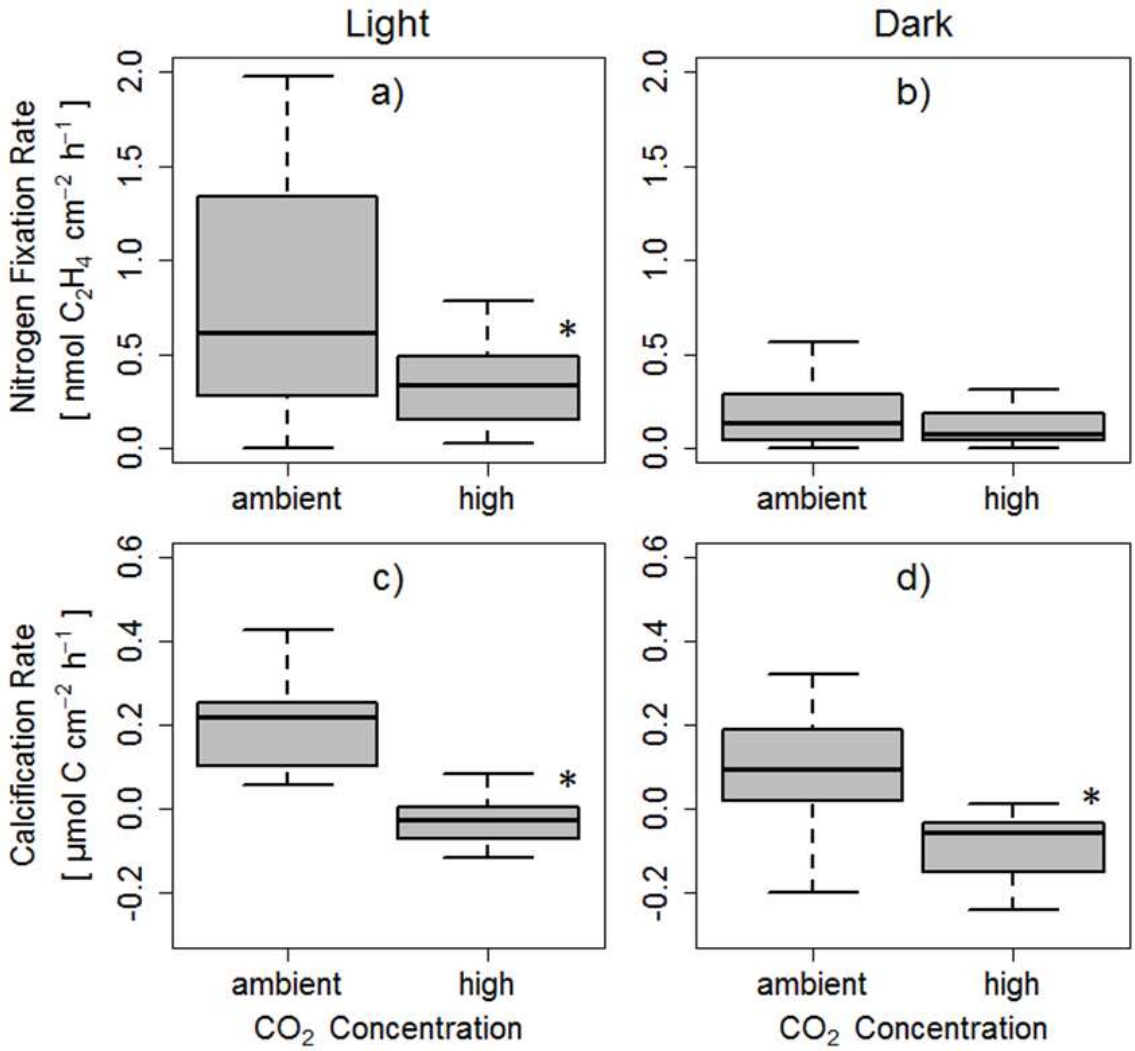

Figure 1: Boxplots for N_2 fixation rates (a,b) and calcification rates (c,d) of *S. hystrix* depending on the CO_2 treatment (n = 15 for N_2 fixation rates and n = 13 for calcification rates) for the light (a,c) period and dark (b,d) period. All N_2 fixation rates are expressed as ethylene (C_2H_4) production rates. All rates were corrected for seawater control and normalized to incubation time and coral surface area. Boxes show upper and lower quartile as well as median of data distribution. Whiskers indicate data points within 1.5 times the interquartile range from the box. Boxplots marked by asterisks (*) are significantly different from each other.

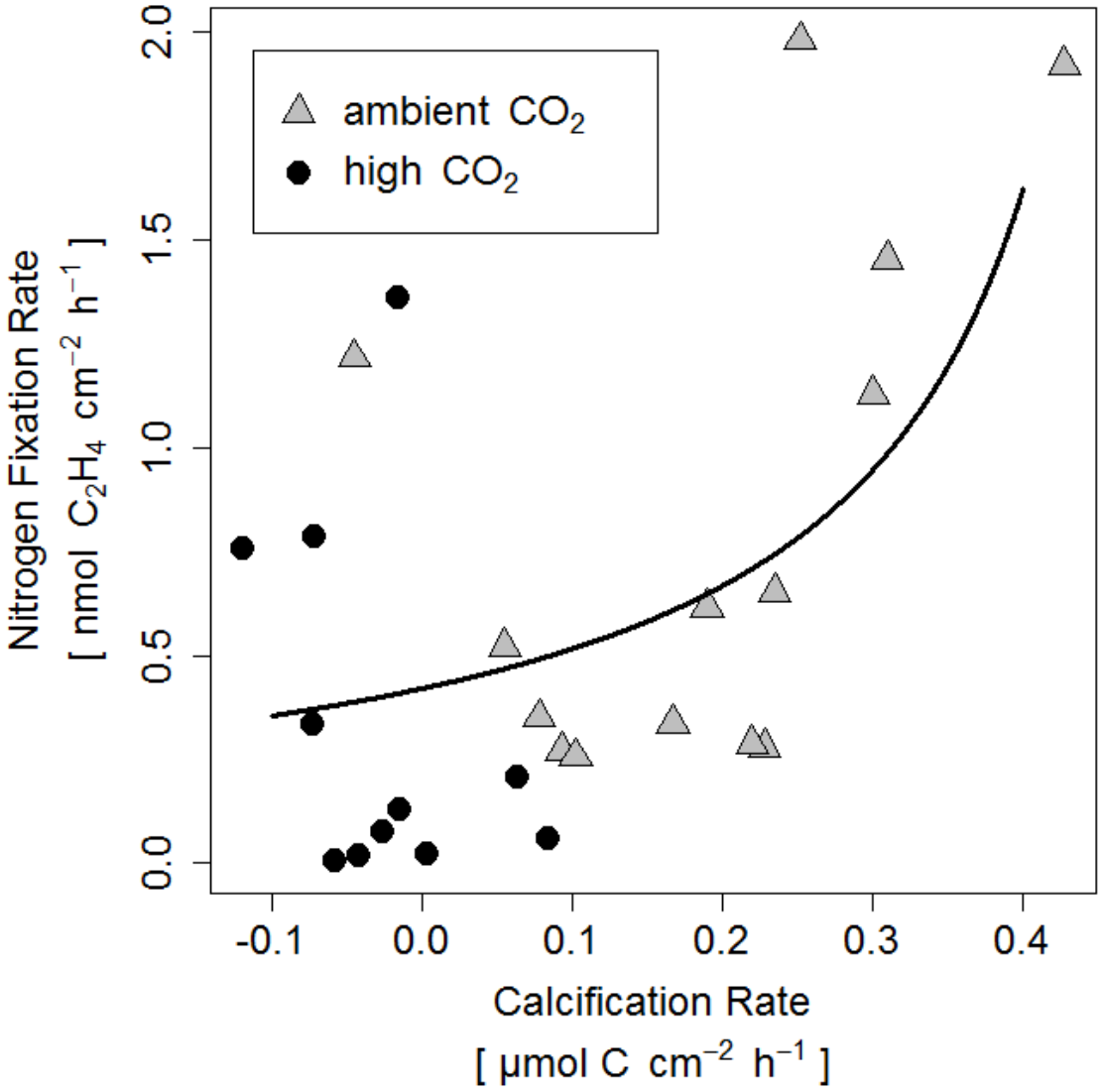

Figure 2: Relationship of N_2 fixation rates and calcification rates of *S. hystrix* incubated in the light under high CO_2 (black points) and control conditions (grey triangles). All rates were corrected for seawater controls and normalized to incubation time and coral surface area. Black curve indicates the best-fitting model ($\chi^2_{(1, N=25)} = 5.21$, $p = 0.03$, Mc Fadden's $R^2 = 0.862$).

Overall, calcification rates ranged from -0.12 to 0.42 µmol C cm^{-2} h^{-1} in the light and -0.24 to 0.32 µmol C cm^{-2} h^{-1} in the dark period (Fig. 1c,d). Calcification rates showed a pronounced response to differences in CO_2 concentrations. Calcification was significantly reduced under high CO_2 conditions compared to ambient CO_2 levels both in the light ($\chi^2_{(1, N=26)}$ = 26.651, p << 0.001) and in the dark period ($\chi^2_{(1, N=26)}$ = 4.55, p << 0.001). At ambient CO_2 concentrations, calcification rates were 0.20 ± 0.03 µmol C cm^{-2} h^{-1} in the light and 0.09 ± 0.04 µmol C cm^{-2} h^{-1}in the dark period. At high CO_2 concentrations, calcification rates were -0.01 ± 0.03 µmol C cm^{-2} h^{-1}in the light and -0.08 ± 0.02 µmol C cm^{-2} h^{-1}in the dark. Since both calcification and N_2 fixation decreased under the ocean acidification scenario, the relationship between these two processes was investigated (Fig. 2).

This revealed a positive exponential correlation of N_2 fixation activity and calcification rates in coral fragments incubated in the light ($\chi^2_{(1, N=25)}$ = 5.21, p = 0.02) as opposed to dark incubations, where the relationship was not significant ($\chi^2_{(1, N=25)}$ = 0.35, p = 0.55).

Differences in CO_2 concentrations had no significant effect on gross photosynthesis ($\chi^2_{(1, N=30)}$ = 0.01, p = 0.90) and respiration rates ($\chi^2_{(1, N=30)}$ = 0.18, p = 0.67) of the coral nubbins. Mean gross photosynthesis was 0.50 ± 0.04 µmol O_2 cm^{-2} h^{-1} under high CO_2 compared to 0.49 ± 0.05 µmol O_2 cm^{-2} h^{-1} under ambient CO_2 conditions. Respirations rates were -0.30 ± 0.03 µmol O_2 cm^{-2} h^{-1} at high CO_2 and -0.28 ± 0.2 µmol O_2 cm^{-2} h^{-1} at low CO_2 conditions respectively.

Discussion

This is the first study showing N_2 fixation associated with *S. hystrix* and demonstrating the effect of elevated CO_2 levels on N_2 fixation.

N_2 fixation has been described for several other coral species, with a pronounced variation between and within species [2,30,32]. To control for the intra-specific differences, manipulative experiments need to use individuals of identical genotype [33]. All experiments in this study where conducted with coral colonies from the same colony. Thus the observed physiological changes can be referred back to treatment conditions.

N_2 fixation is an energy-intensive process [34]. Shashar *et al.* [30] found that N_2 fixation activity was inhibited in corals when photosynthesis was blocked with DCMU, but could be restored when glucose was added to the incubation water. This suggests that coral associated N_2 fixation strongly depends on photosynthetically fixed carbon to fulfil its energetic demands. In the present study, N_2 fixation rates were three to four times higher during the light compared to the dark. This is likely explained by increased availability of fixed carbon by photosynthesis during the light phase. N_2 fixation occurred during times of net O_2 evolution, although O_2 is known to inhibit this process [35]. There are different

mechanisms by which N_2 fixation can take place at times of O_2 evolution [35]. In coral reef sponges for example symbiotic non-heterocystous cyanobacteria, which depend on O_2 for their N_2 fixation, have been suggested to explain high N_2 fixation activity under aerobic conditions [36,37].

N_2 fixation rates were significantly reduced in the ocean acidification treatment compared to the ambient scenario in the light. Other studies reported an increase of N_2 fixation activity under elevated CO_2 conditions for planktonic cyanobacteria due to increased photosynthetic carbon fixation by overcoming of CO_2 limitation [38,39]. This may be the case for planktonic autotrophic diazotrophs, but CO_2 limitation is unlikely to occur in the *S. hystrix* holobiont due to respiration by the coral host. Reduced N_2 fixation rates under elevated CO_2 concentrations have only been described in the planktonic cyanobacterium *Trichodesmium* in combination with low iron availability [17]. Since the experiments carried out in the present study took place in laboratory conditions, it is unlikely that iron limitation caused the lowering of fixation rates in the short time span of the experiment described in the present study. Hence, there has to be another cause for the effects observed. Along with N_2 fixation, calcification of *S. hystrix* was significantly reduced during both light and dark periods. The significant positive correlation between both processes during the light may suggest an indirect linkage of the two processes in the holobiont.

The reduced calcification rates are in good agreement with previous studies reporting similar effects under low pH conditions due to lowered aragonite saturation state [40–42]. Since N_2 fixation and calcification are energy-intensive mechanisms, they likely compete for energy within the coral holobiont. The lowering in the aragonite saturation state makes the calcification process more energy consuming [43,44] Since gross and net photosynthesis were not significantly different between treatments, the increased energy demand by calcification at high CO_2 conditions may create an energy deficit in the coral holobiont. Subsequently, this may also reduce the energy available for heterotrophic diazotrophs in the coral tissue, thereby explaining the decrease in N_2 fixation activity at high CO_2 conditions. Although Anthony *et al.* [41] reported a loss of coral productivity at lower seawater pH during long term experiments, there was no effect of elevated CO_2 on photosynthesis and respiration of the fragments used in the present study, probably due to the short time span of the incubations. It is hence likely that the described long-term drop in productivity will amplify the effects of ocean acidification on N_2 fixation and calcification even more. This is the first evidence that coral associated N_2 fixation can be affected by ocean acidification. The observed decline in N_2 fixation may result in N starvation for both the coral and *Symbiodinium* spp. Together with a reduced skeletal growth this suggests a negative feedback loop for the productivity of the holobiont. The reduction in N_2 fixation may thus exacerbate negative long-term effects of ocean acidification for coral reef functioning. Finally, these findings highlight the importance of N_2 fixation as key process for understanding the response of the coral holobiont to environmental stressors such as ocean acidification. To improve the understanding of interactions between diazotrophs, *Symbiodinium* spp.

and the coral host an interdisciplinary approach is needed, combining ecological and microbiological aspects.

Acknowledgements. We thank Dr. Achim Meyer for his help with the realisation of the experimental set up and Dieter Peterke for his support during the sample analysis. For their support during the experiments we kindly acknowledge the student assistants of the Coral Reef Ecology group Nur Herrea Garcia, Helen O'Neill, Florian Roth and Sabrina Schmalz. We especially thank the editor and the three anonymous reviewers, whose suggestions strongly contributed to the quality of this manuscript. This study was supported by German Research Foundation (DFG) grant Wi 2677/6-1 to C.W.

Literature Cited

1. Muscatine AL, Porter JW, Muscatine L. Corals : to mutualistic symbioses adapted Environments. Bioscience. 1977;27: 454–460.

2. Lesser MP, Falcón LI, Rodríguez-román A, Enríquez S, Hoegh-guldberg O, Iglesias-prieto R. Nitrogen fixation by symbiotic cyanobacteria provides a source of nitrogen for the scleractinian coral *Montastraea cavernosa*. Mar Ecol Prog Ser. 2007;346: 143–152. doi:10.3354/meps07008

3. Grover R, Maguer J-F, Allemand D, Ferrier-Pagès C. Uptake of dissolved free amino acids by the scleractinian coral *Stylophora pistillata*. J Exp Biol. 2008;211: 860–5. doi:10.1242/jeb.012807

4. Lesser MP, Mazel CH, Gorbunov MY, Falkowski PG. Discovery of symbiotic nitrogen-fixing cyanobacteria in corals. Science. 2004;305: 997–1000. doi:10.1126/science.1099128

5. Lema KA, Willis BL, Bourne DG. Corals form characteristic associations with symbiotic nitrogen-fixing bacteria. Appl Environ Microbiol. 2012;78: 3136–44. doi:10.1128/AEM.07800-11

6. Lema KA, Willis BL, Bourne DG. Amplicon pyrosequencing reveals spatial and temporal consistency in diazotroph assemblages of the *Acropora millepora* microbiome. Environ Microbiol. 2014; doi:10.1111/1462-2920.12366

7. Olson ND, Lesser MP. Diazotrophic diversity in the Caribbean coral, *Montastraea cavernosa*. Arch Microbiol. 2013;195: 853–859. doi:10.1007/s00203-013-0937-z

8. Fiore CL, Jarett JK, Olson ND, Lesser MP. Nitrogen fixation and nitrogen transformations in marine symbioses. Trends Microbiol. Elsevier Ltd; 2010;18: 455–463. doi:10.1016/j.tim.2010.07.001

9. Cardini U, Bednarz VN, Foster RA, Wild C. Benthic N_2 fixation in coral reefs and the potential effects of human-induced environmental change. Ecol Evol. 2014; doi:10.1002/ece3.1050

10. Falkowski PG, Dubinsky Z, Muscatine L, McCloskey L. Population control in symbiotic corals. Bioscience. 1993;43: 606–611.

11. Kopp C, Pernice M, Domart-Coulon I, Djediat D, Spangenberg J, Alexander D, et al. Highly dynamic cellular-level response of symbiotic coral to a sudden increase in environmental nitrogen. MBio. 2013;4: e00052–13. doi:10.1128/mBio.00052-13.Updated

12. Cohen A, Holcomb M. Why corals care about ocean acidification: uncovering the mechanism. Oceanography. 2009;22: 118–127. doi:10.5670/oceanog.2009.102

13. Ries JB, Cohen a. L, McCorkle DC. Marine calcifiers exhibit mixed responses to CO_2-induced ocean acidification. Geology. 2009;37: 1131–1134. doi:10.1130/G30210A.1

14. Crook ED, Cohen AL, Rebolledo-Vieyra M, Hernandez L, Paytan A. Reduced calcification and lack of acclimatization by coral colonies growing in areas of persistent natural acidification. Proceeding Natl Acad Sci United States Am. 2013;110: 11044–11049. doi:10.1073/pnas.1301589110/-/DCSupplemental.www.pnas.org/cgi/doi/10.1073/pnas.1301589110

15. Levitan O, Rosenberg G, Setlik I, Setlikova E, Grigel J, Klepetar J, et al. Elevated CO_2 enhances nitrogen fixation and growth in the marine cyanobacterium *Trichodesmium*. Glob Chang Biol. 2007;13: 531–538. doi:10.1111/j.1365-2486.2006.01314.x

16. Czerny J, Barcelos e Ramos J, Riebesell U. Influence of elevated CO_2 concentrations on cell division and nitrogen fixation rates in the bloom-forming cyanobacterium *Nodularia spumigena*. Biogeosciences. 2009;6: 1865–1875. doi:10.5194/bg-6-1865-2009

17. Shi D, Kranz SA, Kim J, Morel FMM. Ocean acidification slows nitrogen fixation and growth in the dominant diazotroph *Trichodesmium* under low-iron conditions. Proceeding Natl Acad Sci United States Am. 2012; E3094–E3100. doi:10.1073/pnas.1216012109/-/DCSupplemental.www.pnas.org/cgi/doi/10.1073/pnas.1216012109

18. Riahi K, Grübler A, Nakicenovic N. Scenarios of long-term socio-economic and environmental development under climate stabilization. Technol Forecast Soc Change. 2007;74: 887–935. doi:10.1016/j.techfore.2006.05.026

19. Sheppard CRC. Coral species of the Indian Ocean and adjacent seas: a synonymized compilation and some regional distributional patterns. Atoll Res Bull. 1987;307. Available: http://www.sciencedirect.com/science/article/pii/S0040162506001387

20. Hoegh-guldbergl O, Smith GJ. The effect of sudden changes in temperature , light and salinity on the population density and export of zooxanthellae from the reef corals *Stylophora pistillata* Esper and Seriatopora hystrix Dana. J Exp Mar Bio Ecol. 1989;129: 279–303.

21. Bongaerts P, Riginos C, Hay KB, Oppen MJH Van, Hoegh-guldberg O. Adaptive divergence in a scleractinian coral : physiological adaptation of *Seriatopora hystrix* to shallow and deep reef habitats. BMC Evol Biol. 2011;11.

22. Lewis E, Wallace D. Program Developed for CO_2 System Calculations (Carbon Dioxide Information Analysis Center, Oak Ridge National Laboratory, US Dept. of Energy, Oak Ridge, TN). ORNL/CDIAC-105 Oak Ridge, Tennessee. 1998;

23. Hardy RWF, Holsten RD, Jackson EK, Burns RC. The acetylene - ethylene assay for N_2 fixation : laboratory and field evaluation. Plant Physiol. 1968;43: 1185–1207.

24. Wilson ST, Böttjer D, Church MJ, Karl DM. Comparative assessment of nitrogen fixation methodologies , conducted in the oligotrophic North Pacific Ocean. Appl Environ Microbiol. 2012;78: 6516–6523. doi:10.1128/AEM.01146-12

25. Chrisholm JRM, Gattuso J-P. Validation of the alkalinity anomaly technique for investigating calcification and photosynthesis in coral reef communities. Limnol Oceanogr. 1991;36: 1232–1239.

26. Nohrstedt HÖ. Conversion factor between acetylene reduction and nitrogen fixation in soil: effect of water content and nitrogenase activity. Soil Biol Biochem. 1983;I: 275–279.

27. Breitbarth E, Mills MM, Friedrichs G, Laroche J. The Bunsen gas solubility coefficient of ethylene as a function of temperature and salinity and its importance for nitrogen. Limnol Oceanogr Methods. 2004;2: 282–288.

28. Zuberer DA, Silver WS. Biological dinitrogen fixation (acetylene reduction) associated with Florida mangroves. Appl Environ Microbiol. 1978;35: 567–575.

29. Gallon JR, Hamadi F. Studies on the effects of oxygen on acetylene reduction (nitrogen fixation) in Gloeothece. J Gen Microbiol. 1984;130: 495–503.

30. Shashar N, Cohen Y, Loya Y, Sar N. Nitrogen fixation (acetylene reduction) in stony corals : evidence for coral-bacteria interactions. Mar Ecol Prog Ser. 1994;111: 259–264.

31. Naumann MS, Niggl W, Laforsch C, Glaser C, Wild C. Coral surface area quantification – evaluation of established techniques by comparison with computer tomography. Coral reefs. 2009;28: 109–117. doi:10.1007/s00338-008-0459-3

32. Williams WM, Broughton V, Broughton WJ. Nitrogen fixation (acetylene reduction) associated with the living coral *Acropora variabilis*. Mar Biol. 1987;94: 531–535.

33. Mascarelli PE, Bunkley-Williams L. An experimental evaluation of the healing in damaged, unbleached and artificially bleached star coral, *Montastraea annularis*. Bull Mar Sci. 1999;65: 577–586.

34. McNarry JE, Burris RH. Energy requirements for nitrogen fixation by cell-free preparations from *Clostridium pasteurianum*. J Bacteriol. 1962;84: 598–599.

35. Gallon JR. The oxygen sensitivity of nitrogenase: a problem for biochemists and micro-organisms. Trends Biochem Sci. 1981;6: 19–23.

36. Wilkinson CR, Fay P. Nitrogen fixation in coral reef sponges with symbiotic cyanobacteria. Nature. 1979;279: 527–529.

37. Mohamed NM, Colman AS, Tal Y, Hill RT. Diversity and expression of nitrogen fixation genes in bacterial symbionts of marine sponges. Environ Microbiol. 2008;10: 2910–21. doi:10.1111/j.1462-2920.2008.01704.x

38. Hutchins DA, Fu F-X, Zhang Y, Warner ME, Feng Y, K P, et al. CO2 control of *Trichodesmium* N_2 fixation, photosynthesis, growth rates, and elemental ratios: implications for past, present, and future ocean biogeochemistry. Limnol Oceanogr. 2007;52: 1293–1304.

39. Garcia NS, Fu F, Hutchins DA. Colimitation of the unicellular photosynthetic diazotroph *Crocosphaera watsonii* by phosphorus, light, and carbon dioxide. 2013;58: 1501–1512. doi:10.4319/lo.2013.58.4.1501

40. Orr JC, Fabry VJ, Aumont O, Bopp L, Doney SC, Feely R a, et al. Anthropogenic ocean acidification over the twenty-first century and its impact on calcifying organisms. Nature. 2005;437: 681–6. doi:10.1038/nature04095

41. Anthony KRN, Kline DI, Diaz-Pulido G, Dove S, Hoegh-Guldberg O. Ocean acidification causes bleaching and productivity loss in coral reef builders. Proceeding Natl Acad Sci United States Am. 2008;105: 17442–17446.

42. Kleypas JS, Yates KK. Coral reefs and ocean acidification. Oceanography. 2009;22: 108–117.

43. Marubini F, Barnett H, Langdon C, Atkinson M. Dependence of calcification on light and carbonate ion concentration for the hermatypic coral *Porites compressa*. Mar Ecol Prog Ser. 2001;220: 153–162. doi:10.3354/meps220153

44. Hohn S, Merico a. Effects of seawater pCO_2 changes on the calcifying fluid of scleractinian corals. Biogeosciences Discuss. 2012;9: 2655–2689. doi:10.5194/bgd-9-2655-2012

Synopsis

This thesis provides a synoptic view on the effects of two factors, ocean acidification (OA), as increased dissolved inorganic carbon (DIC), and increased organic carbon (DOC) availability on the physiological performance of two key coral reef organisms: calcifying green algae and corals. In laboratory studies, various physiological response parameters such as photosynthesis, calcification, nutrient fluxes and nitrogen fixation were investigated in response to the two factors named above. These parameters were tested in corals and algae from the Great Barrier Reef and in green algae from the Mexican Caribbean. To increase the understanding of calcification processes in calcifying green algae, a new calcification model for *Halimeda opuntia* is presented and is expanded towards the effects of high DIC availability on the calcification process.

The effects of elevated DIC

Elevated DIC concentrations affected the growth and calcification of most organisms. These responses were the main physiological changes measured for corals and algae under high DIC concentrations. We observed reduced growth and dark calcification rates in *Acropora millepora,* reduced dark and light calcification rates in *Seriatopora hystrix,* reduced daily calcification rates in *H. opuntia*, and reduced daily calcification rates in *Halimeda incrassata* and *Udothea flabellum*. Our findings confirm recent research that showed a reduction in calcification rates of different *Halimeda* species [1–7], mainly as a result of dissolution processes at night that lead to a reduced inorganic carbon content [5,8]. Although studies found no difference in net calcification, calcification under dark condition showed significant impacts of high DIC concentrations which were outbalanced by increased calcification during light conditions [9]. For *H. incrassata* and *U. flabellum* we could show that calcification under light conditions was significantly reduced by high DIC, and only for *H. opuntia,* we found reduced calcification rates during dark conditions. When we compare these findings to the proposed model of calcification (chapter 5), we see that two distinct processes are affected: the point of primary calcification during light periods and the cementation process during dark periods. In our adaptation of this model to high DIC conditions (chapter 6), we could show that during light conditions, needle formation might even be enhanced due to the presence of higher photosynthetic activity under high DIC conditions. In contrast, under dark conditions, high respirations rates, together with prevailing high DIC concentrations, are reducing the carbonate saturation below dissolution limits and leading to a net dissolution within the segments. Species-specific differences in the magnitude of response in calcification towards high DIC concentrations, observed in our study as well as in other studies [2,5], may result from different metabolic rates. These studies show the weight specific or area specific photosynthesis rate was the highest for *H. opuntia* when compared to the

species *H. digitata* [5] and *H. macroloba* (chapter 3). The increased metabolic rate may also lead to higher calcification rates during light conditions; however, due to the higher respiration rates of *H. opuntia* [10], it has faster dissolution rates than other species. As the cementation process depends on dissolution and re-precipitation of primary calcified aragonite (chapter 6), a higher DIC concentration in the surrounding water might hinder this re-precipitation and lead to the observed dissolution rates under dark conditions. Due to the different structure of primary and secondary calcified aragonite needles and cemented aragonite as a result of re-precipitation, a loss in cemented carbonate in the skeleton might result in a structural deficiency in the skeleton of the alga. Although the overall inorganic carbon content might be similar to algae grown under ambient conditions, these algae might show reduced skeletal strength. These deficiencies might be of special importance when resistance against physical stress is reduced. In addition, after segment shedding the diagenesis of the segments is altered and the derived sediments do not persist as weak cementation eases faster erosion [11]. In addition to a reduced cementation of the green algae, similar observations have been made on corals [11] and are supported by our finding on the dark calcification of both species investigated in this study: *A. millepora* and *S. hystrix.* The dark calcification of these two species was reduced under high DIC conditions, which might also be a result of respiration induced dissolution in combination with high DIC concentrations. For the same species, early life stages have also shown signs of metabolic stress before calcification was initiated [12,13]. This indicates higher respiration rates that might enhance dissolution processes after the onset of calcification as indicated for adult corals in this thesis. Although no effect of high DIC on the primary production of corals was detected in this thesis, the nitrogen fixation rates of *S. hystrix* were reduced compared to the control conditions and showed a significant correlation to calcification rates. In addition to calcification, the primary production of *Halimeda incrassata* and *Udothea flabellum* were also reduced under high DIC conditions. Similar observations have been made in other studies on calcifying green algae [2,5] and indicate photosynthetic impairment due to increased DIC concentrations, leading to a loss in primary production. In summary, these results indicate strong impairment of future biogenic carbonate and primary production of these important reef species. In the light of recent findings suggested in chapter 5 and 7, a loss in structural integrity might have important implications for future carbonate formation, as under high erosion rates, the persistence of *Halimeda* derived sands and also coral reefs might be compromised [14], offering even less buffering capacity towards future ocean acidification.

The effects of elevated DOC

In contrast to high DIC concentrations, elevated DOC concentrations mainly affected the primary production of the organisms investigated. The photosynthesis of *H. macroloba, H. opuntia, A. millepora* and *H. incrassata* was reduced under high DOC conditions. To date, no comparable datasets are available on the physiological effects of high DOC concentrations of corals or algae. From

previous studies, increased bleaching, disease outbreak and eventual mortality are known consequences for corals exposed to high DOC concentrations [15–17]. No sign of disease was observed in this study, however from previous studies it is known that bacterial communities on algae mainly harbour autotrophs [18], and the enrichment of different DOC sources are known to alter these communities [19] and shift them to a more heterotrophic communities, which may reduce the algal physiological and photosynthetic performance. Similar findings on corals have shown that diseased corals harbour distinct bacterial communities compared to healthy corals [20], and the addition of DOC might alter the bacterial communities of healthy corals. In addition, the calcification rates of *H. incrassata* and *U. flabellum* were reduced, indicating an effect of high DOC on the DIC concentration at the boundary layer of the algal tissue. The increase in DIC might be induced through bacterial respiration, which was shown to significantly increase under high DOC conditions [17,21]. This might have similar effects than the DIC treatment described above. As microbial communities shift form auto- to heterotrophy and photosynthesis of the algae is impaired, also the saturation state of aragonite is reduced compared to ambient DOC conditions and calcification is reduced. Furthermore, the outbreak of pathogenic bacteria might also reduce the algal fitness; However, no comparable data are available on this topic. In this thesis, the substance used to enrich water in DOC was glucose, a highly labile carbohydrate and a main component of algal DOC [22] also used in other studies on corals [15–17] . To increase the resolution of this study, a multitude of DOC mixtures tested on different coral reef organisms might provide an insight on how different DOC sources affect algal and coral physiology as they affect bacterial abundance [19]. In this study, bacterial responses are clearly linked to the concentration of glucose, and for future studies, first individual DOC substances have to be tested to address effects of DOC mixtures and identify the most active components that affect coral and algal physiology.

The effects of combined elevated DIC and DOC

Under the combination of elevated DIC and DOC concentrations, both additive and interactive effects were observed. The calcification rate of *U. flabellum* showed further reduction in calcification rates under the combination of both treatments in comparison to the individual treatments. This might be explained by the cumulative negative effects of the individual treatment. The DOC induced shift from auto- to heterotrophic bacterial communities [18] might impair photosynthesis and increase DIC concentration through increased bacterial respiration [23]. Together with the DIC treatment, this leads to amplified negative effects and in this case dissolution of calcified structures. Similar observations were made for *A. millepora* which showed and reduced dark calcification rate under the combination of both treatments.

Summary

This thesis reveals that it is important to investigate the combined effects of global and local factors to predict the physiological consequences of organisms under global climate change in a more realistic manner. This thesis shows that elevated DIC concentrations have strong impacts on primary production rates and calcification rates of both reef algae and corals as previously postulated for other comparable species [24]. The findings indicate poor cementation of algal segments under future acidification scenarios and productivity loss of corals and calcifying algae dominated communities, possibly leading to erosion of reefs and habitat degradation [11,25]. In addition, competition with fleshy macroalgae [26,27] might increase the degradation of reef structures and calcifying species might be replaced with fleshy macro algae. The loss of these biogenic carbonates and the reduction of structural complexity might pose tremendous threats to coral reefs which act as natural buffers against acidification, as well as potential refuges. It is likely that coral reefs might lose their capacity of coastal protection [28] and economic value via food provision, tourism and many other services. Regarding OA, local disturbances such as high DOC concentration might accelerate the process of reef erosion and loss in primary production, thus effort should be made to monitor the concentrations of labile DOC or biological oxygen demand of the water column. Biological oxygen demand as well as community calcification rates, community dark calcification rates, or dark calcification rates of selected individual organisms could be used as first step indicators to identify potential shifts from accretion to erosion of reef communities under future climate change scenarios.

References

1. Sinutok S, Hill R, Doblin MA, Wuhrer R, Ralph PJ (2011) Warmer more acidic conditions cause decreased productivity and calcification in subtropical coral reef sediment-dwelling calcifiers. Limnol Oceanogr 56: 1200–1212. Available: http://cat.inist.fr/?aModele=afficheN&cpsidt=24362064. Accessed 21 February 2014.

2. Price N, Hamilton S, Tootell J, Smith J (2011) Species-specific consequences of ocean acidification for the calcareous tropical green algae *Halimeda*. Mar Ecol Prog Ser 440: 67–78. Available: http://www.int-res.com/abstracts/meps/v440/p67-78/. Accessed 31 October 2011.

3. Robbins LL, Knorr PO, Hallock P (2009) Response of *Halimeda* to ocean acidification: field and laboratory evidence. Biogeosciences Discuss 6: 4895–4918. Available: http://www.biogeosciences-discuss.net/6/4895/2009/.

4. Johnson MD, Price NN, Smith JE (2014) Contrasting effects of ocean acidification on tropical fleshy and calcareous algae. PeerJ 2: e411. Available: https://peerj.com/articles/411.

5. Vogel N, Fabricius KE, Strahl J, Noonan SHC, Wild C, et al. (2015) Calcareous green alga *Halimeda* tolerates ocean acidification conditions at tropical carbon dioxide seeps. Limnol Oceanogr 60: 263–275. Available: http://doi.wiley.com/10.1002/lno.10021.

6. Guinotte JM, Fabry VJ (2008) Ocean acidification and its potential effects on marine ecosystems. Ann N Y Acad Sci 1134: 320–342. Available: http://www.ncbi.nlm.nih.gov/pubmed/18566099. Accessed 10 June 2011.

7. Sinutok S, Hill R, Doblin MA, Kühl M, Ralph PJ (2012) Microenvironmental changes support evidence of photosynthesis and calcification inhibition in *Halimeda* under ocean acidification and warming. Coral Reefs 31: 1201–1213. Available: http://link.springer.com/10.1007/s00338-012-0952-6. Accessed 21 February 2014.

8. Hofmann LC, Heiden J, Bischof K, Teichberg M (2014) Nutrient availability affects the response of the calcifying chlorophyte *Halimeda opuntia* (L.) J.V. Lamouroux to low pH. Planta 239: 231–242. Available: http://www.ncbi.nlm.nih.gov/pubmed/24158465. Accessed 23 January 2014.

9. Vogel N, Uthicke S (2012) Calcification and photobiology in symbiont-bearing benthic foraminifera and responses to a high CO_2 environment. J Exp Mar Bio Ecol 424-425: 15–24. Available: http://linkinghub.elsevier.com/retrieve/pii/S0022098112001736. Accessed 8 August 2012.

10. Smith JE, Price NN, Nelson CE, Haas AF (2013) Coupled changes in oxygen concentration and pH caused by metabolism of benthic coral reef organisms. Mar Biol 160: 2437–2447. Available: http://www.researchgate.net/publication/236588705_Coupled_changes_in_oxygen_concentration_and_pH_caused_by_metabolism_of_benthic_coral_reef_organisms. Accessed 27 July 2015.

11. Manzello D, Kleypas J (2008) Poorly cemented coral reefs of the eastern tropical Pacific: Possible insights into reef development in a high-CO_2 world. Proc Natl Acad Sci U S A 105: 10450–10455. Available: http://www.pnas.org/content/105/30/10450.abstract. Accessed 10 July 2013.

12. Kaniewska P, Campbell PR, Kline DI, Rodriguez-Lanetty M, Miller DJ, et al. (2012) Major cellular and physiological impacts of ocean acidification on a reef building coral. PLoS One 7: e34659. Available: http://www.pubmedcentral.nih.gov/articlerender.fcgi?artid=3324498&tool=pmcentrez&rendertype=abstract. Accessed 6 March 2013.

13. Moya a, Huisman L, Ball EE, Hayward DC, Grasso LC, et al. (2012) Whole transcriptome analysis of the coral *Acropora millepora* reveals complex responses to CO_2-driven acidification during the initiation of calcification. Mol Ecol 21: 2440–2454. Available: http://www.ncbi.nlm.nih.gov/pubmed/22490231. Accessed 7 March 2013.

14. Dove SG, Kline DI, Pantos O, Angly FE, Tyson GW, et al. (2013) Future reef decalcification under a business-as-usual CO_2 emission scenario. Proc Natl Acad Sci U S A 110: 15342–15347. Available: http://www.pubmedcentral.nih.gov/articlerender.fcgi?artid=3780867&tool=pmcentrez&rendertype=abstract. Accessed 15 November 2013.

15. Kuntz NM, Kline DI, Sandin SA, Rohwer F (2005) Pathologies and mortality rates caused by organic carbon and nutrient stressors in three Caribbean coral species. Mar Ecol Prog Ser 294: 173–180. Available: http://www.int-res.com/abstracts/meps/v294/p173-180/.

16. Kline DI, Kuntz NM, Breitbart M, Knowlton N, Rohwer F (2006) Role of elevated organic carbon levels and microbial activity in coral mortality. Mar Ecol Prog Ser 314: 119–125. Available: http://www.int-res.com/abstracts/meps/v314/p119-125/.

17. Haas AF, Al-Zibdah M, Wild C (2009) Effect of inorganic and organic nutrient addition on coral–algae assemblages from the Northern Red Sea. J Exp Mar Bio Ecol 380: 99–105. Available: http://linkinghub.elsevier.com/retrieve/pii/S0022098109003712. Accessed 22 June 2011.

18. Barott KL, Rodriguez-Brito B, Janouškovec J, Marhaver KL, Smith JE, et al. (2011) Microbial diversity associated with four functional groups of benthic reef algae and the reef-building coral Montastraea annularis. Environ Microbiol 13: 1192–1204. Available: http://www.ncbi.nlm.nih.gov/pubmed/21272183. Accessed 27 July 2011.

19. Nelson CE, Goldberg SJ, Wegley Kelly L, Haas AF, Smith JE, et al. (2013) Coral and macroalgal exudates vary in neutral sugar composition and differentially enrich reef bacterioplankton lineages. ISME J 7: 962–979. Available: http://www.ncbi.nlm.nih.gov/pubmed/23303369. Accessed 19 November 2013.

20. Pantos O, Cooney RP, Le Tissier MDA, Barer MR, O'Donnell AG, et al. (2003) The bacterial ecology of a plague-like disease affecting the Caribbean coral *Montastrea annularis*. Environ Microbiol 5: 370–382. Available: http://doi.wiley.com/10.1046/j.1462-2920.2003.00427.x. Accessed 30 July 2015.

21. Haas AF, Nelson CE, Rohwer F, Wegley-Kelly L, Quistad SD, et al. (2013) Influence of coral and algal exudates on microbially mediated reef metabolism. PeerJ 1: e108. Available: http://www.pubmedcentral.nih.gov/articlerender.fcgi?artid=3719129&tool=pmcentrez&rendertype=abstract. Accessed 24 March 2014.

22. Haas AF, Wild C (2010) Composition analysis of organic matter released by cosmopolitan coral reef-associated green algae. Aquat Biol 10. Available: http://www.int-res.com/abstracts/ab/v10/n2/p131-138/. Accessed 17 January 2014.

23. Gregg A, Hatay M, Haas AF, Robinett N, Barott KL, et al. (2013) Biological oxygen demand optode analysis of coral reef-associated microbial communities exposed to algal exudates. PeerJ 1: e107. Available: http://www.pubmedcentral.nih.gov/articlerender.fcgi?artid=3719127&tool=pmcentrez&rendertype=abstract. Accessed 25 April 2014.

24. Anthony KRN, Kline DI, Diaz-Pulido G, Dove SG, Hoegh-Guldberg O (2008) Ocean acidification causes bleaching and productivity loss in coral reef builders. Proc Natl Acad Sci U S A 105: 17442–17446. Available: http://www.ncbi.nlm.nih.gov/pubmed/18988740.

25. Hoegh-Guldberg O, Mumby PJ, Hooten a J, Steneck RS, Greenfield P, et al. (2007) Coral reefs under rapid climate change and ocean acidification. Science 318: 1737–1742. Available: http://www.ncbi.nlm.nih.gov/pubmed/18079392. Accessed 5 July 2011.

26. Johnson MD, Price NN, Smith JE (2014) Contrasting effects of ocean acidification on tropical fleshy and calcareous algae. PeerJ 2: e411. Available:

http://www.researchgate.net/publication/263014583_Contrasting_effects_of_ocean_acidification_on_tropical_fleshy_and_calcareous_algae. Accessed 27 July 2015.

27. Hofmann L, Straub S, Bischof K (2012) Competition between calcifying and noncalcifying temperate marine macroalgae under elevated CO_2 levels. Mar Ecol Prog Ser 464: 89–105. Available: http://www.researchgate.net/publication/233731283_Competition_between_calcifying_and_noncalcifying_temperate_marine_macroalgae_under_elevated_CO_2_levels. Accessed 18 May 2015.

28. Moberg F, Folke C (1999) Ecological goods and services of coral reef ecosystems. Ecol Econ 29: 215–233. Available: http://dx.doi.org/10.1016/S0921-8009(99)00009-9. Accessed 3 June 2013.

Erklärung

Gemas §6 der Promotionsordnung der Universität Bremen für die mathematischen, natur- und ingenieurwissenschaftlichen Fachbereiche vom 14. Marz 2007 versichere ich, dass die Arbeit mit dem Titel

„**The physiology of coral reef calcifiers under local and global stressors**"

1. ohne unerlaubte fremde Hilfe selbstständig verfasst und geschrieben wurde

2. keine anderen als die angegebenen Quellen und Hilfsmittel benutzt wurden

3. die den benutzten Werken wörtlich oder inhaltlich entnommenen Stellen als solche kenntlich gemacht wurden

4. es sich bei den von mir abgegebenen Arbeiten um 3 identische Exemplare handelt.

Bremen, 30.07.2015

_____

Friedrich W. Meyer